UNIVERSIDAD NACIONAL AUTÓNOMA DE MÉXICO

POSGRADO EN CIENCIAS BIOLÓGICAS

INSTITUTO DE ECOLOGÍA

BIOLOGÍA EVOLUTIVA

ÁMBAR DE MÉXICO:

BIOGEOQUÍMICA, TAFONOMÍA Y PALEOBIOLOGÍA

TESIS

QUE PARA OPTAR POR EL GRADO DE:

DOCTOR EN CIENCIAS

PRESENTA:

FRANCISCO RIQUELME ALCANTAR

TUTOR PRINCIPAL: DR. JOSÉ LUIS RUVALCABA SIL, FACULTAD DE CIENCIAS

COMITÉ TUTOR: DR. ABEL MORENO CÁRCAMO, INSTITUTO DE QUÍMICA
DR. JESÚS ALVARADO ORTEGA, INSTITUTO DE GEOLOGÍA

MÉXICO, D.F. DICIEMBRE 2014

UNAM
POSGRADO
Ciencias Biológicas

COORDINACIÓN

Dr. Isidro Ávila Martínez
Director General de Administración Escolar, UNAM
P r e s e n t e

Me permito informar a usted, que el Subcomité de Biología Evolutiva y Sistemática, en su sesión ordinaria del día 29 de septiembre de 2014 aprobó el jurado para la presentación de su examen para obtener el grado de **DOCTOR EN CIENCIAS** del Posgrado en Ciencias Biológicas del alumno **RIQUELME ALCÁNTAR FRANCISCO** con número de cuenta **403024559** con la tesis titulada **"AMBAR DE MÉXICO: BIOGEOQUÍMICA, TAFONOMÍA Y PALEOBIOLOGÍA"**, bajo la dirección del **DR. JOSÉ LUIS RUVALCABA SIL:**

Presidente:	DR. FRANK RAÚL GIO ARGÁEZ
Vocal:	DR. LAURO BUCIO GALINDO
Secretario:	DR. LUIS FELIPE JIMÉNEZ GARCÍA
Suplente:	DR. FERNANDO ALVAREZ PADILLA
Suplente	DR. JUAN DIDIANO MORALES MALACARA

Sin otro particular, me es grato enviarle un cordial saludo

A T E N T A M E N T E
"POR MI RAZA HABLARÁ EL ESPÍRITU"
Cd. Universitaria, D.F. a 18 de noviembre de 2014

DRA. MARÍA DEL CORO ARIZMENDI ARRIAGA
COORDINADORA DEL PROGRAMA

POSGRADO EN CIENCIAS BIOLÓGICAS
COORDINACIÓN

c.c.p. Expediente del (la) interesado (a)

RECONOCIMIENTOS ACADÉMICOS

El presente proyecto de investigación se llevó a cabo dentro los términos y normatividad del programa de Posgrado en Ciencias Biológicas, UNAM. Se reconoce y agradece el apoyo del personal académico y administrativo de la Coordinación y la sede del Instituto de Ecología, UNAM, durante los años 2012-2014.

Este proyecto recibió el apoyo financiero de la beca CONACYT/CVU346471, ciclo escolar 2012 (2) – 2015 (1). Adicionalmente, ha sido parcialmente financiada por la subvención de los siguientes proyectos: PAPIIT-UNAM IN106011, IN403210, CONACYT 131944 MOVIL II.

En particular, se reconoce y agradece el apoyo y dirección académica recibida por el Tutor Principal: Dr. José Luis Ruvalcaba Sil, investigador del Departamento de Física Experimental, Instituto de Física, UNAM.

Se agradece también a los miembros del Comité Tutor conformado por: Dr. Abel Moreno Cárcamo, adscrito al Instituto de Química, UNAM, y Dr. Jesús Alvarado Ortega, adscrito al Instituto de Geología, UNAM, quienes asesoraron y evaluaron el desarrollo del presente trabajo. Sus comentarios y discusiones no necesariamente implican un acuerdo con los puntos de vista y observaciones expresados en este texto y en los artículos publicados.

OTROS RECONOCIMIENTOS ACADÉMICOS Y TÉCNICOS

Se reconoce y agradece la revisión y comentarios del manuscrito realizada por el Comité de Sinodales, el cual quedó conformado por: Dr. Frank Raúl Gío Argáez (Instituto de Ciencias del Mar y Limnología, UNAM), Dr. Lauro Bucio Galindo (Instituto de Física, UNAM), Dr. Luis Felipe Jiménez García (Facultad de Ciencias, UNAM), Dr. Fernando Álvarez Padilla (Facultad de Ciencias, UNAM), Dr. Juan Bibiano Morales Malacara (Facultad de Ciencias, UNAM). Su contribución mejoró significativamente la estructura y contenido del texto final.

Del Instituto de Física, UNAM, se agradece el apoyo del personal del Laboratorio Pelletron: Karim López, Francisco Jaimes y Mauricio Escobar, por el apoyo técnico durante el análisis PIXE. Se agradece a los técnicos y administrativos del Laboratorio de Cristalofísica y Materiales Naturales, por el trabajo realizado en microfotografía. Se agradece al Dr. Arnulfo Martínez Dávalos, por el trabajo realizado en microtomografía computarizada de rayos-X.

Del Instituto de Biología, UNAM, se agradece a Susana Guzmán, por el apoyo en la adquisición de microfotografías.

Del Instituto de Geología, UNAM, se agradece al Dr. Mario Ramos, por el apoyo en el trabajo de campo. Se agradece a Enoch Ortiz, por la preparación de muestras.

Del Museo del Ámbar de Chiapas, se reconoce y agradece a Bibiano Luna y Adriana Kuhn, por el apoyo logístico y préstamo de material para su estudio.

Del Museo del Ámbar Lilia Mijangos, se reconoce y agradece a Luis Zúñiga, Johanna Friessen y Francis Pimentel, por el acceso a la colección y préstamo de material.

Del Instituto Nacional de Antropología e Historia, se agradece al Arqlgo. Jaime Alejandro Bautista Valdespino y Dra. Martha Cuevas, por el apoyo técnico en el registro público de colecciones de ámbar.

Del Laboratorio Nacional de Brookhaven, NY, E.E.U.U., se reconoce y agradece el apoyo de la Dra. Vivian Stojanoff, Dr. Peter Siddons, Dr. Paul Northrup y Dra. Lisa Miller, por el invaluable apoyo logístico y técnico durante los análisis en el Laboratorio de Luz Sincrotrón.

CONTENIDO

LISTA DE FIGURAS

RESUMEN

El ámbar de México incluye una nueva variedad descrita en la Formación Olmos, Cretácico Tardío de Coahuila, ca. 73 Ma. Este primer registro de ámbar cretácico es diferente, química y estratigráficamente, del ámbar fosilífero del Mioceno de Chiapas, ca. 23-15 Ma. Otro ámbar asociado a la **Bacalit**a Buddhue 1935, ha sido recuperado recientemente de la formación El Gallo, Cretácico Tardío de Baja California, ca. 73 Ma. En el presente trabajo de investigación se describen por primera vez las tres variedades de ámbar de México de acuerdo a la nomenclatura de resinas fósiles. **Coahulit**a **nov. var**., patronímico para el ámbar de Coahuila**; Simojovelita nov. var**., para Chiapas, y se establece además una enmienda en la descripción de la **Bacalita,** enmienda Riquelme 2014. La clasificación adoptada aquí está basada en criterios de morfología, biogeoquímica y afinidad botánica. Los marcadores químicos característicos se colectaron usando microespectroscopía de infrarrojo con una fuente de luz Sincrotrón.

El ámbar de Chiapas es el único de entre las tres variedades que preserva inclusiones de plantas, animales y microorganismos. Por lo cual, en la presente investigación también se realizaron análisis biogeoquímicos en la resina basados en espectroscopías de rayos-X usando aceleradores de partículas. Así como un análisis de la estructura y morfología mediante microscopías de alta resolución. De esta manera, en este trabajo se presentan los resultados del primer estudio de tafonomía molecular en el ámbar fosilífero de Chiapas con implicaciones directas en la preservación orgánica.

Finalmente, se ha realizado la sistemática paleontológica de un grupo selecto de artrópodos terrestres preservados en el ámbar de Chiapas. La ocurrencia de estos especímenes fósiles en la historia natural tiene un gran significado, todas las especies fósiles encontradas aquí son nuevas para la ciencia. En el presente trabajo, se describen formalmente tres nuevos géneros y especies de milípedos (orden **Diplopoda**), un género y nueva especie de pseudoescorpión (orden **Pseudoscorpiones**), una nueva especie de escorpión (orden **Scorpiones**), y una nueva especie de insecto microcoryfio (orden **Microcoryphia**). Estos nuevos taxa añaden conocimiento a la biodiversidad y distribución de sus respectivos órdenes para el Mioceno de la América Media.

ABSTRACT

The Mexican amber includes a newly described variety from the Late Cretaceous Olmos Formation in Coahuila, ca. 73 Ma. This first record of cretaceous amber is different, chemically and stratigraphically, from the Miocene fossiliferous amber of Chiapas, ca. 23-15 Ma. Other fossil resin previously known as **Bacalite** Buddhue, 1935, has been recently recovered from the Late Cretaceous El Gallo formation, Baja California, ca. 73 Ma. In the present study, the three varieties of Mexican amber are first described in accordance with the fossil resin nomenclature. **Coahulite nov. var**., patronymic for Coahuila amber; **Simojovelite nov. var**., for Chiapas amber; and an amended description of **Bacalite**, amendment Riquelme 2014 is also stablished. The classification adopted herein is based on morphological, compositional and botanical affinity criteria. The characteristic chemical makers were collected using infrared microspectroscopy with a Synchrotron light source.

The Chiapas amber is the only variety that preserves plants, animals and microorganisms. Furthermore, in the present research, biogeochemistry analyses were carried out using particle accelerators. A structural and morphological analyses using high-resolution microscopy were also applied. Accordingly, this is the first study of molecular taphonomy study on Chiapas amber with direct implications for organic preservation.

Finally, the systematic paleontology of selected terrestrial arthropods in the Chiapas amber has been performed. The occurrence of this fossil specimens in the natural history have a great significance, all fossil species found here are new to science. In this work , three new genera and species of millipedes (order **Diplopoda**), a new genus and species of pseudoscorpion (order **Pseudoscorpiones**), a new species of scorpion (order **Scorpiones**), a new species of microcoryphian insect (order **Microcoryphia**), are formally described. These new taxa add to knowledge of the distribution and biodiversity in their respective orders from the Miocene of Middle America.

CAPITULO 1

INTRODUCCION GENERAL

Este trabajo de investigación se presenta aquí en la modalidad de tesis por artículos publicados (plan 5085), por lo cual, está estructurada en una introducción general (Capitulo 1), artículos científicos publicados en la parte de resultados que es el cuerpo central de este trabajo (Capitulo 2), y en un capítulo final se presentan las conclusiones generales y perspectivas (Capítulo 3).

1. 1 ÁMBAR

El ámbar es una resina vegetal fósil. Su estructura interna es la de un polímero con fases semicristalinas aumentadas por los procesos de fosilización (Riquelme *et al*., 2014a). La polimerización de la resina ocurre a temperatura ambiente, y puede tomar entre unos minutos hasta algunas horas o días a partir de que secreta de la planta (Langenheim, 2003). La fracción volátil se disipa y pierde bajo las condiciones naturales imperantes en el bosque productor. Pero los aceites y ácidos orgánicos persisten, volviéndose químicamente estables, resisten la degradación orgánica y las condiciones de depósito. Los compuestos terpenoides (una clase de hidrocarburos aromáticos) se solidifican aceleradamente al exponerse a la luz y la atmósfera, formando así una masa resinosa endurecida, resistente a los mecanismos típicos de la disolución química. La forma fósil de esta resina es el ámbar (Langenheim, 1969; Anderson, 1992, 1995).

No todas las resinas vegetales fosilizan, la formación del ámbar, que inicia con la polimerización y la maduración química a través del tiempo, implica la formación de compuestos con un mayor peso molecular y el crecimiento de fases semicristalinas. La mayoría de los ámbares son resinas enriquecidas con terpenoides. Pero existen también ámbares con otro

tipo de hidrocarbonos como las resinas sesquiterpenas y las resinas fenólicas, que son menos comunes (Langenheim, 2003).

Al polimerizarse y separarse del árbol la resina entonces se incorpora entre los suelos y sedimentos arenosos y arcillosos, los cuales se litifican convirtiéndose en rocas a través del tiempo geológico. El ámbar es sepultado en este tipo de rocas: areniscas, lutitas, lodolitas, lignitas y carbón. Este proceso de fosilización de la resina es una clase de maduración fisicoquímica que afecta su estructura y composición, endureciéndola, deshidratándola, oxidándola, reduciéndolas otras veces, condensándola, cristalizándola, convirtiéndola en ámbar. Típicamente esto ocurre en depósitos geológicos enriquecidos con carbón orgánico, el cual se asocia a los restos de la masa vegetal de los bosques productores. Sin embargo, en la mayoría de los depósitos de ámbar se observa un transporte por arrastre de sedimentos desde el bosque original donde se formó. Con excepción de algunos depósitos como los de Bitterfeld, New Jersey, Coahuila y Chiapas, donde se pueden observar sedimentos originales al bosque precursor (Grimaldi, 2000; Weistschat y Wichard, 2002, Riquelme *et al*., 2014b)

El tiempo que tarda la maduración de la resina hasta convertirse en ámbar, es un tema insistente y controversial (Anderson, 1996). La maduración de las resinas es un fenómeno todavía bajo estudio. Aunque de manera atenuada, las resinas fósiles permanecen químicamente activas, y las condiciones geológicas de enterramiento de los ámbares son variables. Parámetros físicos relacionados con la mineralogía, como dureza, punto de fusión, gravedad específica, solubilidad, entre otros, se han usado para diferenciar el ámbar de otras resinas o de material no natural como plásticos. Pero el abuso de términos como 'ámbar joven', 'ámbar subfósil', 'copal', 'copal fósil', entre otros, ha aumentado la confusión al clasificar los ámbares. Sin embargo, una escala de tiempo propuesta por el fisicoquímico K. Anderson (*The nature and fate of natural resins in the geosphere VII*: 1997) para clasificar las resinas de acuerdo a su edad de depósito, basada en la datación con carbono-14 de los sedimentos portadores, y que consistente con la composición fisicoquímica de las resinas que, a mayor antigüedad van perdiendo la fracción volátil y las cadenas simples de terpenos (e.g. mono o diterpenos), proporciona una terminología que minimiza la vaguedad y ambigüedad de los términos (Anderson, 1997). De acuerdo a esta clasificación, una resina reciente tendrá de 0 a 250 años. Una resina antigua tendrá de 250 a 5000 años. Una resina subfósil tendrá de 5000 a 40000 años. Las resinas fósiles, las resinitas fósiles y los ámbares, se clasificarán a partir de los 40000 años en adelante. Otra

clasificación general tentativamente se ha basado en sus formas químicas constituyentes. Aunque esta clasificación se aplica a especies de resinas actuales y fósiles (Anderson, 1996; Langenheim, 2003).

Afinidades botánicas

En un informe de los geoquímicos P. S. Bray y K. B. Anderson (*Science 326, 132*: 2009), se ha reportado que las plantas gimnospermas pre-coníferas ya producían resina -un tipo de terpenoide basal- desde hace 320 millones de años, en el periodo geológico del Carbonífero (Bray y Anderson, 2009). Sin embargo, los depósitos más abundantes de ámbar en el planeta se encuentran en rocas asociadas a los periodos geológicos del Mesozoico y Cenozoico (Penney, 2010). Durante gran parte del Mesozoico, las plantas gimnospermas eran la vegetación dominante en los continentes. En este contexto, el ámbar encontrado en estas edades está asociado a coníferas resinosas del orden Pinales, como las familias Araucariaceae (e.g. de árbol actual asociado: pino Kauri), Taxodiaceae (e.g.sequoias y ciprecess), Taxaceae (e.g.tejos), Pinaceae (e.g. pinos comunes), Cupressaceae (e.g. cedros y juníperos) y Podocarpaceae (e.g. rimu o pino rojo). Por otra parte, en un periodo de tiempo más reciente, durante el Cenozoico, otros depósitos abundantes de ámbar están asociados a plantas angiospermas como la familia Fabaceae (gen. *Hymenaea*) ampliamente distribuida en ambientes tropicales y subtropicales. En tiempos todavía más recientes, como en el Pleistoceno, existen también plantas angiospermas como la familia Burseraceae (gen. *Bursera*), que produjo importantes depósitos de resina fósil (Langenheim, 2003).

Nomenclatura mineral

El ámbar es considerado además como un mineral orgánico en la clasificación de minerales de Dana, y un mineral orgánico misceláneo en la clasificación de Nickel-Strunz, dado que es de ocurrencia natural, tiene fases semicristalinas, y se encuentra en depósitos geológicos (Dana, 2014; Strunz, 2014). Su estructura cristalina es compleja porque implica macromoléculas en lugar de átomos o solamente iones. El color y el lustre del ámbar dependerán del grado de la alteración de las substancias orgánicas reactivas, los iones metálicos y las

impurezas minerales presentes en la resina (Langenheim, 2003; Riquelme *et al.*, 2014a). Inicialmente, el ámbar fue nombrado genéricamente como *succinita* por los mineralogistas, de acuerdo a la composición química de un ámbar tipo del Báltico. Sin embargo, existe una cantidad creciente de diferentes nombres asignados a diversos tipos y variedades de ámbar. Mineralogistas de diferentes países han hecho contribuciones a esta quisquillosa e interminable lista: la *gedanita, beckerita, stantienita, krantzita, y glessita* son ejemplos del ámbar de la región del Mar Báltico; *ajkaita, telegdita y kiscellita* se han descrito para Hungría; la *walchovita, muchita* y *neudorfita* se ha caracterizado en las localidades de la República Checa y Eslovaquia; la *rumaenite* de Rumania; la *ambrita* de Nueva Zelanda; la *bucaramangita* de Colombia; la *chemawinita* y/o *cedarita* de Canadá; la *burmita* de Birmania; la *amekita* de Nigeria; la *guyaquilita* de Ecuador; la *ionita* del Plioceno de California; la *retinellita* del Oligoceno de Inglaterra; la *goitschitea*, *bitterfeldita, durglessita*, y *pseudostantienita* de las minas de carbón negro de Bitterfeld en Alemania; la *copalina* de los bosques selváticos de Viena; la c*opalita* de las arcillas azules de Londres; y la *bacalita* de Baja California, inicialmente de origen ambiguo (Vavra, 1993).

Inclusiones

La importancia del ámbar como una resina asociada a un árbol extinto, lo hace en sí misma evidencia de esa vida antigua. El análisis de las resinas fósiles y recientes es un tópico asignado a la quimiotaxonomía de plantas con un alto valor científico (Anderson, 1995; Langenheim, 2003).

Pero el ámbar es también un recipiente natural que preserva inclusiones orgánicas de vida ancestral, tanto de plantas como animales y microorganismos. Es una cápsula del tiempo, un cristal hermético, un sepulcro absurdo, un contenedor congelado, una trampa fosilífera. El valor paleontológico del ámbar es invaluable.

Como el exudado residual brotando de árboles dispersos en bosques antiguos, la resina, de consistencia viscosa, va resbalando lentamente sobre la madera de los troncos, tallos y ramas. Así va capturando todo a su paso: burbujas de aire, gotas de agua mar, vapor de río, vaho de laguna, granos de lluvia, partículas de suelo, minerales, bacterias, hongos, protozoarios, algas, musgos, líquenes, raíces, polen, semillas, hojas, tallos, néctar, maderas, flores diminutas, frutos,

gusanos, tardígrados, bivalvos, gasterópodos, isópodos, hormigas, moscas, chinches, ácaros, miriápodos, escarabajos, tijerillas, mosquitos, abejas, polillas, termitas, cucarachas, mariposas, grillos, libélulas, escorpiones, arañas, pseudoescorpiones, pequeñas lagartijas, geckos , ranas, restos de roedores, y plumas coloridas de las primeras aves con dientes (Durham, 1957; Poinar, 1992; Grimaldi, 1996; Weistschat y Wichard, 2002, Azar *et al.*, 2013). Todas evidencias de vida antigua. Si bien no todos los ámbares son fosilíferos, el ámbar que preserva inclusiones orgánicas en su interior, sean plantas, animales o microbios, funciona como una instantánea de esa vida extinta que quedó inmóvil en el tiempo (Riquelme, 2012).

Primeros estudios con un enfoque naturalista o científico

Los trabajos preliminares de Agrícola, quién utilizó el término latino *succinum* para nombrar el ámbar (*De Nat. Foss.: 231-235*), quedan como uno de los primeros trabajos cientificistas (no aplicando estrictamente el método científico) sobre el ámbar. Agrícola objeta su origen como proveniente del árbol de goma, y en contraste, sostiene que el *succinum* es un material extraído del bitumen enterrado en manantiales submarinos (Agrícola, 1546). Agrícola fue además un pionero del análisis geoquímico de minerales y en sus experimentos químicos logró aislar por primera vez el ácido succínico, en la forma de una sal orgánica de anhídrido extraída de la destilación seca del ámbar del Báltico. El ácido succínico es un inhibidor de la pérdida de iones de potasio en el metabolismo de la célula, por lo que es un antioxidante celular.

Posteriormente, el filósofo naturalista y médico inglés William Gilbert, en su estudio de magnetismo y electrostática conocido como "*De Magnete*" (1600), analizó sistemáticamente el fenómeno de atracción que se produce al frotar ciertas substancias a las que llamó "eléctricos", entre éstas el ámbar, un material arquetípico, y propuso el término de "fuerza eléctrica" (Harmanand y Mitton, 2002).

Existen pocos documentos sobre el inicio del estudio metódico y formal de las inclusiones orgánicas en ámbar antes del siglo XIX. Por ejemplo, está la que se considera la primera monografía sobre plantas y animales embebidos en ámbar del Báltico, publicada por Nathaniel Sendel (*Historia succinorum corpora aliena involventium et nature poere pictorum et caelatorum,* 1742). Esta obra es el resultado del estudio de la colección real de Dresden, patrocinada por el rey de Polonia, Augusto II El Fuerte, ca.1718 (Weistschat y Wichard, 2002).

La obra pionera de Sendel (quizá el primer trabajo evidentemente paleontológico), cataloga los animales de acuerdo a sus hábitos de vida, que incluye insectos voladores, organismos articulados rastreros y animales acuáticos. Escribe además un pequeño capítulo sobre restos y morfologías de plantas. Quedan también las brevísimas observaciones naturalistas sobre el origen de los insectos atrapados en ámbar, escritas por el clérigo, médico y geólogo ingles Joseph Townsend, en su "*A journey through Spain"* (1791). Este geólogo de campo hace comentarios sobre hormigas y moscas preservadas en el ámbar cretácico de Asturias, España. (Zittel, 1901).

Pero el estudio sistemático del ámbar y las inclusiones orgánicas no comenzaría formalmente sino hasta el siglo XIX, en muestras de ámbar del Báltico, predominantemente de los depósitos de la "*Blau Erd*e" de Koningsberg en Prusia. Estos estudios pioneros no serían iniciados por taxónomos profesionales, sino por científicos de formación en física, química y farmacéutica que poseían colecciones personales importantes de ámbar del Báltico. La mayor parte de estos físicos y químicos se volverían entomólogos y botánicos importantes en la historia de la taxonomía. Entre los años de 1830 y 1937, se describen por científicos alemanes, 750 nuevas especies de plantas a partir de material vegetal atrapado en la resina. Por su parte, G.C Berendt y C.L. Koch, entre 1845 y 1854, describen nuevas especies de crustáceos, miriápodos y arañas, entre otros artrópodos. Adicionalmente, en 1836, a partir de estructuras vegetales embebidas en el ámbar, H.R. Goeppert erige la especie *Pinites succinifer* como el probable árbol productor del ámbar del Báltico, actualmente en controversia (Weistschat y Wichard, 2002).

En México

Históricamente, los depósitos en Chiapas son el registro más conocido de ámbar en México. El inicio de su extracción y uso se ubica hacia el año 300 de nuestra era por grupos Zoques que habitaron cerca de las canteras en Chiapa de Corzo, Preclásico Tardío. El arqueólogo Thomas Lee-Whiting (*Ámbar de Chiapas*: 2004), señala que grupos olmecas anteriores ocuparon la zona de los depósitos de Totolapa (ca. 1200 a.n.e), aunque no se ha encontrado ámbar en ese contexto arqueológico (Lee-Whiting, 2004, Lowe, 2004; Riquelme, 2012). El ámbar tuvo un uso ornamental, medicinal y ritual, con un alto valor jerárquico para los pueblos mesoamericanos (Fig.1). Zinacantán, en los Altos de Chiapas, llegó a ser el centro de comercio de ámbar más

importante y los indios zinacantecas controlaban, bajo un celoso cacicazgo, el comercio con otros pueblos, llegando incluso a naciones indias en Costa Rica (Lee-Whiting, 2004; Lowe, 2004; Riquelme, 2012).

A principios del siglo XX el geólogo Emil Böse, adscrito al Instituto Geológico de México, recorre el sureste y describe varios depósitos de ámbar en la zona de Simojovel, Chiapas, ca. 1905 (Lowe, 2004). Böse menciona la bisutería que se hacía con este material por los indígenas locales. Las expediciones en busca de petróleo, iniciadas en la década de 1920 en los estados de Veracruz, Tabasco y Chiapas, favorecen al cazador, etnógrafo y explorador danés Frans Blom (*Historical notes relating to the pre-Columbian amber trade from Chiapas:* 1959), quién se topa con el ámbar colectado en los Altos de Chiapas por indígenas tzotziles y tzeltales (Blom, 1959). Blom adquiere ámbar fosilífero comprando en los mercadillos locales, iniciando así su colección personal. Hasta 1970 realiza continuos viajes por el área, incrementa su colección y se establece en San Cristóbal de las Casas, Chiapas. Interesado en el estudio del ámbar con inclusiones sirve de anfitrión y guía a un equipo de geólogos, entomólogos y botánicos de la Universidad de California en Berkeley, los cuales visitan los sitios y comunidades ambaríferas (Hurd *et al*., 1962). Esta sería la primera expedición científica a las localidades del ámbar de Chiapas. Por ese tiempo también recibe al estudioso y coleccionista de ámbar G.O. Poinar (*Life in amber*: 1992). Entre los botánicos de la primera expedición, destacaba Jean Langenheim (Plant resins: 2003), quien se convertiría en una de las expertas mundiales en resinas vegetales. Entre los entomólogos destaca P.D. Hurd (*The fossiliferous amber of Chiapas, Mexico*: 1962). Estos exploradores e investigadores estuvieron activos en el área de Simojovel y Huitiupán entre 1950 y 1980, publicando los primeros estudios paleobotánicos, geoquímicos, taxonómicos y estratigráficos del ámbar y las inclusiones orgánicas (Hurd *et al.*, 1962, Poinar, 1992; Langenheim, 2003). Eventualmente, Blom donaría toda su colección de inclusiones de plantas y animales a la Universidad de California en Berkeley. En trabajos posteriores se realizarían también los primeros análisis químicos para caracterizar la fuente botánica del ámbar de Chiapas (Fig. 2), las cual se asocia a una planta leguminosa del género *Hymenaea* (Langenheim, 1966; Langenheim y Beck, 1968; Lambert *et al*., 1989).

Actualmente una industria artesanal persiste en torno al ámbar. Hoy en día el ámbar se colecta en su mayoría en las localidades de Simojovel, Totolapa y Estrella de Belén. Se extrae

en canteras a cielo abierto en zonas de derrumbe, socavones y minas de túneles de tiro. Existen depósitos menos explorados dispersos al noroeste y este del estado de Chiapas, tales como los afloramientos en las comunidades de Malpaso, Pueblo Nuevo Solistahuacán, Chenalhó, El Bosque, Pantelhó, y San Andrés Duraznal (Riquelme *et al*., 2014).

Fig. 1. Pectoral de jade en forma de sapo con incrustación de ámbar. Cultura Maya, Yucatán.

1. 2 ANTECEDENTES DIRECTOS

Chiapas

Durante el presente trabajo de investigación, se realizaron tres temporadas de campo, entre 2012 a 2014, en el área ambarífera de Simojovel, Huitupán, Totolapa, San Andrés Duraznal, y Estrella de Belén en Chiapas. Este último sitio, Estrella de Belén cerca de Palenque, fue descubierto entre 2009 y 2010 por campesinos indígenas locales (Fig. 3). Los cuales dieron noticia a una expedición paleontológica-arqueológica representada por la arqueóloga Martha Cuevas (Instituto Nacional de Antropología e Historia), los paleontólogos Jesús Alvarado (Instituto de Geología, UNAM) y el autor del presente trabajo, quienes hacían trabajo de campo en el área.

Los estratos que contienen ámbar en Estrella de Belén se asemejan a aquellos expuestos cerca de Simojovel y Totolapa. La sección de ámbar consiste de lentes de lignitas derivados de la descomposición y litificación de residuos vegetales y suelos. Típicamente aquí se encuentra el ámbar. Capas de arenisca no fisible, de textura fina a gruesa, con laminación cruzada y de espesores variables, están asociadas con la lignita. Intercaladas a la arenisca hay esquistos laminares, con abundantes feldespatos, arcillas tipo bentonita, óxidos de hierro rojizos, copiosos minerales de arcilla y nódulos de pirita. De hecho, la pirita se encuentra frecuentemente embebida en ámbar en los depósitos de Estrella de Belén, la cual es una característica única no compartida en otros sitios. Los estratos que contienen ámbar en Estrella de Belén ocasionalmente se encuentran expuestos de manera angular o casi perpendicular al plano de depósito. Esto indica una fuerte actividad tectónica post-enterramiento. De acuerdo a lo anterior, la litología y el régimen sedimentario son consistentes con un ambiente terrestre-fluvial cercano a la costa. (Boggs, 2009).

Adicionalmente, se atribuye la fuente vegetal del ámbar de Chiapas a una especie extinta del género *Hymenaea* (*sensu* Langenheim, 1966). Este ámbar tiene en común señales químicas con las resinas de la especies actuales *H. courbaril* y *H. verrucosa*, las cuales se distribuyen actualmente en los trópicos (Langenheim, 1995, 2003; Poinar y Brown, 2002; Riquelme *et al*., 2014b). Ámbar asociado con árboles de *Hymenaea* también se encuentran en la República Dominicana, Cuba, Puerto Rico, Haití y Jamaica (Poinar, 1992; Iturralde-Vinent, 2001; Langenheim, 2003). Probablemente, árboles de *Hymenaea* se encontraban dispersos cercanos a la costa en los trópicos del Neógeno de la América Media. Los depósitos de Chiapas y el Caribe comparten una evolución tectónica y sedimentaria semejante que se extiende desde el Mioceno Temprano hasta el Plioceno Medio (Meneses-Rocha, 2001; Iturralde-Vinent, 2006). Por lo tanto, la paleobiota –plantas y animales- presente en el ámbar de *Hymenaea* que ocurre en el Mioceno de la América Media debe estar estrechamente relacionada a niveles taxonómicos como paleogeográficos.

Coahuila

Finalmente, un material apelmazado y resinoso, que aparecía entre las capas de carbón, era ya largamente conocido por los mineros de la zona carbonífera, entre los pueblos de

Múzquiz, Barroterán, Palaú, Sabinas y Piedras Negras, al norte de Coahuila. De acuerdo a la tradición oral, solía utilizarse este material para prender fogatas durante el almuerzo y alumbrarse en las jornadas nocturnas de excavación. Al parecer era altamente combustible. En 2011 se exploró una zona de tajos de carbón inactivos en las proximidades de Palaú en busca de este material por parte del Ingeniero Martín Galicia, de la compañía minera MINOSA. Como resultado las primeras muestras de ámbar fueron recuperadas de entre el corte de una mina a cielo abierto conocida como "Los Menores", localizada a unos 5 kilómetros de Palaú (Fig. 3). Estratigráficamente, las capas de carbón que contienen ámbar corresponden a una sección de la Formación Olmos, con una edad de depósito en el Cretácico Tardío.

Durante la presente investigación se realizaron 2 temporadas de campo, entre 2012 a 2013, en el área de Palaú, Coahuila. Se recuperaron más de 15 trozos distintos, entre medianos y grandes, de formas laminares, apelmazados y encostrados, de entre estos sedimentos de un antiguo bosque paratropical que creció en el Cretácico (Fig. 4)

Baja California

Por otra parte, en 1935 el mineralogista estadunidense J.D. Buddhue describió varias piezas de ámbar de Chiapas adquiridas en una joyería de la Ciudad de México como provenientes de Baja California. No se contaba con los datos sobre la localidad ni el registro estratigráfico del depósito. Aunque la edad era desconocida y la procedencia cuestionable, Buddhue le asignó el nombre mineral de Bacalita, de la conjunción de las sílabas Ba: Baja y Ca: California (Buddhue, 1935). Posteriormente, entre 1962 y 1965 el entomólogo P.D. Hurd y su equipo, así como los geólogos F. H. Kilmer y R. L. Langenheim, reportaron al menos 3 localidades de ámbar con depósitos dispersos en el área cercana a la comunidad de El Rosario, Baja California, a unos 344 kilómetros de la ciudad de Ensenada (Fig. 3). El material era escaso y la resina fósil se presentaba en pequeños nódulos de algunas centímetros, sin embargo, las localidades se ubicaron entre Punta Baja -al sur de El Rosario- y al sur de Punta San José. Preliminarmente, se estableció una edad en el Cretácico Tardío para estos depósitos (Langenheim *et al*., 1965).

En 2010, el paleontólogo Jesús Alvarado, del Instituto de Geología, UNAM, colectó fragmentos de ámbar en sedimentos arenosos cercanos a la costa en Baja California (Fig.5). Los

cuales proporcionó para ser incluidos en esta investigación. Las muestras de ámbar provenían de sedimentos asociados a la localidad fosilífera cretácica conocida como El Gallo, a casi 5 Km al Noroeste de El Rosario y en la misma área de los registros hechos por Langenheim y colaboradores. La ubicación de este punto de colecta tiene las coordenadas latitud 30º 04´02", longitud 115º 47´ 0.5" Oeste.

Fase experimental

Para el estudio de la estructura y composición del material fósil, recientemente, se han implementado metodologías no destructivas, dado el carácter inédito de los fósiles con preservación excepcional. Estas técnicas incluyen microscopías de alta resolución y espectroscopias de alta energía, como el uso de aceleradores con una fuente de protones y otro de luz Sincrotrón (Riquelme *et al*., 2009, 2013). La aplicación sistemática de estas metodologías se definió preliminarmente bajo el concepto de Paleometría (Riquelme *et al*., 2009). Los datos recopilados durante este periodo inicial han sido esenciales para comprender globalmente la fosilización selectiva y han sentado las bases para nuevas interpretaciones y teorías enfocadas en los procesos de preservación de la materia orgánica (Riquelme *et al*., 2013).

El presente proyecto de investigación tiene como plataforma experimental la aplicación de espectroscopias de infrarrojo y rayos-X usando una fuente de luz Sincrotrón, así como otra fuente de protones en un acelerador electrostático. Se realizaron dos estancias de investigación en el Brookhaven National Laboratory, NY, E.U.A.; obteniéndose tiempos de análisis en las siguientes líneas experimentales del National Synchrotron Light Source (NSLS-1): U10B, X15B, X10A, X27A, y X13B (*ver http://www.bnl.gov*). Se realizó otra estancia de investigación en el Soleil Sincrotrón en París, Francia, usando la línea experimental LUCIA (Flank *et al.* 2006) (*ver http://www.synchrotron-soleil.fr/*).

Por otra parte, la presente investigación está fundamentada en trabajos previos que integran análisis químicos, moleculares y microscópicos no destructivos en el material fósil aplicando técnicas analíticas como PIXE (Particle Induced X-ray Emission) y RBS (Rutherford Backscattering), basados en una sonda externa del acelerador 3 MV Pelletron del Instituto de Física, UNAM (Riquelme *et al*., 2014a). PIXE es usado en este trabajo para investigar la

composición multielemental y procedencia de los ámbares evitando el daño o destrucción de la muestra.

Otro de los aspectos críticos en el estudio de las inclusiones orgánicas en ámbar es el examen microscópico a nivel estructural y celular. La microscopía de planos apocromáticos con superposición de múltiples planos de foco y la microscopía de luz infrarroja reflectada, así como la microtomografía computarizada de rayos-X en 3D (micro-CT), se han empleado en el presente trabajo. Estas microscopías han demostrado exitosamente que son técnicas adecuadas para medir, documentar y analizar inclusiones orgánicas con interés taxonómico y tafonómico.

Fig. 2. Ámbar de Chiapas, Mioceno.

Fig. 3. Localidades de ámbar en México, modificado de Riquelme *et al*., 2014b.

Fig. 4. Ámbar de Coahuila, Cretácico.

Fig. 5. Ámbar de Baja California, Cretácico.

1.3 LÍNEAS DE INVESTIGACIÓN

Ámbares

i. Se caracteriza a nivel estructural y composicional los tipos de ámbar de México, haciendo énfasis en la fuente paleobotánica y la nomenclatura mineral. Como resultado, se reportan dos nuevas resinas fósiles no descritas anteriormente para el Cretácico de México, ubicadas en Coahuila y Baja California. Se establece además una nomenclatura para el ámbar de Chiapas. Esta clasificación de lo ámbares de México contribuye a una nueva propuesta de la clasificación genérica de los ámbares y las resinas fósiles en el mundo. La metodología para clasificar las resinas fósiles en el grupo de los minerales orgánicos aún no está resuelta.

Tafonomía molecular

ii. Se aborda por primera vez el estudio de las inclusiones preservadas de animales y plantas en el ámbar de Chiapas basados en la química molecular. Se obtienen los primeros datos de la dinámica fisicoquímica en el proceso de ambarización de esta resina, con implicaciones en la preservación excepcional de la materia orgánica. Este estudio a pequeña escala contribuye de manera significativa al entendimiento de la preservación del material biológico ancestral, tópico de la tafonomía molecular.

Sistemática paleontológica

iii. La sistemática paleontológica es una de las ramas fundamentales de la paleobiología, la cual combina los métodos de la neontología en las ciencias naturales y los conceptos de la paleontología en las ciencias de la tierra. Como resultado de los avances en la aplicación de microscopías de alta resolución en el presente trabajo, que innovaron en la manera de registrar, procesar y mostrar las inclusiones en ámbar, se pueden observar morfologías virtualmente completas y detalladas de los organismos con interés taxonómico. Consecuentemente, se describen nuevos géneros y especies de milípedos (orden Diplopoda), pseudoscorpiones (orden

Pseudoscorpiones), escorpiones (orden Scorpiones) y archeognatos (orden Microcoryphia =Archeognata), los cuales fueron preservados selectivamente dentro del ámbar de Chiapas. Este estudio contribuye significativamente al conocimiento de la diversidad de Diplopoda, Pseudoscorpiones, Scorpiones, y Microcoryphia, en el Nuevo Mundo. La descripción y registro de estas nuevas especies fósiles tiene una notable importancia evolutiva y biogeográfica para la distribución de las especies actuales.

Fig. 6. Milípedo en ámbar de Chiapas, Mioceno.

1.4 PRESENTACIÓN GENERAL DE LOS ÁMBARES DE MÉXICO

Las resinas fósiles son exudados de plantas que preservan firmas químicas de ácidos orgánicos, aceites esenciales (terpenoides) y sales minerales, los cuales están asociados con determinada especie vegetal, con la identidad mineral y el depósito geológico. En consecuencia, se plantean varias preguntas con respecto a las afinidades botánicas, el registro fósil y la nomenclatura mineral de las resinas fósiles, donde se incluyen los ámbares (Langenheim, 2003; Anderson, 1992; Vavra, 1993).

El ámbar de Chiapas (Fig. 2), con una edad estimada en el Mioceno Temprano-Medio (ca.23 a 15 Ma.), ha sido considerado durante largo tiempo como el único depósito geológico de ámbar en México (Langenheim, 2003; Lee-Whiting, 2004; Lowe, 2004). Sin embargo, en los últimos dos años se ha colectado de entres capas de rocas enriquecidas con carbón orgánico cerca de Palaú, Coahuila, una nueva variedad de ámbar no reportada anteriormente (Fig. 4). Estos estratos pertenecen a la Formación Olmos, con una edad estimada en el Cretácico Tardío, ca. 73 Ma. (Eguiluz de Antuñano, 2001). De manera adicional, otra variedad de ámbar se ha colectado recientemente en el sitio fosilífero conocido como "El Gallo", Cretácico Tardío (ca. 73 Ma.), cerca de El Rosario, Baja California (Fig. 5), a unos 344 kilómetros de la ciudad de Ensenada (Morris, 1981; Johnson *et al*., 2006). El primer registro de resina fósil en esta área fue reportado inicialmente por Langenheim *et al.* (1965). Como resultado de varios viajes de geología de campo, entre 1962 y 1965, Langenheim y colaboradores describieron tres lugares hacia el sur de El Rosario con restos de resina fósil, los cuales fueron interpretados como ámbar y lo asociaron al registro geológico de la Bacalita, mencionada previamente por Buddhue en 1935.

Inicialmente, el término Bacalita fue erigido en la nomenclatura de minerales orgánicos para una nueva variedad de ámbar que tentativamente se asumía provenía de Baja California, a pesar de la naturaleza incierta de la resina (no se presentó un análisis de su composición) y el origen ambiguo del registro, cuyo depósito y edad geológica eran entonces desconocidos (Buddhue, 1935; Langenheim *et al.*, 1965). Más tarde, sobre la base de las exploraciones geológicas arriba mencionadas, Langenheim y colaboradores (1965) sugieren que las rocas del Cretácico en las proximidades de El Rosario, eran probablemente la fuente de la Bacalita.

En el presente estudio, muestras de ámbar recientemente colectadas de los depósitos geológicos de Chiapas, Coahuila y Baja California, han sido caracterizados siguiendo la metodología usada para restos fósiles y utilizando microespectroscopía de Infrarrojo por transformada de Fourier (micro-FTIR) usando una fuente de luz Sincrotrón. Los resultados tienen implicaciones directas en la nomenclatura de las resinas fósiles. La clasificación adoptada en este trabajo está basada en criterios morfológicos y la composición de las resinas, además de su afinidad botánica. Dos nuevos términos se proponen para el ámbar de Coahuila y Chiapas, así como una enmienda en el registro del ámbar de Baja California.

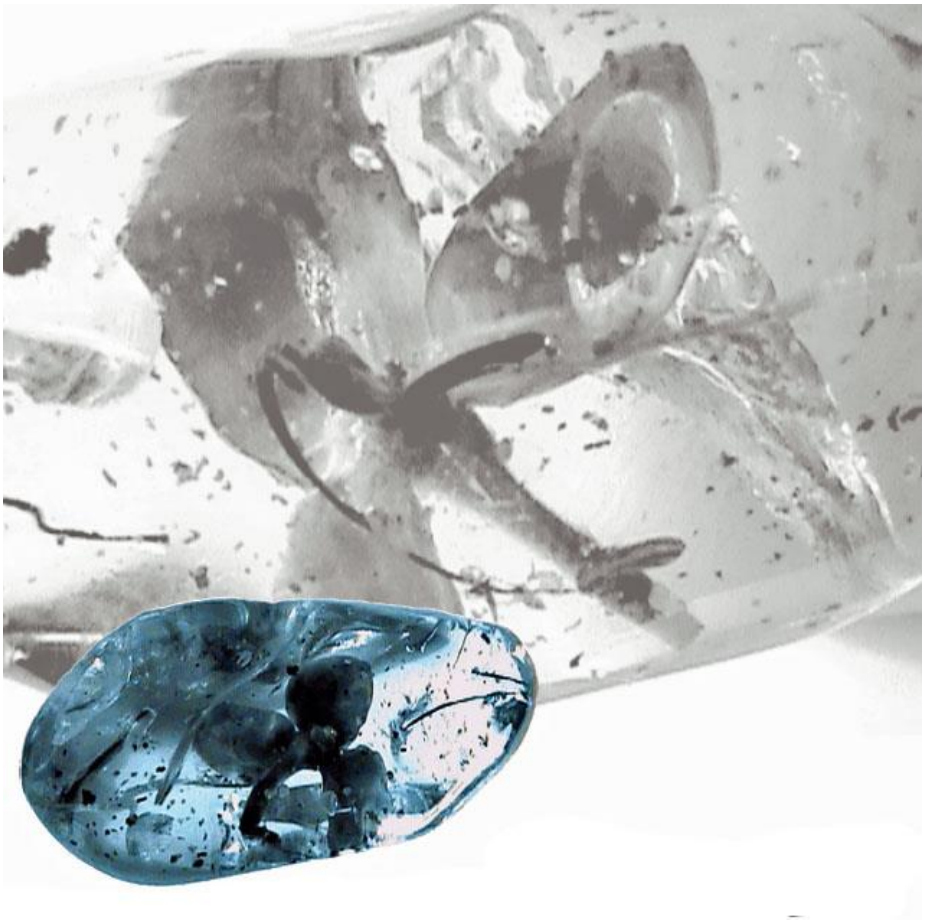

Fig. 7. Flor de *Hymenaea* en ámbar de Chiapas, Mioceno. Fotomicrografía de infrarrojo.

Ámbar de Coahuila

Coahuilita nov. var.

(Figs. 4 y 8)

Localidad y horizonte. Mina de carbón "Los Menores", cerca de Palaú, Coahuila, México (Fig.3). Localizada en las coordenadas: latitud 27° 50' 57" N, longitud 101° 24' 20" O. Esta sección, enriquecida con carbón orgánico, pertenece a la Formación Olmos, Cretácico Tardío, ca. 73 Ma. (Martínez-Hernández *et al*., 1980; Estrada-Ruiz *et al*., 2008).

Etimología. Patronímico por el estado de Coahuila. Las capas de carbón con ámbar están expuestas al norte del estado, en la región conocida como la "Región Carbonífera".

Ambiente Geológico. El ámbar ocurre en rocas de la Formación Olmos, con una edad estimada del Cretácico Tardío, Campaniano-Maastrichtiano. Esta unidad geológica consiste principalmente en secuencias de areniscas finas a gruesas, conglomerados y arcillas que se depositaron en un ambiente de planicie deltaica (Estrada-Ruiz *et al*., 2008). Adicionalmente, se encuentran capas interestratificadas de lodolitas con abundante materia orgánica y carbón bituminoso asociadas con un ambiente de pantanos y lagunas someras. Restos fósiles de plantas, incluyendo hojas, frutos y madera, se recolectan típicamente en estas rocas. El conjunto de plantas fósiles está ligado a un paleambiente de bosque paratropical (Martínez-Hernández, 1980; Estrada-Ruiz *et al.*, 2008). En consecuencia, el ámbar se encuentra depositado en los sedimentos asociados con el bosque productor, ningún rasgo de transporte desde sedimentos alóctonos es observable.

Notas tafonómicas. El ámbar se encuentra *in situ* entre las capas de carbón, se presenta en forma de nódulos o de hojas con un tamaño variable no mayor a los 15 cm. Muestra frecuentemente texturas encostradas y comprimidas a causa de los procesos de litificación y sepultamiento, además de superficies semicristalinas brillantes producidas por intemperismo. Varias muestras con formas laminares preservan moldes y costras asociados a la corteza del árbol productor. Otras muestras con formas nodulares revelan capas deposicionales episódicas,

lo cual es consistente con diferentes épocas de producción de la resina. La resina se acumuló sucesivamente formando una masa endurecida de capas multilaminares. Árboles resiníferos actuales presentan variaciones estacionales similares con el incremento del depósito de resina durante la estación de lluvias, tal como se demuestra en Langenheim (2003).

Diagnosis. Resina fósil de color amarillo, pardo-anaranjado y negro; brillo translúcido vítreo a graso, flexible, muy resistente a la fractura, dureza igual al yeso mineral, insoluble al alcohol y acetona; depositado en forma de nódulos multilaminares y placas encostradas. Ámbar no fosilífero, preserva fragmentos de suelo, carbón y materia vegetal es su interior; su afinidad botánica es una resina diterpenoide aromática, enriquecida con fracciones volátiles producida actualmente por los pinos y el liquidámbar.

Observaciones. El mapa composicional por micro-FTIR muestra el perfil químico del anillo cíclico, de los componentes carbonilo y de los hidrocarbonos aromáticos en la Coahuilita, los cuales son rasgos diagnósticos para resinas vegetales. De acuerdo a lo anterior, la Coahulita coincide mejor con las resinas diterpenoides aromáticas, enriquecidas con fracciones volátiles (Riquelme *et al*., 2014b). Las bandas de absorción IR se asemejan a la observadas en los espectros de resinas actuales producidas por árboles de la familia de los pinos y el liquidámbar. La banda de absorción centrada a 3287 cm-1 se encuentra alterada por la pérdida de moléculas con enlaces OH causado por un proceso de deshidratación, puede ser un indicador del grado de alteración diagenética en resinas antiguas por el proceso de maduración (Riquelme et al., 2014b).

Fig. 8. Ámbar de Coahuila, Cretácico.

Ámbar de Baja California

Bacalita Buddhue, 1935; enmienda Riquelme 2014

(Fig. 5)

Localidad y horizonte. El sitio fosilífero "El Gallo", a 5 km NO de El Rosario, Baja California, México (Fig.3). Longitud 30 º 04 '2 "N, latitud 115 º 47' 0.5" O. Esta sección es conocida informalmente como la formación El Gallo, Cretácico Tardío, ca. 73 Ma. (Morris, 1981; Johnson *et al.*, 1996, 2006).

Etimología. Como se asignó por Buddhue, 1935. Nombre derivado de las sílabas Ba: Baja y Cal: California.

Ambiente geológico. Los sedimentos donde se encuentra el ámbar se componen de arcillas de color gris a ocre-amarillento y areniscas de grano fino, los cuales fueron depositados en un ambiente de planicie costera transicional. Estos estratos costeros pertenecen a la formación el Gallo. Análisis estratigráficos y radiométricos establecen una edad en el Cretácico Tardío, en el límite del Campaniano-Maastrichtiano (Morris, 1981; Johnson *et al.*, 1996, 2006). Otros restos fósiles de peces, reptiles, dinosaurios, mamíferos, invertebrados marinos y restos de madera y hojas, son colectados típicamente de estos estratos (Morris, 1981; Johnson *et al*., 2006; Prieto-Márquez *et al*., 2012).

Notas tafonómicas. El ámbar se encuentra entre nódulos carbonosos no mayores a 5 cm de tamaño. Es frágil, se rompe fácilmente y se encuentra en cantidades mínimas. Intercalados con los nódulos, se encuentra también materia orgánica, madera carbonizada, impresiones de hojas y restos de huesos indeterminados. Los nódulos de ámbar se encuentran fraccionados y dispersos entre los sedimentos arenosos, los cuales muestran una sedimentación cruzada. Esto sugiere que el ámbar fue redepositado a partir de los sedimentos originales al bosque productor. Probablemente, el ámbar proviene de rocas más antiguas.

Diagnosis. Resina fósil de color pardo-amarillo a rojizo, brillo translúcido vítreo a nublado; insoluble en alcohol o acetona, de superficie encostrada a toscamente pulida por erosión, frágil y de apariencia cristalina, fraccionada, con abundantes fracturas y microporos; depositado en diminutos nódulos carbonosos < 5 cm. Ámbar no fosilífero, contiene restos de suelo y polen en su interior; su afinidad botánica es la resina de coníferas actuales, de la familia de los pinos, como la colofonía o el rosín.

Asignación original. Término propuesto por Buddhue, 1935, conservado por Langenheim *et al.*, 1965. Ámbar originario de Baja California, sin descripción de la morfología ni composición química. Afinidad botánica desconocida.

Descripción. Ámbar de color pardo-amarillo a rojizo, con un brillo translúcido vítreo a nublado, no es soluble en alcohol o acetona, con una superficie toscamente pulida por la erosión, es frágil y de apariencia cristalina, altamente fraccionado, aparece en pequeños nódulos redondeados alcanzando unos pocos centímetros de tamaño (< 5 cm.); resiste ataque de ácidos suaves > pH 4.5; no despide olor al quemarse; muestra abundantes fracturas y microporos; es una resina no fosilífera, únicamente fragmentos de suelo y de polen indeterminado se observan atrapados en su interior.

Observaciones. Las impurezas minerales reactivas se incrementan durante el entierro y la fosilización, lo cual afecta la composición y estructura de las cadenas principales de carbono en las resinas fósiles; esto se refleja notablemente en los espectros de IR y el perfil químico de la Bacalita, tal como se observa en la deformación de las bandas (Riquelme, 2014b).

Por otra parte, el primer reporte de la Bacalita que data de 1935, es ambiguo y la descripción original es muy escueta (Buddhue, 1935). Posteriormente, la composición, las afinidades botánicas y las características físicas de muestras atribuibles a la Bacalita, reportada en las exploraciones de 1965, cerca de El Rosario, no fueron descritas formalmente (Langenheim *et al.*, 1965). Desafortunadamente, la ubicación actual de estas muestras es incierta, las cuales carecen de un catálogo formal.

Por considerar que la descripción original es confusa y pobre en detalles, en el presente trabajo se acepta el término Bacalita, pero se propone una diagnosis y una descripción formal

dentro de la nomenclatura de las resinas fósiles. La diagnosis enmendada se basa en los resultados del análisis composicional y la descripción de muestras recientemente recuperadas de la formación el Gallo (Cretácico Tardío), en el área de El Rosario, Baja California. El origen de estas muestras es consistente con el depósito geológico previamente reportado por Langenheim y colaboradores (1965) en el área de El Rosario, y que fue interpretado preliminarmente como la procedencia sedimentaria de la Bacalita. De acuerdo a lo anterior, en la diagnosis inicial presentada aquí, se evita hacer referencia a un nuevo nombre mineral que eventualmente se reduzca a una sinonimia.

Ámbar de Chiapas

Simojovelita var. nov.
(Fig. 2)

Localidad y horizonte. Mina de ámbar "La Pimienta", Municipio de Simojovel de Allende, Chiapas, México (Fig.3). Situado a 17 ° 9 '21 "N, 92 ° 45' 9" W. La sección de ámbar pertenece a los estratos de la Formación Mazantic y Balumtum, Mioceno, ca. 23-13 Ma. (Frost y Langenheim, 1974; Poinar, 1992; Graham, 1999; Perrilliat *et al.*, 2010).

Etimología. Patronímico por el pueblo de Simojovel. Históricamente, el centro de acopio y comercio del ámbar proveniente de los Altos de Chiapas.

Ambiente Geológico. El ámbar se encuentra en rocas de las Formaciones Mazantic y Balumtum, con una edad estimada en el Mioceno Temprano-Medio (Perrilliat *et al.*, 2010). Los depósitos de ámbar están asociados con un ambiente de línea de costa y tierras bajas continentales (Graham, 1999; Perrilliat *et al.*, 2010). La biota fósil, incluyendo plantas y animales, tanto en los sedimentos como embebidos en ámbar, está vinculada a un bosque subtropical (Graham, 1999; Langenheim, 2003; Solórzano-Kraemer, 2010; Riquelme *et al*., 2014).

Notas tafonómicas. En muestras de mano, el ámbar tiene diversas formas y tamaños, aparece como masas encrostadas, como gotas, como placas multilaminadas, como tubos y conos similares a estalactitas, y como aglomerados en forma de tortas. Estas formas no muestran necesariamente el estado original de las secreciones resiníferas del árbol productor, ya que pueden ser transformadas por la intensa compresión y el reordenamiento químico de los compuestos (la temperatura de transición cristal-líquido del ámbar de Chiapas es cercano a los 100° C), los cuales ocurren durante el entierro y los procesos diagenéticos.

Diagnosis. Resina fósil de color amarillo dorado, naranja, rojizo, marrón, negruzco, amarillo ocre, amarillo citrino, amarillo lechoso, excepcionalmente verde y azul al observarse por refracción; brillo translúcido vítreo, dureza semejante al yeso mineral, liviano, con abundantes planos de fractura y microestratos pardo-rojizos, nódulos y abundantes burbujas; insoluble al alcohol o acetona, resiste ataques de ácidos suaves > pH 3.5, temperatura de transición vítrea a ~100 °C; depositado en forma de masas encrostadas, tubulares y cónicas similares a estalactitas, gotas, placas multilaminadas y aglomerados. Ámbar fosilífero, preserva minerales, suelo, microorganismos, plantas y animales en su interior; su afinidad botánica es la resina actual de una leguminosa del género *Hymenaea.*

Descripción. En muestras pulidas, este ámbar tiene una amplia gama de colores, desde los más comunes amarillo dorado, naranja, rojizo, marrón, negruzco, amarillo ocre, amarillo citrino, amarillo lechoso, y rara vez, verde y azul, tal como se puede observar por refracción. Su brillo es translúcido vítreo, por su raya tiene una dureza semejante al yeso mineral, es liviano y muestra abundantes planos de fractura. Su temperatura de transición vítrea es ~100 °C. Resistente a ataques de ácidos suaves > pH 3.5. Al quemarse despide un olor acre dulzón. En secciones delgadas transversales, muestra líneas longitudinales pardo-rojizas, nódulos y copiosas burbujas con líquidos indeterminados -¿aceites esenciales de la resina?- conservados en su interior. Este ámbar es fosilífero, su característica más conspicua: microorganismos, plantas y animales atrapados en su interior, están preservados a detalle, algunos organismos pueden presentar características celulares. Igualmente, preserva suelo y minerales autigénicos en su interior, como sales carbonatadas y pirita.

Observaciones. Este tipo de ámbar es conocido desde tiempos precolombinos y ha sido estudiado formalmente por varias disciplinas, como la arqueología, la botánica, la química y la paleontología, entre otras, publicando trabajos con estándares científicos a partir de 1959 (Hurd, 1962, Langenheim, 1966; Lee-Whiting, 2004; Lowe, 2004). Sin embargo, previo al presente trabajo, su inclusión en la nomenclatura de minerales orgánicos no había sido considerada. Por lo cual, no se le conoce anteriormente con un nombre mineral.

El ámbar de las canteras de Simojovel está estrechamente relacionado con los exudados resiníferos de plantas actuales del género *Hymenaea* (*sensu* Langenheim, 1966). Análisis químicos comparativos a muestras de ámbar colectado en las canteras de Simojovel y Totolapa, mostraron una afinidad botánica similar entre ellos asociado a *Hymenaea,* ambos ámbares son químicamente idénticos (Lambert *et al.,* 1989; Langenheim, 2003). Ambos ámbares también comparten el mismo registro geológico (Perrilliat *et al*., 2010; Durán-Ruiz *et al*., 2013; Riquelme *et al*., 2014). En consecuencia, un mismo nombre mineral puede ser utilizado para este tipo de ámbar, el cual puede encontrarse en distintos depósitos a lo largo de los Altos de Chiapas, incluyendo Totolapa, Simojovel y Palenque.

A partir de estudios químicos basados en espectroscopia IR, Langenheim (2003) sugiere que este ámbar coincide mejor con un tipo de exudado resinoso de la especie actual *Hymenaea courbaril.* Adicionalmente, los rasgos diagnósticos en los espectros IR de la Simojovelita en la región entre 1500 a 650 cm-1, también se asemejan a la resina actual de *Hymenaea verrucosa*, conocido como "Copal de África" (Riquelme *et al*., 2014b). Esto sugiere que la Simojovelita conserva huellas químicas en una posición intermedia entre las resinas actuales de *H. courbaril y H. verrucosa.* Una nueva revisión de las afinidades botánicas de ámbar recuperado en varias canteras de los Altos de Chiapas, incluyendo Palenque, Totolapa, Pueblo Nuevo, Chenalhó, Huitiupán y Puente Nacional, aumentando la toma de muestras y aplicando microespectroscopías IR, Raman, y espectrometría de masas, se encuentra actualmente en curso por el autor del presente trabajo.

1.5 TAFONOMÍA MOLECULAR Y ACELERADORES DE PARTÍCULAS

Aproximación conceptual

La tafonomía surge intuitivamente, aunque no conceptualmente, a la par que la Paleontología. Desde los juegos retóricos de la escuela pitagórica versus la escuela platónica, en donde se discutía sobre el origen biológico de los fósiles (siglo VI al V a.C.), y pasando por los primeros trabajos descriptivos de fósiles hechos por Georgius Agricola, Konrad von Gesner, Nicolaus Steno, Leonardo da Vinci, y Robert Hooke (siglos XVI y XVII), hasta la época moderna de la paleontología inaugurada en la *Histoire Naturelle* de George-Louis Buffon (1749), la evolución adaptativa de Jean-Baptiste Lamarck en *Philosophie zoologique* (1809), la anatomía comparada de George Cuvier en *Le Règne animal distribué d'après son organisation*: (1817), el estructuralismo geológico de Charles Lyell en *Principles of Geology* (1830), y la selección natural de Charles Darwin en *The origin of species* (1859), se va dando respuesta a la pregunta inicial hecha por estos autores fundamentales: ¿Qué tipo de organismos se preservan? Pero a ésta pregunta iba también emparejada otra inmediata: ¿Por qué se preservan?

Precisamente, la tafonomía es una disciplina que aborda ésta otra cuestión: las causas y condiciones de preservación del material fósil en la historia natural del planeta. Es decir, procesa y examina las condiciones y causas de la preservación de los organismos con implicaciones directas en su biología, historia de vida y procesos evolutivos. Aunque fue definida conceptualmente en la época moderna (siglo XX), la tafonomía explica los procesos que rigen la preservación de la materia orgánica a través del tiempo, la cual cubre un amplio rango de organismos, edades geológicas y ambientes sedimentarios diversos. La tafonomía tiene un papel clave en la paleobiología (Behrensmeyer *et al.,* 2000). El paleontólogo ruso Iván Yefrémov propone el término tafonomía (*Las leyes del enterramiento,* 1940), y establece una definición que se ha vuelto clásica. Para Yefrémov, la tafonomía es el estudio de los procesos biológicos, físicos y químicos que ocurren durante la muerte, enterramiento y preservación de los organismos a lo largo del tiempo geológico (Yefrémov, 1940). Recientemente, sin embargo, la tafonomía puede ser definida como el estudio de la relación entre la materia orgánica y los ambientes minerales a través del tiempo. Así pues, este tiempo puede establecerse en edades geológicas o en un tiempo más reciente medido en días, semanas, meses, años; y la materia

orgánica incluye desde biomoléculas y microorganismos, hasta organismos multicelulares, como vertebrados, invertebrados y plantas; así como los ambientes minerales pueden abarcar desde suelos, substratos, permafrost, polímeros semicristalinos, y rocas. La tafonomía es, básicamente, una ciencia forense.

Lo anterior implica nuevas aproximaciones, tanto conceptuales como metodológicas, un ejemplo de esto es el concepto de *Biomineralización*, introducida en el estudio de los procesos de preservación selectiva, la cual sucede en horas o días después de la muerte de los organismos, preservando tejidos blandos intactos, como la que ocurre en el ámbar. Además, aborda la idea de que la fosilización selectiva es un fenómeno biológico (no únicamente mineralógico), que afecta al material orgánico a pequeña escala mediante reacciones biogeoquímicas entre macromoléculas orgánicas y fases minerales, preservando tejidos, células y biomoléculas (Riquelme *et al.*, 2013).

El presente trabajo se enmarca en la aplicación reciente de técnicas analíticas en fisicoquímica que han sido particularmente útiles en el estudio tafonómico del material fósil, en el cual típicamente se requiere un enfoque científico multidisciplinario (Stankiewicz *et al.*, 1998). De hecho, las nuevas metodologías implementadas en la investigación de tejidos blandos fósiles y macromoléculas, comprenden análisis microscópicos de alta resolución y estudios fisicoquímicos con técnicas analíticas de mayor sensibilidad. En la actualidad, por citar algunas metodologías novedosas, se desarrollan análisis del material fósil mediante espectrometrías no destructivas usando radiación con aceleradores de partículas (Fig. 9). Estos se aplican para explorar los aspectos básicos del material biológico preservado en depósitos antiguos. En la información que se genera se reconoce un nivel de análisis estructural y otro composicional. Por otra parte, aplicando técnicas microscópicas de alta definición se identifican elementos de origen biológico: e.g. tejidos, células, biopolímeros; así como ultraestucturas cristalinas y semicristalinas propias del sedimento portador de fósiles. Adicionalmente, mediante el análisis del estado químico, es posible encontrar marcadores que son indicadores diagnósticos muy útiles para entender los procesos de preservación selectiva de la materia orgánica. Este tipo de estudios a pequeña escala del material biológico ancestral forman parte de la paleobiología moderna y la llamada tafonomía molecular (Briggs, 2003; Schweitzer *et al*., 2008).

De esta manera, podemos estudiar la preservación de organismos atrapados en ámbar, la cual está determinada por las características fisicoquímicas de la resina, en particular, su química

molecular, su estructura interna y cristalinidad parcial. El ámbar está formado estructuralmente por cadenas muy largas de macromoléculas hidrocarbonadas. Cuando secreta como un líquido viscoso, durante la síntesis de la planta, la resina está compuesta por cadenas cortas de macromoléculas, pero se va transformando en un polímero -extremadamente sólido- al formarse cadenas más grandes sintetizadas a partir de las pequeñas durante el proceso de polimerización (Callister, 2000). Existe un estado semicristalino en polímeros de ocurrencia natural como el ámbar, diferente al que ocurre en minerales (Callister, 2000). Esto implica que cristalizan las macromoléculas, en lugar de solamente los iones o los átomos como en los minerales. Por lo tanto, la longitud de la cadena de las macromoléculas y su composición química, influyen en la capacidad del ámbar de solidificarse y de cristalizar parcialmente. Así pues, el organismo que cae en la resina queda atrapado permanentemente por la rápida solidificación de ésta. La consolidación de la resina protege al organismo de la degradación orgánica, que es ubicua en la naturaleza, preservando sus delicadas estructuras y tejidos. Con los aceleradores de partículas podemos medir y comprobar -o replantear- la dinámica fisicoquímica de estos procesos. A la fecha, el presente trabajo de investigación representa el primer estudio de tafonomía molecular sobre los procesos de fosilización en el ámbar de Chiapas, el cual involucra aspectos biogeoquímicos, moleculares y ultraestructurales.

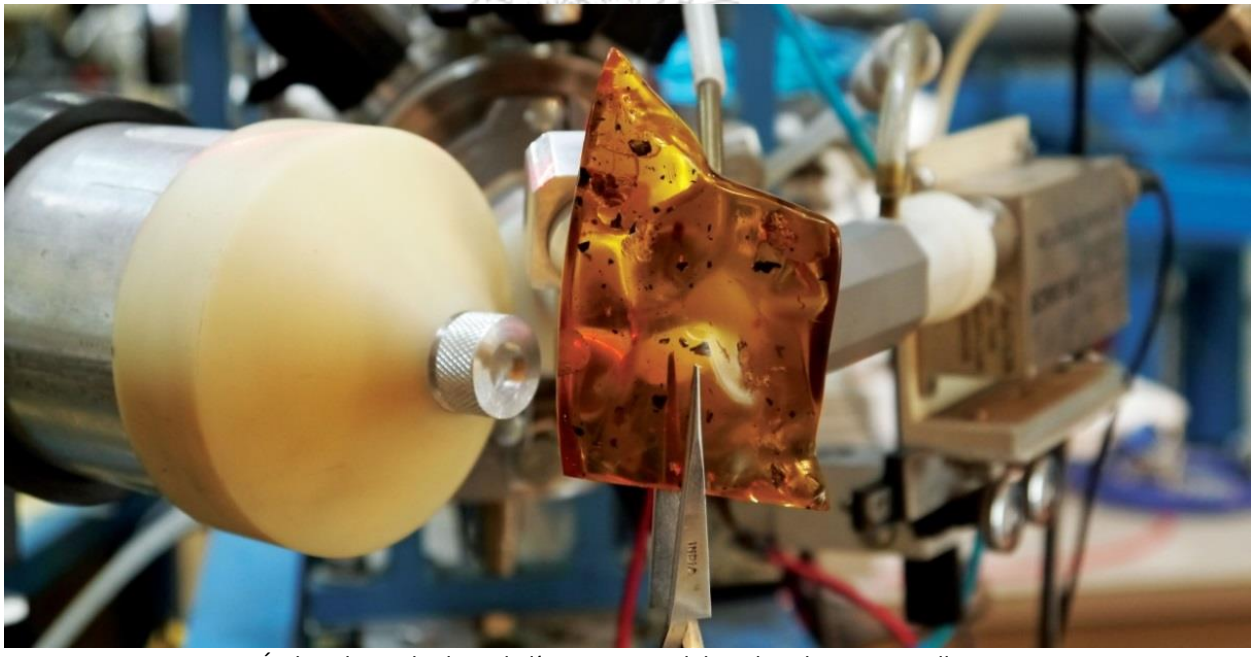

Fig. 9. Ámbar de Coahuila en la línea externa del Acelerador 3MeV Pelletron.

1.6 SISTEMÁTICA PALEONTÓLOGICA

El caso de los artrópodos terrestres en el ámbar en Chiapas

Los afloramientos de ámbar agrupados en las Montañas de Chiapas forman parte de un Lagerstätte fósil del Mioceno, ca. 23-15 Ma., cuya característica más notable es que contiene una paleobiota preservada de manera excepcional (Riquelme *et al*., 2014, 2014a). Esta preservación de tejidos duros y blandos en plantas, animales y microorganismos fue causado por un rápido endurecimiento de la resina vegetal, seguido por una interrupción de la descomposición orgánica (Riquelme *et al.*, 2014a). Existe un número notable de artrópodos terrestres presentes en la paleobiota del ámbar de Chiapas, entre los que destacan por su biodiversidad y el reciente descubrimiento de ejemplares completos y virtualmente intactos, los milípedos (orden **Diplopoda**), los pseudoscorpiones (orden **Pseudoscorpiones**), los escorpiones (orden **Scorpiones**), y los microcoryfios (orden **Microcoryphia** =Archeognata).

Típicamente, es posible detectar morfotipos asociados a diferentes familias actuales que se distribuyen en los trópicos de América, desde la parte más sureña de Norte América hasta el norte de Sudamérica. Una primera evaluación de estos morfotipos indica que son especies no conocidas para la ciencia. En algunos casos, como los milípedos y los microcoryfios, no existe un registro fósil previo. Consecuentemente, su descripción formal es una cuestión que se torna imprescindible y contribuye significativamente al conocimiento de la historia natural de cada uno de sus respectivos grupos taxonómicos.

El reconocimiento de nuevas especies biológicas en el material fósil conjunta la sistemática y la paleontología, cuyo propósito es la reconstrucción de la historia de la vida en el planeta. Esta sistemática paleontológica combina los métodos de la neontología en las ciencias naturales y los conceptos de la paleontología en las ciencias de la tierra. Por lo cual, forma una de las ramas fundamentales de la paleobiología.

Orden Diplopoda Blainville, 1844

La biología, ecología, morfología y filogenia de los milpiés ha sido descrita exhaustivamente en algunos textos clásicos (Hopkin y Read, 1992; Sierwald y Bond, 2007;

Shear, 2011). Los milpiés se han adaptado exitosamente a los hábitats del suelo y la hojarasca en todos los climas subárticos. Contribuyen en gran medida en los ciclos del suelo de los bosques templados y tropicales. Pero la preservación fósil de los milpiés es muy inusual, sobre todo porque tienen hábitos terrestres y tejidos no recalcitrantes, los cuales no resisten los procesos de fosilización (Fig.6). El registro fósil más antiguo de los milpiés se encuentra en las rocas del Silúrico Medio en Escocia (Wilson y Anderson, 2004). Un resumen del registro geológico de Diplopoda se encuentra en otra parte (Sierwald y Bond, 2007; Shear, 2011). Consecuentemente, existe un gran sesgo en el registro fósil durante el Mesozoico, con la excepción de los espirobólidos del Cretácico Superior de Mongolia y la ocurrencia de la especie (posiblemente mal asignada) *?Xylobius mexicanus* Müllerried, 1942 en el Jurásico Tardío-Cretácico Medio del centro de México (Müllerried, 1942). Sin embargo, la mayoría de los miembros de los taxa extintos se encuentran sobre todo en Lagerstätten fósiles, tal como ocurre en los nódulos piritizados del Carbonífero de Gran Bretaña y en los depósitos de ámbar en el Cenozoico de Europa y de América Central (Wilson y Anderson, 2004).

Uno de los registros fósiles más abundantes se encuentra en el Paleógeno de Europa, específicamente, en el ámbar del Báltico (Keilbach, 1982). Otro grupo de fósiles se han encontrado en los depósitos de ámbar más jóvenes en el Neógeno de la República Dominicana (Santiago-Blay y Poinar, 1992). A la fecha, no se había registrado o descrito formalmente ningún fósil de milpiés en el ámbar de Chiapas, el cual comparte edades geológicas similares, ambientes sedimentarios y afinidades paleobotánicos con el ámbar dominicano. En este estudio, tres nuevos géneros y tres nuevas especies de milpiés se describen e ilustran en el ámbar de Chiapas por vez primera (Fig. 10).

Orden Microcoryphia (=Archaeognatha) Verhoeff, 1904

Los microcoryfios son uno de los primeros linajes de insectos. Son insectos pequeños, primitivos, ectognatos, sin alas, que viven actualmente en ambientes templados y tropicales (Sturm y Machida, 2001) (Fig.11). Los microcoryfios ocurren en el suelo, hojarasca, corteza de árbol, piedras fracturadas, cerca de cuerpos de agua, y costas rocosas. La sistemática de Microcoryphia ha sido revisada y discutida en los trabajos de Sturm y Bach de Roca (1993) y Mendes (2002). El orden Microcoryphia (=Archaeognatha) comprende las familias

Meinrtellidae, Machilidae, y algunos géneros *incertae sedis,* con algunos pocos representantes fósiles distribuidos en ambos hemisferios (Sturm y Machida, 2001).

En América, existe una especie fósil de la familia Meinrtellidae descrita en el ámbar del Neógeno de la República Dominicana: *Neomachilellus (Praeneomachilellus) dominicanus* Sturm y Poinar, 1997, y otro conocido como *Meinirtellus sp*., que se ha reportado en el copal de Venezuela (Mendes, 1997). Existe un primer registro en el ámbar de Chiapas, un ejemplar hembra provisionalmente asignado al género *Neomachilellus* (Wygodzinsky, 1971). Otro ejemplar macho depositado en el Museo Americano de Historia Natural, Nueva York, EE.UU., ha sido mencionado brevemente por Sturm y Poinar (1997). Hasta ahora, el status de ambos ejemplares es incierto. En el presente trabajo, se describe una nueva especie basada en ejemplares de macho y hembras que se han colectado en los últimos dos años de los estratos cerca de Simojovel, Totolapa, Huitiupán, y Estrella de Belén, en las montañas de Chiapas (Fig.11).

Orden Pseudoscorpiones De Geer, 1778

La biología e historias de vida de los pseudoescorpiones (Arachnida: Pseudoscorpiones) ha sido ampliamente investigada en varias especies vivientes (Weygoldt, 1969). La radiación adaptativa de los pseudoscorpiones incluye todos los ambientes subárticos. Ocurren en el suelo, hojarasca, corteza de árbol, pasto, cuevas, rocas fracturadas, lodos y arenas costeras. La cladística y filogenia molecular del grupo se ha examinado en múltiples contribuciones (Harvey 1992; Murienne *et al.,* 2008). Sin embargo, la preservación fósil de los pseudoscorpiones es extremadamente rara. Las formas fósiles son poco conocidas excepto en ámbar. Sus pequeñas, lábiles cutículas quitinizadas son fácilmente destruidas por el enterramiento profundo y la litificación. Las formas más antiguas de pseudoescorpiones en el registro geológico provienen de los estratos arcillosos del Devónico Medio cerca de Gilboa, Nueva York, EE.UU. (Shear *et al.,* 1989; Schawaller *et al*., 1991; Dunlop, 1996). En el Mesozoico sólo se conoce un fósil en ámbar del Cretácico en los estratos de Grassy Lake, Alberta, Canadá (Schawaller, 1991). En el Cenozoico, la mayoría de las especies fósiles descritas se encuentran en los depósitos de ámbar del Paleógeno del Báltico y el Neógeno de la República Dominicana, así como los depósitos más jóvenes de copal en Madagascar y Colombia (Henderickx *et al*., 2012; Schawaller, 1980; Judson, 2010).

Poco se sabe sobre los pseudoescorpiones fósiles en el ámbar de Chiapas. Un morfotipo de chernetido, con identidad taxonómica incierta, es el único fósil documentado previamente (Schawaller 1982). En el presente trabajo, se describe por primera vez una especie fósil de pseudoescorpión en el ámbar de Chiapas (Fig.12).

Orden Scorpiones Koch, 1851

El registro fósil de la orden Scorpiones Koch, 1851 actualmente alcanza 118 especies descritas, de las cuales hay 112 especies provenientes de depósitos de ámbar en todo el mundo (Lourenço y Weitschat 2005; Dunlop *et al*., 2008). Una lista completa de los escorpiones fósiles descritos hasta ahora puede consultarse en Dunlop *et al.* (2014). El registro de escorpiones en ámbar data desde el Cretácico Temprano-Medio.

En los depósitos de ámbar del Nuevo Mundo se han encontrado en estratos del Neógeno de la República Dominicana y México. De los cuales, se han erigido nuevas especies en los géneros Centruroides Marx, 1890, Microtityus Kjellesvig-Waering, 1966, y Tityus Koch, 1836. Estas especies son *Centruroides nitidus* Thorell, 1876; *Centruroides beynai* Schawaller, 1979; *Microtityus ambarensis* Schawaller, 1982; *Tityus geratus* Santiago-Blay y Poinar, 1988, *Tityus (Brazilotityus) hartkorni* Lourenço, 2009, y *Tityus azari* Lourenço, 2013, todos ellos provenientes del ámbar de la República Dominicana; mientras que solamente una especie, *Tityus knodeli* Lourenço, 2014, ha sido descrita recientemente del ámbar de Chiapas (Dunlop *et al.*, 2014; Lourenço, 2014).

La ocurrencia de escorpiones fósiles en el ámbar de Chiapas es muy rara. A la fecha, sólo hay dos fósiles conocidos. Uno de ellos ha sido asignado tentativamente dentro del género *Centruroides* (estatus incierto) y la especie *T. knodeli,* mencionada anteriormente (Santiago-Blay y Poinar, 1993; Lourenço, 2014). Los escorpiones del ámbar de Chiapas son formas modernas que vivieron en un ambiente de manglar durante el Mioceno. Por lo tanto, hay variaciones intraespecíficas significativas que nos permitan determinar nuevas especies estrechamente relacionadas con los morfotipos actualmente distribuidos en el Neotrópico del Caribe, América Central y Sudamérica. En este trabajo, se describe una nueva especie colocada en el género *Tityus*, familia Buthidae (Fig.13).

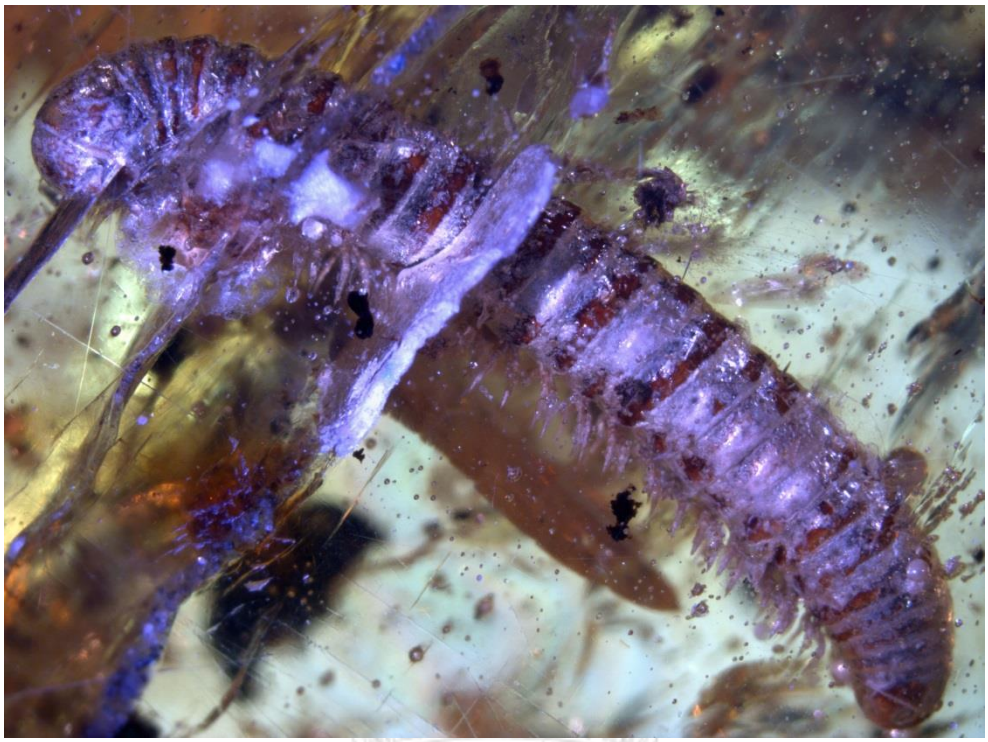

Fig. 10. Milípedo, inclusión en ámbar de Chiapas, Mioceno.

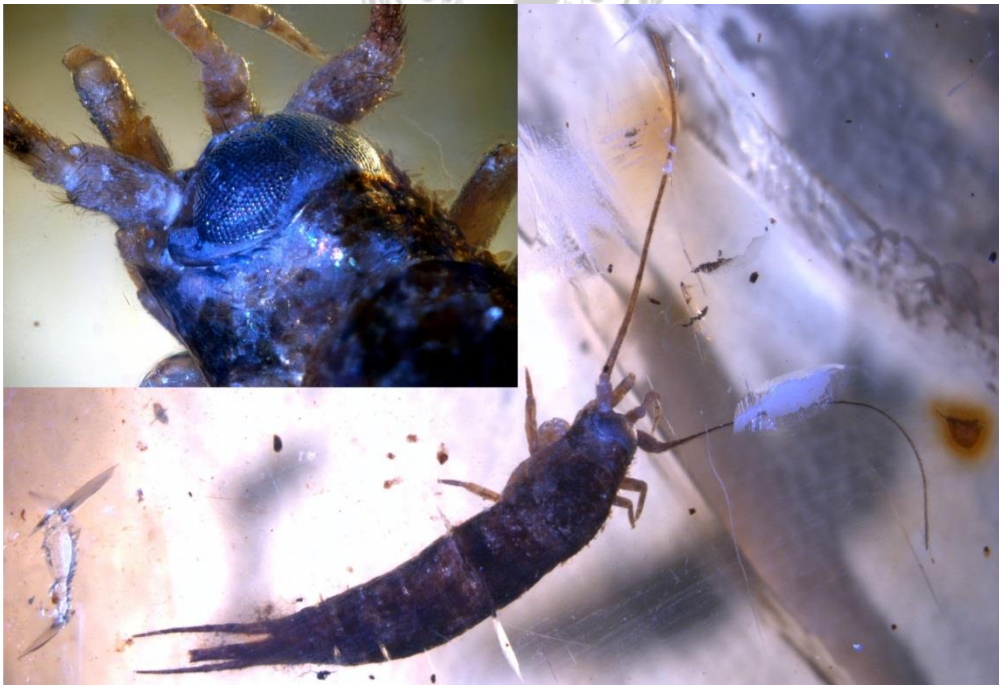

Fig. 11. Microcoryfio, inclusión en ámbar de Chiapas, Mioceno.

Fig. 12. Pseudoescorpión, inclusión en ámbar de Chiapas, Mioceno.

Fig. 13. Escorpión, inclusión en ámbar de Chiapas, Mioceno.

1. 7 PLATAFORMA EXPERIMENTAL

Micro-FTIR: Fourier Transform Infrared Microspectroscopy

Se utilizó la línea experimental U2B del sincrotrón NSLS-1 (Fig. 14), ubicado en el laboratorio Brookhaven, NY, E.U.A. (http://beamlines.ps.bnl.gov/beamline.aspx?blid=U2B). Se obtuvieron espectros infrarrojo (IR) característicos y mapas composicionales en muestras pulidas, fracturadas, sin preparar, extraídas directamente del ámbar con ayuda del microscopio. Los espectros IR se colectaron en la región media de 4000 a 650 cm^{-1}, a una resolución de 4 cm^{-1} y > 250 escaneos por punto. Los mapas composicionales se colectaron en un área de 20x20 μm. El espesor de las muestras fue menor a 50 μm para reducir las saturación (ruido) de los espectros IR. Para disminuir el tiempo de preparación de las muestras no se requirió de pelletización, tal como se muestra en los experimentos de Wolfe *et al.* (2009). Esto también evita la distorsión en la señal de los grupos hydroxyl (OH^-), los cuales son huellas químicas características en las resinas vegetales fósiles, así como se demuestra en los resultados presentados por Tappert *et al.* (2011). Se usaron ambos métodos de transmitancia y reflectancia en infrarrojo para la obtención de los espectros y mapeos estructurales, y el programa Opus V6.5 para procesar los espectros y micromapas.

En los espectros IR característicos se identificaron los grupos funcionales diagnósticos correlacionados con la composición de la resina y el origen botánico. Estos rasgos característicos fueron incluidos en la diagnosis de cada variedad de ámbar, los cuales ahora forman parte de su descripción quimiotaxonómica formal (Riquelme *et al.*, 2014b).

La espectroscopía de infrarrojo por transformada de Fourier (FTIR) ha sido una técnica ampliamente usada en análisis de resinas vegetales fósiles y recientes (Beck *et al*., 1964; Langenheim y Beck, 1968; Derrick *et al*., 1999; Vandenabeele *et al.*, 2003; Trevisani *et al.*, 2005; Wolfe *et al*., 2009) El espectro de infrarrojo (IR) muestra señales químicas llamadas regiones 'fingerprints' (sic) o huellas digitales, las cuales están relacionadas a la identidad y afinidad botánica de las resinas fósiles y recientes (Beck *et al*., 1964, Vavra, 1993; Langenheim, 2003; Tappert *et al*., 2011). Estas huellas químicas diagnósticas permiten elucidar la procedencia, la afinidad botánica y la variedad mineral de los ámbares y otras resinitas fósiles (Trevisani *et al.*, 2005; Wolfe *et al*., 2009). Las asignaciones de regiones diagnósticas

(fingerprints) en los espectros IR en resinas fósiles y recientes han sido publicadas en numerosos trabajos y forman parte de amplias librerías de espectros IR actualmente disponibles (Trevisani *et al*., 2005; Wolfe *et al*., 2009; Tappert *et al*., 2011, entre otros). Adicionalmente, los principios básicos del uso de la microespectroscopía FTIR usando una luz sincrotrón se puede revisar en múltiples contribuciones (Potts *et al.,* 1995; Carr y Williams, 1997; Dumas y Miller, 2003, entre otros).

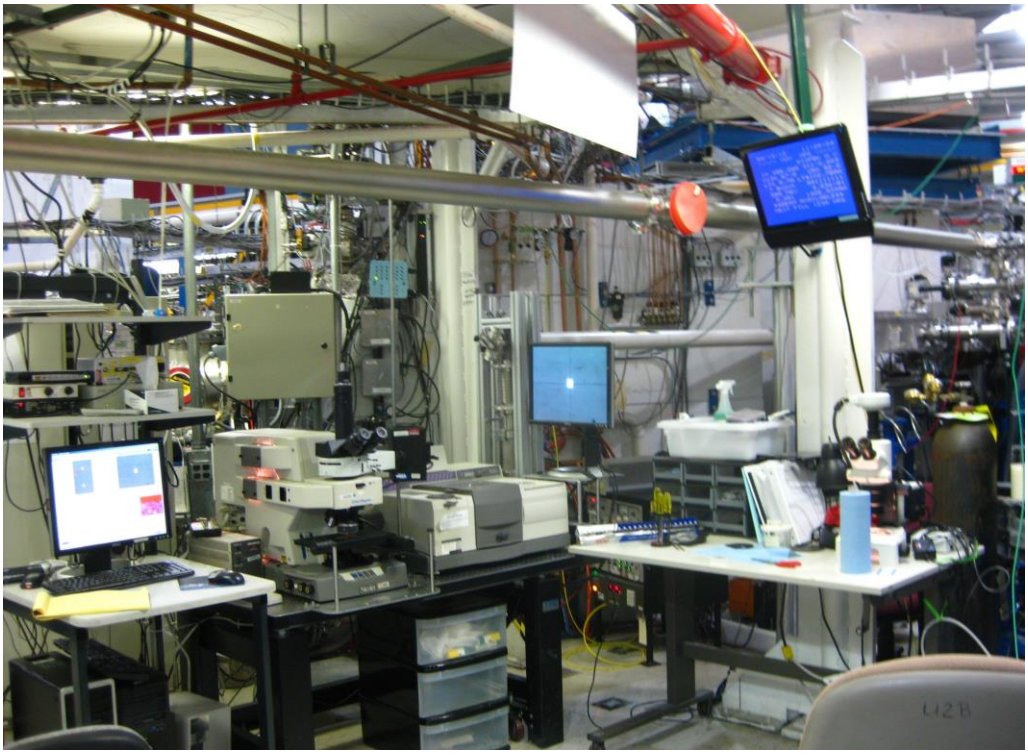

Fig. 14. Línea experimental U2B NSLS-1, Laboratorio Brookhaven.

XANES: X-ray Absorption Near Edge Structure spectroscopy

Se utilizó la línea experimental X15B del sincrotrón NSLS-1 (Fig. 15), ubicado en el laboratorio Brokhaven, NY, E.U.A (http://beamlines.ps.bnl.gov/beamline.aspx?blid=X15B). Se cuantificó la especiación del azufre directamente proporcional a la intensidad de absorción de rayos-X, calibrando para una energía estándar de 2482.6 eV. Se empleó el programa de acceso libre Athena con la función IFEFFIT para la interpretación y ajuste de los espectros característicos (Ravel y Newville, 2005) La intensidad y distancia de los picos en el espectro K-XANES fueron asignadas a especies de azufre de acuerdo al consenso en la literatura, y siguiendo la identificación establecida para los grupos funcionales presentes en el azufre orgánico, se asignó su respectivo estado de oxidación. La cuantificación de especies de azufre presente son indicares diagnósticos del endurecimiento acelerado del ámbar de Chiapas, seguido de un efecto inhibidor de la degradación orgánica de las inclusiones atrapadas en su interior (Riquelme *et al.*, 2014a).

La espectroscopía XANES (X-ray Absorption Near Edge Structure) basada en el uso de una fuente de luz sincrotrón, es una poderosa herramienta para identificar los mecanismos de incorporación y especiación de elementos ligeros en materiales sólidos, líquidos, gases y coloides (Sham, 2002). El uso de este método en la identificación y cuantificación de especies de elementos orgánicos en una variedad de materiales y substancias naturales ha sido ampliamente demostrado en múltiples experimentos (Morra *et al.*, 1997; Xia *et al*., 1998). Los resultados obtenidos mediante esta técnica funcionan como marcadores químicos característicos de los procesos de especiación elemental en la materia orgánica. Tiene la ventaja de emplearse en muestras sin preparar o en bajas concentraciones (Sham, 2002). La espectroscopía XANES puede ser usada además de manera no invasiva en material fósil invaluable, cuya naturaleza única limita el uso de técnicas tradicionales. Esta otra ventaja impacta de manera importante en el uso de la espectroscopía XANES para estudiar material fósil o subfósil (Riquelme, 2014a).

A la fecha, no existe literatura disponible que muestre la caracterización de resinas fósiles o recientes aplicando espectroscopía XANES (Langenheim, 2003). En este estudio se ha utilizado por primera vez en ámbares fosilíferos. La identificación y cuantificación de azufre orgánico en la resina tiene implicaciones en la preservación excepcional y los procesos de ambarización o endurecimiento de ésta a través del tiempo geológico (Riquelme, 2014a).

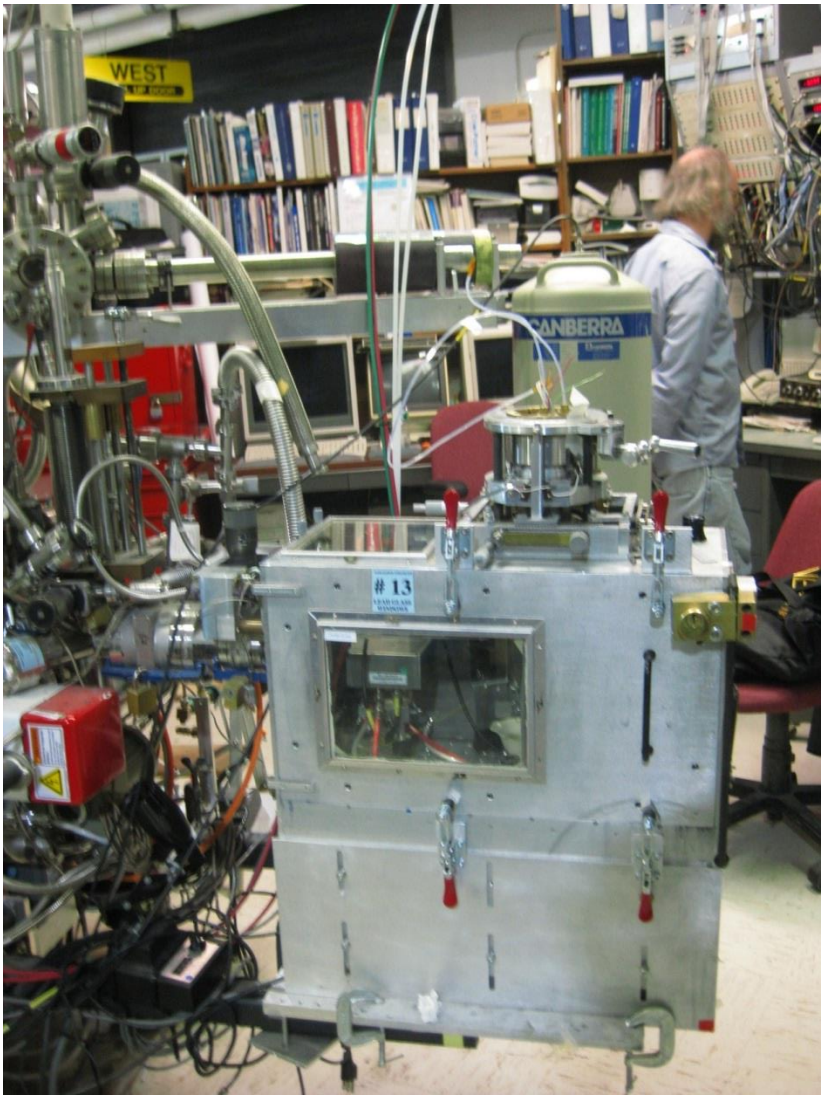

Fig. 15. Línea experimental X15B NSLS-1, Laboratorio Brookhaven.

PIXE: Particle Induced X-ray Emission spectroscopy

RBS: Rutherford Backscattering

Se utilizó la sonda externa de protones del acelerador 3MeV Pelletron (Fig. 16), Instituto de Física, UNAM (Ruvalcaba *et al.*, 2008). Para investigar las abundancias elementales de diferentes muestras de ámbar se utilizó simultáneamente PIXE (Particle Induced X-ray Emission) y RBS (Rutherford Backscattering), a una intensidad de 150 eV, y un tiempo de radiación de 5 minutos. Se usaron los programas AXIL y PIXEINT para el procesamiento, ajuste y análisis iterativo de los espectros de rayos-X resultantes (Fig.17). La cuantificación de las energías e intensidades relativas en los picos de los espectros fue usada para determinar la composición elemental de los ámbares (Riquelme *et al*., 2014).

Existen múltiples métodos para cuantificar la composición química en una muestra, pero PIXE tiene la ventaja de ser una técnica no destructiva, se aplica en muestras sin preparar, y tiene además una alta sensibilidad para detectar elementos traza mayores al Na (Z>11). PIXE analiza la superficie de un material orgánico o inorgánico y puede examinar un área determinada sin alterar su estructura o composición. Esto cobra importancia cuando se analiza ejemplares fósiles únicos.

PIXE es ampliamente usado en el análisis multielemental de materiales en contexto arqueológico (Ruvalcaba, 2008), pero su uso en material paleontológico es más reciente, por ejemplo, se ha utilizado para analizar hueso y tejidos blandos preservados (Goodwin *et al*., 2007; Riquelme *et al.*, 2009, 2013). Los principios teóricos y dispositivos experimentales de PIXE son ampliamente explicados e ilustrados en Johansson *et al*. (1995). No tenemos conocimiento, a la fecha, de trabajos publicados de PIXE en análisis de resinas vegetales fosilizadas. Sin embargo, un trabajo previo en muestras de resinas (incluyendo ámbar de Chiapas) colectadas en contexto arqueológico puede consultarse en Lowe y Ruvalcaba (2000). En la presente investigación, los datos obtenidos combinando PIXE/RBS fueron usados como marcadores químicos de las fuentes a partir de la composición relativa de los ámbares (Riquelme *et al*., 2014a).

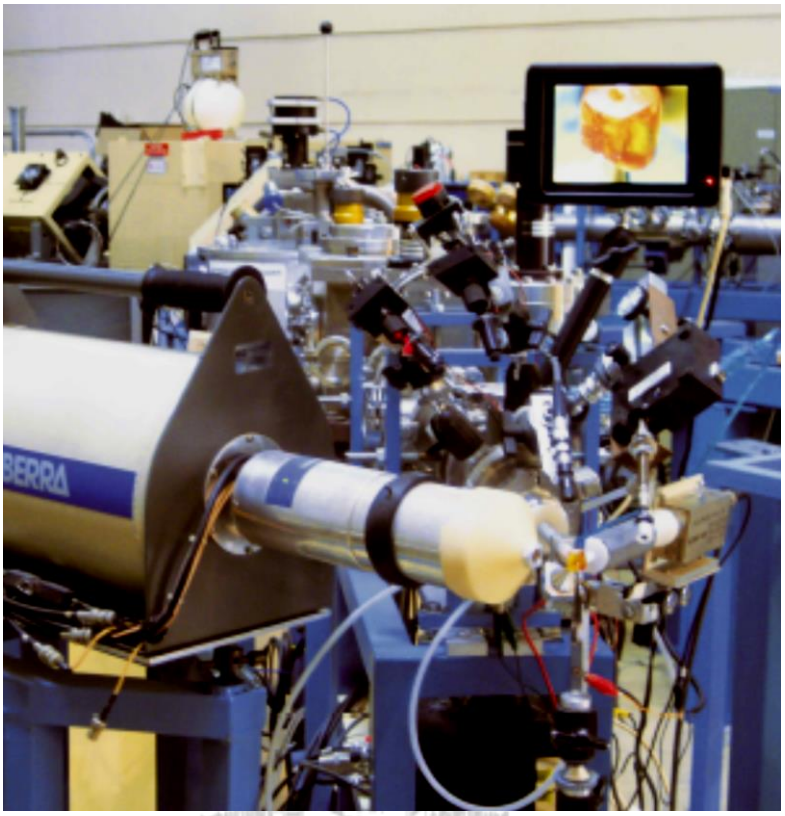

Fig. 16. Línea experimental externa del Acelerador Pelletron, Instituto de Física, UNAM.

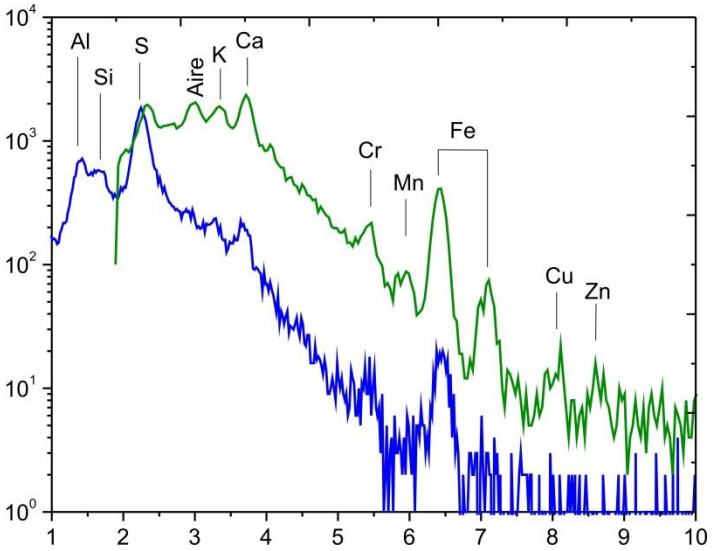

Fig. 17. Espectro PIXE característico del ámbar de Chiapas, Mioceno. Tomado de Riquelme *et al*., 2014a.

Microscopía de filtros infrarrojos y planos apocromáticos

Se utilizaron tres microscopios y cámaras digitales CCD con o sin filtros infrarrojos adaptados, y lámparas de tungsteno y luz blanca LED como fuentes convenientes de radiación infrarroja. Las muestras no requirieron de un tratamiento previo. El equipo consintió de un microscopio Leica Z16 APO-A, con un microsistema modular de 6.3X/1 y 16x/1, lentes apocromáticos y una cámara Leica CCD DFC90. Así como otro microscopio Carl Zeiss V16, con un microsistema modular de 16x/16, lentes apocromáticos y una cámara AxioCam CCD, perteneciente a la Unidad de Informática para la Biodiversidad (UNIBIO), Instituto de Biología, UNAM. Para el incremento de contraste se aplicó un alcance estándar de entre 115X a 920X, con luz blanca reflejada/transmitida. Para la sobreimposición de imágenes se usó un módulo multifocal con más de 32 planos por imagen y escaneo por área de >0.5 mm^2. Se usaron los programas Leica Application Suite®, ZEN SP2®, y Corel Photo-Paint® X6, para procesar y editar las imágenes. Adicionalmente, se usó un microscopio Edmond E- Zoom 6V con filtros infrarrojos y una cámara digital Axio Cam CCD, perteneciente al laboratorio Pelletron, Instituto de Física, UNAM. Para incrementar el contraste se aplicó un alcance entre 50X a 480X con luz blanca reflejada/transmitida, y Corel Photo-Paint® X6 para procesar las imágenes.

La microscopía estereoscópica de planos apocromáticos muestra el objeto de estudio con morfologías bien definidas, fidelidad de color, impresión espacial y detalles de estructuras diminutas (Fig. 6). Para generar una imagen con una mayor profundidad de campo y contraste de relieves, se tomaron primeramente imágenes múltiples sobre el eje-Z del campo focal, en un rango de entre 32 a 90 imágenes. Luego se aplicó una sobreimposición de éstas, generando así una imagen única con alta resolución (Riquelme *et al*., 2011).

Los filtros infrarrojos adaptados al microscopio son sensitivos a la longitud de onda del infrarrojo cercano, bloquean la luz visible, pero transmiten el infrarrojo en el rango de 750 a 1400 nm. La luz reflejada disminuye en este intervalo luminoso provocando que el ámbar se torne transparente. Esto permite visualizar las inclusiones orgánicas virtualmente a detalle (Fig. 18). Mayores detalles sobre los principios y aplicaciones de la fotografía de infrarrojo son presentados en otra parte (Miller, 1994; Maldague, 2001).

Fig. 18. Fotomicrografía de infrarrojo de la flor de *Hymenaea*, inclusión en ámbar de Chiapas, Mioceno.

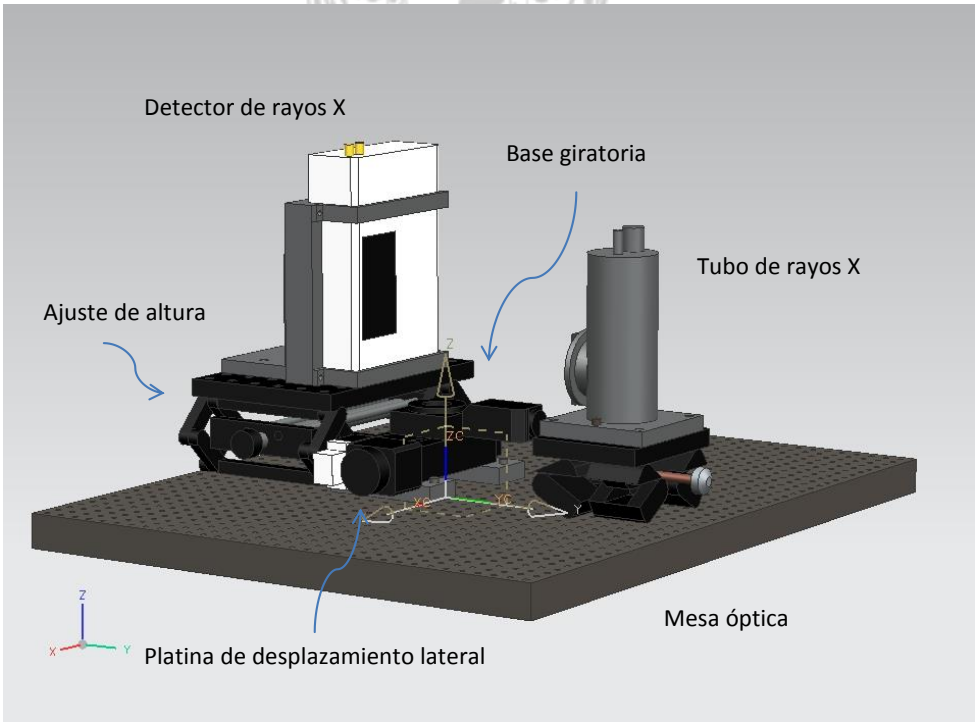

Fig. 19. Esquema del dispositivo experimental del Microtomógrafo de rayos-X (Martínez-Dávalos, 2012), Instituto de Física, UNAM. Imagen proporcionada por A. Martínez Dávalos (IF-UNAM).

Microtomografía computarizada de rayos-X

Se utilizó un microtomógrafo computarizado (micro-CT) construido en el Instituto de Física, UNAM (Fig. 19). Una descripción detallada del dispositivo experimental puede consultarse en (Martínez-Dávalos, 2010). El sistema micro-CT está basado en un tubo de rayos-X Oxford Instruments Apogee XTG5011, con ánodo de tungsteno, tamaño de punto focal de 35 μm, y acoplado a un panel detector aplanado Rad-icon Shad-o-Box 2048. Se aplicó una corrección a las imágenes para cancelar el ruido oscuro, inconformidades de campo plano, y decaimiento de pixeles. Para la reconstrucción tomográfica se aplicó el algoritmo Feldkamp-Davis-Kress (Feldkamp *et al.,* 1984), un filtro Hamming con 0.7 de frecuencia de corte, y un programa interno escrito en MATLAB. Para el post-procesamiento y edición final de las imágenes 3D se usaron los programas libres ImageJ (Rasband, 2012) y OsiriX (Rosset *et al*., 2004).

El uso de la microtomografía computarizada de rayos-X en inclusiones de ámbar usando una fuente de luz Sincrotrón se ha aplicado exitosamente en muestras de ámbar del Báltico (Tafforeau *et al*., 2006; Lak *et al*., 2008; Perreau y Tafforeau, 2011). Sin embargo, es una técnica costosa y no disponible en un ámbito general. El presente trabajo representa la primera demostración de las posibilidades de recuperar imágenes en 3D de los artrópodos fósiles atrapados en el ámbar de Chiapas (Fig. 20, Video S1), utilizando una tecnología hecha en el laboratorio por Martínez-Dávalos (2010), la cual es una alternativa a la utilización de una fuente de luz de sincrotrón.

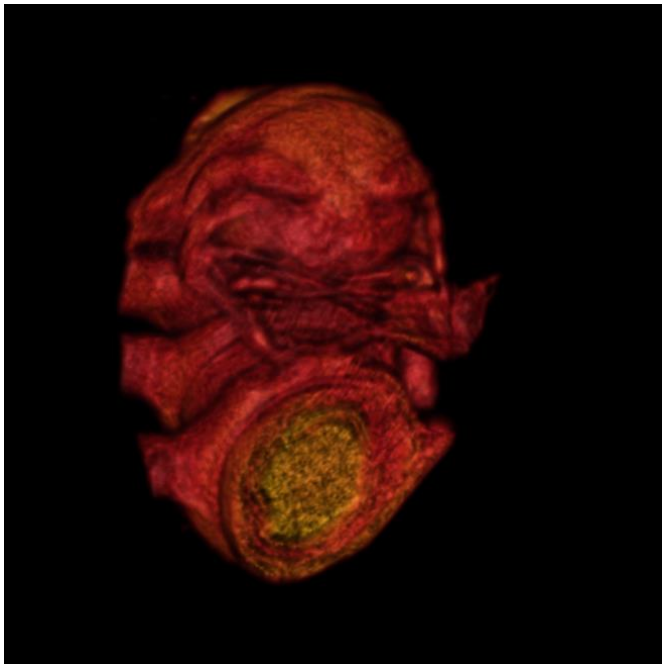

Fig. 20. Microtomografía de rayos-X de un milípedo (corte transversal), inclusión en ámbar de Chiapas, Mioceno. Imagen proporcionada por A. Martínez Dávalos (IF-UNAM).

CAPITULO 2 RESULTADOS

2.1 LISTA DE ARTICULOS PUBLICADOS

Sección A: Publicados**, c**on arbitraje, indizados Thomson Reuters (ISI).

1. Riquelme, F., Northrup, P., Ruvalcaba-Sil, J.L., Stojanoff, V., Siddons, D.P., and Alvarado-Ortega, J. 2014a. Insights into molecular chemistry of Chiapas amber using infrared-light microscopy, PIXE/RBS, and sulfur K-edge XANES spectroscopy. **Applied Physics A 116** (1): 97-109.

2. Riquelme, F., Ruvalcaba-Sil, J.L., Alvarado-Ortega, J., Estrada-Ruiz, E., Galicia-Chávez, M., Porras-Múzquiz, H., Stojanoff, V., Siddons, D.P., and Miller, L. 2014b. Amber from México: Coahuilite, Simojovelite and Bacalite. **MRS Proceedings 1618,** OPL Cambridge University Press, doi:10.1557/opl.2014.466.

3. **Riquelme**, F., Alvarado-Ortega, J., Ramos-Arias, M., Hernández, M., Le Dez, I., Lee-Whiting, T. A., and Ruvalcaba-Sil J.L., 2014. A fossil stemmiulid millipede (Diplopoda: Stemmiulida) from the Miocene amber of Simojovel, Chiapas, Mexico. **Historical Biology 26** (4): 415-427.

4. Riquelme, F., Hernández-Patricio, M., Martínez-Dávalos,A., Rodríguez-Villafuerte, M., Montejo-Cruz,M., Alvarado-Ortega, J., Ruvalcaba- Sil, J.L., and Zúñiga-Mijangos, L. 2014. Two flat-backed Polydesmidan millipedes from the Miocene Chiapas-Amber Lagerstätte, Mexico**. Plos One 9** (8): e105877. doi:10.1371/journal.pone.0105877

5. Riquelme, F., Piedra-Jiménez, D.F., Córdova-Tabares, V., and Luna-Castro, B. 2014. A new chernetid pseudoscorpion from the Miocene Chiapas-Amber Lagerstätte, Mexico. **Canadian Journal of Earth Sciences** 51: 902-908.

6. Riquelme, F., Montejo -Cruz, M., Luna-Castro, B., Zúñiga-Mijangos, L. 2015. Fossil jumping-bristletail from Chiapas Amber: Neomachilellus (Praeneomachilellus) ezetaelenensis sp. nov. (Microcoryphia: Meinertellidae). **Neues Jahrbuch für Geologie und Paläontologie 275** (1): 93-106.

Sección B: Sometidos, con arbitraje, indizados Thomson Reuters (ISI).

7. Riquelme, F., Villegas-Guzmán, G., González-Santillán, E., Córdova-Tabares, V., Piedra-Jiménez, D., Francke O., Estrada-Ruiz, E., Luna-Castro, B. 2014. New scorpion species from the Miocene Chiapas-Amber Lagerstätte. **Plos One.**

Sección C: Publicados, con arbitraje. Este artículo es externo al protocolo pero fue realizado como consecuencia directa del presente trabajo de investigación.

8. Riquelme, F., and Hill, D. E. 2013. Insights into amber salticids from the Neogene of Middle America, with the first report of Marpissinae (Araneae: Salticidae) from the Chiapas amber. **†Peckhamia 106.2**: 1-5.

2.2 ARTÍCULO 1: "Insights into molecular chemistry of Chiapas amber using infrared-light microscopy, PIXE/RBS, and sulfur K-edge XANES spectroscopy".

Síntesis: En este trabajo se combinaron las espectroscopías PIXE/RBS (Particle Induced X-ray Emission / Rutherford retrodispersión) y XANES (absorción de rayos X Estructura Cerca de punta) para identificar la cantidad de azufre orgánico en el ámbar de Chiapas. Inicialmente, las muestras de ámbar fueron examinadas usando microscopia con filtros infrarrojos. El ámbar es transparente a la luz infrarroja, las plantas y animales embebidos son fácilmente visibles, mostrando morfologías a detalle, como si se estuvieran sumergidas en una solución acuosa. Los datos de PIXE/RBS muestran que la proporción de azufre en ámbar es significativamente mayor que la encontrada en resinas recientemente formada, de acuerdo con los procesos biogeoquímicos que transforma la resina en ámbar en depósitos geológicos. Los espectros XANES confirman la abundancia de azufre y revela especies de azufre en estados de oxidación reducidos e intermedios. Casi no se encontró sulfato, mientras que las resinas recientes muestran típicamente fracciones de azufre oxidado. Esto indica que el azufre oxidado, más lábil, decae durante la fosilización y la maduración de la resina, la cual debe producirse en condiciones de deficiencia de oxígeno. Las implicaciones directas de la presencia de azufre en la preservación orgánica también se discute aquí. Los compuestos de azufre orgánico funcionan como un aditivo del polímero que promueve una intensa solidificación de la resina. Esto restringe la temprana degradación-oxidante de la biomateria embebida en el ámbar, y proporciona una mayor estabilidad frente a los cambios químicos que ocurren a través del tiempo geológico.

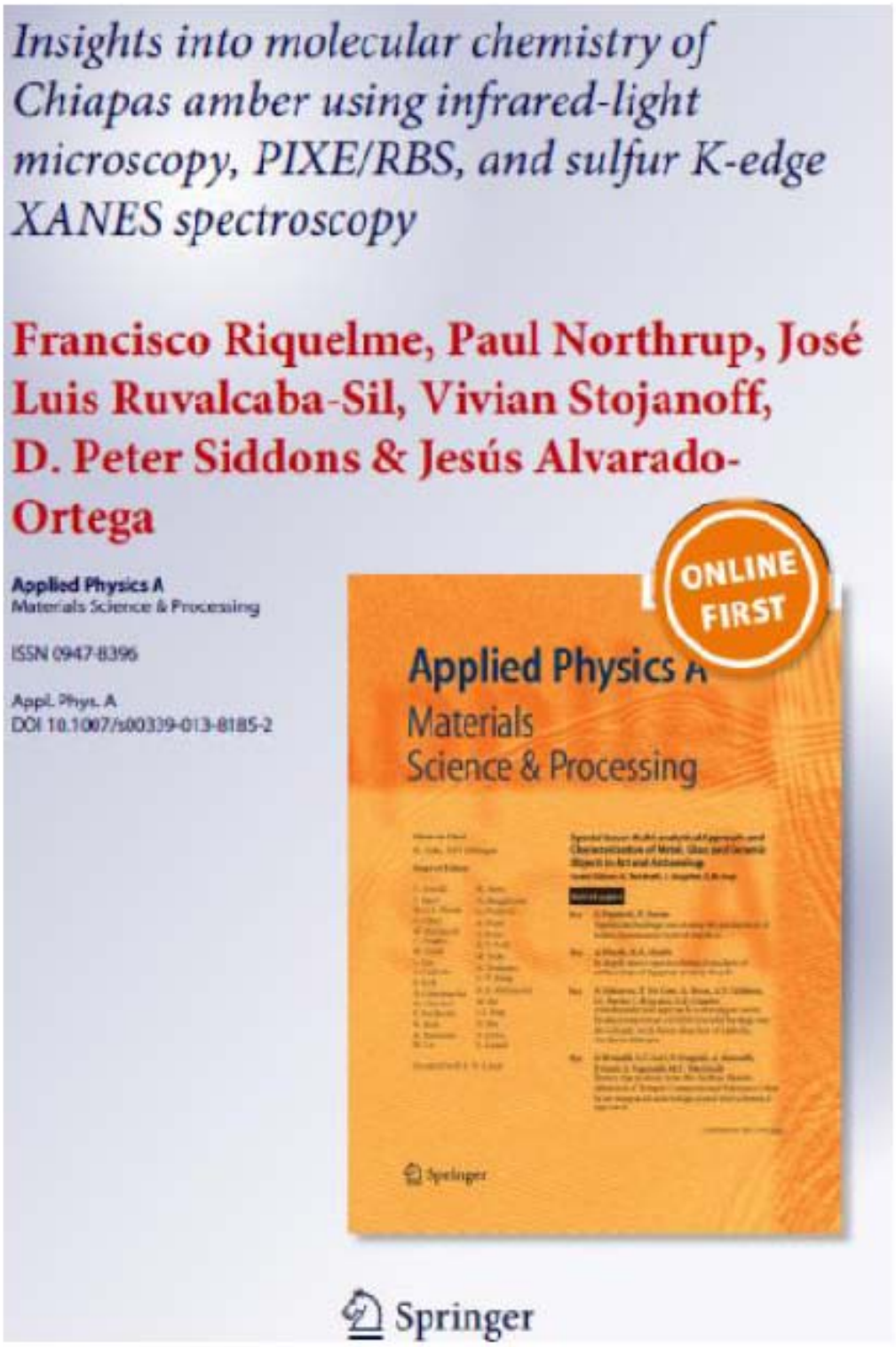

Fig. 21. Imagen general del artículo 1 publicado.

2.3 ARTÍCULO 2: “Amber from México: Coahuilite, Simojovelite and Bacalite”

Síntesis: En este trabajo se describen las tres variedades conocidas de ámbar en México, de acuerdo a la nomenclatura de minerales orgánicos. **Coahuilita** var. nov., de la Formación Olmos, Cretácico, en Coahuila; **Simojovelita** var. nov., de las Formaciones Balumtum y Mazantic, Mioceno Temprano-Medio, en Chiapas; y se propone una enmienda en la descripción de la **Bacalita**, Buddhue 1935, de la formación El Gallo, Cretácico, en Baja California. La caracterización de los ámbares está soportada por análisis de microespectroscopía FTIR usando una fuente de luz Sincrotrón.

MRS

CAMBRIDGE UNIVERSITY PRESS

Amber from México: ***Coahuilite, Simojovelite and Bacalite***

Francisco Riquelme[1,2], José Luis Ruvalcaba-Sil[2], Jesús Alvarado-Ortega[3], Emilio Estrada-Ruiz[4], Martin Galicia-Chávez[5], Hector Porras-Múzquiz[6], Vivian Stojanoff[7], D. Peter Siddons[7], Lisa Miller[7]

[1] Posgrado en Ciencias Biológicas, Universidad Nacional Autónoma de México, Cuidad Universitaria, C.P. 04510, D. F., Mexico.
[2] Instituto de Física, Universidad Nacional Autónoma de México. Apartado Postal 20-364, Mexico D.F. 01000, Mexico. e-mail: riquelme.fc@gmail.com
[3] Instituto de Geología, Universidad Nacional Autónoma de México, Ciudad Universitaria, Mexico D.F. 01000, Mexico.
[4] Escuela Nacional de Ciencias Biológicas, Instituto Politécnico Nacional, Mexico DF 11340, Mexico.
[5] Grupo MINOSA, Unidad Minerales Monclova, Coahuila 26350, Mexico.
[6] Museo de Múzquiz, Múzquiz Centro, Coahuila 26340, Mexico.
[7] Photon Science Directorate, Brookhaven National Laboratory, Upton, New York, USA.

ABSTRACT

Coahuilite, a new variety of amber is described from the Late Cretaceous Olmos Formation (ca. 73 Ma.), Coahuila, north of México. This amber is totally distinct chemically and stratigraphically from the Miocene Chiapas amber (ca. 23-13 Ma.), Southern México, which according to mineral nomenclature is currently known as *Simojovelite* var. nov. Additionally, an emended description of *Bacalite* is proposed, based on the physicochemical analysis and geological record of a fossil resin recently recovery from the Late Cretaceous El Gallo Formation (ca. 73 Ma.), Baja California, northwestern México. The results are supported by characterization of such ambers using synchrotron-based Infrared (FTIR) microspectroscopy.

Keywords: Amber, Coahuilite, Simojovelite and Bacalite, micro-FTIR

Fig. 22. Imagen general del artículo 2 publicado.

2.4 ARTÍCULO 3: "A fossil stemmiulid millipede (Diplopoda: Stemmiulida) from the Miocene amber of Simojovel, Chiapas, Mexico".

Síntesis: En este trabajo se describe un nuevo género y especie de milpiés del orden Stemmiulida (Diplopoda), basados en un ejemplar hembra adulta atrapado en el ámbar del Mioceno de Simojovel, en Chiapas, México. Este ejemplar se distingue de sus congéneres actuales por una combinación de caracteres diagnósticos y es la primera especie de milípedo descrita en el ámbar de Chiapas. La nueva especie es ahora conocida como *Parastemmiulus elektron*.

Historical Biology, 2013
http://dx.doi.org/10.1080/08912963.2013.778843

Taylor & Francis

A fossil stemmiulid millipede (Diplopoda: Stemmiulida) from the Miocene amber of Simojovel, Chiapas, México

Francisco Riquelme[a]*, Jesús Alvarado-Ortega[b], Mario Ramos-Arias[b], Miguel Hernández[c], Isabelle Le Dez[d], Thomas A. Lee Whiting[d] and José Luis Ruvalcaba Sil[e]

[a]Posgrado en Ciencias Biológicas, Instituto de Física, Universidad Nacional Autónoma de México, AP 20-364, D.F., México; [b]Instituto de Geología, Universidad Nacional Autónoma de México, Circuito de la Investigación S/N, Ciudad Universitaria, 04510, D.F., México; [c]Posgrado en Ciencias Biológicas, Facultad de Ciencias, Universidad Nacional Autónoma de México, Circuito Interior S/N, Ciudad Universitaria, 04510, D.F., México; [d]Escuela de Arqueología, Centro Superior de Investigaciones México y Centroamérica, Universidad de Ciencias y Artes de Chiapas, Chiapas, México; [e]Instituto de Física, Universidad Nacional Autónoma de México, AP 20-364, D.F., México

(Received 11 December 2012; final version received 19 February 2013)

A fossil millipede representative of the order Stemmiulida is described on the basis of a well-preserved adult female trapped in amber from the Miocene of Simojovel, Chiapas, south-eastern México. The fossil specimen is named as *Parastemmiulus elektron*, a new genus and species. As observed in extant stemmiulids, this fossil shows a reduced number of ocelli, the distal larger than the proximal, as well as a total of 46 trunk segments including 2 apodous segments in front of the telson. The head of this ancient stemmiulid has three ocelli and a Tömösvary organ, characteristics not reported before in Stemmiulida, requiring the diagnosis of the order to be emended.

http://zoobank.org/urn:lsid:zoobank.org:pub:361400A8-37D4-421F-B4FD-A0AD62BE538C

Keywords: Chiapas amber; Miocene; Stemmiulida; *Parastemmiulus*

Introduction

Millipedes (Diplopoda) are one of the earliest known air-breathing terrestrial animal groups. The modern forms of diplopods had differentiated by the Late Silurian (Almond 1985; Shear 1998; Shear et al. 2000; Shear and Edgecombe 2010). Although trackways from the Borrowdale Volcanic Group (Ordovician) have been attributed to millipedes (Johnson et al. 1994; Wilson 2006), the oldest unequivocal records of millipedes are the fossil specimens of *Albadesmus almondi*, *Pneumodesmus newmani* and *Cowiedesmus eroticopodus* from the mid-Silurian Cowie Formation in Scotland (Wilson and Anderson 2004). The fossil record of Diplopoda in México is extremely scarce, consisting only of *Xylobius mexicanus* Müllerried, 1942 from the Late Jurassic/Mid Cretaceous, of which the taxonomic identity is still uncertain (Shear et al. 2009).

Millipedes are widely distributed in all subarctic environments including tropical and temperate forest, short tree savannas, grasslands, coastal plains and deserts (Shelley 2007; Shelley and Golovatch 2011). Millipedes live in leaf litter, soil, beneath stones, bark, wood and caves. Millipedes have played an exceptional ecological role in terrestrial ecosystems from both temperate and tropical environments around the globe, as they are efficient biological agents of nutrient fluxes through soil detritus fragmentation (Crawford 1992).

Currently, millipedes comprise about 10,000 described species, representing 16 orders and 145 families and an estimated recent global fauna of more than 80,000 species (Shelley 2003, 2007). This makes them the third most diverse class of terrestrial arthropods after Insecta and Arachnida (Brewer et al. 2012). The Neotropical distribution of millipedes in México, Caribbean islands and Central and South America comprises between 1200 and 1800 species. Accordingly, there is an estimated about 498 species in 14 orders, 39 families and 117 genera distributed in México (Bueno-Villegas et al. 2004).

Most fossil millipedes preserved in amber are known from Baltic deposits dated as Eocene, including representatives of the orders Glomerida, Polydesmida, Chordeumatida, Julida, Polyzoniida and Polyxenida (Keilbach 1982). The Miocene Dominican amber includes numerous millipedes such as representatives of Glomeridesmida, Polyzoniida, Polydesmida, Spirostreptida, Siphonophorida and Stemmiulida (Shear 1981, 1987, 1998; Santiago-Blay and Poinar 1992; Pérez-Asso and Pérez-Gelabert 2001). Unfortunately, the single specimen interpreted as a stemmiulid by Santiago-Blay and Poinar (1992) is very

*Corresponding author. Email: riquelme.fc@gmail.com

This article was originally published with errors. This version has been amended. Please see Corrigendum (DOI: http://dx.doi.org/10.1080/08912963.2013.824264)

Fig. 23. Imagen general del artículo 3 publicado.

2. 5 ARTÍCULO 4: "Two flat-backed Polydesmidan millipedes from the Miocene Chiapas-Amber Lagerstätte, México".

Síntesis: En este trabajo se describen dos nuevos géneros y especies de milpiés del orden Polydesmida (Diplopoda), basados en dos ejemplares fósiles atrapados en ámbar del Mioceno de Chiapas, México. Los datos morfológicos fueron colectados usando microscopia de filtros infrarrojos y microtomografía computarizada de rayos-X en 3D. Estos fósiles representan las primeras especies de polidésmidos descritas para el ámbar de Chiapas.

OPEN ACCESS Freely available online

PLOS | ONE

Two Flat-Backed Polydesmidan Millipedes from the Miocene Chiapas-Amber Lagerstätte, Mexico

Francisco Riquelme[1,2]*, Miguel Hernández-Patricio[3], Arnulfo Martínez-Dávalos[2], Mercedes Rodríguez-Villafuerte[2], Maira Montejo-Cruz[4], Jesús Alvarado-Ortega[5], José L. Ruvalcaba-Sil[5], Luis Zúñiga-Mijangos[6]

1 Posgrado en Ciencias Biológicas, Universidad Nacional Autónoma de México, Ciudad Universitaria, D.F., México, 2 Instituto de Física, Universidad Nacional Autónoma de México, Ciudad Universitaria, D.F., México, 3 Subcoordinación de Información Biótica, Comisión Nacional para el Conocimiento y Uso de la Biodiversidad, Tlalpan, D.F., México, 4 Facultad de Ciencias, Universidad Nacional Autónoma de México, Ciudad Universitaria, D.F., México, 5 Instituto de Geología, Universidad Nacional Autónoma de México, Ciudad Universitaria, D.F., México, 6 Museo del Ámbar Luis Mijangos, San Cristóbal de las Casas, Chiapas, México

Abstract

Two species of fossil polydesmidan millipedes (Diplopoda, Polydesmida) embedded in amber are described from Miocene strata near Simojovel, in the Chiapas Highlands, Mexico. *Mastidesmus pacchtun* gen. et sp. nov., placed into Chelodesmidae Cook, 1895, and *Antarrhoeus adamantis* gen. et sp. nov., assigned in the family Platyrhacidae Pocock, 1895. Morphological data from fossil specimens have been recovered using 3D X-ray micro-computed tomography and regular to infrared-reflected microscopy. Both fossil species are recognizable as new primarily but not exclusively, by collum margin modification and remarkable paranotal and metatergite dorsal sculpture.

Citation: Riquelme F, Hernández-Patricio M, Martínez-Dávalos A, Rodríguez-Villafuerte M, Montejo-Cruz M, et al. (2014) Two Flat-Backed Polydesmidan Millipedes from the Miocene Chiapas Amber Lagerstätte, Mexico. PLoS ONE 9(8): e105877. doi:10.1371/journal.pone.0105877

Editor: Andrew Hajos, Sars International Centre for Marine Molecular Biology, Norway

Received May 16, 2014; **Accepted** July 30, 2014; **Published** August 29, 2014

Data Availability: The authors confirm that all data underlying the findings are fully available without restriction. All relevant data are within the paper and its Supporting Information files.

Funding: Research has been partially founded by the following granting-projects: PAPIIT-UNAM IB100913-2, IB400313 and CONACYT 131644. The funders had no role in study design, data collection and analysis, decision to publish, or preparation of the manuscript.

Competing Interests: The authors have declared that no competing interests exist.

* Email: riquelme.fo@gmail.com

Introduction

The ecology, life history, physiology, morphology and phylogeny of millipedes (class Diplopoda) have been comprehensively reviewed in a few classical texts [1–3]. Millipedes have successfully adapted to soil and litter habitats in all subarctic climates. They contribute hugely into soil cycles from both temperate and tropical forest. The fossil preservation of millipedes is very unusual mostly because they have terrestrial habits and non-recalcitrant tissues and cuticles. The oldest fossil record of millipedes is from the Mid-Silurian rocks in Scotland [4]. The geological record of Diplopoda is summarized elsewhere [1–3]. Accordingly, there is a large gap in the Mesozoic fossil record with the exception of the spirobolid millipedes from the Late Cretaceous of Mongolia and the presumably millipede *?Xyulias stevensons* Millennich, 1912 from the Late Jurassic/Mid-Cretaceous of Central Mexico [5,6]. However, most members of the extinct taxa are notably found as Fossil Lagerstätten, as seen in the Late Carboniferous inclusions nodules from Britain and Cretaceous amber from Europe and Middle America [7–11].

The wedge-packing type millipedes are generally represented by the order Polydesmida, whose fossil record dates back to the Paleocene of Europe in Baltic amber [3,9]. Several polydesmidan millipedes from the younger deposits at the Neogene Middle America have also been recorded in Dominican Republic amber [10]. Millipedes from Miocene aged Chiapas amber (ca. 23–15 Ma.), Mexico, which has similar geological ages, sedimentary environments and paleobotanical affinities with Dominican ambers, are only known for a recently described siemuliidal species [11]. In this study, two fossil polydesmidan millipedes from the Chiapas amber are named and illustrated.

The fossil material studied has been mine recovered from two private collections with geographic references. As a result of field geology and chronological provenance analysis, we track the source of millipede-embedded amber to the mine of the Guadalupe Victoria site, near Simojovel in Chiapas, México (Fig. 1). Morphological data was collected by micro-imaging of fossil specimens using a non-destructive 3D X-ray micro-computed tomography (CT) and high-resolution microscopy with regular light to infrared-pass lens. The X-ray micro-CT scanning of a millipede specimen, as presented here, is also the first demonstration about the possibilities to recovery 3D images of fossil arthropods embedded in Chiapas amber using a laboratory-made technology, as alternative to the use of a synchrotron light source.

Two new, extinct genera *Mastidesmus* and *Antarrhoeus* and two new species are described herein. The fossil genus *Antarrhoeus* has been assigned to the family Platyrhacidae Pocock, 1895 and *Mastidesmus* to Chelodesmidae Cook, 1896. Currently both fossil species *Mastidesmus pacchtun* **gen. et sp. nov.** and *Antarrhoeus adamantis* **gen. et sp. nov.** have been defined by available somatic characters (Fig. 2, 3, 4, 5). *A. adamantis* shows an exposed gonopods in dim on ring 7; however, it represents a stadium 7 male with relatively immature gonopods, from which the gonopodal characters cannot be unambiguously assessed. To our

Fig. 24. Imagen general del artículo 4 publicado.

2.6 ARTÍCULO 5: "A new chernetid pseudoscorpion from the Miocene Chiapas-Amber Lagerstätte, Mexico"

Síntesis: *Mayachernes maatiatus*, un nuevo género y especie de pseudoescorpión de la familia Chernetidae (Arachnida: Pseudoscorpiones), es descrito en el ámbar de Chiapas, México. Esta nueva especie fósil está representada por un ejemplar adulto macho con tejidos blandos/duros conservados con gran detalle. Los datos anatómicos fueron recolectados mediante microscopía de alta resolución usando luz regular y filtros infrarrojos. *M. maatiatus* es la primera especie fósil de pseudoescorpión descrita en el ámbar de Chiapas.

NRC Research Press

RAPID COMMUNICATION

A new chernetid pseudoscorpion from the Miocene Chiapas – Amber Lagerstätte, Mexico

Francisco Riquelme, Dulce F. Piedra-Jiménez, Víctor Córdova-Tabares, and Bibiano Luna-Castro

Abstract: *Mayachernes manitalus*, a new genus and species of pseudoscorpions of the family Chernetidae (Arachnida: Pseudoscorpionida), is described from the Miocene Chiapas – Amber Lagerstätte, south of Mexico. This new fossil species represents an adult male specimen with hard-soft tissues preserved in great detail. It differs from all other living chernetids by a combination of diagnostic characters. Anatomical data were collected using high-resolution microscopy with regular to infrared-reflected light. *Mayachernes manitalus* is the first newly described fossil species of pseudoscorpion from the Chiapas amber. This taxon also adds to knowledge of the Chernetidae diversity in the southernmost part of North America at the Neogene.

Résumé : **Mayachernes manitalus**, un nouveau genre et espèce de pseudoscorpion de la famille Chernetidae (Arachnida: Pseudoscorpionida) est décrit provenant du Miocène Chiapas – Amber Lagerstätte, au sud du Mexique. Cette nouvelle espèce de fossil représente un spécimen adulte de sexe masculin avec des tissus durs et mous étonnamment préservés en détail. Ses caractères morphologiques le différent de tous les autres chernetides vivants. Les données anatomiques ont été recueillies à l'aide d'un microscope utilisant les lumière visible et passe infrarouge lointain. Cette découverte donne lieu à la première description, dans l'ambre du Chiapas, d'une espèce fossile de pseudoscorpion. Aussi ce taxon ajoute à la connaissance de la diversité de Chernetidae dans la partie la plus méridionale de l'Amérique du Nord au Néogène.

Introduction

Biology and life histories of pseudoscorpions (Arachnida: Pseudoscorpionida) have been widely investigated in several living species (Weygoldt 1969). Adaptive radiation of pseudoscorpions includes all subarctic environments. They occur in soil, litter, tree bark, grass, caves, fractured rocks, swamps muds, and seashore sands. Cladistics and molecular phylogeny have been examined elsewhere (Harvey 1992; Murienne et al. 2008). However, fossil preservation of pseudoscorpions is extremely rare. Fossil forms are poorly known except in amber. Their small, labile, chitinized cuticles are easily destroyed by deep burial and lithification. The oldest pseudoscorpion forms in the geological record date back to the Mid-Devonian argillaceous strata near Gilboa, New York, USA (Shear et al. 1989; Schawaller et al. 1991; Dunlop 1996). The only known Mesozoic occurrence of chernetid is a specimen embedded in amber from Cretaceous coal in Grassy Lake, Alberta, Canada (Schawaller 1994). In contrast, the majority of described fossil species are found in Cenozoic deposits from the Paleogene Baltic and Neogene Dominican Republic amber and younger copal sites from Madagascar and Colombia (i.e., Schawaller 1980; Judson 2000, 2010; Hendericks et al. 2012).

Little is known about fossil pseudoscorpions in the Chiapas amber, Mexico, which is botanically and geologically contemporary to the Dominican Republic amber (Langenheim 2003). A chernetid morphotype with uncertain taxonomic identity is the only fossil previously documented (Schawaller 1983). In the present work, the first fossil species of pseudoscorpion in the Chiapas amber is described and illustrated based on an adult male specimen. This fossil pseudoscorpion is diagnosed herein as *Mayachernes manitalus* gen. et sp. nov. (family Chernetidae Menge, 1855). The fossil body is intact and shows true color morphology. Also cuticle and other tissues are gracefully preserved at detail. The morphology of *M. manitalus* seems notably similar to some living species of Institernes clade. However, it separates from its extant congeners by a combination of diagnostic characters, such as the granulated sculpture and furrows on carapace, the trichobothria pattern on pedipalp, tarsus with basal tactile seta, tibia IV with two setae, and genitalia shape, among others.

According to Harvey (2003), the order Pseudoscorpionida globally comprises 26 extant families with 454 genera and 3600 species, whose record is constantly growing worldwide. Fossil pseudoscorpions have been placed in one family with 11 genera and 41 species (Harvey 2003). Diversity in Mexico is considerably high, currently represented by 38 extant families, with 64 genera and 167 species (nearly 4.7% of the global species richness) (Cihaltic 2004; Córdova-Tabares and Villegas-Guzmán 2013; Villegas-Guzmán 2013; Francke 2014). As mentioned earlier in the text, there is one fossil pseudoscorpion known in Mexico (Schawaller 1983). The new species *M. manitalus* placed into Chernetidae is restricted to Neogene amber of the Middle America, which includes Chiapas and the Antilles Islands amber (particularly the Dominican Republic).

Depositional environment and fossilization

Amber embedded pseudoscorpion studied here comes from an amber site known as La Pimienta near Simojovel, Chiapas, which belongs to a fossil Lagerstätte with early–middle Miocene age

Received 15 May 2014. Accepted 7 August 2014.

Paper handled by Associate Editor Jiasu Jin.

F. Riquelme. Posgrado en Ciencias Biológicas, Universidad Nacional Autónoma de México, Ciudad Universitaria, C.P. 04360, D.F., México.
D.F. Piedra-Jiménez. Laboratorio de Aracnología, Facultad de Ciencias, Universidad Nacional Autónoma de México, Ciudad Universitaria, Coyoacán, C.P. 04360, D.F., México.
V. Córdova Tabares. Laboratorio de Acarología, Escuela Nacional de Ciencias Biológicas, Instituto Politécnico Nacional, Casco de Santo Tomás, C.P. 11340, D.F., México.
B. Luna Castro. Museo del Ámbar de Chiapas, Barrio de Mazariegos S/N, La Merced, C.P. 29224, San Cristóbal de las Casas, Chiapas, México.
Corresponding author: Francisco Riquelme (e-mail: riquelme.f@gmail.com).

Can. J. Earth Sci. 52: 963–968 (2014) dx.doi.org/10.1139/cjes-2014-0137 Published at www.nrcresearchpress.com/cjes on 22 September 2014.

Fig. 25. Imagen general del artículo 5 publicado.

2.7 ARTÍCULO 6: "Fossil jumping-bristletail from Chiapas Amber: *Neomachilellus (Praeneomachilellus) ezetaelenensis* sp. nov. (Microcoryphia: Meinertellidae)".

Síntesis: En este trabajo se describe una nueva especie de microcoryfio, *Neomachilellus (Praeneomachilellus) ezetaelenensis* sp. nov., a partir de ejemplares (macho + hembras) bien preservados colectados en los depósitos de ámbar cerca de Simojovel, Totolapa y Estrella de Belén en Chiapas, México. El subgénero Praeneomachilellus Sturm y Poinar, 1997 en el género Neomachilellus Wygodzinsky, 1953 comprende una especie fósil descrita en el ámbar Mioceno de la República Dominicana y una especie actual de Puerto Rico. De esta manera, *N. (Praeneomachilellus) ezetaelenensis* es la primera especie que se describe en el ámbar de Chiapas. Este taxón añade conocimientos sobre la biodiversidad del orden Microcoryphia en la parte más meridional de América del Norte en el Mioceno.

N. Jb. Geol. Paläont. Abh.
Stuttgart, January 2015

Article

Fossil jumping-bristletail from the Chiapas amber: *Neomachilellus (Praeneomachilellus) ezetaelenensis* sp. nov. (Microcoryphia: Meinertellidae)

Francisco Riquelme, Maira Montejo-Cruz, Bibiano Luna-Castro, and Luis Zuñiga-Mijangos

With 8 figures

Abstract: A new species of jumping-bristletail, *Neomachilellus (Praeneomachilellus) ezetaelenensis* sp. nov. (Microcoryphia: Meinertellidae), is described from the Miocene amber collected in the Mountains of Chiapas, southwestern Mexico. This study is based on amber microcoryphian insect newly recovered from rocks near the towns of Simojovel, Totolapa and Estrella de Belén. These amber sites are part of a Conservation Lagerstätte with remarkable preserved paleobiota. On the basis on male and female specimens, *N. (Praeneomachilellus) ezetaelenensis* sp. nov., is illustrated and diagnosed herein by a combination of diagnostic characters. Morphological data were collected using high-resolution microscopy with regular to adapted infrared-pass lens. The subgenus *Praeneomachilellus* Sturm & Poinar, 1997 into the genus *Neomachilellus* Wygodzinsky, 1953 comprises one described fossil species from the Miocene Dominican Republic amber and one extant species from Puerto Rico. Thus, *N. (Praeneomachilellus) ezetaelenensis* is the first species of this group to be described in the Chiapas amber that adds insights into Microcoryphia biodiversity at the southernmost part of North America.

Key words: Miocene, Chiapas amber, Microcoryphia, Meinertellidae, *Neomachilellus*, Jumping bristletail.

1. Introduction

Microcoryphians (= Archaeognatha) commonly called Jumping-bristletails are one of the earliest insect lineages. They are small, primitive, ectognathous wingless insects that currently live in temperate and tropical environments (Sturm & Machida 2001). Microcoryphians occur in soil, leaf litter, tree bark, fractured stones, nearby water pounds, and rocky nearshores. Systematics of Microcoryphia Verhoeff, 1904 has been reviewed and discussed elsewhere (Sturm & Bach de Roca 1993; Mendes 2002). The order Microcoryphia comprises the families Meinertellidae, Machilidae, and some *incertae sedis* genera with extant and few fossil representatives distributed at both Hemispheres (Sturm & Machida 2001).

In spite of very poor fossil record of Microcoryphia, modern forms are found as fossils in amber at different deposits and geological ages. A few fossils have been recorded in amber from Lebanon, Myanmar, Spain, New Jersey, Baltic, Dominican Republic, Mexico (Chiapas), and Venezuela copal (Mendes & Wunderlich 2013; Getty et al. 2013).

Basal archaeognatha like forms associated with Microcoryphia and its sister group Zygentoma (=Thysanura) are recorded as fragmentary fossils in Early to Middle Devonian shale from Quebec, Canada and New York, US, respectively (Shear et al. 1984, La-

DOI: 10.1127/njgpa/2015/04a3

0 0// //49/2015/04a3 80.0

Fig. 26. Imagen general del artículo 6 publicado.

2.8 ARTÍCULO 7: "New scorpion from the Miocene Chiapas-Amber Lagerstätte".

Síntesis: En este trabajo se describe una nueva especie de escorpión basado en un ejemplar macho adulto excepcionalmente preservado en el ámbar de Chiapas, Mioceno Temprano, México. La diagnosis de la nueva especie corresponde con el género *Tityus* Koch, 1836, familia Buthidae. Por lo tanto, se le conoce ahora como *Tityus apozonalli* sp. nov. Igualmente, se discute su posición filogenética dentro de los taxones fósiles de la superfamilia Buthoidea y sus relaciones filogenéticas con los actuales clados de *Tityus* que viven en el Neotrópico de América. Este nuevo taxón se suma al conocimiento de los escorpiones del Nuevo Mundo que rara vez se encuentran en el ámbar del Neógeno de la América Media.

PLOS ONE

New fossil scorpion from the Chiapas Amber Lagerstätte

–Manuscript Draft–

Manuscript Number:	PONE-D-14-51462
Article Type:	Research Article
Full Title:	New fossil scorpion from the Chiapas Amber Lagerstätte
Short Title:	New fossil scorpion from the Chiapas Amber Lagerstätte
Corresponding Author:	Francisco Riquelme Universidad Nacional Autonoma de México Mexico City, MEXICO
Keywords:	Chiapas amber, Miocene, Scorpiones, Buthidae, Tityus.
Abstract:	A new species of scorpion is described based on entire adult male rarely preserved in a cloudy amber from Miocene rocks in the Chiapas Highlands, Mexico. The amber-bearing beds in Chiapas constitute a Conservation Lagerstätte with outstanding organic preservation inside plant resin. The new species is diagnosed by having putative characters that correspond largely with the genus Tityus Koch, 1836 (Scorpiones, Buthidae). Accordingly, it is now referred to as Tityus apozonalli sp. nov. Its phylogenetic position among fossil taxa of the family Buthidae from both Dominican and Mexican amber is testing herein. Close relationships with the extant Tityus-like clades that live now in the Neotropics are also discussed. This new taxon adds to knowledge of the New World scorpions rarely found in amber from the Neogene of Middle America.
Order of Authors:	Francisco Riquelme
	Gabriel Villegas-Guzmán
	Edmundo González-Santillán
	Víctor Córdova-Tabares
	Oscar F. Francke
	Dulce Piedra-Jiménez
	Emilio Estrada-Ruiz
	Bibiano Luna-Castro

Fig. 27. Imagen general del artículo 7 sometido.

2.9 ARTÍCULO 8: "Insights into amber salticids from the Neogene of Middle America, with the first report of Marpissinae (Araneae: Salticidae) from the Chiapas amber".

*Síntesis***:** Este trabajo presenta el primer registro de arañas del genero Marpissinae (Araneae: Salticidae) en el ámbar de Simojovel, Chiapas. A la fecha, no se conocía este grupo en el ámbar de Chiapas o de la República Dominicana. Adicionalmente, se comenta y discute sobre la extinción y dispersión de la paleobiota del ámbar de Chiapas que, como se expresa aquí, pudo ocurrir por alopatría, inducida por cambios geológicos.

PECKHAMIA 106.2. 29 August 2013, 1–3
urnlsid.zoobank.org:pub:3D939741-F2A4-4FDC-A565-300877412C03 (registered 27 AUG 2013)
ISSN 2161–8526 (print)
ISSN 1944–8120 (online)

Insights into amber salticids from the Neogene of Middle America, with the first report of Marpissinae (Araneae: Salticidae) from the Chiapas amber

Francisco Riquelme[1] and David E. Hill[2]

[1] Instituto de Física, Universidad Nacional Autónoma de México, AP 20-364, D.F. Mexico. *email corresponding author:* riquelme.fe@gmail.com
[2] 213 Wild Horse Creek Drive, Simpsonville, South Carolina 29680-6519, USA

Abstract. The genera and species of fossil salticids from the European Baltic amber (Paleogene) are more diverse than salticids from the geologically younger Neogene deposits of Dominican and Chiapas amber. However, the latter are more diverse than Baltic amber at the subfamily level and also include close relatives of modern species. This diversity may reflect the presence of ancestor taxa for extant North American groups. The relatively modern forms of the Neogene suggest a broader divergence since the Miocene within the tropics. Here we add the discovery of a fossil salticid that appears to be a marpissine (cf. *Mauvia* C. L. Koch, 1846) from the Miocene Chiapas amber (southern México). The tectonic and sedimentary evolution of South Mexico, Central America and the Antilles from the Paleogene to Neogene that caused short-term cyclical changes in climate may have also driven the early dispersal and introduction of marpissines from Middle America into southern North America.

Key words: Chiapas amber, Miocene, Middle America, Salticidae, Marpissinae

Resumen. Los géneros y las especies de salticidos fósiles del ámbar Báltico en Europa (Paleógeno) son más diversos que los salticidos de los más recientes depósitos de ámbar del Neógeno de República Dominicana y Chiapas. Sin embargo, estos últimos son más diversos que los del ámbar del Báltico a nivel de subfamilias y también muestran parentescos cercanos con especies modernas. Las formas relativamente modernas del Neógeno sugieren una más amplia divergencia desde el Mioceno en los trópicos. Se incluye aquí el descubrimiento de un salticido fósil, seguramente marpisino (cf. *Mauvia* C. L. Koch, 1846) en el ámbar de Chiapas (Mioceno) sur de México. La evolución tectónica y sedimentaria del Sur de México, Central América y las Antillas durante el Paleógeno al Neógeno que causó cambios cíclicos de periodos cortos en el clima también puede haber conducido a una temprana dispersión e introducción de marpisinos desde la América Media hacia el sur de Norte América.

Palabras claves: Ámbar de Chiapas, Mioceno, América Media, Salticidae, Marpissinae

Introduction

Fossil spiders, including amber salticids have been fully cataloged based on criteria used for living spiders (Dunlop, Penney and Jekel, 2013). Several monographs of amber and copal spiders from the Cretaceous to Tertiary of Europe, Africa, Asia and America have also been published separately by Wunderlich (2004a, 2008, 2011, and 2012), reflecting his use of different criteria. Fossil representatives of the Salticidae occur in the amber deposits of the Paleogene and Neogene of Europe and the Americas (Wunderlich, 2004a; Penney and Selden, 2011; Dunlop, Penney and Jekel, 2013). This includes the Paleogene amber deposits from Bitterfeld, Baltic, Rovno and younger (Neogene) strata from the Dominican Republic. These recent reviews do not include the salticid records from the Neogene Chiapas amber (Southern México) that were previously published by Petrunkevitch (1971) and García-Villafuerte and Penney (2003). Both reports of Chiapas salticids were associated with the Simojovel quarries that belong to the Lower Miocene Balumtum and Mazantic Shale strata. Petrunkevitch (1971) described a representative of Salticidae *Incertae sedis* since this specimen was too poorly preserved to identify further, while García-Villafuerte and Penney (2003) described a representative of the genus *Lyssomanes*. Additionally, a putative new member of the subfamily Marpissinae (Araneae: Salticidae) from the Chiapas amber is reported here for the first time. Although limited, this fossil record increases our knowledge of

Fig. 28. Imagen general del artículo 8 publicado.

Insights into molecular chemistry of Chiapas amber using infrared-light microscopy, PIXE/RBS, and sulfur K-edge XANES spectroscopy

Francisco Riquelme, Paul Northrup, José Luis Ruvalcaba-Sil, Vivian Stojanoff, D. Peter Siddons & Jesús Alvarado-Ortega

Applied Physics A
Materials Science & Processing

ISSN 0947-8396

Appl. Phys. A
DOI 10.1007/s00339-013-8185-2

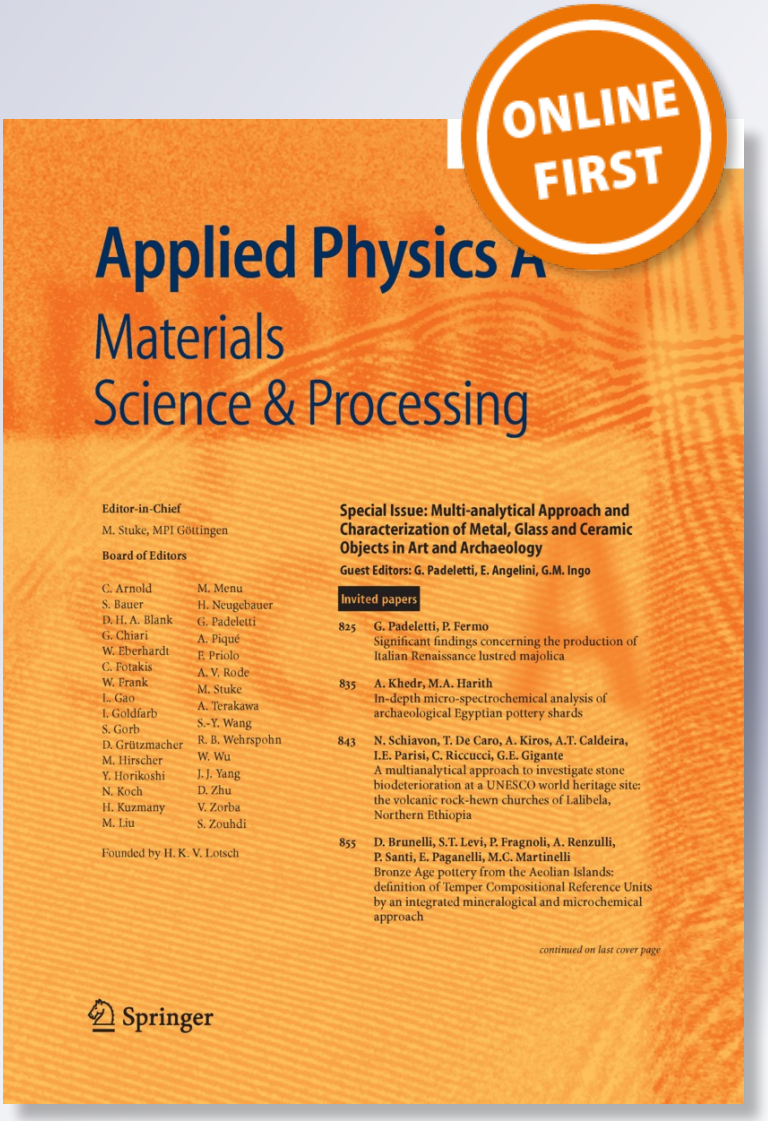

Springer

Appl. Phys. A
DOI 10.1007/s00339-013-8185-2

Applied Physics A
Materials Science & Processing

Insights into molecular chemistry of Chiapas amber using infrared-light microscopy, PIXE/RBS, and sulfur K-edge XANES spectroscopy

Francisco Riquelme · Paul Northrup · José Luis Ruvalcaba-Sil · Vivian Stojanoff · D. Peter Siddons · Jesús Alvarado-Ortega

Received: 26 September 2013 / Accepted: 29 November 2013

Abstract Chiapas amber is a natural occurring fossil resin structurally composed of long macromolecule chains with semicrystalline phases associated with both fossil and polymerization process. The most conspicuous characteristic of this fossil polymer is that it preserves ancient organic inclusions. In the present work, PIXE/RBS spectrometry (particle-induced X-ray emission/Rutherford backscattering) were combined with complementary K-edge XANES spectroscopy (X-ray absorption near-edge structure) to identify the amount of sulfur in Chiapas amber. Initially, the amber samples were examined using infrared reflected photomicrography. Amber is transparent to infrared light and so embedded plants and animals are easily visible, showing them in extraordinary detail, as if they were immersed in a water-like solution. The PIXE/RBS data show that the proportion of sulfur in amber is significantly higher than that found in recently formed resins, consistent with the biogeochemical process that transforms the resin into amber during long-term burial in geological deposits. The sulfur K-edge XANES spectra from amber confirm the sulfur abundance and reveal sulfur species in the reduced and intermediate oxidation states in amber. Almost no oxidized sulfur was found, whereas the recent resins show mostly oxidized sulfur fractions. This indicates that labile oxidized sulfur decays during fossilization and resin maturation must occur under conditions of oxygen depletion. The implications of the presence of sulfur in amber for organic preservation is also discussed here. Sulfur compounds work as a polymer additive that promotes intense resin solidification. This restricts the early oxidant-specific biodegradation of the embedded biomatter and, over geological time, provides greater stability against chemical changes.

1 Introduction

The Chiapas amber-bearing beds are exposed in localities belonging to the Mazantic Shale and Balumtum Sandstones strata, which date as early-middle Miocene in age, ca. 23–13 Ma [1–3]. The three major deposits are near the towns of Simojovel, Huitiupán and Totolapa, located in the Chiapas Highlands in southern México [4]. These geological deposits represent transitional sediments associated with a nearshore, mangrove-like environment [5]. The most conspicuous characteristic of the Chiapas amber is that shows embedded animals and plants with delicate tissues preserved almost intact [6]. The resin-producing tree of Chiapas amber is closely related with the extant legume *Hymenaea courbaril,* on the basis that their resins are chemically similar, sensu Langenheim, 1963 [1]. The secondary metabolites of resin-producing trees generate a wide range of terpenoids, carboxylic acids and associated alcohols in the form of resin, as response to ecological

F. Riquelme (✉) · J. L. Ruvalcaba-Sil
Instituto de Física, Universidad Nacional Autónoma de México, 20-364 Mexico, DF, Mexico
e-mail: riquelme.fc@gmail.com

P. Northrup
Department of Geosciences, Stony Brook University, National Synchrotron Light Source, Brookhaven National Laboratory, Upton, NY, USA

V. Stojanoff · D. Peter Siddons
Photon Science Directorate, Brookhaven National Laboratory, Upton, NY, USA

J. Alvarado-Ortega
Instituto de Geología, Universidad Nacional Autónoma de México, 04510 Mexico, DF, Mexico

Published online: 10 December 2013

pressures, such as insect and microbial attacks or climate changes [7]. The specific variability of terpenoids and carboxylic acids has been used extensively in chemotaxonomic characterization of plant resins [8]. In particular, the chemotaxonomic classification of Chiapas amber has been studied typically based on infrared spectroscopy and Carbon-13 NMR methods [9–11]. In addition, botanical affinities of Chiapas amber when compared with other world-wide ambers have been studied applying mass spectrometry techniques [12, 13], and thermal analysis [14]. However, the structure and molecular chemistry of Chiapas amber, with implication for its exceptional organic preservation, remain still unexplored.

Plant resins are naturally occurring polymers. However, not all plant resins can fossilize [7, 15]. The solidification of fossil resins is determined by their physicochemical characteristics; particularly, the molecular chemistry, polymeric chain configuration, and partial crystallinity. As a viscous liquid during plant synthesis, the resin has short molecular chains, but is transformed into a high polymer which is extremely solid because large macromolecules are synthesized from the smaller ones during the polymerization process at ambient temperature of the surrounding forest [16]. Thus, the fossil resins are structurally composed of very long molecular chains that are affected by the increased molecular weight [16]. In addition, the crystalline state exists in polymeric materials, such as fossil resins, but this involves macromolecules instead of ions or atoms only [16]. Thus, the length of the polymer chains, their structure and chemistry influence the ability of fossil resin to solidify and to partially crystallize. Accordingly, the rapid solidification and partial crystallinity of amber increase the preservation potential of the organic inclusions trapped within it, because they inhibit the organic decay.

The resin fossilization, or the physicochemical process that transform a resin into amber in geological deposits, is also poorly understood [7, 15]. To describe this process the term that has been conventionally used is *maturation* [7, 8, 15], some authors use the term *amberization* too [2]. The chemical changes that occur during resin maturation have been tentatively considered as part of the oxidative processes that arise from the conditions of depositional environments [2, 14]. However, the biogeochemical interactions with sediments during long-term burial, which include a chemical dissolution under oxygen deficiency, recrystallization of organic substances, and reuptake of mineral impurities and metal ions, must be considered.

In the present study, a combination of PIXE/RBS spectrometry (particle-induced X-ray emission/Rutherford backscattering) and K-edge XANES spectroscopy (X-ray absorption near-edge structure) was applied to measure the sulfur signatures in fossiliferous Chiapas amber, with implications for resin fossilization and organic preservation.

The fossiliferous amber samples were first analyzed by infrared reflected microphotography using stereomicroscopes coupled with IR-pass lens, CCD imaging systems sensitive to the IR spectrum, and an intense white fluorescent light as a source that radiates well into the IR spectrum. Infrared-pass filters are sensitive to wavelengths of near-infrared spectrum, absorbing visible light, but transmitting infrared in the bands of 750 to 1,400 nm [17]. The infrared light is slightly absorbed or reflected by amber, making visible the embedded biomatter in detail. The use of infrared-light microscopy is here first proposed to solve the problematic cloudiness and luster in amber induced by visible light. At the present, this technique has never applied before in amber studies. The principles and uses of infrared photography are described elsewhere [17–19].

After infrared microimaging, here the major and trace elements were quantitatively determined by simultaneous PIXE/RBS spectrometry based on a highly focused proton beam used to carry out point analyses in freshly fractured and polished amber samples. Light and heavy elements (with $Z > 12$) were measured in both PIXE/RBS spectra. The major and trace elements are useful fingerprints to understand the chemical composition of fossiliferous amber. A previously published analysis of archeological Chiapas amber applying PIXE has been performed by Lowe and Ruvalcaba-Sil [20]. RBS using protons measures mainly the scattering due to carbon of amber, so it is possible to quantify the integrated charge deposited on the sample during the proton beam measurements. From these data, X-rays from the sample can be normalized. However, RBS shows a poor resolution to detect heavier elements in low concentrations [21]. Furthermore, PIXE is complementary used to detected low concentrations of heavier elements than carbon. In the present work, the carbon fitting is no reported because RBS data are relative to other elements detected in the sample. Accordingly, during the experimental runs, the carbon fitting of RBS spectra and the depth chemical profile have shown a quite homogeneous surface composition in samples. PIXE/RBS measurements were focused on identify the amount of sulfur in fossiliferous amber. A detailed review and application of PIXE/RBS methods are given in Johansson et al. [21]. The advantage of the PIXE/RBS methods is the measurement precision that is obtained for peak energy and peak fitting of the X-ray spectrum; this provides quantitative information of element concentrations that can be used as potential biogeochemical fingerprints [22].

Finally, synchrotron-based sulfur K-edge XANES measurements are utilized to focus on the organic sulfur speciation in amber. These organic sulfur compounds can work as markers linked to the resin-producing plant and to molecular interactions within resin. The chemistry of sulfur is critical to understand several processes of resin polymerization [23]. In addition, in materials science studies,

sulfur compounds have been extensively investigated as polymer additives [24].

Synchrotron-based K-edge XANES is a powerful analytical tool to elucidate the chemical properties of both organic and nonorganic material, applied in various fields, such as chemistry, biochemistry, materials, and earth sciences [25, 26]. The physics and methods of K-edge XANES spectroscopy are described elsewhere [27]. XANES spectra also provide direct nondestructive experimental measurement of the sulfur oxidation state in materials that cannot be obtained by other techniques, under less-than-perfect sample conditions, and at low concentrations [28, 29]. The S K-edge XANES spectra are dominated by a large peak representing the 1 *s*–2*p* electron transition. The position (energy) of this peak is sensitive to the effective oxidation state of the S atom, and so is indicative of the type of S compound (e.g., sulfate, sulfonate, thiol). In mixed samples, fitting of the magnitude of different peaks can be used to quantify the content of various classes of sulfur compounds [28–33].

The infrared-light microscopy, PIXE-RBS and synchrotron-based XANES are basically noninvasive and are appropriate techniques for the analysis of exceptionally preserved fossils. These specimens are unique evidence of ancient life and should be kept safe from destructive experimental methods [34].

2 Experimental

2.1 Sample description

Amber with organic inclusions comes from the three major deposits in the Chiapas Highlands, Southern México. These are known as a fossil Lagerstätte [4, 6]. One group is from the quarries at the west end of the town of Totolapa, latitude 16°32′42.85″N, longitude 92°40′58.67″W. The second group is from the quarries at the east of the town of Simojovel, latitude 17°8′27.60″N, 92°41′34.08″W. The third group is from quarries at the west of the town of Huitiupán, latitude 17°10′13.01″N, longitude 92°41′24.57″W. Fossil organisms are represented by the well-preserved specimens of animals: spider, ant, fly, mosquito, centipede, and pseudoscorpion; as well as plant structures: leaf, flower, and wood. The samples T2 (1HNFG-0534) and *H. allendis* belong to the Museo de Paleontología 'Eliseo Palacios Aguilera', Chiapas. No specific permits were required for the samples analysis. For comparison, sampling includes recent resins from the legume tree *Hymenaea courbaril*, and copal resin from *Bursera* sp. These were collected from two different localities from Chiapas and Veracruz in the South of México. A relatively simple technique for sample preparation was used in PIXE/RBS and XANES experiments: amber samples were freshly fractured, cut, polished and cleaned by mechanical techniques and deionized water. All samples were not exposed to solvents to avoid contamination or deposition of any chemical residues.

2.2 Infrared imaging

Digital Infrared photomicrographs were acquired using a Carl Zeiss® SteREO.V12 Apochromatic-zoom and Edmond® E-Zoom 6 V video system with adapted infrared-pass filters for a range of 680–720 nm, and coupled to a CCD imaging system sensitive to the infrared spectrum. For the best relief contrast, multiple pictures ($\simeq$34) were taken at different positions of the *Z* axis over a field; image superimposition of multiple pictures resulted in a unique image with high depth of field; using a zoom range of 2.4× to 575×, and AxioVision® and Corel® Photo-Paint®X5 software for image processing. A reflected/transmitted white fluorescent light, electronic flash, and tungsten lamps were conveniently used as an infrared radiation source.

2.3 Ion beam analysis

Element concentrations were quantitatively determined using simultaneous particle induced X-ray emission (PIXE) and Rutherford backscattering (RBS) spectrometries on the external proton beam of 3 MeV at the Tandem Pelletron Accelerator of UNAM [35]. The beam spot at the sample surface was 1 mm diameter. Light element fluorescence lines were detected by a Si-PIN Amptek detector (150 eV resolution for Mn-Kα line) with a 1-mm diameter Ta collimator and a helium jet to improve detection of low energy X-rays. Heavier elements were detected using a LEGe detector set at 15 cm from the sample without any filter. In this way, X-ray absorption by air in the detection path was used to reduce the light element fluorescence detection. Backscattered protons were collected in a passivated implanted planar silicon (PIPS) detector under vacuum using a collimator of 2 mm diameter. PIXE and RBS spectra were collected for 5 min; several measurements were carried out on each sample. The efficiency of detection of the PIXE system was determined using pellets of standard reference materials of sediments from NIST (SRM 2704, SRM 2711). AXIL code and the PIXEINT program [36] were used to determine the elemental concentrations (wt %). This paper focuses on sulfur (S), other lighter elements from aluminum (Al) to iron (Fe) were also detected.

2.4 Synchrotron-based K-edge XANES spectroscopy

Sulfur K-edge XANES spectra were measured at beamline X15B at the National Synchrotron Light Source. X15B is

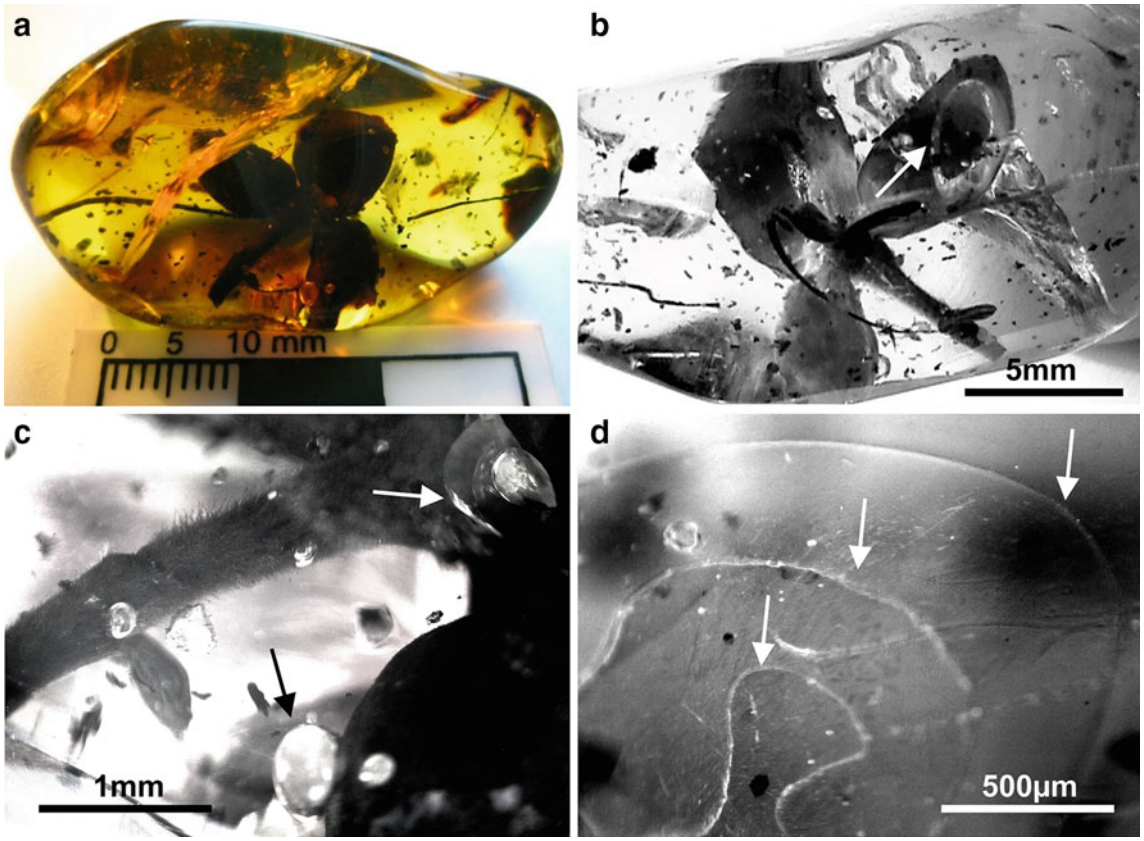

Fig. 1 Contrasting images using visible light and infrared. Flower of *H. allendis* under visible light (**a**), the same specimen applying infrared reflected photomicrography (**b**), *arrows* indicate nectar ring (**b**) and nectar drops (**c**), as well as a wave-like pattern in amber matrix (**d**)

optimized for X-ray absorption spectroscopy in the 1–5 keV energy range, and provides a focused monochromatic X-ray beam of ~0.5 mm to the sample in a helium-atmosphere sample chamber. Sulfur K alpha fluorescence (directly proportional to absorption) was measured using a germanium detector, and was normalized to incident beam intensity as measured with an ionization chamber just before the sample position. Incident-beam energy was calibrated to a dilute sulfate standard (sulfate in calcite), and an energy of 2,482.6 eV was assigned to the sulfate peak of the absorption spectrum. Darkening of the samples (fossil or living plant resins) under X-rays was not observed and no significant decreases of the relative intensities of the peak related to sulfates were observed during experimental runs. Peak fitting for the current study was performed using the Athena program in the IFEFFIT software package [37, 38]. Fitted peaks were assigned to species according to consensus in the literature [25, 26, 28–31], and their relative areas, corrected for differing absorption cross-section, were used to determine the fraction of each species present [25, 29]. Finally, according to [25, 26, 28–32], the organic sulfur functional moieties are grouped according to their respective oxidation states.

3 Results and discussion

3.1 Physical documentation

Infrared photomicrography of amber with organic inclusions are depicted in black and white (Figs. 1, 2, and 3). The visible light that produces color from a narrow band of wavelengths (continuous spectrum approximately from 380 to 750 nm) is blocked by the infrared-pass lens, which acts as a barrier filter over the digital camera lens and transmits only near-infrared longer wavelengths, extending from 750 to 1,400 nm [17, 39]. Amber is transparent to infrared radiation in this wavelength range.

The opacity, strong luster, and saturated coloration of amber, as a result of visible light incidence (the refractive index of amber is 1.54), are absent under infrared light. This allows the detailed morphology of embedded plants and animals to appear as if they were immersed in a water-like solution. Regularly, the Chiapas amber shows a crystalline luster with a variety of colors, including the most common golden yellow, citrine yellow, brownish orange, blackish brown, red, milky yellow, and rarely, green and blue. The opacity and color of amber also depends on the degree of diagenetic alterations by the reacting organic

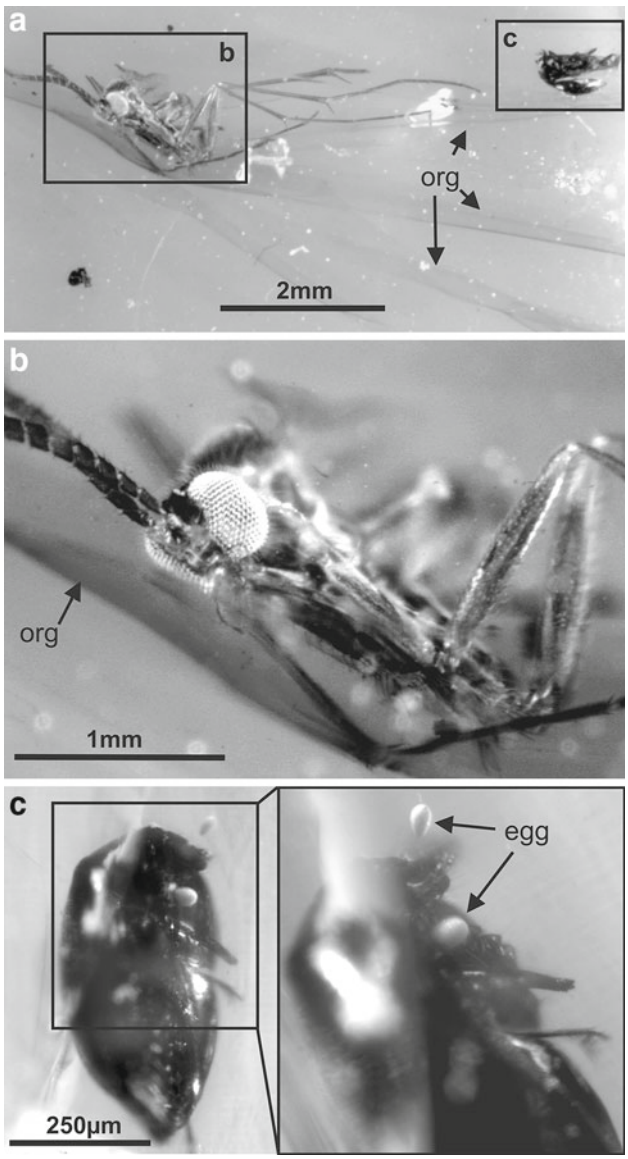

Fig. 2 Amber sample with embedded mosquito and beetle as shown by infrared reflected photomicrography (**a**). Closed views of mosquito (**b**) and bettle (**c**); *arrows* indicate the longitudinal bands of organic fluid-like (*org*) (**a**, **b**), and egg-like structure (*egg*) adjacent to beetle (**c**)

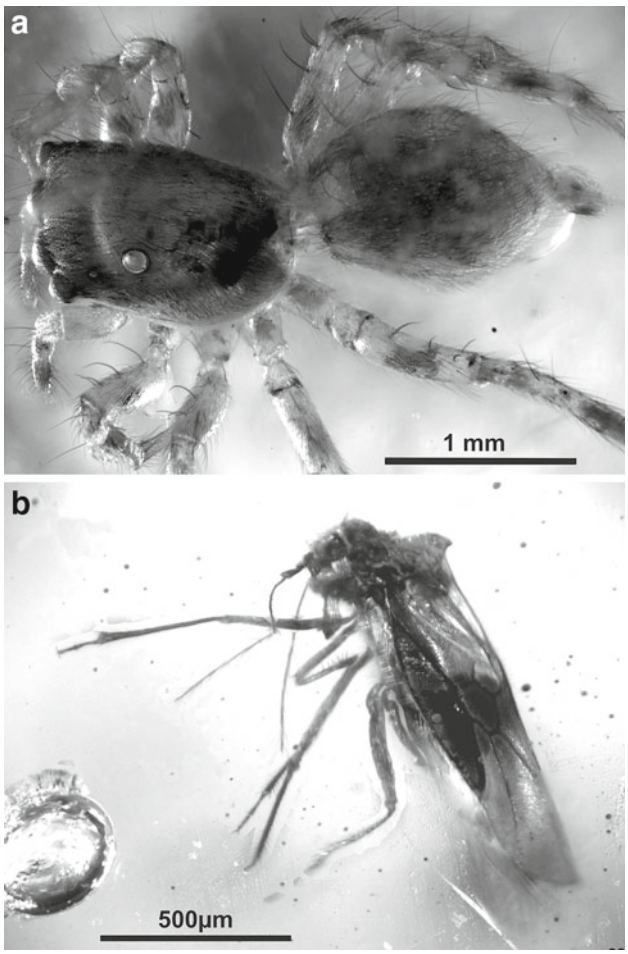

Fig. 3 Infrared reflected photomicrographs of fossil spider and fly trapped in Chiapas amber

substances within the resin, as well as metal ions and mineral impurities from sediments.

Amber absorbs high energy radiations, i.e., ultraviolet and X-rays; however, as shown in Figs. 1, 2, and 3, the infrared light it is transmitted through amber before it is absorbed by the bodies of the organisms trapped within it, which are optically denser than the resin. This permits us to detect their delicate morphologies and tissues that are observed according to the black and gray scale, as is already presented in the literature of colors under infrared light: black when infrared is absorbed; gray when this is reflected; and bright-white when infrared is luminescent [40–42].

Figure 1a and b shows images of the flower of *Hymenaea allendis* (sample S1/the holotype) contrasting visible light with infrared light. The biology of the *H. Allendis* is described elsewhere [43], this plant is strongly associated with the amber-producing tree. Figure 1b and c shows a nectar ring and nectar drops, which are also finely recrystallized and preserved totally embedded in the amber matrix. Both nectar remains and fossil resin responded differently to infrared, in accordance to chemical differences and contrasting timing between crystallization of nectar polysaccharides and the polymerization of amber terpenoids. A wave-like pattern is also observed in the structure of amber associated with the dynamics of the viscous flow of the resin during secretion and rapid polymerization (Fig. 1d). This also suggests that the resin solidification may occur at different velocities.

On the other hand, animal exoskeletons such as mosquito and beetle (Fig. 2), as well as spider and fly (Fig. 3), which are poorly visible through the overlaying thick amber, are clearly visible and detail-rich by infrared

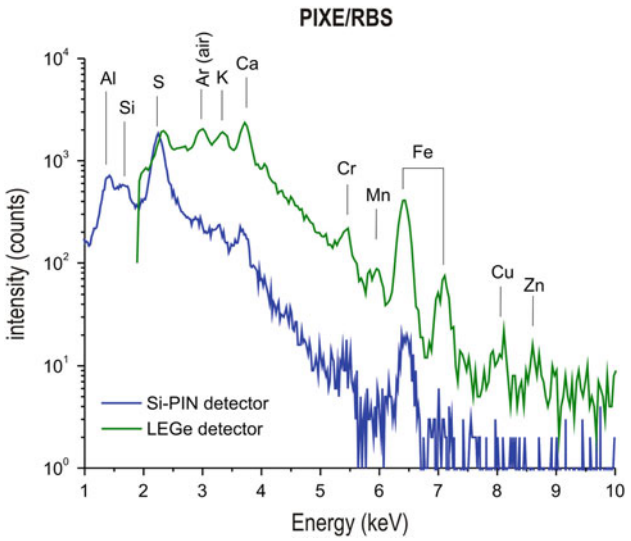

Fig. 4 Typical PIXE/RBS spectra of fossiliferous amber as shown in sample T1 with embedded spider

reflected microscopy. Other delicate features linked to modes of preservation are also observable, for instance, the longitudinal dissolution bands surrounding animal bodies, which are linked to organic fluid remain from animal decay; these were transported through the polymeric structure of amber (Fig. 2a, b). The egg-like structures preserved close to a beetle are detected (Fig. 2c), and the three-dimensional morphologies of spider and fly (Fig. 3a, b) are seen in detail as well.

3.2 PIXE/RBS data analysis

PIXE/RBS spot-analyses were performed on different micro-zones of amber samples. The ion beam takes a measurement on the sample surface; however, each organic inclusion was placed near the amber surface: ≈100–500 μm deep, except for sample T1 with embedded spider that is closest to the surface about <50 μm. Elements of measurable abundance were determined by PIXE/RBS peak energy and peak fitting (Fig. 4). As shown in Table 1, the elements of interest identified within amber were aluminum, silicon, sulfur, potassium, calcium, chromium, manganese, iron. Traces of copper and zinc were also detected in a few samples (Fig. 4), however, the signal of these elements is very weak or unobservable at the majority of the samples, for that reason they were not included in Table 1. In contrast, all experimental runs detected sulfur at high abundance in amber, whereas lower amounts in recent resins were observed. Concentrations of other elements varied markedly in both fossil and recent resins. The amount of each major element was determined in weight percentage.

The averages (wt %) of sulfur for each sample (Table 1) show that amber with slightly higher values are those with mosquitoes (T2 and S2), centipede (H13), and pseudoscorpion (H14). The most well-preserved organisms are spider (T1), ants (T5 and S3), and flower of *H. allendis* (S1), which also show significant sulfur concentrations. If the biology and mode of preservation of the embedded organisms can significantly affect the elemental distribution in the amber microfabric, one would expect to see differences between distinct analyzed spots on the same sample. The measurements were taken at 'hot spots' located at the position of the organic inclusions (i.e., animal bodies) and others located away from them. However, no significant variation in sulfur content at different spots in the same amber sample was observed.

The beam range using a 3 MeV proton beam to analyze amber with a density of about 1.1 g/cm^3, can reach about 150 μm. However, the X-ray absorption is different for the elements depending on their characteristic X-ray energies. Considering this fact, the analyzed depth can be calculated from the natural logarithm of the ratio of emitted and incident beams divided by the product of the material density and the X-rays mass attenuation factor. Then, the total absorption (99 %) of the X-ray intensity corresponds for Al, Si, S, K, Ca, and Fe to 0.9, 1.8, 3.8, 12, 20, and 60 μm, respectively. This means that for sulfur, independently of the analytical technique based on X-ray detection, the maximum analyzed depth is <4 μm. Since the organic inclusions in the amber are under more than 50 μm, PIXE probes the amber surface only.

On the other hand, as shown in Table 1, the living plant resins that lack organic inclusions (samples R1 and CP), show a lower sulfur content than amber with embedded fossil organisms. In addition, comparing these recent resins with amber sample T11 (Totolapa), which also lacks organic inclusions, and amber sample T22 (Totolapa) with a poorly preserved leaf, both groups of samples show a low sulfur content. The Totolapa amber samples T11 and T22 also show different sulfur signal with respect to other ambers from the same locality. Samples T11 and T22 come from the bottom sediments within the deposit, dominated by layers of sandstone, in which carbonaceous rocks, linked to plant material and ancient soils, are scarce. The rest of the samples come from sediments with carbonaceous-rich material. The geological section of Totolapa amber is presented elsewhere [4]. The ancient environment of amber is represented by both nearshore sands and rich-mud soils [4–6].

As shown in Fig. 5, the sulfur average data from each amber locality was tested as a chemical signal of geographical source, or provenance marker. Sulfur concentrations have been compared to observe if these elemental abundances were consistent within each locality. The data show that the sulfur concentrations in amber were fairly consistent for Simojovel and Huitiupán. The samples from Totolapa show, however, more variability, in accordance to

Table 1 Multielemental analysis of amber and living plant resins using PIXE

Sample	Fossil inclusion *Totolapa*	Spot	Al Weight (%)	Si	S	Cl	K	Ca	Cr	Fe	Average S^a
			±8 %	±10 %	±8 %	±12 %	±12 %	±15 %	±15 %	±12 %	
T11	No inclusions	1	0.679	0.180	0.438	0.021	0.006	0.015	0.002	0.015	0.39 ± 0.03
		2	1.530	0.139	0.303	0.020	0.006	0.007	0.006	0.006	
		3	1.210	0.189	0.306	0.027	0.011	0.019	0.002	0.015	
		4	0.359	0.182	0.502	0.024	0.006	0.012	0.001	0.010	
T22	Leaf	1	0.194	0.139	0.585	0.020	–	0.005	–	0.005	0.42 ± 0.03
		2	2.165	–	0.253	–	0.009	0.014	0.003	0.012	
T3	Fly	1	–	0.326	0.574	–	–	–	–	–	0.59 ± 0.05
		2	–	0.273	0.599	–	–	–	–	–	
		3	–	0.292	0.590	–	–	–	–	–	
T5	Ant	1	–	–	0.720	–	–	–	–	–	0.61 ± 0.05
		2	0.230	0.420	0.421	0.003	0.018	0.014	–	0.017	
		3	–	–	0.685	0.016	0.011	–	–	–	
T1	Spider	1	–	–	0.675	0.007	0.022	0.003	–	–	0.69 ± 0.06
		2	–	–	0.691	0.002	0.017	0.003	–	–	
		3	–	0.014	0.698	–	0.011	0.002	–	–	
T2	Mosquito	1	–	–	0.750	–	–	–	–	–	0.73 ± 0.06
		2	–	–	0.725	–	0.001	–	–	–	
		3	–	0.028	0.714	–	–	–	–	–	
	Huitiupán										
H13	Centipede	1	–	–	0.727	–	–	–	–	–	0.73 ± 0.06
		2	–	–	0.750	–	–	–	–	–	
		3	–	–	0.720	–	–	–	–	–	
H14	Pseudoscorpion	1	–	0.079	0.690	–	–	–	–	–	0.72 ± 0.06
		2	–	–	0.740	–	–	–	–	–	
		3	–	–	0.720	–	–	–	–	–	
	Simojovel										
S5	Wood	1	–	0.198	0.634	–	–	–	–	–	0.65 ± 0.5
		2	–	0.159	0.653	–	–	–	–	–	
		3	–	0.120	0.671	–	–	–	–	–	
S4	Leaf	1	0.138	0.153	0.562	0.023	0.014	0.006	–	–	0.64 ± 0.05
		2	0.041	0.021	0.709	–	–	–	–	–	
S1	Flower	1	–	–	0.676	–	0.030	–	–	–	0.64 ± 0.05
	H. allendis	2	–	0.060	0.618	0.018	0.032	–	–	–	
	Holotype	3	–	0.052	0.650	0.008	0.025	–	–	–	
		4	–	0.051	0.603	0.018	0.041	0.003	–	–	
S9	Spider	1	0.141	0.146	0.565	0.032	0.008	0.005	–	–	0.62 ± 0.05
		2	–	0.100	0.680	–	–	–	–	–	
S2	Mosquito	1	–	–	0.740	–	–	–	–	–	0.72 ± 0.06
		2	–	0.072	0.693	–	–	–	–	–	
		3	–	0.087	0.672	0.007	–	0.003	–	–	
S3	Ant	1	–	0.083	0.688	–	–	–	–	–	0.60 ± 0.05
		2	–	–	0.720	–	–	–	–	–	
		3	0.197	0.291	0.384	0.073	0.023	0.015	–	–	
	Living plant resin										
R1	No inclusions	1	–	0.081	0.689	–	–	–	–	–	0.33 ± 0.03
H. courbaril		2	0.398	0.315	0.061	0.132	0.080	0.073	–	–	
		3	–	0.862	0.234	–	–	0.056	–	–	
CP	No inclusions	1	1.020	0.263	0.401	–	–	–	–	–	0.40 ± 0.03

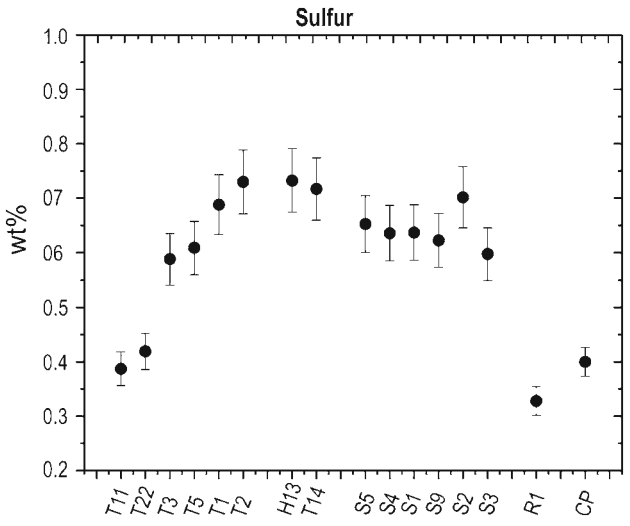

Fig. 5 Relative sulfur averages in amber and living plant resins from different sites based on PIXE/RBS analysis. The amounts are expressed in weight percentage (wt %), and uncertainties are ± 0.08

the lithological variation that is observed here, and described above [4–6]. Simojovel shows a sulfur average of 0.64–65 wt %; Huitiupán 0.72–0.73 wt %, and Totolapa 0.39–0.73 wt %. In contrast, samples of *Hymenaea courbaril* and *Bursera* sp., both grouped as living plant resins, show an average of 0.33–0.40 wt %. The use of the extant resin from *Hymenaea courbaril* as a control is plausible, since it is chemically the most closely related to Chiapas amber [1, 7, 9, 10].

According to the discussion above, the ability to measure sulfur in recent and fossil resins is very important as the level of this element could be used as a "fingerprint" of amber. Silicon is another element that is present at significant concentrations (Table 1), also strongly associated with soils and sediments (sandstones and clay). This should be evaluated in future sampling in the hope that the application of PIXE can be sensitive enough to detect more trace elements in amber.

3.3 Organic sulfur compounds

The nonlinear least square fitting of experimental S K-edge XANES spectra showing the various oxidation states of sulfur in the representative samples of both amber and living plant resins is presented in Fig. 6; and the normalized S K-edge XANES spectra for five amber samples from different sites are shown in Fig. 7. Sample H1 is from Huitiupán, samples S1 and S2 are from Simojovel, and samples T1 and T2 from Totolapa. Likewise, samples of the living plant resins from two different localities (Chiapas and Veracruz, south of México) are compared in Fig. 8. As shown in Table 2 (fossiliferous amber) and Table 3 (living plant resins), deconvolution of the spectra into distinct peak positions for each observed organic sulfur species is presented in keV and Gaussian component peaks are derived from curve-fitting analysis of the spectra according to literature [25, 29].

The amber samples with well-preserved organisms show a relative increase of the peak energy around 2.4735, 2.4767, 2.4801 and 2.4811 keV (Fig. 7), this is indicative of reduced and intermediate S species. In contrast, there is a lower signal at ≥2.4822 keV, corresponding to sulfate, which is the most oxidized sulfur species. Individual peaks that have been detected and assigned to organic species, include thiol/thioether/heterocyclic S at ~2.4735 and cyclic-thioethers around 2.4742–2.4745 keV. There is overlap in the reported peak positions of thiol/thioether/heterocyclic S, but the higher energy peak positions are consistent with more aromatic structures [25, 26, 28–32]. Accordingly, the first peak at ~2.4735 keV has been identified as thiol/thioether/heterocyclic S (aromatic rings) and the second peak at ~2.4742 to 2.745 keV (present only in the living plant resins) as a distinctly different cyclic thiother (Fig. 7). There are other individual peaks assigned to sulfoxide (+2) at ~2.4767 keV, sulfite (+3.7) at ~2.4783 keV, and sulfonate (+5) at 2.4811 keV. A shoulder attributed to sulfone (+4) at ~2.4801 keV has been also identified in several samples (Fig. 7).

For example, the thiol/thioether/heterocyclic S peak is dominant in the sample T1 with the embedded spider, whereas the sulfoxide peak is not obvious. However, some sulfoxide fraction was still estimated to be present based on peak fitting data (Table 2). For the sample S1, both sulfone (2.4801 keV) and sulfate shoulders (2.4826 keV) are noted on each side of the sulfonate peak. The sample S1 (with the embedded flower of *H. allendis*) is the only amber that shows evidence of sulfate fraction (+6) (see Fig. 7; Table 2). Here a smaller signal in the energy region of sulfite (2.4783 keV) has also been observed (Fig. 7).

The relative abundances of the main sulfur species for amber and living plant resins according to their relative areas were also estimated [25, 29, 30]. Table 2 shows values for amber and Table 3 for living plant resins. Table 4 shows the standard compounds and peak positions according to literature [25, 29, 30]. The intermediate organic S shows an important contribution from sulfoxide ranging from 17.6 to 23.7 % of total S; sulfone ranging from 15.7 to 29.6 % of total S; and sulfonate ranging from 20.4 to 38 % of total S (Table 2). The respective abundances of sulfite and sulfone were not quantified because their relative peaks are heavily overlapped. In addition, there is an important contribution from thiol/thioether/heterocyclic S (aromatic rings), which significantly varies in two amber samples. For example, the sample S1 shows the smallest amount (4.6 % of total S) and T1 the largest (76.4 % of total S). In sample T1, the organic thiol/

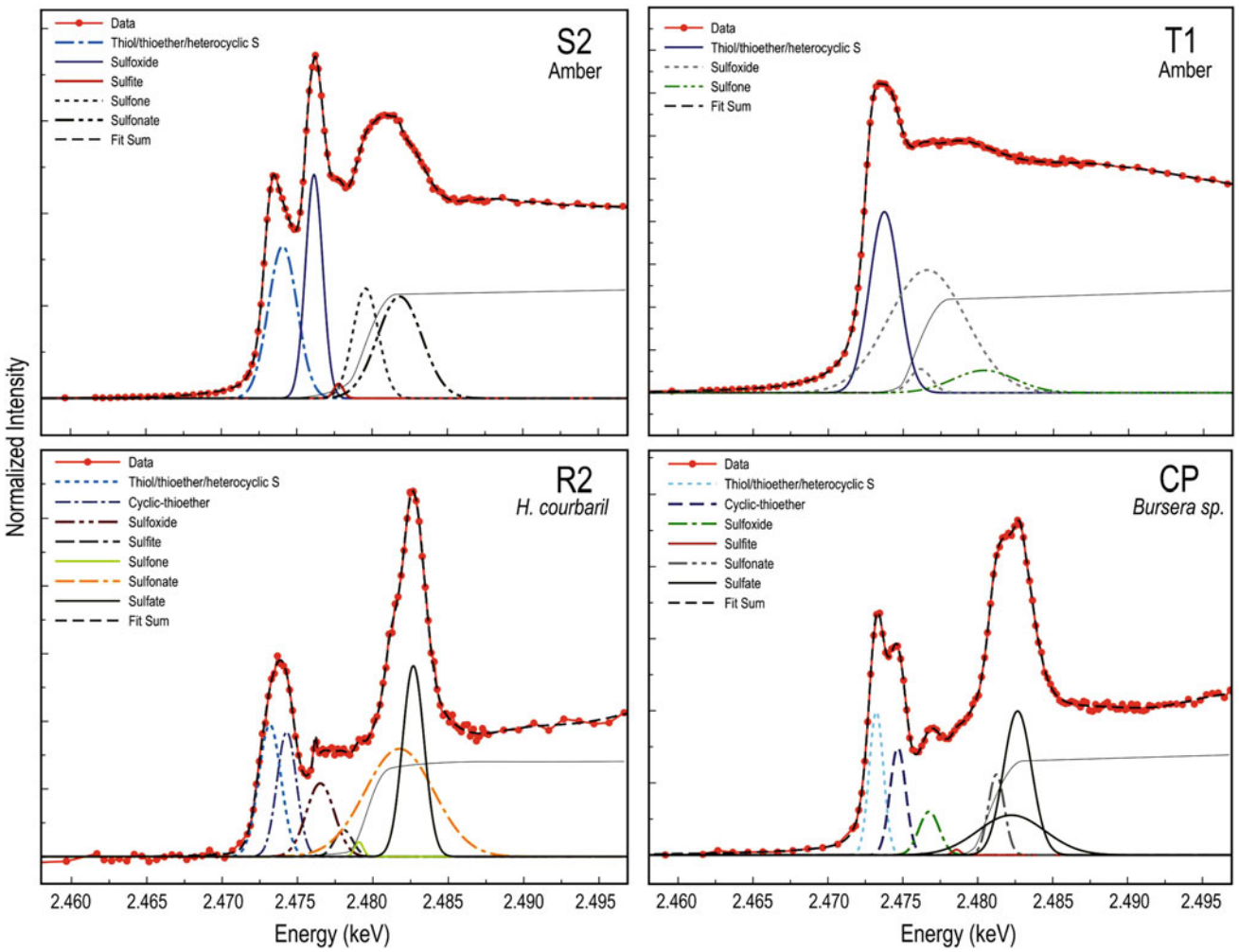

Fig. 6 Nonlinear least square fit of experimental S K-edge XANES spectra from representative samples of both amber and living plant resins. The *dotted black line* shows the best fit of the data in *solid red line*; *top* fossiliferous ambers; *bottom* living plant resins

thioether/heterocyclic S (peak position at 2.4735 keV) is the most important compound of total sulfur. This is very intriguing because T1 is the amber sample with the most well-preserved animal, here the spider carcass is almost intact and preserved soft tissues remain. According to previously reported measurements [25, 26, 28–30, others], a variety of compounds could be represented by this peak, from thiols to heterocyclic S. Further spectroscopic measurements, including EXAFS (extended X-ray absorption fine structure) are being analyzed to better define these species. Interestingly, organic disulfide species are not evident in the amber samples. These species would be represented by a peak at lower energy than any observed here.

On the other hand, the thiol/thioether/heterocyclic S is also an important peak signal for all the living plant resins, as shown in Fig. 8. But there are two different peaks present here. The lower-energy one is at ~2.4734 keV, very similar to the peak observed in the amber (aromatic rings). The second peak is at ~2.742 to 2.745 keV, which is not seen in the amber (Fig. 8). This peak best matches with cyclic-thiothers that show a high-energy bonding structure as presented in previously published reports [30–32]. As shown in Table 3, the estimated fraction of these two species in sample CP (*Bursera* sp.) shows thiol/thioether/heterocyclic S with 13.1 % and cyclic-thiothers with 11.7 % of total S; sample R1 (*H. courbaril*) shows 31.4 and 19.2 %; and sample R2 (*H. courbaril*) shows 17.8 and 16.4 %, respectively.

The intermediate S fractions also occur in significant amounts in living plant resins, such as sulfoxide from 4.7 to 16.4 %, and sulfonate from 7.4 to 30.4 % of total sulfur. However, these resins remarkably show larger signals in the energy region of the most oxidized S compounds, particularly the organic sulfate at 2.4826 keV (Fig. 8). For instance, sample CP shows 39.8 % of total S, sample R2 49.6 % of total S, and sample R1 32.3 % of total S (Table 3). The relative abundances of thiol/thioether/

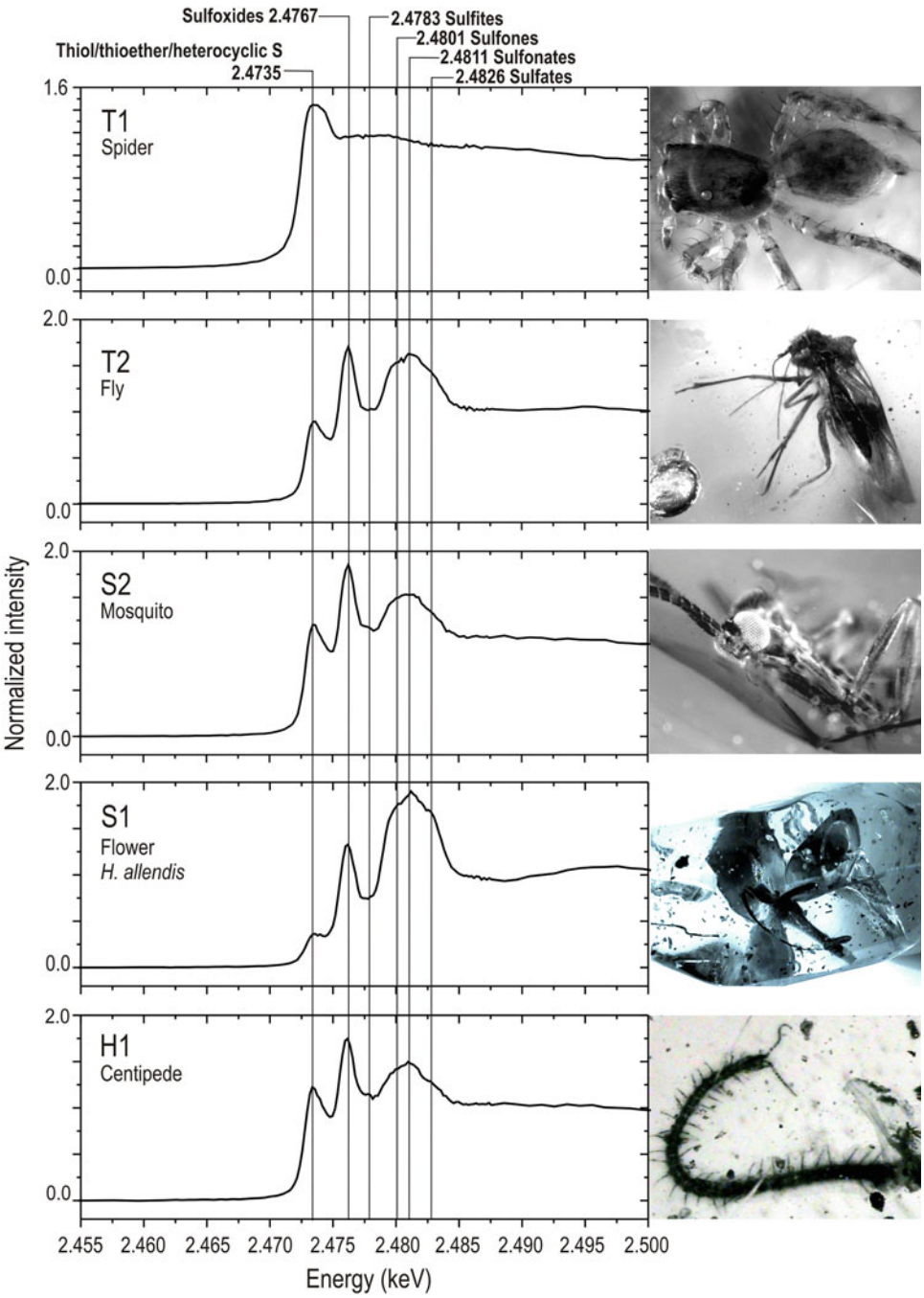

Fig. 7 Normalized S K-edge XANES spectra of fossiliferous amber samples studied from the three major sites of Chiapas, a fossil Lagerstätte: T1 and T2 from Totolapa; S1 and S2 from Simojovel; and H1 from Huitiupán

heterocyclic S and sulfate in R1 are more variable; however, the sulfate abundance is also significant like the other samples. According to the results above, organic sulfate is one of the most conspicuous features in the recent resins from *Hymenaea* and *Bursera* sources (Table 3).

This variation of sulfur species between recent and fossil resins appears to be the result of maturation processes that occurred in the physicochemical history of fossil resins [1, 2, 7, 8, 15]. Thus, organic sulfate is mostly associated with immature recent resins. This implies that organic sulfate was formed during resin production, mostly driven by acid-soluble ions present in the resin, which subsequently interact with the more volatile sulfur fraction to scavenge internal oxygen to form sulfate locally. Typically organic sulfate has a soluble salt structure, which reacts strongly with water [33, 44]. This suggests that sulfate present in the newly formed resin has been eventually mobilized and leached out upon increasing water-solubility and temperature during the early burial. Hence, the organic sulfate is decayed markedly during deposition and is transformed during fossilization to less labile compounds. The cyclic-thiother fraction is also lost in amber (Figs. 7, 8).

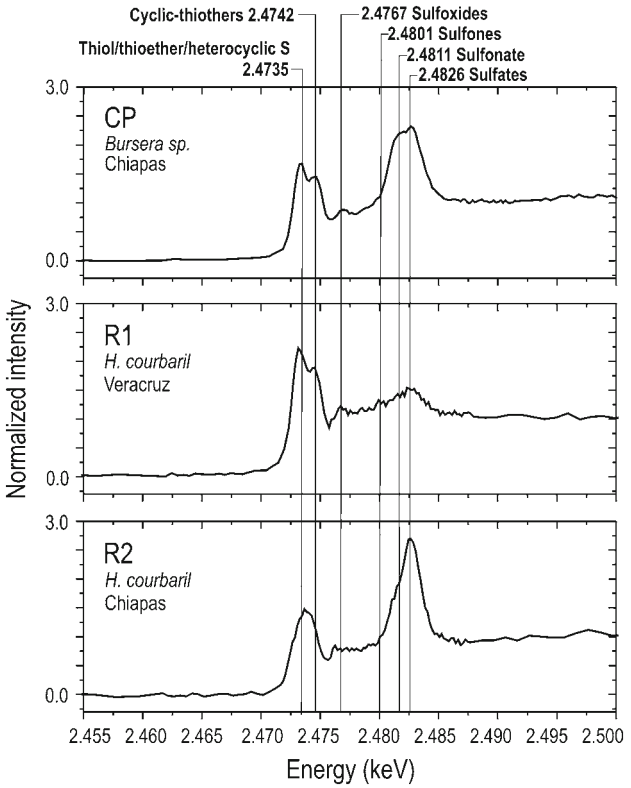

Fig. 8 Normalized S K-edge XANES spectra of living plant resin collected from two areas of south of México (Veracruz and Chiapas); *Bursera* sp. resin is well known as copal and *H. courbaril* resin is closely related to Chiapas amber

According to the S K-edge XANES spectra, the amber with well-preserved organisms is characterized by dominance of intermediated to reduced sulfur species, almost no sulfate was found, i.e., the sample T1 embedded spider with preserved soft tissues (Table 2; Fig. 7). Hence, the organosulfur speciation is important to understand the preservation process of biomatter within amber or subfossil resins. The amber experienced extensive exposure to air and water during deposition into the original forest, as well as oxidizing conditions during early burial in soils. But the nature of the fossil resin resists oxidation and excludes any oxygen within the inner structure which would otherwise cause a rapid oxidative degradation of the embedded biomatter. Thus, the sulfur compounds in amber should be part of the mechanism responsible for resistance to oxidation.

4 Conclusion

Imaging of organic inclusions in amber is an important topic, which has been, to date, very problematic to solve due to opacity of the fossil resins. The synchrotron-based X-ray microtomography has been successfully applied elsewhere [45, 46]. But the advantage of the new practice of infrared reflected photomicrography of fossiliferous amber or subfossil resins, as presented here, is that it provides rapid and detailed information about the organic inclusions and resin matrix. The accomplished information is critical in the paleobiological studies of amber that includes analysis of modes of preservation (Taphonomy) and Systematics. Finding tools and materials to improve this technique would be essential to use it routinely.

On the other hand, from the results above we conclude that the lower concentration of total sulfur from living plant resins significantly contrast with the higher level of fossiliferous amber. An exception is the sample T22 that shows poorly preserved leaf. As presented here, the organic sulfur concentration is an important element in the plant resin composition, which tends to increase in

Table 2 Relative abundances of the main sulfur species for each amber using XANES spectroscopy

Compound	Observed peak energy (keV)	Gaussian peak energy (keV)	Adjusted peak area (a.u.)	Fraction (%)
	T1 Spider	Arachnida		
Heterocyclic S	2.4737	2.4736	1.54	76.4 ± 0.6
Sulfoxide	2.4771	2.4770	0.48	23.6 ± 1.0
Sulfone	2.4806	2.4802	ND	ND
	T2 Fly	Diptera		
Heterocyclic S	2.4735	2.4736	1.15	12.5 ± 2.4
Sulfoxide	2.4762	2.4760	1.92	20.7 ± 2.3
Sulfite	2.4780	2.4782	ND	ND
Sulfone	2.4804	2.4800	2.66	28.8 ± 2.2
Sulfonate	2.4812	2.4814	3.51	38.0 ± 2.0
	S2 Mosquito	Diptera		
Heterocyclic S	2.4735	2.4738	1.76	12.0 ± 3.0
Sulfoxide	2.4762	2.4762	3.11	21.4 ± 2.8
Sulfite	2.4778	2.4776	ND	ND
Sulfone	2.4801	2.4800	4.32	29.6 ± 2.7
Sulfonate	2.4808	2.4812	5.38	37.0 ± 2.5
	S1 Flower	*H. allendis*		
Heterocyclic S	2.4734	2.4730	0.66	4.6 ± 3.0
Sulfoxide	2.4761	2.4762	2.59	17.9 ± 2.9
Sulfite	2.4776	2.4780	ND	ND
Sulfone	2.4802	2.4800	2.27	15.7 ± 2.9
Sulfonate	2.4812	2.4810	5.97	41.4 ± 2.4
Sulfate	2.4826	2.4822	2.94	20.4 ± 2.9
	H1 Centipede	Chilopoda		
Heterocyclic S	2.4734	2.4738	1.29	12.4 ± 2.5
Sulfoxide	2.4762	2.4762	1.82	17.6 ± 2.5
Sulfite	2.4780	2.4782	ND	ND
Sulfone	2.4800	2.4800	2.55	24.5 ± 2.4
Sulfonate	2.4810	2.4814	4.72	45.5 ± 2.0

Table 3 Relative abundances of the main sulfur species for each living plant resins using XANES spectroscopy

Compound	Observed peak energy (keV)	Gaussian peak energy (keV)	Adjusted peak area (a.u.)	Fraction (%)
	CP copal	*Bursera* sp.		
Thiol/thioether/ heterocyclic S	2.4734	2.4734	1.41	13.1 ± 2.6
Cyclic-thiothers	2.4744	2.4742	1.28	11.7 ± 2.6
Sulfoxide	2.4770	2.4768	0.51	4.7 ± 2.7
Sulfite	2.4777	2.4782	ND	ND
Sulfone	2.4796	2.4800	ND	ND
Sulfonate	2.4818	2.4816	3.26	30.4 ± 2.3
Sulfate	2.4826	2.4822	4.26	39.8 ± 2.1
	R1 resin	*H. courbaril*		
Thiol/thioether heterocyclic S	2.4732	2.4735	1.86	31.4 ± 1.7
Cyclic-thiothers	2.4745	2.4742	1.14	19.2 ± 1.8
Sulfoxide	2.4767	2.4762	0.57	9.7 ± 1.9
Sulfite	2.4785	2.4782	ND	ND
Sulfone	2.4794	2.4800	ND	ND
Sulfonate	2.4815	2.4811	0.44	7.4 ± 2.0
Sulfate	2.4823	2.4825	1.91	32.3 ± 1.7
	R2 resin	*H. courbaril*		
Thiol/thioether heterocyclic S	2.4736	2.4734	1.44	17.0 ± 2.2
Cyclic thiothers	2.4742	2.4746	1.40	16.4 ± 2.2
Sulfoxide	2.4762	2.4762	0.49	5.8 ± 2.4
Sulfite	2.4780	2.4782	ND	ND
Sulfone	2.4794	2.4879	ND	ND
Sulfonate	2.4810	2.4811	0.95	11.2 ± 2.3
Sulfate	2.4826	2.4822	4.21	49.6 ± 1.7

Table 4 Standard compounds and peak positions

Compound	Functional group	Electronic oxidation state	Peak energy (keV)
Thiol/thioether heterocyclic S	(Aromatic rings)	0.5/1	2.4735[a]
Cyclic-thiothers		0.5/1	2.4742[a]
Sulfoxide	R-SO-R′	2	2.4767[a] 2.4762[b]
Sulfite	SO_3	3.7	2.4783[a] 2.4785[b]
Sulfone	R-SO_2-R′	4	2.4801[a] 2.4805[b]
Sulfonate	R-SO_3	5	2.4811[a] 2.4813[b]
Sulfate	SO_4	6	2.4823[a] 2.4827[b]

[a] Mean value from Orthous-Daunay et al. [25]

[b] Mean value from Prietzel et al. [30]

accordance with the biogeochemical process that transforms the resin into amber throughout the geological time. Complex chemical interactions occur between resin and soils into the depositional environment. Reactive sulfur is abundant in organic-rich soils from wetlands [31–33, 44], such as the ancient environment under which the amber-producing forest grew. So the organic sulfur in recent resins is associated with the uptake from organic-rich soils and amber can increase sulfur reuptake from the soils and sediments under conditions of long-term burial, in which temperature and pressure greatly increase. This implies that organic sulfur is related to the original biogenic signal in Chiapas amber, which may reflect lifetime characteristics and strong interactions with sulfur-rich soils that became rocks through geological time. Typically fossils react with minerals from rocks. The increased temperature in long-term burials works as a natural oven that chemically transforms any organic material. The glass–liquid transition of Chiapas amber observed in the laboratory starts about 100 °C (pers. obs.). Thus, sulfur content can increase in the resins during amber maturation.

Accordingly, the high abundance of sulfur in fossiliferous amber from Chiapas is a particular biogeochemical marker with implications for organic matter preservation. Sulfur works as polymer additive that promotes a rapid solidification of the resin [23, 24, 47], therefore, this significantly restricts the early decay of embedded organisms. Polymer encapsulation also provides greater stability against chemical changes in the geological conditions.

In addition, the chemical change that occurred during geological maturation of amber has long been considered to be induced by oxidative processes that arise from the conditions of burial and sediment lithification [2, 14]. However, the S K-edge XANES data show that the most oxidized sulfur species decay in amber, suggesting that resin maturation occurs under oxygen-poor chemical reactions instead of oxygen-scavenging reactions, or was favored by oxygen depletion during diagenetic process.

Although this research has important implications for Chiapas amber, further work and discussion will be required to assess whether sulfur species can be applicable as informative biomarkers for fossiliferous amber from other localities worldwide.

Acknowledgments We thank Karim López, Francisco Jaimes, and Mauricio Escobar, for their technical support during the experimental runs at the Pelletron Accelerator Laboratory, IF-UNAM. We also thank Dr. Lauro Bucio from IF-UNAM, for the valuable comments that enriched the manuscript discussion. We thank Biol. Gerardo Carbot and Biol. Marco A. Coutiño, from the Museo de Paleontologia 'Eliseo Palacios Aguilera', Chiapas, they facilitated the holotype of *H. allendis* and sample T2. The editor and referees provided useful suggestions that improved the manuscript. This research is part of the PhD-granting program in Biological Sciences at the UNAM, financially supported by CONACYT, also partially supported by UNAM-PAPIIT IN106011 and IN403210 grants, as well as CONACYT 131944 MOVIL II endowment.

References

1. J.H. Langenheim, Ciencia **24**, 201–211 (1966)
2. G.O. Poinar Jr., *Life in Amber* (Stanford University Press, Stanford, 1992).
3. M.C. Perrilliat, F.J. Vega, M.A. Coutiño, J. S. Am. Earth Sci. **30**, 111–119 (2010)
4. C. Duran-Ruiz, F. Riquelme, M. Coutiño-José, G. Carbot-Chanona, G. Castaño-Meneses, M. Ramos-Arias, Can. J. Earth Sci. **50**, 495–502 (2013)
5. A. Graham, Am. J. Bot. **86**, 17–31 (1999)
6. F. Riquelme, J. Alvarado-Ortega, M. Ramos-Arias, M. Hernández, I. Le Dez, T.A. Lee-Whiting, J.L. Ruvalcaba-Sil, Hist. Biol. (2013). doi:10.1080/08912963.2013.778843
7. Langenheim, J., *Plant Resins: Chemistry, Evolution, Ecology, and Ethnobotany* (Timber Press Inc., Portland, 2003)
8. K.B. Anderson, R. Winans, R. Botto, Org. Geochem. **18**(6), 829–841 (1992)
9. A. Cunningham, I.D. Gay, A.C. Oehlschlager, J.H. Langenheim, Org. Geochem. **22**, 965–968 (1983)
10. J.B. Lambert, J.S. Frye, T.A. Lee, C.J. Welch, G.O. Poinar Jr, Archaeol. Chem. **4**, 381–388 (1989)
11. R.H. Brody, H.G. Edwards, A.M. Pollard, Spectrochim. Acta A Mol. Biomol. Spectrosc. **57**(6), 1325–1338 (2001)
12. L. Carlsen, A. Feldthus, T. Klarskov, A. Shedrinsky, J. Anal. Appl. Pyrol. **43**, 71–81 (1997)
13. L. Tonidandel, E. Ragazzi, G. Roghi, P. Traldi, Rapid Commun. Mass Spectrom. **22**(5), 630–638 (2008)
14. E. Ragazzi, G. Roghi, A. Giaretta, P. Gianolla, Thermochim. Acta **404**, 43–54 (2003)
15. K.B. Anderson, J.C. Crelling, ACS Symp. Ser. **617**, xi–xvii (1995)
16. W.D. Callister Jr., Polymer structures, in *Materials Science and Engineering, an Introduction* (Wiley, New York, 2000), pp. 447–517
17. X.P. Maldague, *Theory and Practice of Infrared Technology for Nondestructive Testing*, vol. 130 (Wiley, New York, 2001), p.704
18. H.L. Gibson, *Photography by Infrared: Its Principles and Applications*, 3rd edn (Wiley, New York, 1978), p. 572
19. J.L. Miller, *Principles of Infrared Technology: A Practical Guide to the State of the Art* (The University of Michigan, Michigan, 1994), p. 578
20. L. Lowe, J.L. Ruvalcaba Sil, Antropología y Técnica. IIA-UNAM **6**, 41 (2000)
21. S.A.E. Johansson, J.L. Campbell, K.G. Malmqvist, in *Chemical Analysis: Series of Monographs on Analytical Chemistry and its Applications*, ed. by J.D. Widefrodner (Wiley, New York, 1995)
22. F. Riquelme, J. Alvarado-Ortega, J.L. Ruvalcaba-Sil, M. Aguilar-Franco, H. Porras-Muzquiz, Revist. Mexicana Cien. Geol. (2013, in press)
23. A. Kultys, Sulfur-containing polymers, in *Encyclopedia of Polymer Science and Technology* (Wiley, New York, 2002)
24. E.J. Goethals, J. Macromol. Sci. Part C **2**(1) (1968)
25. F.R. Orthous-Daunay, E. Quirico, L. Lemelle, P. Beck, V. de Andrade, A. Simionovici, S. Derenne, Earth Planet. Sci. Lett. **300**, 321–328 (2010)
26. M.J. Morra, S.E. Fendorf, P.D. Brown, Geochim. Cosmochim. Acta **61**, 683–688 (1997)
27. D.C. Koningsberger, R. Prins (eds.), *X-ray Absorption: Principles, Applications, Techniques of EXAFS, SEXAFS, and XANES*, vol. 91 (Wiley, New York, 1988)
28. A.W. Schroth, B.C. Bostick, M. Graham, J.M. Kaste, M.J. Mitchell, A.J. Friedland, J. Geophys. Res. **122**, GO4011 (2007)
29. K. Xia, F. Weesner, W.F. Bleam, P.R. Bloom, U.L. Skyllberg, P.A. Helmke, Soil Sci. Soc. Am. J. **62**, 1240–1246 (1998)
30. J. Prietzel, A. Botzaki, N. Tyufekchieva, M. Brettholle, J. Thieme, W. Klysubun, Environ. Sci. Technol. **45**(7), 2878–2886 (2011)
31. D. Solomon, J. Lehmann, C.E. Martinez, Soil Sci. Soc. Am. J. **67**, 1721 (2003)
32. D. Solomon, J. Lehmann, I. Lobe, C.E. Martinez, S. Tveitnes, C.C. Du Preez, W. Amelung, Eur. J. Soil Sci. **56**, 621–634 (2005)
33. M.A. Vairavamurthy, D. Maletic, S. Wang, B. Manowitz, T. Eglinton, T. Lyons, Energy Fuels **11**(3), 546–553 (1997)
34. F. Riquelme, J.L. Ruvalcaba-Sil, J. Alvarado-Ortega, Boletín de La Sociedad Geológica Mexicana **61**(2), 177–183 (2009)
35. J.L. Ruvalcaba Sil, L. Manzanilla, E. Melgar, R. Lozano Santa Cruz, X-Ray Spectrom. **37**, 96–99 (2008)
36. P. Van Espen, K. Janssens, J. Nobels, Chemomet. Intell. Lab. Syst. **1**(1), 109–114 (1986)
37. M. Newville, J. Synchrotron Radiat. **8**, 96–100 (2001)
38. B. Ravel, M. Newville, J. Synchrotron Radiat. **12**, 537–541 (2005)
39. J. James (2007) The relevant regions of the electromagnetic spectrum, in *Spectrograph Design Fundamentals*, vol. 6–9 (Cambridge University Press, Cambridge, 2007)
40. C. Bridgman, H.L. Gibson, Stud. Conserv. **8**(3), 77–83 (1963)
41. B. Fiske, L.S. Morenus, Book Paper Group Ann. **23**, 21–32 (2004)
42. G. Verhoeven, J. Archeol. Sci. **35**, 3087–3100 (2008)
43. L. Calvillo-Canadell, S. Cevallos-Ferriz, L. Rico-Arce, Rev. Palaeobot. Palynol. **160**(3–4), 126–134 (2009)
44. M.B. McBride, *Environmental Chemistry of Soils* (Oxford University Press, New York, 1994), p. 406
45. P. Tafforeau, R. Boistel, E. Boller, A. Bravin, M. Brunet, Y. Chaimanee, P. Cloetens, M. Feist, J. Hoszowska, J.-J. Jaeger, R.F. Kay, V. Lazzari, L. Marivaux, A. Nel, C. Nemoz, X. Thibault, P. Vignaud, S. Zabler, Appl. Phys. A Mater. Sci. Process. **83**, 195–202 (2006)
46. M. Lak, D. Néraudeau, A. Nel, P. Cloetens, V. Perrichot, P. Tafforeau, Microsc. Microanal. **14**, 251–259 (2008)
47. O. Nuyken, G. Reuschel, F. Siebzehnruebl, Makromol. Chem., Macromol. Symp. **26**, 313–331 (1989)

Mater. Res. Soc. Symp. Proc. Vol. 1618 © 2014 Materials Research Society
DOI: 10.1557/opl.2014.466

Amber from México: *Coahuilite, Simojovelite and Bacalite*

Francisco Riquelme[1,2], José Luis Ruvalcaba-Sil[2], Jesús Alvarado-Ortega[3], Emilio Estrada-Ruiz[4], Martin Galicia-Chávez[5], Hector Porras-Múzquiz[6], Vivian Stojanoff[7], D. Peter Siddons[7], Lisa Miller[7]

[1] Posgrado en Ciencias Biológicas, Universidad Nacional Autónoma de México, Cuidad Universitaria, C.P. 04510, D. F., Mexico.
[2] Instituto de Física, Universidad Nacional Autónoma de México. Apartado Postal 20-364, Mexico D.F. 01000, Mexico. e-mail: riquelme.fc@gmail.com
[3] Instituto de Geología, Universidad Nacional Autónoma de México, Ciudad Universitaria, Mexico D.F. 01000, Mexico.
[4] Escuela Nacional de Ciencias Biológicas, Instituto Politécnico Nacional, Mexico DF 11340, Mexico.
[5] Grupo MINOSA, Unidad Minerales Monclova, Coahuila 26350, Mexico.
[6] Museo de Múzquiz, Múzquiz Centro, Coahuila 26340, Mexico.
[7] Photon Science Directorate, Brookhaven National Laboratory, Upton, New York, USA.

ABSTRACT

Coahuilite, a new variety of amber is described from the Late Cretaceous Olmos Formation (ca. 73 Ma.), Coahuila, north of México. This amber is totally distinct chemically and stratigraphically from the Miocene Chiapas amber (ca. 23-13 Ma.), Southern México, which according to mineral nomenclature is currently known as *Simojovelite* var. nov. Additionally, an emended description of *Bacalite* is proposed, based on the physicochemical analysis and geological record of a fossil resin recently recovery from the Late Cretaceous El Gallo Formation (ca. 73 Ma.), Baja California, northwestern México. The results are supported by characterization of such ambers using synchrotron-based Infrared (FTIR) microspectroscopy.

INTRODUCTION

Fossil resins are natural occurring plant exudates that preserve chemical signatures of terpenoids, organic acids and mineral salts, which are associated with particular tree species, mineral identity and geological deposits. Consequently, there are several questions that arise regarding botanical affinities, fossil record and organic mineral nomenclature [1,2]. The Miocene amber-bearing rocks from the Chiapas Highlands spanning in age from 23 to 13 Ma., have been long considered as the only geological deposit of amber in México [1], (Figure 1). However, over the past two years a new variety of amber, not previously described, has been collected from a series of coal-rich beds near Palaú, Coahuila, north of México (Figure 1). These strata belong to the Olmos Formation, dated as late Cretaceous, ca. 73 Ma. [3]. In addition, another variety of fossil resin has been recently collected by the present authors (Alvarado-Ortega s. str.) from the Late Cretaceous fossiliferous site known as 'El Gallo', ca. 73 Ma., near El Rosario, Baja California (Figure. 1), about 344 km from the city of Ensenada [4,5]. The first record of fossil resin from this geographic area has been previously reported by [6]. As a result of several field trips between 1962 and 1965, Langenheim and co-workers described three sites towards the

south of El Rosario with fossil resins remains that they interpreted as amber. Initially, the term of *Bacalite*, erected in the amber nomenclature, was proposed by Buddhue since 1935, for a new variety of amber that he assumes came from Baja California, in spite of the ambiguous origin and age of these samples at the first [7,8]. Later, based on the geological explorations, Langenheim *et al*. [6,8] suggest that the Cretaceous rocks in the vicinities of El Rosario were probably the source of *Bacalite.*

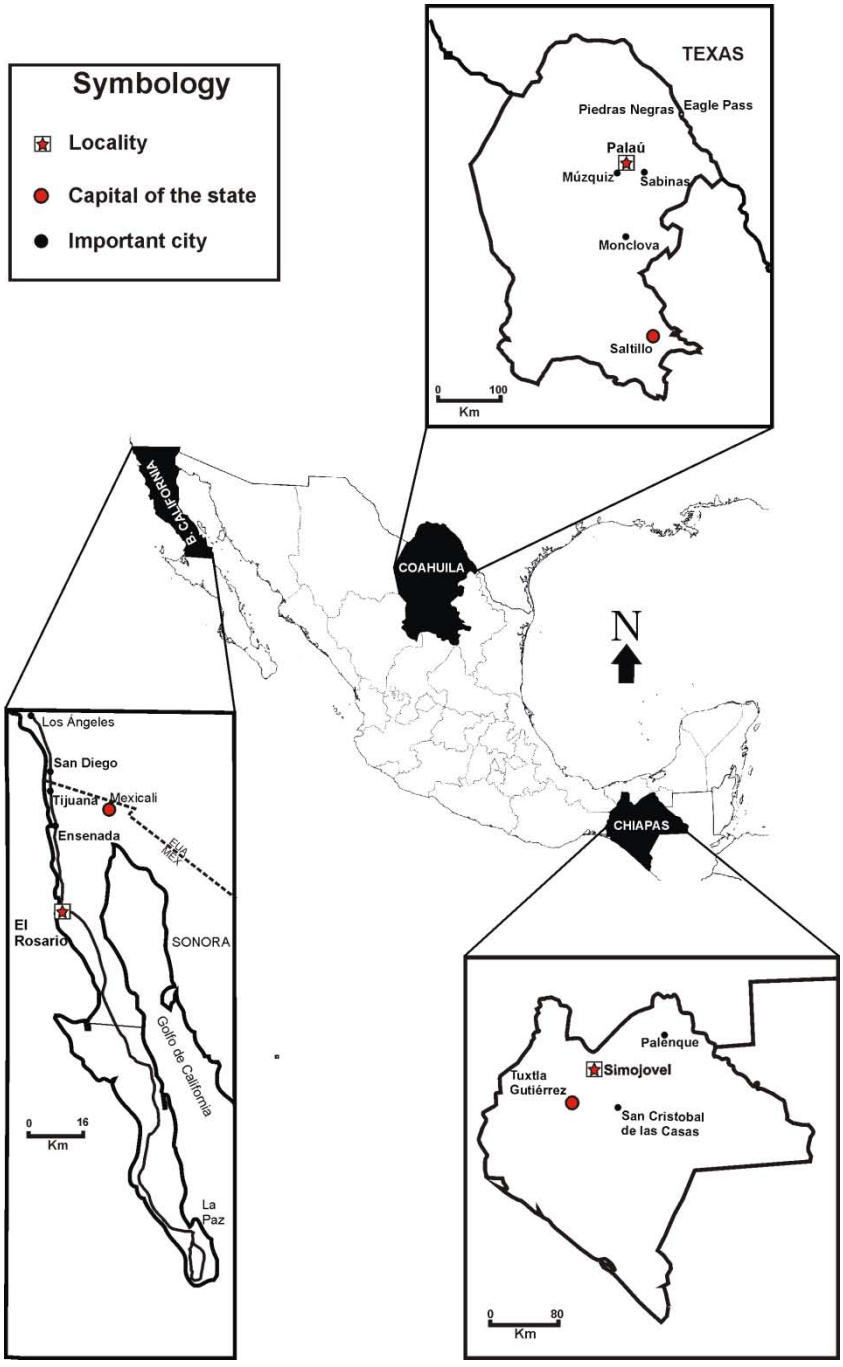

Figure 1. Location of amber deposits in México.

Infrared spectroscopy (IR) is widely used for analytical studies of fossil and recent plant resins [9-12]. The IR spectrum shows particular fingerprints regions related to identity and botanical affinities of both amber and recent resins. This allows to elucidate the provenance, botanical affinities and mineral species of ambers and others fossil resins [1,9, 13-14]. The assignments of infrared spectral features in fossil and recent resins have been published in numerous works [11-12,14]. In the present study, amber samples recently collected from the geological deposits of Chiapas, Coahuila and Baja California, México, have been characterized using Synchrotron-based Infrared (FTIR) microspectroscopy, with direct implications in fossil resin nomenclature.

MATERIAL AND METHODS

Samples

Amber from Coahuila was recovery in a section of the Late Cretaceous Olmos Formation, at the coal mine known as "Los Menores", near Palaú, northern Coahuila, Mexico (Figure 1). Amber from Chiapas was collected from the Miocene Mazantic and Balumtum strata at the amber site known as "La Pimienta", near Simojovel, in the Chiapas Highlands, Mexico (Figure 1). Amber from Baja California was collected from rocks at the Late Cretaceous fossiliferous site known as "El Gallo", near El Rosario, northern Baja California, Mexico (Figure 1).

Micro-FTIR analysis

The absorption spectra were collected in the mid-IR region from 4000 to 650 cm^{-1} range using a MCT-A (Mercury Cadmium Telluride) detector equipped with a Nicolet Continuum IR microscope at U2B beamline of the National Synchrotron Light Source, Brookhaven National Laboratory. The spectral resolution was set to 4 cm^{-1} and 256 scans/ pixel. Baseline correction was performed by concave rubberband at 5 iterations and 50 points using Opus V6.5 software. Micro-FTIR mapping was performed using the synchrotron source, with a beam aperture size of 60 x 60 microns and Omnic V7.2 software was used for IR-images processing. IR spectra were collected from polished, freshly fractured samples that were microscopically extracted from the hardened amber with no embedded inclusions or mineral crusts. Sample thickness was less than 50 μm to avoid IR spectra oversaturation. For a less time-consuming sample preparation, pelletization was not needed as seen in [12]. This also prevents the signal distortion of hydroxyl (OH^-) groups, which are characteristic in ancient resins as demonstrated by Tappert *et al.* [14]. The basics of infrared analysis using a synchrotron light source is presented elsewhere [15-16].

RESULTS AND DISCUSSION

Coauhilite *var. nov.*

Geological setting.

This amber was found in rocks from the Olmos Formation, dated as late Cretaceous, Campanian-Maastrichtian [3]. This geological unit consists mainly of alternating sequences of

sandstones, fine to coarse conglomerates and clays that were deposited in a deltaic plain environment [17]. Interbedded mud-clays and bituminous coal associated with swamps and lagoons are also exposed in these strata. Fossil plant remains including, leaves, fruits and wood are commonly collected in these rocks. The fossil plant assemblage is linked to a paratropical rainforest [17-18]. Accordingly, amber was deposited in the sediments associated with the forest that produced the resin; no other transport from foreign sediments is observable.

Locality and age

The coal mine known as "Los Menores", near Palaú, Coahuila, México. Located at 27° 50' 57" N, 101° 24' 20" W. This coal deposit belongs to the Late Cretaceous Olmos Formation, ca. 73 Ma. (Figure 1).

Etymology

For the State of Coahuila, the amber-bearing coal beds are exposed at the north of the state, in the so-called "Region Carbonífera".

Description

In polished samples, *Coahuilite* shows a vitreous glossiness from translucent to greasy, with a yellow color, varies from blackish to orange-brown, is flexible, elastic and resistant to fracture, with mineral gypsum hardness, not soluble in alcohol or acetone, resistant to soft acids attack, is a non-fossiliferous amber, soil fragments and indeterminate plant remains are only observable embedded into resin matrix.

Figure 2 shows the results of micro-FTIR analysis of freshly fractured samples. The broad absorption band centered at 3287 cm-1 is assigned to symmetrical stretching of O-H bonds from the carboxylic acid remains. Another strong C-H stretch at 2929-2865 cm-1 is attributed to molecular arrangement of CH3 methyl and methylene end groups, which is characteristic of cyclic ring structure from tree resins. There is also a strong C=O carbonyl stretch at 1707-1600 cm-1 corresponding to C=O carboxylic esters and acids groups from plant resins. The IR map shows the chemical profile of cyclic ring (also called the resin acid), carbonyl compounds and aliphatic hydrocarbons in amber; which are diagnostic features in fossil and recent resins [Fig. 2b]. Absorption features of C-H bending centered at 1411 and 1308 cm-1 are assigned to aliphatic hydrocarbons (Figure 2b). The prominent sharp peak at 1513 cm-1 is attributed to C-C stretching, which corresponds to aromatic hydrocarbons from volatile-rich resins. This absorption band resembles those observed in resin spectra from extant trees of the pine family and liquidambar [14-19]. Other absorption features located at 1220, 1070 and 1016 cm-1 also show similarities with those present in volatile-rich resins [14]. Additional peaks at 812 and 753 cm-1 are assigned to terminal olefins. Other organic salts are present at concentrations close to the detection limits as indicated by the weak peaks and shoulders observed in the 1500-650 cm-1 region. Accordingly, the Cretaceous amber from Coahuila resembles with volatile-rich, aromatic diterpenoid resins [14, 20].

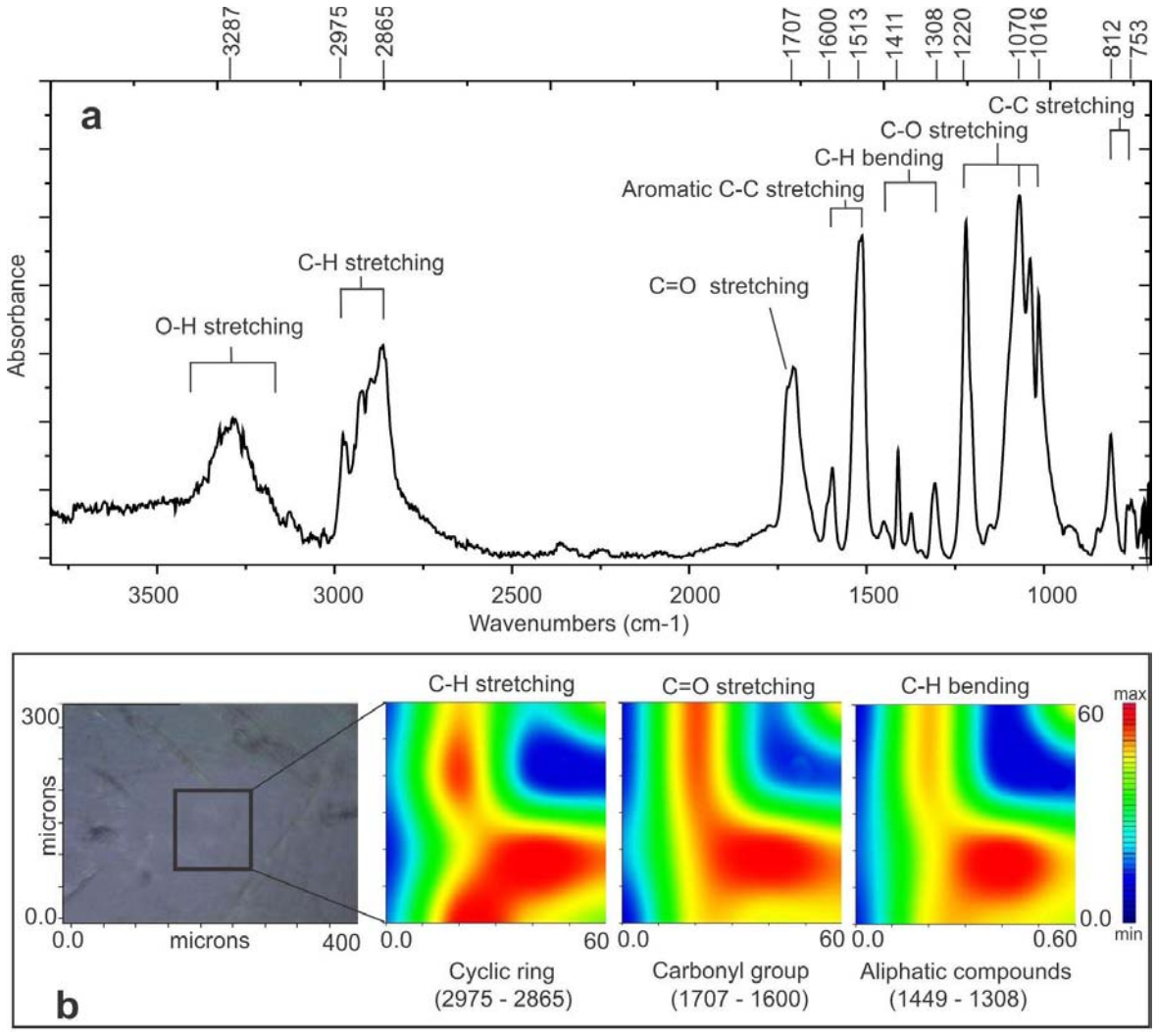

Figure 2. Representative synchrotron infrared spectrum of *Coahuilite* (a) and infrared images of diagnostic chemical signatures of amber: cyclic ring, carbonyl group and aliphatic hydrocarbons (b).

Remarks

Amber occurs in the coal sediments as nodules or in sheets of variable thickness and no longer than 15 cm. Heavy compressed due lithification process, this amber shows encrusted textures to bright, semicrystalline surfaces due to weathering. Molds and crust linked to tree bark are also observable in amber with sheet forms. Several amber samples (mostly nodular shapes) show depositional episodic layers; this is consistent with different events of production. The resin was successively accumulated forming a hardened mass with multilaminar layers. Living resin-producing trees show similar seasonal variations with increased resin depositions during summer as demonstrated in [1].

Simojovelite var. nov.

Geological setting

This amber occurs in rocks from the Mazantic and Balumtum Formations, dated as early-middle Miocene in age [21]. The amber deposits are associated with nearshore and lowlands sediments [22]. Fossil biota, both plants and animals, are also linked to a subtropical forest [23, 24].

Locality and age

The amber mine known as "La Pimienta", Municipality of Simojovel de Allende, Chiapas, México. Located at 17° 9' 21" N, 92°45' 9" W. The amber section from "La Pimienta" belongs to the Mazantic and Balumtum strata, early-middle Miocene, ca. 23-13 Ma.

Etymology

For the town of Simojovel, Chiapas. Currently is the area with the most profuse amber sites.

Description

In hand samples from geological deposits, *Simojovelite* occurs in diverse shapes and sizes, such as encrusted lumps, drops, multi-laminated plates, stalactite-like tubes and cones, and cake-shaped agglomerates. These forms do not necessarily show the original state of tree secretions, because they can be transformed by intense compression and chemical rearrangements during burial and diagenetic processes. A diverse range of color from the most common golden-yellow to ochre, orange, reddish, brown, blackish, citrine-yellow, milky-yellow, can be observed in polished *Simojovelite* samples, and rarely, green and blue as seen by refraction light. Its glossiness is vitreous translucent, with gypsum-like hardness, light weight and heavy fracture planes. Not soluble in alcohol or acetone, this amber is resistant to soft acid attacks but fractioned by liquid nitrogen. Its glass transition temperature is about 100 °C. In thin sections, *Simojovelite* shows longitudinal reddish lines, copious bubbles and lumps with indeterminate liquids (essential oils from the resin?) preserved within them. *Simojovelite* is remarkable fossiliferous amber: microorganisms, plants and animals with cellular features are well-preserved embedded within it.

Figure 3 shows the FTIR spectrum with a broad absorption band centered at 3400 cm-1 with variable amplitude; this is assigned to symmetrical stretching of O-H bonds from the carboxylic acid remains. Other absorption feature located at ≈3200 cm-1 linked to C-H monoalkyl stretch shows a deviation indicating a heavy overlapping due chemical alteration by fossilization. The strong C-H stretching vibration at both prominent peaks 2923 and 2860 cm-1 of CH3 methyl and methylene end groups reveals the cyclic ring structure from *Simojovelite*. The prominent peak at 1700 cm-1 attributed to strong C=O carbonyl stretch of carboxylic esters and acids groups is very characteristic for this type of amber [6]. The IR maps of both cyclic ring and carbonyl compound show a variable distribution into resin microfabric (Figure 3b). Absorption bands at 1440-1378 cm-1 region of C-H aliphatic hydrocarbons and its

corresponding IR map in Figure 3b, they show doublet bands, which is consistent with a crystalline lattice effect in the resin. The absorption feature at 1235-970 cm-1 region with several peaks and shoulders is attributed to C-O stretching of aromatic esters and secondary alcohols. The weak C-C stretching at ≈846 cm-1 of unsaturated olefins is also observed (Figure 3).

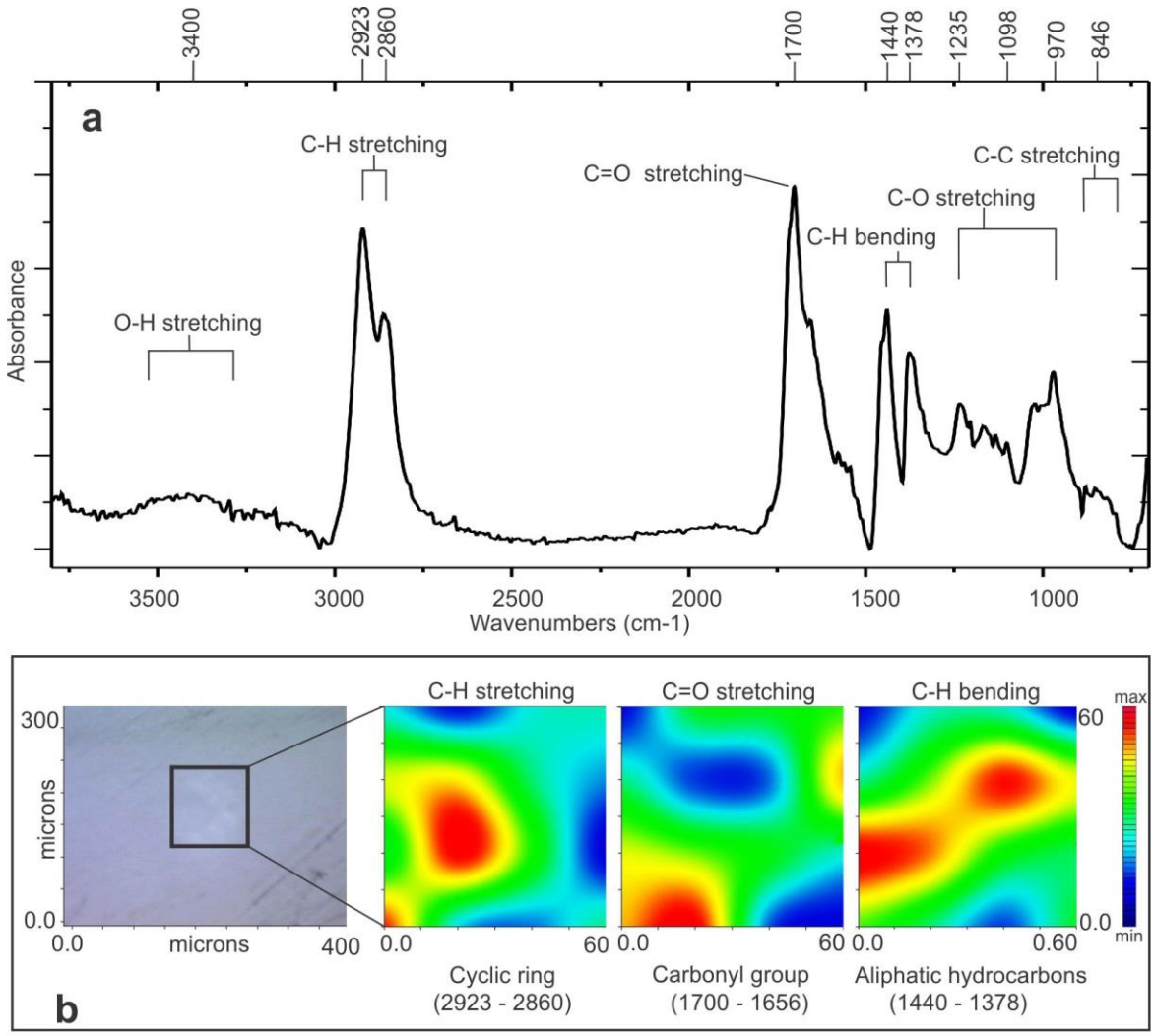

Simojovelite var. nov., Amber, Miocene, Chiapas

Figure 3. Representative synchrotron infrared spectrum of *Simojovelite* (a) and infrared images of diagnostic chemical signatures (b).

Remarks

This type of amber is widely known since pre-Columbian times and also formally studied for several disciplines, including paleontology, archeology, botany and chemistry from about 1959 [1, 23]. However, its inclusion into the organic mineral nomenclature never was considered

before. Amber from Simojovel is closely related with the plant exudates of the living species of *Hymenaea* tree [*sensu* 25]. Further analyses of amber collected from two major deposits near Simojovel and Totolapa showed the amber of these two sources to be chemically identical [1, 26]. Both also share the same geological record [21, 24, 27]. Accordingly, the same generic mineral name can be used for this type of amber widely distributed in several sites at the Chiapas Highlands, including Totolapa, Simojovel and Palenque.
Based on comparative chemical studies, Langenheim [25] suggested that this amber best matches with a resinous exudate of the extant tree species *Hymenaea courbaril*. Additionally, the IR spectra features of *Simojovelite* (particularly in the fingerprint region at 1500-650 cm-1) as presented here, also resembles those observed in *Hymenaea verrucosa* resin (African copal), as seen in the spectra libraries elsewhere [i.e. 28]. This may suggests that *Simojovelite* preserves chemical signatures in an intermediate position between *H. courbaril and H. verrucosa* extant resins. A new revision of botanical affinities of amber from several sites in the Chiapas Highlands, which increase the sampling, is currently in progress for the authors of the present paper.

Bacalite [7]

Geological setting

Amber is found in shoreline sediments at the fossiliferous site informally known as El Gallo Formation, dated as late Cretaceous in age, Campanian-Maastrichtian boundary [4, 29]. The amber-bearing sediments are composed of gray to yellowish-brown mud and fine-grained sandstones, which have been deposited in a transitional coastal plain. Other fossils, such as fishes, reptiles, dinosaurs, mammals, marine invertebrates and wood, are typically collected from this area [4, 29-30]. Amber occurs within carbonaceous lumps no larger than 5 cm in size. Dissolved organic matter, carbonized wood, leaf impressions and indeterminate bone fragments are also interbedded with amber lumps, which are found fractioned and dispersed into fine homogeneous sands. This suggests that amber was redeposited from the original sediments of the resin-producing forest. Probably, amber comes from older rocks.

Locality and age

The fossiliferous site known as “El Gallo”, 5 km NW of El Rosario, Baja California, México. Located at 30º 04´ 2" N, 115º 47´ 0.5" W. The strata of “El Gallo” are late Cretaceous, ca. 73 Ma. (Figure 1).

Etymology

As assigned by Buddhue, 1935. Name derived from syllables Ba: Baja and Cal: California.

Amended description

Bacalite is reddish to brownish yellow, with glossiness from vitreous translucent to cloudy, not soluble in alcohol or acetone, crudely polished by weathering, brittle and crystalline,

heavy fractioned, appears as small rounded lumps of a few centimeters in size, is a non fossiliferous amber, only soil and pollen fragments are hardly recognizable trapped within it.
As shown in amber FTIR spectrum (Figure 4), the stretching O-H band centered at 3420 cm-1 is reduced and peaked, strongly altered by fossilization. The absorption feature bell-shape centered at ≈3180 cm-1 attributed to C-H stretching terminal alkenes is also altered. In contrast, the absorption band at of CH3 methyl/methylene groups from the cyclic ring structure is prominent and sharp with particular three peaks at 2910, 2870 2845 cm-1. The other important peak at 1693 cm-1 assigned to strong C=O carbonyl stretch of carboxylic esters and acids is broad at the bottom and sharp at top.

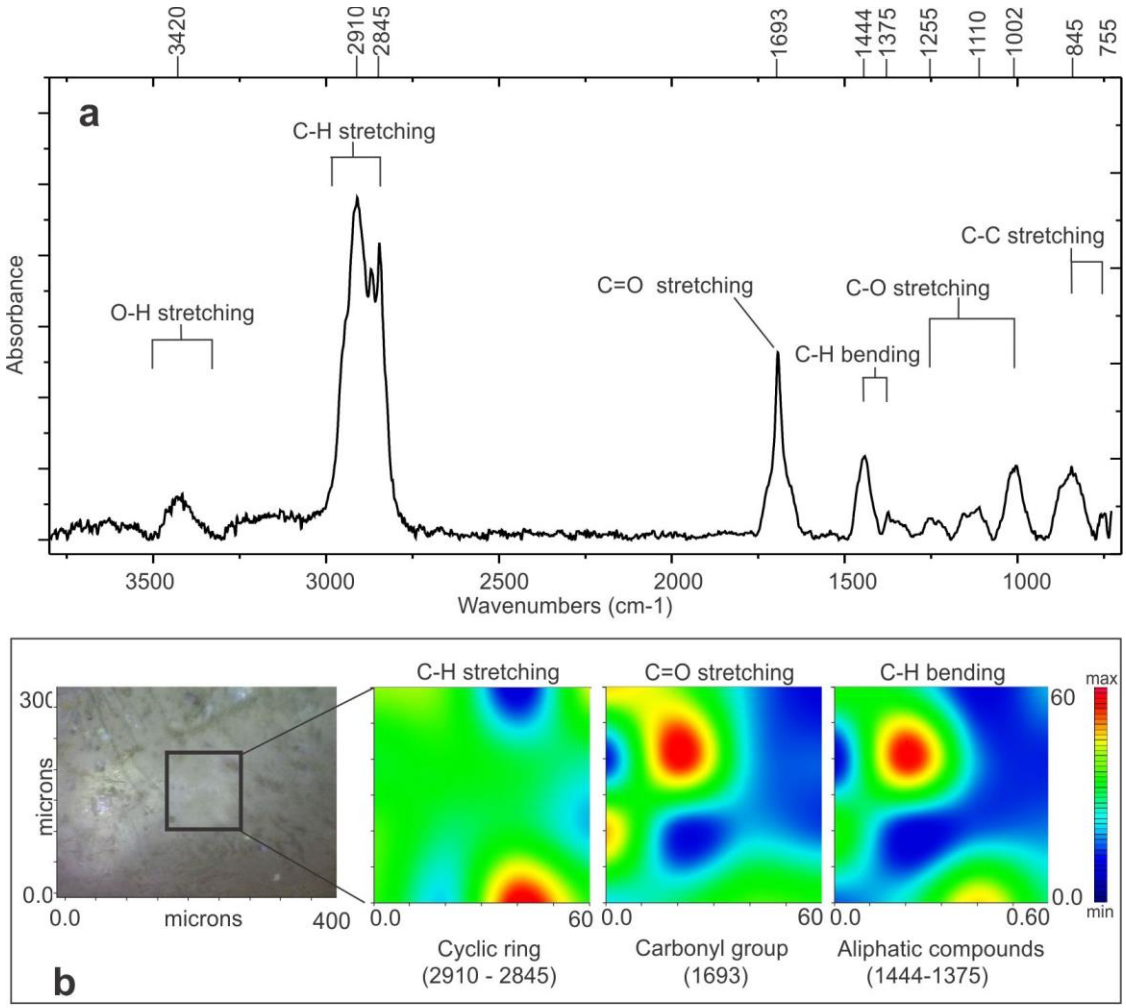

Bacalite, Amber, Cretaceous, Baja California

Figure 4. Representative synchrotron infrared spectrum of *Bacalite* (a) and infrared images of diagnostic chemical signatures (b).

Reactive mineral impurities increasing during burial and fossilization also affect the carbon backbones of fossil resins; this is reflected in IR spectra and chemical profile (Fig. 4b). Additional particular peak at 1444 cm-1 of aliphatic CH-methyl group are sharp and well-

defined, whereas peaks at 1255, 1110 and 1002 cm-1 of unsaturated and aromatic esters are reduced and overlapping. Finally, the peak at 845 cm-1 of unsaturated olefins is also detected. According to above, the IR spectrum of *Bacalite* resembles those observed in resinous exudates from extant conifers trees, such as colophony or rosin from the pine family, which grow in sandy soil near the sea [14, 20, 31].

Remarks

The first report of *Bacalite* was ambiguous [7]. The composition, botanical affinities and physical characteristics of *Bacalite* were not described subsequently to geological fieldworks surrounding El Rosario [6]. The location of these amber samples is today uncertain. In the present paper, the term of *Bacalite* is accepted but it is proposed an amended description within the amber nomenclature, according to description of recently recovery samples as presented here. Therefore, this Cretaceous amber from El Rosario, Baja California, México, associated with resins from conifer trees, is currently known as *Bacalite*.

CONCLUSIONS

The synchrotron-based FTIR microspectroscopy support *Coahuilite,* as a new variety of amber from the Cretaceous of Northern México. Also provides the first chemical data to describe the botanical affinities of *Bacalite.* Currently both fossil resins are the oldest record of amber from México. Since past decades, the only amber known from México with certainty was the amber from the Miocene of Chiapas, in southern México, which is closely related with amber from the Neogene Dominican Republic and the Antilles because share botanical affinities and geological history. However, amber from the Cretaceous of Baja California and Coahuila are strongly associated with geological ages and botanical affinities of fossil resins from North America. This study represents the first approach to characterize these types of ambers with implications for organic mineral nomenclature compared with elsewhere.

ACKNOWLEDGMENTS

Authors thank Dra. Marina Vega from Centro de Geociencias-UNAM; Dr. Eli Stavitski from National Synchrotron Light Source at the Brookhaven National Laboratory; Dr. Lauro Bucio from Instituto de Física-UNAM; Dr. Mario Ramos from Instituto de Geología-UNAM; Bibiano Luna from the Museo del Ámbar de Chiapas, and Luis Zuñiga from the Museo del Ámbar Lilia Mijangos, Chis., for technical support. The editor and anonymous reviewers provided useful comments that improved the manuscript. This research was supported by the Posgrado en Ciencias Biologicas at the Universidad Nacional Autónoma de México, financied by a PhD/CONACYT grant. Also it was partially supported by UNAM-PAPIIT IN106011 and UNAM-PAPIIT IN402813 grants, as well as CONACYT 131944 MOVIL II endowment.

REFERENCES

1. J. H., Langenheim, *Plant resins: chemistry, evolution, ecology and ethnobotany* (Timber Press, 2003) p. 586.
2. K.B. Anderson, R.E. Winans, R.E. Botto, *Organic Geochemistry* **18**, 829-841 (1992).

3. S. Eguiluz de Antuñano, "Geologic evolution and gas resources of the Sabinas Basin in northeastern Mexico" in *The western Gulf of Mexico Basin: Tectonics, sedimentary basins, and petroleum systems*, C. Bartolini, R. T. Buffler, and A. Cantú-Chapa (eds.), AAPG Memoire **75**, 241-270. (2001).
4. W.J. Morris, *Journal of Paleontology* **55** (2), 453-462 (1981).
5. M.E. Johnson, J. Ledesma-Vazquez, B. G. Baarli, *Journal of Coastal Research* **223**, 574-580 (2006).
6. J. H. Langenheim, C. W. Beck, *Science* **149**, 52–54 (1965).
7. J.D. Buddhue, 1935. "A variety of amber from Baja (Lower) California, Mexico", in *Rocks and Minerals*, (Peekskill, 1935) vol. 10, p. 171.
8. R.L. Lanhenheim, J.D. Budduhe, G. Jelinek, *Journal of Paleontology* **39**, 283-287 (1965).
9. C. Beck, E. Wilbur, S. Meret, *Nature* **201**: 256-257 (1964).
10. J.H. Langenheim, C.W. Beck, *Catalogue of infrared spectra of fossil resins (ambers) I. North and South America*. Botanical Museum Leaflets (Harvard University, 1968.) vol. 22 (3), pp. 65-120.
11. E. Trevisani, C.A. Papazzoni, E. Ragazzi, G. Roghi. G., *Palaeogeography, Palaeoclimatology, Palaeoecology* **223**, 260-274 (2005).
12. A.P. Wolfe, R. Tappert, K. Muehlenbachs, M. Boudreau, R. C. McKellar, J. F. Basinger, A. Garrett, *Proceedings of Royal Society* B **276**, 3403-341 (2009).
13. N. Vavra, "Chemical Characterization of Fossil Resins ("Amber")" in *A Critical Review of Methods, Problems and Possibilities: Determination of Mineral Species, Botanical Sources and Geographical Attribution*. *Proceedings of a Symposium held in Neukirchen am Großvenediger 1990*, Abh.Geol. B.-A: 147-157 (1993).
14. R. Tappert, A.P. Wolfe, R.C. McKellar, M.C. Tappert, K. Muehlenbachs, *Int. J. Plant Sci.* **172**,120-138 (2011).
15. G.L. Carr, G.P. Williams, "Infrared microspectroscopy with synchrotron radiation" in *Accelerator-Based Infrared Sources and Applications, SPIE Conf. Proc*. **3153**, 51-59 (1997).
16. P. Dumas, L. Miller, *Vib. Spectrosc.* **32**, 3–21 (2003).
17. E. Estrada-Ruiz, G.R. Upchurch, S.R.S. Cevallos-Ferriz. *Gulf Coast Association of Geological Societies Transactions* **58**, 273-283 (2008).
18. E. Martínez-Hernández, L. Almeida-Leñero, M. Reyes-Salas, Y. Betancourt-Aguilar, *Estudio palinógico para la determinación de ambientes en la cuenca Fuentes-Río Escondido (Cretácico Superior), región de Piedras Negras, Coahuila.* Instituto de Geología, Universidad Nacional Autónoma México, Revista **4**, 167-185 (1980).
19. National Gallery, "INR00225 *Liquidambar orientalis*" in *Infrared and Raman Users Group Spectral Database, Edition 2007*. Edited by B. Price, B. and B. Pretzel, (IRUG, 2007) vol. 1 (8), pp. 368.
20. M.R. Derrick, D. Stulik, J.M. Landry, *Infrared Spectroscopy in Conservation Science* (The Getty Conservation Institute, 1999) p. 235: Appendix I.
21. Perrilliat, M., Vega, F., Coutiño, M., *Journal of South American Earth Sciences* **30**, 111-119 (2010).
22. A. Graham, A. *American Journal of Botany* **86** (1):17–31 (1999).
23. M.M. Solórzano-Kraemer, "Mexican Amber" in *Biodiversity of fossils in amber from the major world deposits*, edited by D. Penney (Siri Scientific Press, 2010) pp. 42-56.

24. F. Riquelme, J. Alvarado-Ortega, M. Ramos-Arias, M. Hernández, I. Le Dez, T.A. Lee-Whiting, J.L. Ruvalcaba-Sil. *Historical Biology*, 1-13 (2013). DOI: 10.1080/08912963.2013.778843
25. J.H. Langenheim, *Botanical Source of Amber from Chiapas, Mexico (Fuente botánica del ámbar de Chiapas, México),* Ciencia **24,** 5-6, pp. 201-210 (1966).
26. J.B. Lambert, J.S. Frye, T.A. Lee, C.J. Welch, G. Poinar, *Archaeological Chemistry* **4**, 381-388 (1989).
27. C. Durán-Ruiz, F. Riquelme, M. Coutiño-José, G. Carbot-Chanona, G. Castaño-Meneses, M. Ramos-Arias, *Canadian Journal of Earth Sciences* **50** (5), 495-502 (2013).
28. Victoria and Albert Museum, 2007. "INR00165 *Hymenaea verrucosa* resin" in *Infrared and Raman Users Group Spectral Database, Edition 2007*. Edited by B. Price, B. and B. Pretzel, (IRUG, 2007) vol. 1 (8), pp. 165.
29. M.E. Johnson, J. Ledesma-Vazquez, H.C. Clark, J.A. Zwiwbel, *Geological Society of America Bulletin* **108**, 708-721 (1996).
30. A. Prieto-Márquez, L.M. Chiappe, S.H. Joshi, *PLoS ONE* **7** (6), e38207 (2012).
31. Hungarian National Museum, 2007. "INR00341 Colophony American" in *Infrared and Raman Users Group Spectral Database, Edition 2007*. Edited by B. Price, B. and B. Pretzel, (IRUG, 2007) vol. 1 (8), pp. 341.

Historical Biology, 2013
http://dx.doi.org/10.1080/08912963.2013.778843

Taylor & Francis
Taylor & Francis Group

A fossil stemmiulid millipede (Diplopoda: Stemmiulida) from the Miocene amber of Simojovel, Chiapas, México

Francisco Riquelme[a]*, Jesús Alvarado-Ortega[b], Mario Ramos-Arias[b], Miguel Hernández[c], Isabelle Le Dez[d], Thomas A. Lee-Whiting[d] and José Luis Ruvalcaba-Sil[e]

[a]*Posgrado en Ciencias Biológicas, Instituto de Física, Universidad Nacional Autónoma de México, AP 20-364, D.F., México;* [b]*Instituto de Geología, Universidad Nacional Autónoma de México, Circuito de la Investigación S/N, Ciudad Universitaria, 04510, D.F., México;* [c]*Posgrado en Ciencias Biológicas, Facultad de Ciencias, Universidad Nacional Autónoma de México, Circuito Interior S/N, Ciudad Universitaria, 04510, D.F., México;* [d]*Escuela de Arqueología, Centro Superior de Investigaciones México y Centroamérica, Universidad de Ciencias y Artes de Chiapas, Chiapas, México;* [e]*Instituto de Física, Universidad Nacional Autónoma de México, AP 20-364, D.F., México*

(*Received 11 December 2012; final version received 19 February 2013*)

A fossil millipede representative of the order Stemmiulida is described on the basis of a well-preserved adult female trapped in amber from the Miocene of Simojovel, Chiapas, south-eastern México. The fossil specimen is named as *Parastemmiulus elektron*, a new genus and species. As observed in extant stemmiulids, this fossil shows a reduced number of ocelli, the distal larger than the proximal, as well as a total of 46 trunk segments including 2 apodous segments in front of the telson. The head of this ancient stemmiulid has three ocelli and a Tömösváry organ, characteristics not reported before in Stemmiulida, requiring the diagnosis of the order to be emended.

http://zoobank.org/urn:lsid:zoobank.org:pub:361400A8-37D4-421F-B4FD-A0AE63BE538C

Keywords: Chiapas amber; Miocene; Stemmiulida; *Parastemmiulus*

Introduction

Millipedes (Diplopoda) are one of the earliest known air-breathing terrestrial animal groups. The modern forms of diplopods had differentiated by the Late Silurian (Almond 1985; Shear 1998; Shear et al. 2009; Shear and Edgecombe 2010). Although trackways from the Borrowdale Volcanic Group (Ordovician) have been attributed to millipedes (Johnson et al. 1994; Wilson 2006), the oldest unequivocal records of millipedes are the fossil specimens of *Albadesmus almondi*, *Pneumodesmus newmani* and *Cowiedesmus eroticopodus* from the mid-Silurian Cowie Formation in Scotland (Wilson and Anderson 2004). The fossil record of Diplopoda in México is extremely scarce, consisting only of ?*Xylobius mexicanus* Müllerried, 1942 from the Late Jurassic/Mid-Cretaceous, of which the taxonomic identity is still uncertain (Shear et al. 2009).

Millipedes are widely distributed in all subarctic environments including tropical and temperate forest, short-tree savannas, grasslands, coastal plains and deserts (Shelley 2007; Shelley and Golovatch 2011). Millipedes live in leaf litter, soil, beneath stones, bark, wood and caves. Millipedes have played an exceptional ecological role in terrestrial ecosystems from both temperate and tropical environments around the globe, as they are efficient biological agents of nutrient fluxes through soil detritus fragmentation (Crawford 1992).

Currently, millipedes comprise about 10,000 described species, representing 16 orders and 145 families and an estimated recent global fauna of more than 80,000 species (Shelley 2003, 2007). This makes them the third most diverse class of terrestrial arthropods after Insecta and Arachnida (Brewer et al. 2012). The Neotropical distribution of millipedes in México, Caribbean islands and Central and South America comprises between 1200 and 1800 species. Accordingly, there is an estimated about 498 species in 14 orders, 39 families and 117 genera distributed in México (Bueno-Villegas et al. 2004).

Most fossil millipedes preserved in amber are known from Baltic deposits dated as Eocene, including representatives of the orders Glomerida, Polydesmida, Chordeumatida, Julida, Polyzoniida and Polyxenida (Keilbach 1982). The Miocene Dominican amber includes numerous millipedes such as representatives of Glomeridesmida, Polyzoniida, Polydesmida, Spirostreptida, Siphonophorida and Stemmiulida (Shear 1981, 1987, 1998; Santiago-Blay and Poinar 1992; Pérez-Asso and Pérez-Gelabert 2001). Unfortunately, the single specimen interpreted as a stemmiulid by Santiago-Blay and Poinar (1992) is very

*Corresponding author. Email: riquelme.fc@gmail.com
This article was originally published with errors. This version has been amended. Please see Corrigendum (DOI: http://dx.doi.org/10.1080/08912963.2013.824264)

fragmentary (a headless adult female) and poorly preserved, so it is doubtful whether it could be accurately diagnosed.

The new species described in this work is based upon an exceptionally preserved specimen of Stemmiulida from the Miocene Chiapas amber deposits. Accordingly, this fossil represents the first unquestionable record of the order Stemmiulida, which provides a valuable record of the class from the Neogene.

Geological setting

The numerous amber-rich outcrops exposed nearby the town of Simojovel, State of Chiapas, México, constitute a Konservat-Lagerstätte with a large accumulation of fossil resin and one of the richest fossil assemblages of plants and animals from an ancient subtropical forest biome. Those amber-bearing beds are also exposed in the vicinities of the town of Huitiupán, Totolapa, Malpaso, Pueblo Nuevo Solistahuacán and Estrella de Belem in the Chiapas Highlands (Figure 1).

Historically, amber has been extracted since pre-Columbian peoples who primary settled in Simojovel, Huitiupán and Totolapa areas (Langenheim 2003; Lee-Whiting 2004). A traditional industry around amber craft still persists, typically extracting amber from outcrops surrounding Simojovel. The collection of the present stemmiulid has been possible through the efforts of local craftsman and the indigenous community-owned quarry of La Guadalupe, near the village of Guadalupe Victoria II, Municipality of Simojovel. This is located between coordinates 17°07′58″N and 92°48′19″W, at an altitude of 1587 m.s.l. (Figure 1). The amber-bearing beds of La Guadalupe represent the bottom of the Mazantic Shale strata, for which a Miocene age is suggested based on an associated mollusk assemblage (Perrilliat et al. 2010).

The Chiapas amber-bearing beds have been assigned to a section of the Mazantic Shale and Balumtum Sandstone strata (Early–Middle Miocene) exposed near the town of Simojovel (Langenheim 1966; Poinar 1992; Graham 1999; Grimaldi 2003; Perrilliat et al. 2010; among others). Lignites containing amber linked to La Quinta strata assigned to the transition between the Late Oligocene and Early Miocene have also been preliminarily mentioned in Frost and Langenheim (1974), and later in Poinar (1992) and Graham (1999). Other studies recently published suggest that amber from Simojovel has been deposited within the boundaries of the Early Miocene period (Vega et al. 2009; Perrilliat et al. 2010). In addition, a lower Middle Miocene age has been proposed by Solórzano-Kraemer (2007, 2010) linked to Dominican and Puerto Rican ambers based on their coeval insect faunas.

Paleobotanical affinities of Chiapas amber associated with a legume tree of the genus *Hymenaea* Linnaeus, 1753 have been published elsewhere (*sensu* Langenheim 1966; Lambert et al. 1989; Poinar 1992; Graham 1999; Poinar and Brown 2002; Calvillo-Canadell et al. 2009; among others).

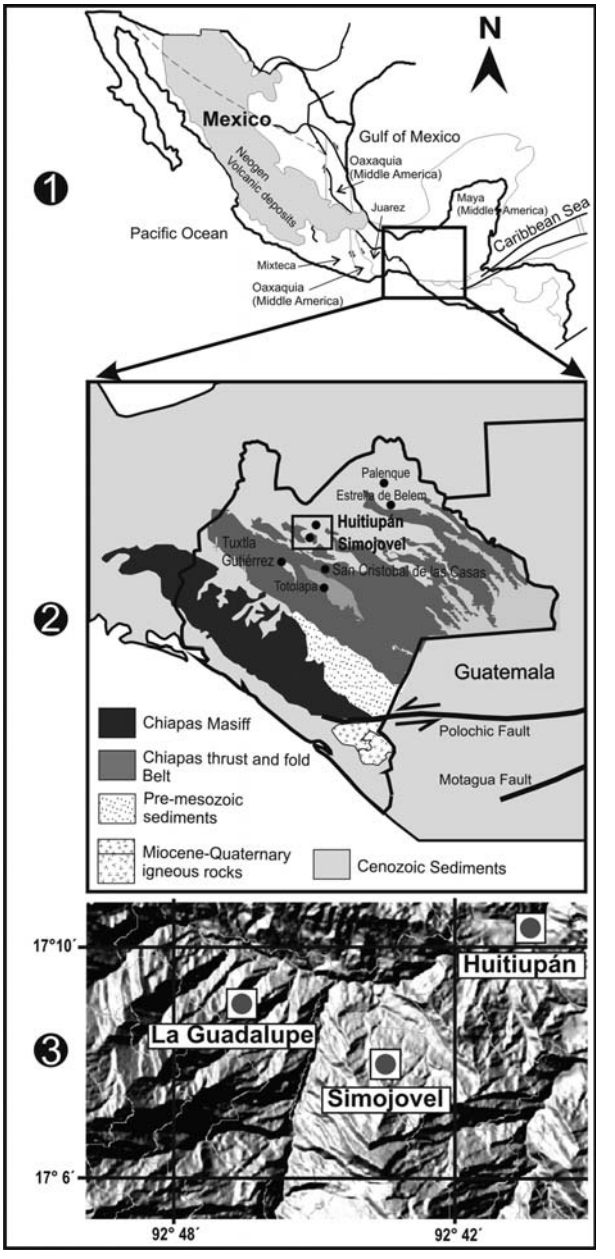

Figure 1. Location of Simojovel-Huitiupán amber-rich area and schematic representation of the Cenozoic sedimentary cover for Chiapas thrust–fold belt in the context of the Mexican tectonostratigraphic terranes (1) and (2); La Guadalupe amber-bearing deposit from where the specimen studied here was collected (3).

The Mazantic Shale and Balumtum Sandstone units are linked to nearshore and continental settings, which are part of the Cenozoic sedimentary cover from the geologic province referred as the Chiapas Thrust–Fold Belt (Figure 1) (Sedlock et al. 1993; Padilla and Sánchez 2007; Mandujano-Velázquez and Keppie 2009). Four tectono-sedimentary sub-regions have been identified in this geological province

(Meneses-Rocha 2001) and the Simojovel sections are included into the Eastern part of the geological sub-region described as the strike-slip fault. According to this, an oblique collision that formed E–W sinistral transcurrent faults and WNW-trending folds they moved and uplifted from the Oligocene to Middle Miocene (Meneses-Rocha 2001; Mandujano-Velázquez and Keppie 2009). This tectonic phenomenon switched the sedimentary regime affecting the depocentres from an open sea setting with carbonate platforms to confined paleobasins with continental influence associated with the Chiapas Massif (pre-Mesozoic basement), which produced a large volume of terrigenous sediments. Accordingly, the Highlands proliferated and the coastline migrated northward during the Late Miocene–Early Pliocene, in a manner that is consistent with the extinction of the amber paleobiota (Figure 2).

In this geological context, the amber deposits of Simojovel represent quite restricted outcrops with an apparently analogous sedimentary regimen. Those sections are composed of organic-rich lignite lenses, interbedded friable shales and non-fissile, coarse to fine grained sandstones. They also contain widely persistent grey to green bentonite-like clay, sandstone nodules, siltstone, bioclastic carbonates and stratified deposits of brown to red iron oxides. The Early to Middle Miocene sedimentary successions exposed at Simojovel show compositional changes in carbonate, siliciclastic and organic-rich carbonaceous beds that suggest a system eventually controlled by short-term cyclical changes in climate.

Materials and methods

Preparation. A relatively simple technique for sample preparation was used for microscopic analysis: amber has been cut and polished to get closer to the specimen. The micrographs were acquired based on apochromatic-zoom microscopy methods described in Riquelme et al. (2011).

Anatomical abbreviations. The nomenclature and anatomical abbreviations used in this manuscript follow Blower (1985) and Enghoff et al. (1993). *Abbreviations*: anm, antennomere; ca, cardo; cl, collum; oc, ocellum; cio, canal interocular; coa, canal between the ventral ocellum and antenna; ctd, central triangular depression of the head capsle; gl, gnathal lobe; gp, gnatochilarium; hyp,

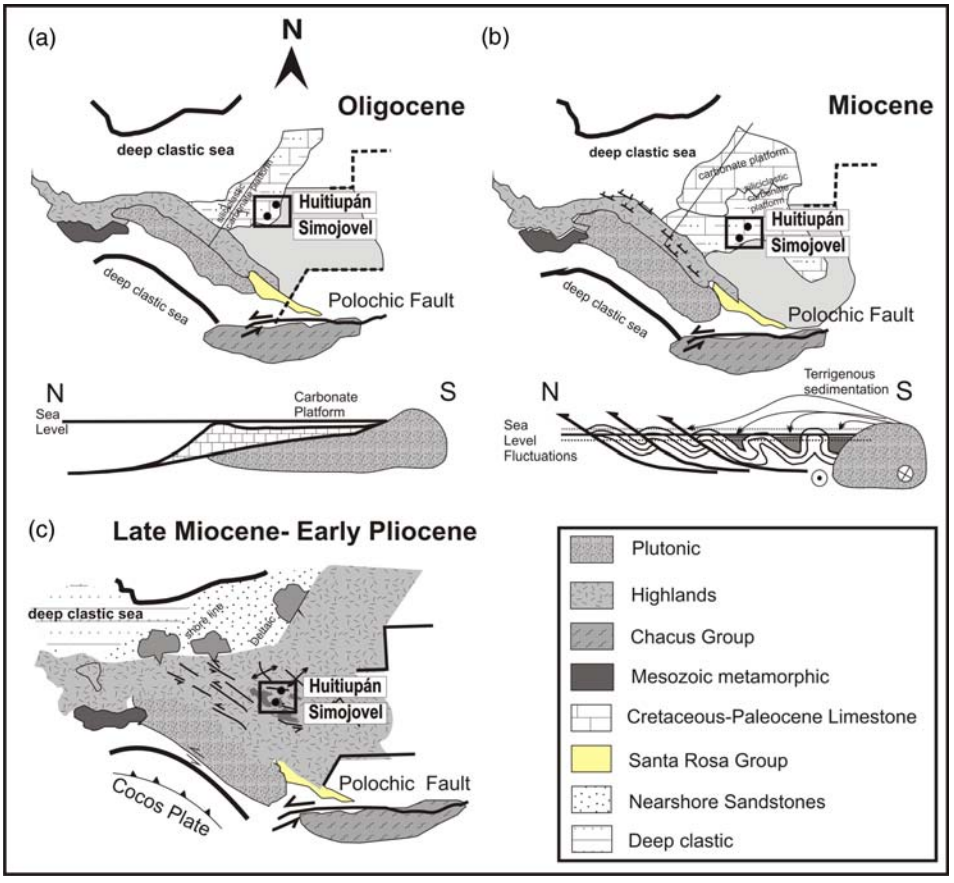

Figure 2. Schematic representation of tectonic and sedimentary evolution of Chiapas in the context of the depositional environment of amber Lagerstätte. The sedimentary pattern of carbonate platform during the Oligocene (a); the oblique convergence during the Oligocene–Middle Miocene with an intense sedimentary switch that produced isolated basins, which represents the amber deposition (b); the Highlands proliferate and the coastline has migrated northward during the Late Miocene–Early Pliocene (c); modified from Meneses-Rocha (2001).

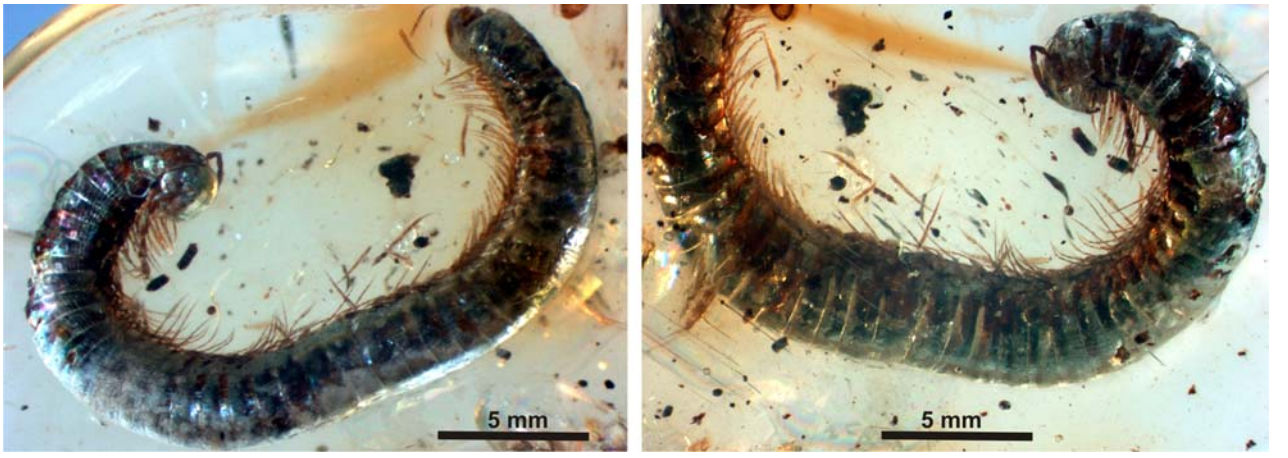

Figure 3. INAH.2661.PF.14.IPMP00003296 holotype and single specimen as far known as *P. elektron* gen. and sp. nov. from La Guadalupe quarry, Municipality of Simojovel, Chiapas, México.

hypoproct; il, incisura lateralis; l, leg; lgs, longitudinal sulcus of the head capsule; lk, lateral keel; lts, lateral sulcus of the head capsule; mz, metazonite; o, ocellus; pap, paraproct; par, preanal ring; pz, prozonite; s, trunk segment; se, seta; sp, spinneret; spm, suture between the prozonite and metazonite; st, stipes; to, Tömösváry organ; ts, tergital suture; anatomical elements of the right and left sides are denoted as (r) and (l), respectively.

Institutional acronym. INAH, Instituto Nacional de Antropología e Historia, México.

Taphonomic notes. True colour is observed in the specimen and some crystalline paste-like in the cuticle around several diplosegments, probably a calcium-rich salt (Figures 3 and 4). It seems that this is caused by chemical reactions of calcium-enriched cuticle with the resin during polymerisation. This type of preservation is a snapshot depicting a restricted organic decay that might occur in minutes or at most a few hours after the organism's death. This is consistent with the accelerated polymerisation of the plant resin under Neotropical temperatures (Langenheim 2003). After polymerization, the plant resin is still chemically active and starts to mature over a longer period of time in geological deposits. However, the amber maturation process in the present stemmiulid specimen does not appear to have significantly affected the organic preservation. This amber is yellow, crystalline, semi-clear and hardened.

There is a granulose structure between sternites (eight segment) associated with soil particles or fungal remains trapped in this particular position (Figure 4). The position of the carcass does not permit the nature of this structure to be determined. In extant female specimens of Stemmiulida, this granular structure is not observed, but recent stemmiulids usually show soil and organic particles in the narrow spaces between sternites.

Other taphonomic characteristics are: a tiny structure resembling an indeterminate egg preserved close to the right side of the labrum (Figures 4 and 5), decay features in 9–12 and 45–46 segments in which the dorsal surfaces have partially disappeared and dark-brown masses with no describable details are also observed here (Figures 3, 8 and 9). There are also several soil particles and plant remains within the amber, such as a carbonaceous stem fragment located perpendicular to the stemmiulidan body.

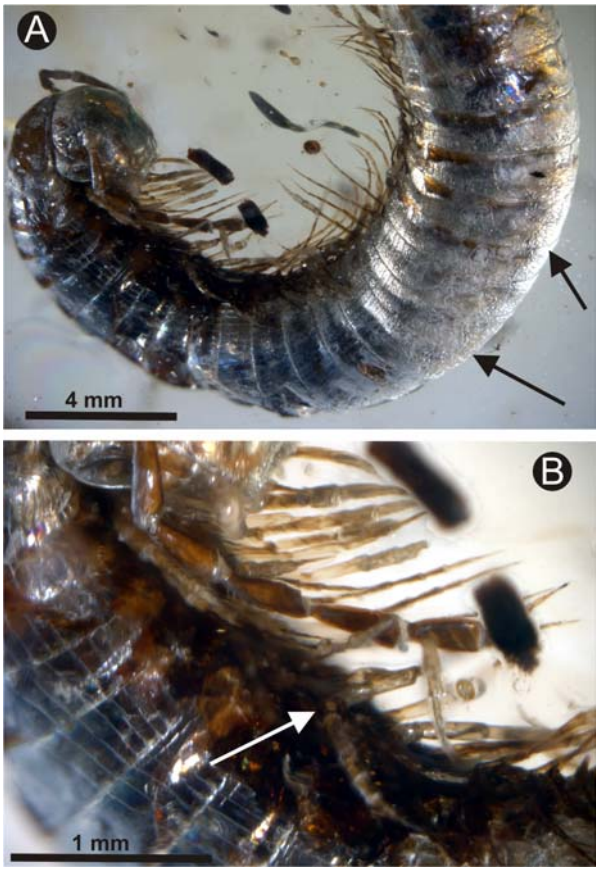

Figure 4. A crystalline paste-like substance in the cuticle covering several trunk segments (arrows) (A), granulose structure between legs of segment 8 as shown by arrow (B).

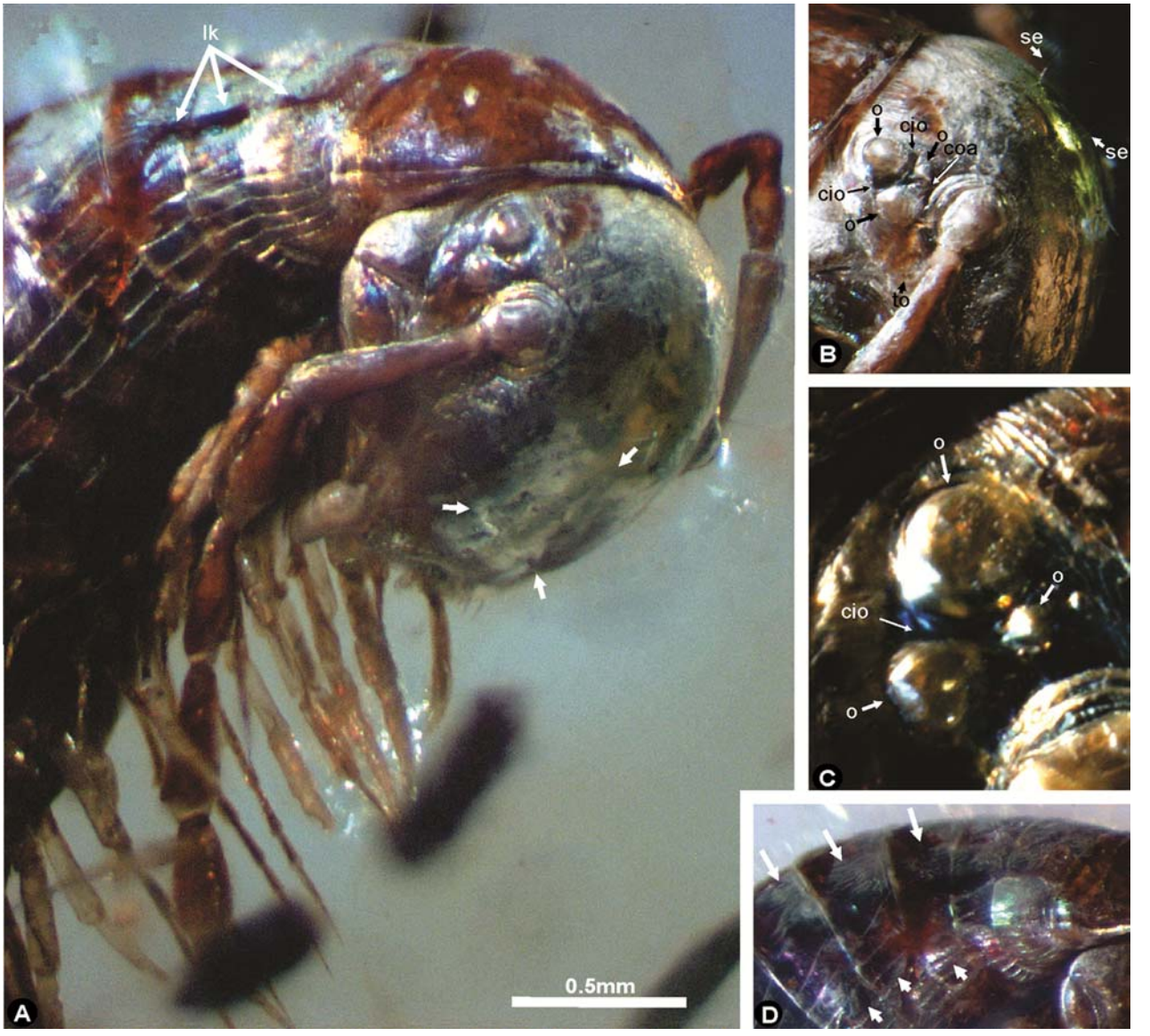

Figure 5. Head and anterior segments of INAH.2661.PF.14.IPMP00003296 holotype of *P. elektron* gen. and sp. nov., photographed under different lighting conditions and microscopical images superimposition ($Z > 30$) to avoid amber cloudiness. (A) General view, the arrows in front of the head shows a triangular shallow depression, lateral keel (lk). (B) Closer view at the head, abbreviations: cio, canal interocular; coa, canal between the ventral ocellum and antenna; o, ocellus; se, seta. (C) Closer view at the ocellus field. (D) Ornament of the first trunk segments as shown by arrows.

Systematic paleontology

Class Diplopoda de Blainville, 1844 (in Gervais, 1844)

Subclass Helminthomorpha Pocock, 1887

Order Stemmiulida Pocock, 1894

Emended diagnosis. Helminthomorph millipedes with cylindrical body, 0–3 ocelli of irregular size, when present the posterior ocellus is the larger, trunk composed of 39–60 segments with two apodous segments before telson, tergites dorsally showing a longitudinal groove, leg pair 1 enlarged in adult males, gonopods comprise anterior legs of segment 7.

Family STEMMIULIDAE Pocock, 1894

Genus **Parastemmiulus** *gen. nov*

Type species. Parastemmiulus elektron sp. nov. (see below).

Etymology. The name is derived from Greek; prefix ‘para’ meaning ‘alongside’ is added to *Stemmiulus*, in inference to similarities shared between this genus and *Stemmiulus* Gervais, 1844; and ‘elektron’ meaning ‘amber’, in inference to that was the earliest name given to amber in the ancient past.

Diagnosis. The diagnosis of the type and single species is extensive to the genus (see below).

Parastemmiulus elektron *sp. nov*

Holotype. INAH.2661.PF.14.IPMP00003296 entire female, ca. 21 mm in total length (Figure 2), deposited in the amber collection SUCCINUM2661, certified by INAH, at the San Cristobal de Las Casas, Chiapas, México.

Occurrence. The specimen is preserved embedded in amber from lignite beds of the Miocene Mazantic Shale strata at La Guadalupe Quarry, Municipality of Simojovel, State of Chiapas, México (Figure 1).

Diagnosis. Stemmiulid millipede with cylindrical trunk formed by 46 segments, including two apodous segments immediately anterior to the telson; ocellar field composed of three ocelli; ocelli and antenna connected through two open canals, one between the ocelli and the other projected from the anterodorsal ocellus to the border of the antennal socket; head with a triangular shallow depression whose corners give rise to three shallow grooves or sulci, one dorsolongitudinal and two tranverse-lateral; antennomere 2 the largest in the antenna; metazonites of haplosegments with lateral keels; metazonites of all haplosegments and first four diplosegments with two ornament patterns: straight, long and parallel grooves cover the lateral metazonite surfaces, short and sinuous grooves cover their dorsal surfaces (Figures 5–7).

Description

General characteristics. The single specimen known represents an entire adult female with exoskeleton heavy sclerotised. The total length is about 21 mm including head and trunk. The trunk height is 1.3 mm along segments 6–36, and it tends to decrease slightly in front of and behind these segments. The head is hemispherical and flat in the bottom. The trunk is composed of 46 segments; it is long and cylindrical, with a longitudinal and continuous tergite suture at the top except on the collum. In cross section, the segments are oval, slightly higher than wide. The position of the legs is completely ventral and each leg arises practically side-by-side with its pair. The length of the legs is regular along the trunk and is about half the maximum body height. Although the specimen shows a homogeneous reddish-dark brown colour, its legs are brownish and hyaline (Figures 3–5).

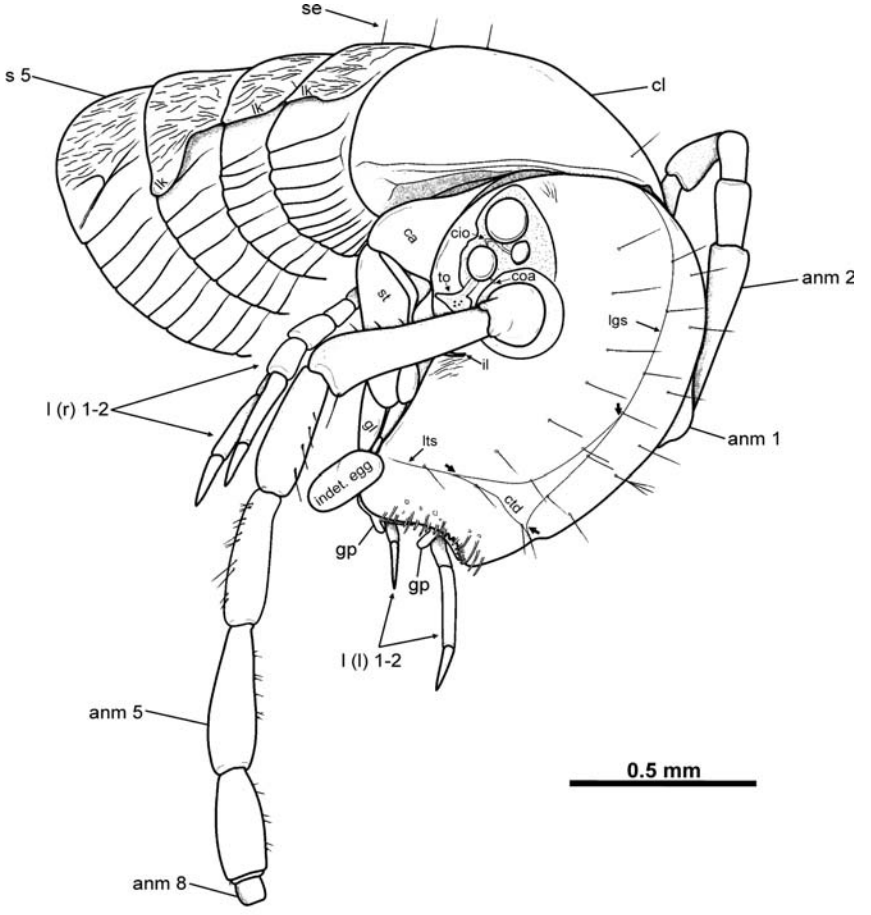

Figure 6. Line drawing of the head and first trunk segments of *P. elektron* (based on Figure D). Abbreviations: anm, antennomere; cl, collum; gp, gnatochilarium, l (l), left leg; l (r), right leg; se, seta.

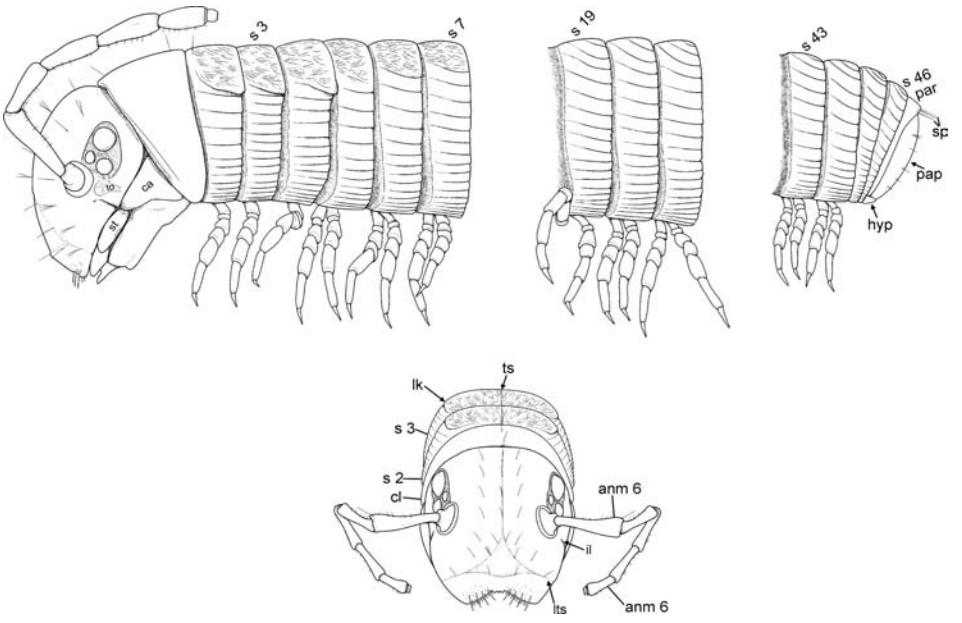

Figure 7. Reconstruction of the trunk and head in lateral and frontal view. Abbreviations: anm, antennomere; ca, cardo; cl, collum; hyp, hypoproct; il, incisura lateralis; lk, lateral keel; st, stipes; lts, lateral sulcus of the head capsule; pap, paraproct; par, preanal ring; s, trunk segments; sp, spinneret; ts, tergital suture; to, Tömösváry organ.

Head. The head capsule is spherical, flat on the bottom, and has an obtuse depression in its anterior edge or labrum. The head surface is irregularly roughened except behind the eyes and in a small lateral area of the clypeus where the rugosities form longitudinal ridges (Figures 5–7).

The clypeal area has a central triangular shallow depression, whose corners project to form three shallow grooves or sulci. Dorsally, a longitudinal sulcus on the head capsule runs along the vertex and frons, whereas the two lateral sulci project towards the external lateral clypeus (Figures 5–7).

The head has numerous setae set in small trichopores. Seven trichopores in a line along the longitudinal sulcus are equally spaced from each other; these are arranged almost in parallel with the same number of lateral trichopores located on each side of the head, which are set in between the antennae and the longitudinal sulcus. In the clypeal area, trichopores are located along the triangular depression margins, two in the middle of its lateral margins and four along its ventral margin. Fourteen trichopores are aligned on the labral margin dorsally. All thrichopores bear one seta but those in the longitudinal sulcus have two or three setae on each (Figures 5–7).

The V-shaped medial arc of the labrum has three small teeth; the central tooth is in the commissure and the others are in a lateral position, close to the first. A series of labral bristles like straight spines are set along the entire edge of the labrum; these have similar size and are equally spaced, projected forward and clearly thicker than the setae along the head capsule (Figures 5–7).

Three ocelli occupy an ocellar field, which is a shallow and triangular depression behind the antenna (Figures 5 and 6). On the right side, the three ocelli are well-exposed; they show different sizes and shapes, and have a noticeable convex cornea. The posterior ocellus is rounded and about three times larger than the intermediate sized ocellus; it is aligned longitudinally with the smallest and single ocellus situated just behind the antenna. The intermediate-size ocellus is also rounded and about three times larger than the smallest ocellus. On the other side of the head, the eye is only partially exposed because the left antenna covers it; nevertheless the largest and intermediate-sized ocelli are visible, and the former is positioned behind and above the last, as occurs with the right eye.

Within the ocellar field are two deep wide canals, perhaps sensory ocular canals, associated with the ocelli and antenna (Figures 5 and 6). The first is sinuous and occupies the interocular space, running from posterior of the ventral ocellum, reaching the anterior edge of the posterior ocellus and ending at the ventral edge of the anterior dorsal ocellus. The second of these canals is straight and connects the anterodorsal edge of the smallest ocellus and the posteroventral edge of the antennal socket.

Gnathochilarium and mandible elements are only partially visible because the ventral surface of the head is inclined against and very close to the first body segments (Figures 5–7). Nonetheless, in both lateral views of the head the cardo, stipes and gnathal lobe of the mandible are exposed, and beneath the labrum two bulbous gnathochilarial palps are visible.

The Tömösváry organ is present below the antenna and between the incisura lateralis and the ocellar field (Figures 5–7). This forms a superficial inverted pear-shaped depression that seems to have five or six pores and is almost as large as the ventral ocellus. This depression has a branch that reaches the anterior edge of that ocellus. The presence of a Tömösváry organ is verifiable only on the right side of the head because on the left side, the antenna also covers this area.

Antennae. The antennae are large, each arising from a dorsolateral socket (Figures 5–7). Each antenna is composed of eight articles or antennomeres. Antennomere length provides the following series: $2 > (3 \approx 4 \approx 5) > (1 \approx 6) > 8 > 7$. Antennomere 2 is the longest in the series; it is twice as long as antennomeres 3–5, two and half times longer than antenommeres 1 and 6. Antennomere 7 is so small that its length is less than a quarter of that seen in antennomere 8; which represents one-fifth the length of antennomere 1. All antennomeres are slender, cylindrical and slightly wider towards the apex except the first antennomere, which has a spherical base. It is not possible to see the occurrence of sensitive cones in the apex of antennomere 8 probably because they are tiny. The antennomeres are ornamented with numerous setae which are smaller than those of the head capsule.

Trunk. The trunk is composed of 46 segments, including the collum, 3 haplosegments, 40 diplosegments and 2 apodous segments. The telson (which includes the preanal ring, two paraprocts and a hypoproct) is not included in this account.

The collum shape resembles an orange slice; its dorsal length is almost equal to that of the first two podous trunk segments. This segment is gently curved laterally and articulated with the entire rear of the head capsule and the anterior edge of the first trunk segment. The collum outer surface is almost totally smooth except for a thicker cuticle band near its anterior edge and by the three curved grooves at its lateroventral corner. Two long setae are longitudinally aligned at the top of the collum (Figures 5–7).

The body is cylindrical and has a narrow longitudinal tergital suture throughout its dorsal edge (it does not go through the collum), although the segments behind the collum show some differences in shape and ornament. The trunk is almost totally cylindrical and reaches its maximum height along segments 5–40. The subsequent segments (41–46) are also cylindrical, but their height is significantly reduced. The first segments (collum and segments 2–4) are less high, ovoid and dorsoventrally depressed (Figures 5–7). The trunk segments strongly overlap each other, so the metazonite of one covers the prozonite of the subsequent; nonetheless, a straight suture is visible between the prozonites and metazonites of some segments (i.e. 3, 6 and 13–16) (Figure 8). The waist or the slope behind this suture that establishes the level of the overlapping between trunk segments is inconspicuous.

Figure 8. Dorsal and lateral view of anterior trunk segments. Abbreviations: anm, antennomere; ca, cardo; cl, collum; mz, metazonite; pz, prozonite; spm, suture between the prozonite and metazonite; ts, tergital suture; s, trunk segment.

The metazonite of each haplosegment (segments 2–4) bears a longitudinal lateral keel or ridge. In segments 2 and 3, the keels are almost straight and slightly elevated, whereas it is higher and curved in segment 4. Below these keels, the haplosegments are ornamented with longitudinal straight and uniformly separated grooves that run all along the metazonites. The dorsal surface of haplosegments, between the lateral keels, the metazonites are ornamented with shorter, sinuous, closely spaced, non-parallel grooves.

Although metazonites of all diplosegments lack lateral keels, the ornamental pattern of short and sinuous grooves seen in the dorsal surface of haplosegments is also present along the top of the metazonites of the first four diplosegments (5–8). Ornament on the tops of the subsequent diplosegments (9–13) is poorly preserved (Figure 8). The remaining surface preserved on the metazonites of these diplosegments (5–8) and all the remaining diplosegments (9–46) is covered with longitudinal straight grooves that run all along the metazonites, in which this ornament tends to be increasingly separated and inclined up and forward. In the posterior segments, this tilting tendency of the metazonite grooves is stronger, so even the lateral basal grooves are no longer parallel to the tergite suture. Apparently the trunk segments have no ozopores or setae.

Each leg has seven articles, of which the pretarsus occupies the apex and is substantially the length of all. The legs of haplosegments are practically the same length but thicker than those of the diplosegments. Sternites are not observable due to the density and cloudiness of the amber.

Telson. The posterior end of the trunk is constituted by two apodous segments (45 and 46 in the series) that precede the tail or telson. This involves a thicker preanal segment that surrounds a pair of stout paraprocts that at

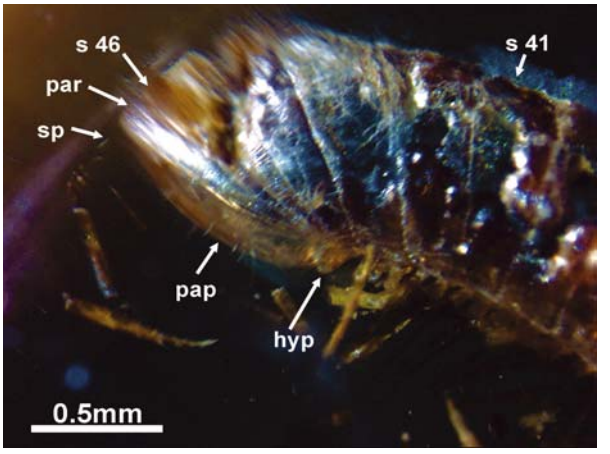

Figure 9. Closer view of posterior trunk segments. Abbreviations: hyp, hypoproct; pap, paraproct; par, preanal ring; sp, spinneret; s, trunk segment.

least have four setae along the anal opening (Figure 9). The triangular small anal ventral scale or hypoproct borders the paraprocts ventrally and probably has four short setae along its dorsal edge. The epiproct is a very small dorsoposterior projection of the preanal segment and at least has a pair of very short spinnerets or setal groups located on each side of the body.

Remarks

Currently Diplopoda comprises 10 extinct and 16 extant orders, but several phylogenetic relationships are controversial (Sierwald and Bond 2007, p. 41; Shear and Edgecombe 2010).

Cladistic analyses of Diplopoda on the basis of morphological characters have been carried out by Enghoff (1984) and Sierwald et al. (2003). However, the placement of extinct orders in a phylogenetic scheme is until now speculative. Additional phylogenetic relationships of extinct groups have been provided elsewhere (Hannibal and Feldmann 1981; Kraus and Brauckmann 2003; Sierwald et al. 2003; Wilson and Anderson 2004; Wilson 2005; Wilson and Hannibal 2005; Sierwald and Bond 2007; Shear and Edgecombe 2010). Readers are encouraged to consult those previously published works for a more detailed discussion, which is only complemented in this study. Figure 10 shows our knowledge of millipedes in a context of phylogenetic relationships.

Eugnatha has been grouped in two superorders: Juliformia that comprises Julida, Spirostreptida and Spirobolida; and Nematophora, which includes Stemmiulida, Callipodida and Chordeumatida. Juliformia species are easily recognisable because they show an enlarged collum that covers the rear of the head. In contrast, Nematophora species show setae or spinnerets in the telson. However, the

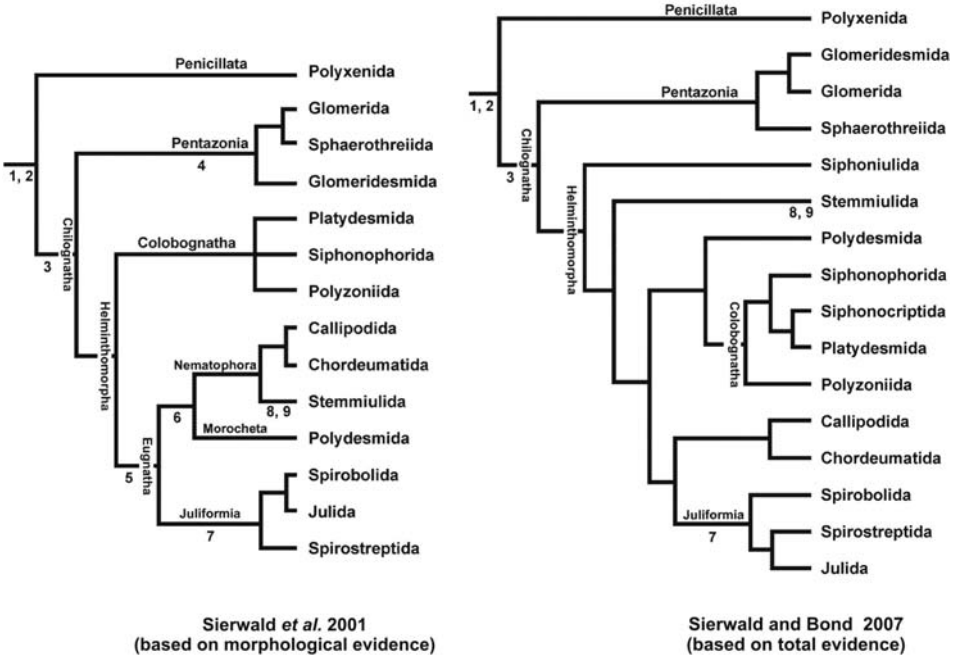

Figure 10. Phylogenetic hypotheses of Diplopoda. The taxonomical determination of *P. elektron* is based on the distribution of the following characteristics and putative synapomorphies. (1) Diplosegments; (2) legless collum; (3) cuticle calcified; (4) labrum with a single median tooth (vs. labrum with three teeth in Helminthomorpha); (5) gnathochilarial palps; (6) telson with spinnerets; (7) enlarged collum covering the head rear (vs. relatively small collum); (8) reduced number of ocelli 3–0; (9) when there are more than two ocelli, the posterior one is always the larger.

relationships of two extant anophthalmous orders are unclear: the Siphoniulida is rare *incertae sedis* group, in which the head has a peak-shaped anterior edge; whereas the Polydesmida forms an unnamed group with Nematophora (Figure 10). The inclusion of the present fossil as a member of the superorder Nemathophora is well-supported because it has a relatively small collum that does not cover the rear of the head, as well as showing spinnerets in the telson.

The attempt to resolve the phylogenetic relationships of the enigmatic order Siphoniulida has thus far led to a poorly resolved hypothesis (Sierwald et al. 2003: figure 2), in which the Eugnatha collapses (Figure 10). Other analyses using nucleotide, amino acid and total evidence data (Regier et al. 2005; Sierwald and Bond 2007) also reject the monophyly of Eugnatha, which suggests that the order Siphoniulida represents the sister group of an unnamed clade that involves Stemmiulida and other helminthomorph orders (Figure 10).

Regardless of such complex phylogenetic relationships between both fossil and extant millipedes, it is possible to assure the taxonomic affinities of *P. elektron* at ordinal level. Considering both extant and extinct millipede orders, Stemmiulida is the only order that combines a drastic reduction of the number of ocelli, and differences in sizes of those ocelli are observed. It also shows differences in the relative lengths of antennomeres, in which antennomere 2 is the largest. All those features are present in this fossil and support its inclusion into the small order Stemmiulida, which contains only one family.

The genus-level taxonomy of Stemmiulida is also problematic. Hoffman (1980) recognised seven stemmiulid genera including the type genus, *Stemmiulus* Gervais, 1844, as well as *Diopsiulus* Silvestri, 1897; *Prostemmiulus* Silvestri, 1916; *Paurochaeturus* Silvestri, 1916; *Plusiochaeturus* Silvestri, 1916; *Nethoiulus* Brölemann, 1920; and *Scoliogmus* Loomis, 1941. In contrast, Mauriès and Golovatch (2006) recognised only two genera, the monotypic *Scoliogmus* and put the other genera as synonymous with *Stemmiulus* (with 153 nominal species). Later, Mauriès et al. (2010) described a cave dweller and anophthalmous stemmiulid from Vietnam as *Eostemmiulus caesus*. Shear (2011) saw a need for broader analyses before reduction in the number of genera can be accepted.

Previously described Stemmiulida genera have no Tömösváry organ (Mauriès and Golovatch 2006), and their number of ocelli ranges between 2 and 0 (Silvestri 1916; Hoffman 1999; Mauriès et al. 2010; among others). Accordingly, genus placement of this fossil stemmiulid is based on the presence of more than two ocelli and the Tömösváry organ, not reported before in other stemmiulidans. There are also two exposed canals (probably sensory canals) between the antennal base and ocellar field that connect the ocelli with the antenna. In addition, there are several ornaments on the first trunk segments including lateral keels in the haplosegments, as well as two groove patterns covering the metazonites of segments 2–8, short and sinuous grooves above the keels and straight and long grooves beneath.

The third ocellum is identified and described here because its position into ocellar field best matches with such structure, and its appearance and composition are similar to other two ocelli (Figure 5(C)). No previously published studies in any living stemmiulid species have documented or interpreted these features into the ocellar field – near ocelli and having the same appearance of these – as a lump or protuberance with no morphological significance. There is also no evidence in the present fossil specimen that shows this kind of features as a consequence of fossilisation or decay alteration. There is no previously published literature of amber inclusions taphonomy that reports this as an ordinary preservation pattern. Particularly, in exceptionally preserved fossils from Lagerstätten that shows three-dimensional body preservation with cellular features, which is the case for the present fossil stemmiulidan as noted in its remarkable preservation state.

The stemmiulidans share a reduced number of ocelli as one of the most conspicuous characteristics. In this context, the third ocellus observed on the right side of the head from this fossil specimen might not correspond in number with those ocelli of the left side, in which only two ocelli are observable because the left antenna obscures the third ocellus (if present); however, the third ocellus as seen in *P. elektron* strongly suggests a good diagnostic character. If the three-ocelli state is interpreted as a hypothetical teratological feature, whether the third ocellus is present at the left side or not seems to be ambiguous and is rejected here. Records of individual variation in the number of ocelli in stemmiulidans are previously reported only in *Diopsulus latens* Silvestri, 1916, the holotype of which shows 2–1 ocelli. Currently no formal inferences from other stemmiulidans that show 3–2 ocelli (neither 2–0 nor 1–0 combination) are previously published.

The Tömösváry organ is recognised due to its position, size, composition and appearance (Figure 5(B)); also bears pores as described above. It should be mentioned that there is a depression in the Tömösváry organ position that recent stemmiulidans possess. To our knowledge, no current published studies have examined how this depression in recent stemmiulidans is associated with the Tömösváry organ, which remains not fully understood so far.

Accordingly, it seems that *Parastemmiulus* is a 'primitive' representative of Stemmiulida. Certainly it is the oldest known stemmiulidan but also shows putative plesiomorphic characters shared with other representatives of the millipede orders such as the Tömösváry organ and more than two ocelli, which point to close relationships with primitive members of millipedes. The presence of Tömösváry organ in *P. elektron*, which is absent in genera *Stemmiulus*, *Scoliogmus* and *Eostemmiulus* (Mauriès and Golovatch, 2006), may represent a plesiomorphic

character shared with Callipodida, Chordeumatida and Polydesmida (Sierwald and Bond 2007).

In addition, Enghoff et al. (1993), who observed the ontogenetic changes in members of the Stemmiulida based on the ratio between segments with and without legs, have shown that the mode of anamorphosis in stemmiulidans induces a new addition of body segments during every moult persisting after sexual maturity and reaching higher stages, thus, adult stemmiulids may have 35–54 segments and 2 apodous segments before the telson. Accordingly, *P. elektron* has 46 segments; however, its haplosegments show small lateral keels (Figure 5(A)) resembling those that are transformed into the true paranota in other millipedes (i.e. some species within Chordeumatida, Platydesmida, Polydesmida). In fact, the lateral keels are not present in living stemmiulidans species that show totally cylindrical segments. However, there is no evidence to suggest that these putative keels in *P. elektron* at both sides of the body with totally symmetry and placed in similar segments were produced by fossilisation as a result of struggle or post-mortem water loss or post-burial compression because the struggle typically produce disarticulation, water loss induces soft tissues dissolution and amber works as a protective barrier (a kind of hardening capsule) against adjacent sediments lithification and diagenetic transformation. Furthermore, the ornaments above and below of these keels are symmetrically placed, suggesting that these are true features and certainly these are not artefacts of fossilisation or decay alteration.

Discussion

The probable fossil record of stemmiulidans is previously known from Dominican amber (Santiago-Blay and Poinar 1992), but very little can be said about this fossil because of a single fragmentary specimen with a very poor state of preservation as a consequence of severe taphonomic damage; this makes it impossible to observe diagnostic characters and restricts the discussion.

In this context, *P. elektron* from the Miocene Chiapas amber represents the first unquestionable record of the order Stemmiulida. It might also be considered as a 'primitive' representative of this order on the basis of several putative plesiomorphic characters that it shares with other orders of Diplopoda. This provides new insights into systematics and biogeography of Stemmiulida.

The recognition of *P. elektron* as a new genus and species within the Stemmiulida forced us to discuss its possible relationships with other stemmiulid members. The taxonomic history of the genera is rather misunderstood and is still disputable. However, understanding the diversity and phylogenetic relationships within the Stemmiulida is a challenging task that requires a major resolution and fine revision of the putative stemmiulids, a goal that goes beyond the scope of this study.

Currently Stemmiulida shows a pantropical distribution with >150 species. In the Americas, stemmiulids are reported in Brazil, Ecuador, Peru, Venezuela, Antillas Islands, Guatemala, Honduras, Costa Rica and Panama, as well as in southern México (Bueno-Villegas et al. 2004). Recently, Shelley et al. (2012) have reported a potential establishment in Florida, USA. Stemmiulids in Africa show a sub-Saharan distribution between the Atlantic and Indian oceans, from Senegal to Kenya, Tanzania and northern Malawi (Mauriès 1985, 1989). In Asia, stemmiulids are present in subtropical areas of India, Sri Lanka, Vietnam, and islands of Indonesia, Halmahera and Papua New Guinea (Silvestri 1916; Carl 1941; Mauriès 1981; Mauriès and Golovatch 2006).

Unfortunately, there is a huge gap in the stemmiulidan fossil record that does not permit the inference of the phylogenetic and dispersal processes that give rise to current diversity at Stemmiulida. Regardless of this paleontological gap, the only hypothesis of the origins and dispersal of Stemmiulida has been tentatively proposed in Shelley and Golovatch (2011). According to these authors, the origin of the order Stemmiulida is inferred on Gondwana in the Early Ordovician and is primarily a southern/Gondwanan distribution except for secondary dispersals in México/Central America probably spread from South American source areas. Although limited, the occurrence of *P. elektron* helps in filling such gap as it is the oldest known stemmiulid.

Acknowledgements

This paper was submitted as part of the PhD-granting programme of Biological Sciences at the UNAM, financially supported by CONACYT. Funding to J.A.O. is provided by UNAM-PAPIIT grant 106011; additional support granted by PAPIIT-UNAM IN403210 and CONACYT endowment 131944.We thank Stefano Calabro, from the amber collection SUCCINUM2661 at San Cristobal, Chis., who generously helped in this project. We also thank Noé Lopez, Rene Hernández and Luis Zuñiga for field assistance at the Simojovel amber deposits. We thank Susana Guzmán (UNIBIO-UNAM) for photomicrograph assistance; and Dra. Ma. Del Carmen Perrilliat for access to the Colección Nacional de Paleontología, IGL-UNAM. We also appreciate the comments, corrections and critics from Drs Julian Bueno, Greg Edgecombe and Rowland Shelley, who kindly urged to prepare this manuscript; our communication and discussions do not necessarily imply their agreement with the views expressed here. The editor and referees also provided useful suggestions that improved the manuscript.

References

Almond JE. 1985. The Silurian–Devonian fossil record of the Myriapoda. Philos Trans Roy Soc Lond Ser B. 309:227–237.

Blower JG. 1985. Millipedes. In: Kermack DM, Barnes RSK, editors. Synopsis of the British fauna. London: Linn. Soc 242 p.

Brewer MS, Sierwald P, Bond JE. 2012. Millipede taxonomy after 250 years: classification and taxonomic practices in a mega-diverse yet understudied arthropod group. PLoS ONE. 7(5):e37240, 12 p.

Brölemann HW. 1920. Myriapodes receuillis par D.J.M. de la Fuente. Memor Reale Soc Española Hist Nat. 11(4):125–147.
Bueno-Villegas J, Sierwald P, Bond JE. 2004. Diplopoda. In: Llorente BJ, Morrone JJ, Yáñez O, Vargas I, editors. Biodiversidad, Taxonomía y Biogeografia de Artrópodos de México: Hacia una síntesis de su conocimiento. IV. México: UNAM p. 569-599, 660 p.
Calvillo-Canadell L, Cevallos-Ferriz S, Rico-Arce L. 2009. Miocene *Hymenaea* flowers preserved in amber from Simojovel de Allende, Chiapas, Mexico. Rev Palaeobot Palynol. 160(3–4):126–134.
Carl J. 1941. Diplopoden aus Südindien und Ceylon. 2. Teil: Nematophora und Juliformia. Rev Suis Zool. 48(22):569–714.
Crawford CS. 1992. Millipedes as model detritivores. Ber Nat-Med Verein Innsbruck. 10:277–288.
Enghoff H. 1984. Phylogeny of millipedes: a cladistic analysis. Zool Z Syst Evolforsch. 22(1):8–26.
Enghoff H, Dohle W, Blower JG. 1993. Anamorphosis in millipedes (Diplopoda): the present state of knowledge with some developmental and phylogenetic considerations. Zool J Linn Soc Lond. 109:103–234.
Frost SH, Langenheim RL. 1974. Cenozoic reef biofacies, tertiary larger Foraminifera and scleractinian corals from Chiapas, Mexico. De Kalb (IL): Northern Illinois University Press. p. 388.
Gervais P. 1844. Études pour servir a l'histoire des myriapodes (These de Zoologie). Doctorat es-Sciences Naturelles, Zoologie. Faculté des Sciences de Paris (Bourgogne et Martinet Publ). 36 p
Graham A. 1999. Studies in neotropicalpaleobotany. XIII. An Oligo-Miocene palynoflora from Simojovel (Chiapas, Mexico): America J Botany 86(1):17–31.
Grimaldi DA. 2003. In: Abrams HN, editor. Amber: window to the past. New York: American Museum of Natural History.
Hannibal JT, Feldmann RM. 1981. Systematics and functional morphology of oniscomorph millipedes (Arthropoda: Diplopoda) from the Carboniferous of North America. J Paleontol. 55(4):730–746.
Hoffman RL. 1980. Classification of the Diplopoda. Genève: Mus. Hist. Nat 237 pp.
Hoffman RL. 1999. Checklist of the millipeds of North and Middle America., Virginia Museum of Natural History Special Publication Number 8 p. 1–584
Johnson EW, Briggs DEG, Suthren RJ, Wright JL, Tunnicliff SP. 1994. Nonmarine arthropod traces from the subaerial Ordovican Borrowdale Volcanic Group. English Lake District. Geol Mag. 131:395–406.
Keilbach R. 1982. Bibliographie und Listeder Artentierischer Einschlüsse in fossilen Harzensowieihrer Aufbewahrungsorte. Deut Entomol Z, Neue Folge. 29(129–286):301–491.
Kraus O, Brauckmann C. 2003. Fossil giants and surviving dwarfs. Arthropleurida and Pselaphognatha (Atelocerata, Diplopoda): characters, phylogenetic relationships and construction. Verh Nat Ver Hambg. 40:5–50.
Lambert JB, Frye JS, Lee TA, Welch CJ, Poinar GO. 1989. Analysis of Mexican amber by carbon-13 NMR spectroscopy. Archaeol Chem. 4:381–388.
Langenheim JH. 1966. Botanical source of amber from Chiapas, Mexico. Ciencia. 24:201–211.
Langenheim JH. 2003. Plant resins: chemistry, evolution, ecology and ethnobotany. Portland (OR): Timber Press. p. 141–304.
Lee-Whiting TA. 2004. Ámbar de Chiapas: historia, ciencia y estética. México: Gobierno del Estado de Chiapas 276 p.
Linnaeus C. 1753. Species Plantarum. Stocklom: Impresis Laurentii Salvii, Tomus II, 673 p.
Loomis HF. 1941. Millipeds collected in Puerto Rico and the Dominican Republic by Dr. P.J. Darlington in 1938. Bull Mus Comp Zool. 88(2):17–80.
Mandujano-Velázquez JJ, Keppie JD. 2009. Middle Miocene Chiapas fold and thrust belt of Mexico: a result of collision of the Tehuantepec Transform/Ridge with the Middle America Trench. Vol. 327. London: The Geological Society. p. 55–69, Special Publications.
Mauriès JP. 1981. Craspedosomida, Stemmiulida et Cambalida (Myriapoda: Diplopoda) de Sri Lanka (Ceylan). Entomol Scand Suppl. 11:33–62.
Mauriès JP. 1985. Contributions to the knowledge of the mountain fauna of Malawi (Mission R. Jocqué). 5. Diplopoda Stemmiulida. Rev Zool Afr. 99:41–146.
Mauriès JP. 1989. Révision des stemmiulides: espèces nouvelles et peu connues d'Afrique (Myriapoda, Diplopoda). Bull Mus Nat d'Hist Nat, 4e Sér, Sec A, Zool. 11(3):605–637.
Mauriès JP, Golovatch SI. 2006. Stemmiulus deharvingi sp. n., the first Stemmiulida to be reported from Indonesia (Diplopoda: Stemmiulida). Arthropoda Selecta. 15:91–98.
Mauriès JP, Golovatch SI, Geoffroy JJ. 2010. Un nouveau genre et une nouvelle espèce de l'ordre Stemmiulida du Viet-Nam (Diplopoda). Arthropoda Selecta. 19:73–80.
Meneses-Rocha JJ. 2001. Tectonic evolution of the Ixtapagraben, an example of a strike-slip basin in southeastern Mexico: implications for regional petroleum systems. In: Bartolini C, Buffler RT, Cantú-Chapa A, editors. The Western Gulf of Mexico Basin: tectonics, sedimentary basins, and petroleum systems. Vol. 75. Tulsa (OK): American Association of Petroleum Geologists Memoir. p. 183–216.
Müllerried FKG. 1942. Fósiles raros de México. I. El primer miriópodo fósil de México, encontrado en el estado de Puebla. Anal Inst Biol. 13:711–717.
Padilla y Sánchez RJ. 2007. Evolución geológica del sureste mexicano desde el Mesozoico al presente en el contexto regional del Golfo de México, Boletín de la Sociedad Geológica Mexicana, tomo LIX, no. 1:19–42.
Pérez-Asso AR, Pérez-Gelabert DE. 2001. Checklist of the millipeds (Diplopoda) of Hispaniola. Bol SEA. 28:67–80.
Perrilliat MC, Vega FJ, Coutiño MA. 2010. Miocene mollusks from the Simojovel area in Chiapas, southwestern Mexico. J South Am Earth Sci. 30:111–119.
Pocock RI. 1887. On the classification of the Diplopoda. Ann Mag Nat Hist (Ser 5). 20:283–295.
Pocock RI. 1894. Contributions to our knowledge of the Arthropod Fauna of the West Indies. Part III. Diplopoda and Malacopoda, with a supplement on the Arachnida of the Class Pedipalpi. J Linnean Soc (Zool) Lond. 24:473–544, pls. 37-40.
Poinar GO. 1992. Life in amber. Palo Alto (CA): Stanford University Press. p. 29–46.
Poinar GO, Brown AE. 2002. *Hymenaea mexicana* sp. nov. (Leguminosae: Caesalpiniodeae) from Mexican amber indicates Old World connections. Bot J Linnean Soc. 139:125–132.
Regier JC, Wilson HM, Shultz JW. 2005. Phylogenetic analysis of Myriapoda using three nuclear protein-coding genes. Mol Phylogenet Evol. 34:147–158.
Riquelme F, Ruvalcaba-Sil JL, Alvarado-Ortega J, Espinosa-Matías S, Martínez MC, Rodríguez I, Perrilliat MC, Ortiz E, Guzman S, Durán CA, et al., 2011. Processing and displaying 3D images of fossil insect and plants preserved in amber based on apochromatic-zoom microscopy and infrared microimaging. CIACEM proceedings Acta Microsc. 20(1, Suppl. B):2.
Santiago-Blay JA, Poinar GO. 1992. Millipeds from Dominican amber, with the description of two new species (Diplopoda: Siphonophoridae) of Siphonophora. Ann Entomol Soc Am. 85(4):363–369.
Sedlock RL, Ortega-Gutiérrez F, Speed RC. 1993. Tectonostratigraphic terranes and tectonic evolution of México. Geol Soc Am Special Paper. 278:153.
Shear WA. 1981. Two fossil Millipedes from the Dominican amber (Diplopoda: Chytodesmidae, Siphonophoridae). Myriapodologica. 1:51–54.
Shear WA. 1987. Myriapod fossils from the Dominican amber. Myriapodologica. 7:43.
Shear WA. 1998. The fossil record and evolution of Myriapoda. In: Fortey RA, Thomas RH, editors. Arthropod relationships. London: Chapman & Hall pp. 211–212, 383 pp.
Shear WA. 2011. Class Diplopoda de Blainville in Gervais, 1844. In: Zhang Z-Q, editor. Animal biodiversity: an outline of higher-level classification and survey of taxonomic richness. Vol. 3148 Zootaxa. p. 159–164.
Shear WA, Edgecombe GD. 2010. The geological record and phylogeny of the Myriapoda. Arthropod Struct Dev. 39:174–190.

Shear WA, Selden PA, Gallet JC. 2009. Millipedes from the Grès à Voltzia, Triassic of France, with comments on Mesozoic millipedes (Diplopoda: Helminthomorpha: Eugnatha). Int J Myriapodol. 1:1–13.

Shelley RM. 2003. A revised, annotated, family-level classification of the Diplopoda. Arthropoda Selecta. 11(3):187–207.

Shelley RM. 2007. Taxonomy of extant Diplopoda (Millipeds) in the modern era: perspectives for future advancements and observations on the global diplopod community (Arthropoda: Diplopoda). In: Zhang Z-Q, Shear WA, editors. Linnaeus tercentenary: progress in invertebrate taxonomy. Vol. 1668 Zootaxa. p. 1–766.

Shelley RM, Edwards GB, Bogan AE. 2012. First recorded introduction of the milliped order Stemmiulida (Eugnatha: Nematophora): potential establishment in Florida, USA, and new records from Mexico; northward range extension into southern Tamaulipas. Insecta Mundi. 0245:1–5.

Shelley RM, Golovatch SI. 2011. Atlas of myriapod biogeography. I. Indigenous ordinal and supra-ordinal distributions in the diplopoda: perspectives on taxon origins and ages, and a hypothesis on the origin and early evolution of the class. Insecta Mundi. 0158:1–134.

Sierwald P, Bond JE. 2007. Current status of the myriapod Class Diplopoda (millipedes): taxonomic diversity and phylogeny. Annu Rev Entomol. 52:401–420.

Sierwald P, Shear WA, Shelley RM, Bond JE. 2003. Millipede phylogeny revisited in the light of the enigmatic order Siphoniulida. J Zool Syst Evol Res. 41:87–99.

Silvestri F. 1897. Viaggio del Dr. Enrico Festa nell'Ecuador e regioni vicine. V. Chilopodi e diplopodi. Boll Musei Zool Anatom comp Reale Univ Torino. 12:1–18.

Silvestri F. 1916. Contribuzione alla Conoscenza degli Stemmiuloidea (Diplopoda). Boll Lab Zool Gen Agraria, Portici. 10:287–354.

Solórzano-Kraemer MM. 2007. Systematic, palaeoecology, and palaeobiogeography of the insect fauna from Mexican amber. Palaeontogr Abteilung A. 282(1–6):1–133.

Solórzano-Kraemer MM. 2010. Mexican amber. In: Penney D, editor. Biodiversity of fossils in amber from the major world deposits. Manchester: Siri Scientific Press. p. 42–56.

Vega FJ, Nyborg T, Coutiño MA, Solé J, Hernández-Monzón O. 2009. Neogene Crustacea from southeastern Mexico. Bull Mizunami Fossil Mus. 35:51–69.

Wilson HM. 2005. Zosterogrammida, a new order of millipedes from the Middle Silurian of Scotland and the Upper Carboniferous of Euramerica. Palaeontology. 48:1101–1110.

Wilson HM. 2006. Juliformian millipedes from the Lower Devonian of Euramerica: implications for the timing of millipede cladogenesis in the Paleozoic. J Paleontol. 80:638–649.

Wilson HM, Anderson LI. 2004. Morphology and taxonomy of Paleozoic millipedes (Diplopoda: Chilognatha: Archipolypoda) from Scotland. J Paleontol. 78:169–184.

Wilson HM, Hannibal JT. 2005. Taxonomy and trunk-ring architecture of pleurojulidan millipedes (Diplopoda: Chilognatha: Pleurojulida) from the Pennsylvanian of Europe and North America. J Paleontol. 79(6):1105–1119.

OPEN ACCESS Freely available online

PLOS ONE

Two Flat-Backed Polydesmidan Millipedes from the Miocene Chiapas-Amber Lagerstätte, Mexico

Francisco Riquelme[1,2]*, Miguel Hernández-Patricio[3], Arnulfo Martínez-Dávalos[2], Mercedes Rodríguez-Villafuerte[2], Maira Montejo-Cruz[4], Jesús Alvarado-Ortega[5], José L. Ruvalcaba-Sil[2], Luis Zúñiga-Mijangos[6]

1 Posgrado en Ciencias Biológicas, Universidad Nacional Autónoma de México, Ciudad Universitaria, D.F., México, **2** Instituto de Física, Universidad Nacional Autónoma de México, Ciudad Universitaria, D.F., México, **3** Subcoordinación de Inventarios Bióticos, Comisión Nacional para el Conocimiento y Uso de la Biodiversidad, Tlalpan, D.F., México, **4** Facultad de Ciencias, Universidad Nacional Autónoma de México, Ciudad Universitaria, D.F., México, **5** Instituto de Geología, Universidad Nacional Autónoma de México, Ciudad Universitaria, D.F., México, **6** Museo del Ámbar Lilia Mijangos, San Cristóbal de las Casas, Chiapas, México

Abstract

Two species of fossil polydesmidan millipedes (Diplopoda: Polydesmida) embedded in amber are described from Miocene strata near Simojovel, in the Chiapas Highlands, Mexico. *Maatidesmus paachtun* **gen. et sp. nov.**, placed into Chelodesmidae Cook, 1895, and *Anbarrhacus adamantis* **gen. et sp. nov.**, assigned in the family Platyrhacidae Pocock, 1895. Morphological data from fossil specimens have been recovered using 3D X-ray micro-computed tomography and regular to infrared-reflected microscopy. Both fossil species are recognizable as new primarily but not exclusively, by collum margin modification and remarkable paranotal and metatergite dorsal sculpture.

Citation: Riquelme F, Hernández-Patricio M, Martínez-Dávalos A, Rodríguez-Villafuerte M, Montejo-Cruz M, et al. (2014) Two Flat-Backed Polydesmidan Millipedes from the Miocene Chiapas-Amber Lagerstätte, Mexico. PLoS ONE 9(8): e105877. doi:10.1371/journal.pone.0105877

Editor: Andreas Hejnol, Sars International Centre for Marine Molecular Biology, Norway

Received May 14, 2014; **Accepted** July 20, 2014; **Published** August 27, 2014

Data Availability: The authors confirm that all data underlying the findings are fully available without restriction. All relevant data are within the paper and its Supporting Information files.

Funding: Research has been partially founded by the following granting-projects: PAPIIT-UNAM IN105913-2, IN402813 and CONACYT 131944. The funders had no role in study design, data collection and analysis, decision to publish, or preparation of the manuscript.

Competing Interests: The authors have declared that no competing interests exist.

* Email: riquelme.fc@gmail.com

Introduction

The ecology, life history, physiology, morphology and phylogeny of millipedes (class Diplopoda) have been comprehensively reviewed in a few classical texts [1–3]. Millipedes have successfully adapted to soil and litter habitats in all subarctic climates. They contribute largely into soil cycles from both temperate and tropical forest. The fossil preservation of millipedes is very unusual mostly because they have terrestrial habits and non-recalcitrant tissues and cuticles. The oldest fossil record of millipedes is from the Mid-Silurian rocks in Scotland [4]. The geological record of Diplopoda is summarized elsewhere [1–3]. Accordingly, there is a large gap in the Mesozoic fossil record with the exception of the spirobolid millipedes from the Late Cretaceous of Mongolia and the presumably millipede *?Xylobius mexicanus* Müllerried, 1942 from the Late Jurassic/Mid-Cretaceous of Central Mexico [5,6]. However, most members of the extinct taxa are notably found in Fossil Lagerstätten, as seen in the Late Carboniferous ironstone nodules from Britain and Cenozoic amber from Europe and Middle America [7–11].

The wedge-pushing type millipedes are generally represented by the order Polydesmida, whose fossil record dates back to the Paleogene of Europe in Baltic amber [8,9]. Several polydesmidan millipedes from the younger deposits at the Neogene Middle America have also been recorded in Dominican Republic amber [10]. Millipedes from Miocene aged Chiapas amber (ca. 23-15 Ma.), Mexico, which has similar geological ages, sedimentary environments and paleobotanical affinities with Dominican amber, are only known for a recently-described stemmiulid species [11]. In this study, two fossil polydesmidan millipedes from the Chiapas amber are named and illustrated.

The fossil material studied has been now recovered from two private collections with geographic references. As a result of field geology and chemical provenance analysis, we track the source of millipede-embedded amber to the rocks of the Guadalupe Victoria site, near Simojovel in Chiapas, México (Fig. 1). Morphological data was collected by microimaging of fossil specimens using a nondestructive 3D X-ray micro-computed tomography (CT) and high-resolution microscopy with regular light to infrared-pass lens. The X-ray micro-CT scanning of a millipede specimen, as presented here, is also the first demonstration about the possibilities to recovery 3D images of fossil arthropods embedded in Chiapas amber using a laboratory-made technology, as alternative to the use of a synchrotron light source.

Two new, extinct genera *Maatidesmus* and *Anbarrhacus* and two new species are described herein. The fossil genus *Anbarrhacus* has been assigned to the family Platyrhacidae Pocock, 1895 and *Maatidesmus* to Chelodesmidae Cook, 1895. Currently both fossils species *Maatidesmus paachtun* **gen. et sp. nov**. and *Anbarrhacus adamantis* **gen. et sp. nov**. have been defined by available somatic characters (Fig. 2, 3, 4, 5). *A. adamantis* shows an exposed gonopods in situ on ring 7; however, it represents a stadium 7 male with relatively inmature gonopods, from which the gonopodal characters cannot be unambiguously assessed. To our

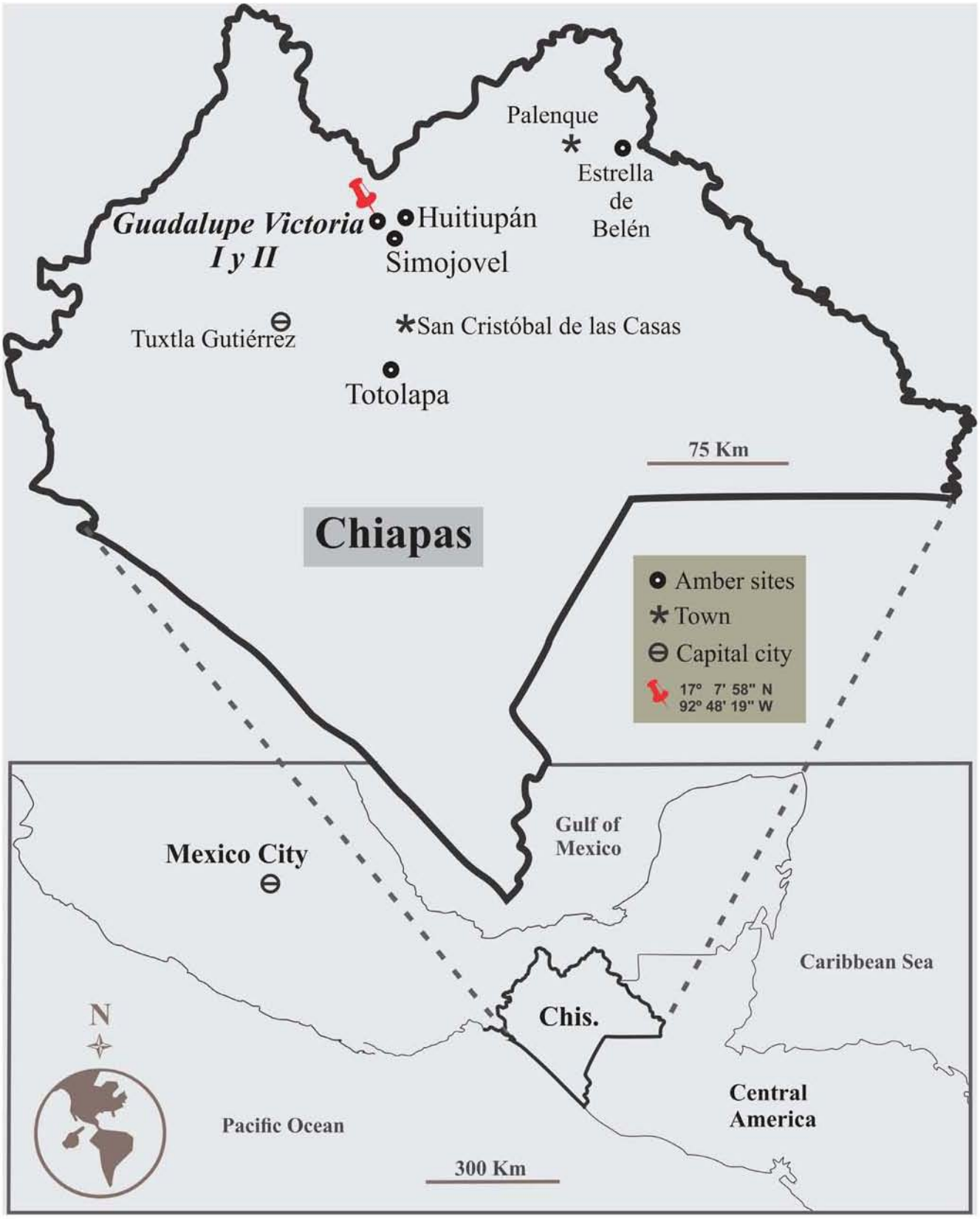

Figure 1. Location of the amber sites: Guadalupe Victoria I and II, Municipality of Simojovel de Allende, Chiapas, southern Mexico.
doi:10.1371/journal.pone.0105877.g001

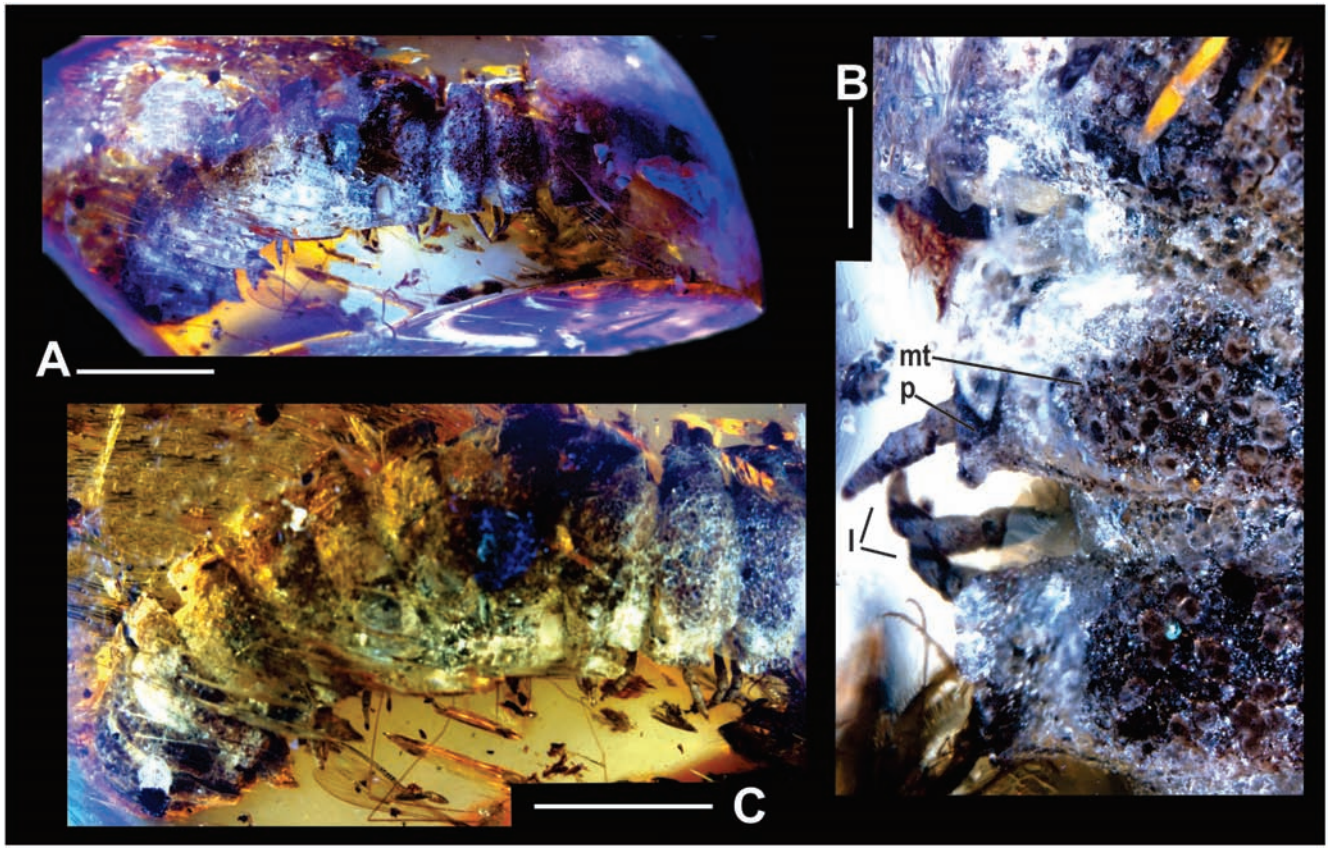

Figure 2. ***Maatidesmus paachtun*** **nov. gen. and sp., holotype.** (A) General view, scale bar 5 mm. (B) Close dorsal view of first segments, scale bar 1 mm. (C) Close dorsal view of metatergite and paranota in mid-body rings, scale bar 5 mm. See anatomical abbreviations in the main text.
doi:10.1371/journal.pone.0105877.g002

knowledge, there are no previous formal descriptions of polydesmidan millipedes in the Chiapas amber, whose fossil record in the Neogene of Middle America provides some insight into origins and dispersal of New World Polydesmida millipedes from the Neotropics of North America to South America.

Geological setting

The Guadalupe Victoria site near the town of Simojovel in Chiapas, Mexico, is characterized by carbonate and terrigenous sequences that resemble those exposed in the amber outcrops at the La Pimienta and Los Pocitos sites, also close to Simojovel [11–15]. The amber section consists of organic-rich lignite lenses, interbedded shales and coarse-fine grained sandstones with abundant iron oxides and pyrite nodules. The amber-bearing beds surrounding Simojovel primarily belong to the Mazantic shale and Balumtum sandstone strata dated as early to middle Miocene [11–15]. Preliminary, another outcrop with amber lumps was assigned to the Late Oligocene La Quinta unit [13]. However, the occurrence of this outcrop that presumably contains amber has not been recently verified in the field.

The amber-bearing rocks are the results of the nearshore and lowland sedimentation at the edge of the Chiapas Thrust–Fold Belt, which formed the Mountains of Chiapas spanning from the end of the Oligocene to mid-Pliocene [16]. Several amber localities sorted in the Mountains of Chiapas near Simojovel, Huitiupán, Totolapa, and Palenque (Estrella de Belén), they constitute an Amber Lagerstätte with extraordinary fossil preservation (Fig. 1). Taphonomy of arthropods, plants and microorganisms embedded in amber show a unique preservation of hard/soft tissues suggesting that organic decay was drastically interrupted [17]. Occurrence of small-sized vertebrates is infrequent and they are less preserved.

Palynology on amber sediments demonstrates that it represents a mangrove-like environment [18]. It is generally accepted that Chiapas amber was deposited in a subtropical forest with a Neotropical *Hymenaea* tree species recognized as the plant source [19–20]. Additionally, the biogeochemical data using synchrotron-based infrared microspectroscopy and organic mineral nomenclature of Chiapas amber has also been reviewed in a recently published contribution [21].

Material and Methods

Fossil specimens studied here come from the amber pits known as the Guadalupe Victoria site, also known as "La Guadalupe" [11], which includes two indigenous communities (predominantly Tzeltal and Tzotzil): Guadalupe Victoria I and II, near the town of Simojovel, Chiapas, southern Mexico (Fig. 1). Both specimens are preserved in golden-yellow amber with glossiness from translucent to cloudy. Crude amber pieces with embedded millipedes were collected by anonymous indigenous miners. Specimen LZ.MALM.28 is currently housed in the public collection of the Museo del Ámbar Lilia Mijangos (MALM), San Cristobal de las Casas, Chiapas, Mexico. This collection is formally certified by the Instituto Nacional de Antropología e Historia (INAH) and curated by the present researchers (Riquelme, Montejo-Cruz and Hernandez-Patricio s. str.). Specimen IGM.4544 (Instituto Geológico Mexicano) is now housed in the Colección Nacional de

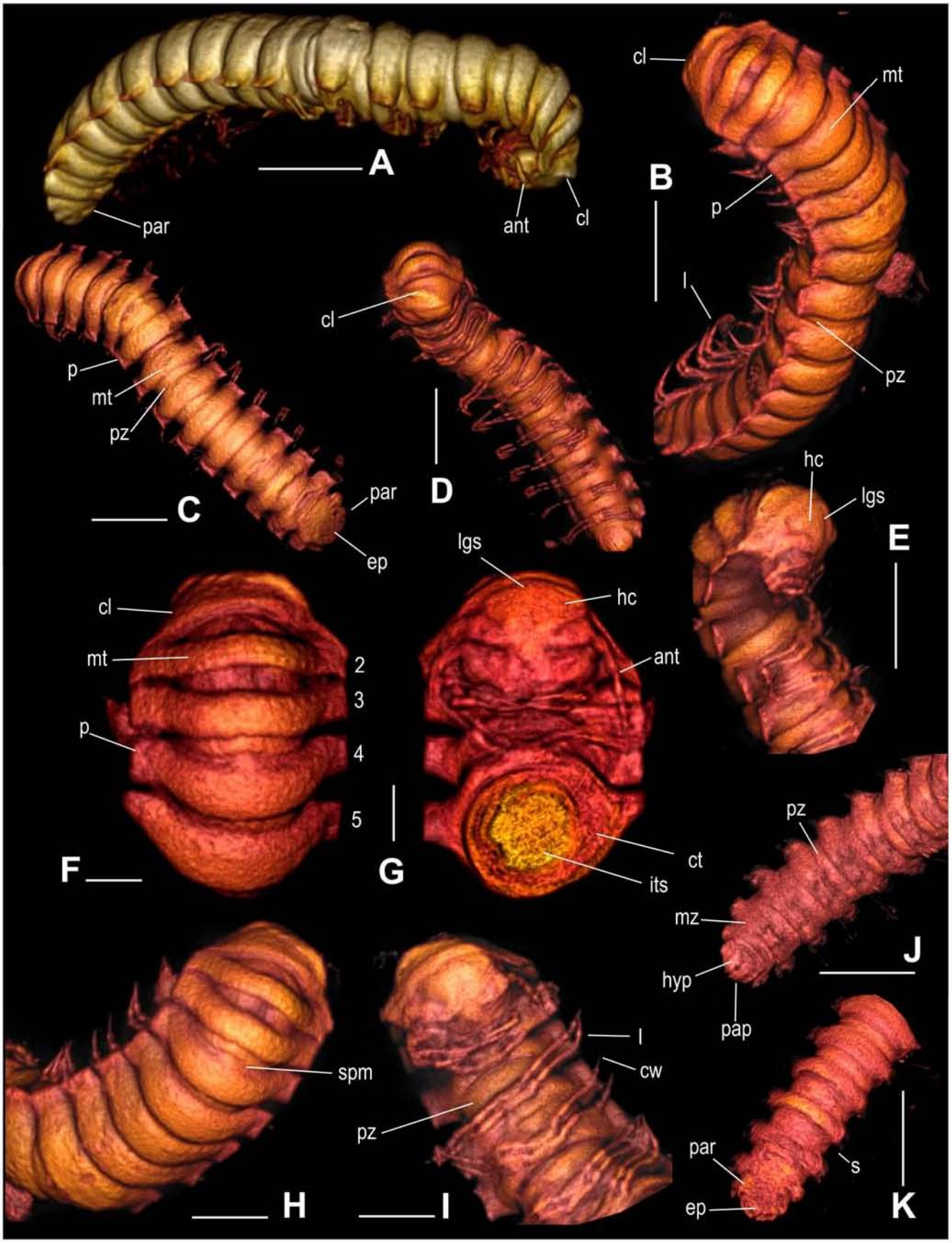
A
par
ant
cl
B
cl
mt
p
l
pz
C
p
mt
pz
par
ep
D
cl
E
hc
lgs
F
cl
mt
p
2
3
4
5
G
lgs
hc
ant
ct
its
H
spm
I
l
cw
pz
J
pz
mz
hyp
pap
K
par
s
ep

Figure 3. *Maatidesmus paachtun* nov. gen. and sp., holotype, 3D micro-CT reconstruction. (A–D): General view, scale bar 5 mm. E) Head, collum and first segments in lateral view, scale bar 5 mm. (F) Dorsal view of first segments, scale bar 2 mm. (G) Ventral view of head with a cross section of first segments, scale bar 2 mm. (H) Collum, metaterga and paranota in dorsal view, scale bar 3 mm. (I) Head and legs in dorsal view, scale bar 3 mm. (J) Last segments in ventral and dorsal view (K), respectively, scale bar 5 mm. All 3D images are expressed in virtual colors. See anatomical abbreviations in the main text.
doi:10.1371/journal.pone.0105877.g003

Paleontología, Instituto de Geología, Universidad Nacional Autónoma de México (IGL-UNAM). No specific permits were required for the specimen description and paleontology fieldwork. A provenance analysis was carried out in amber samples using Fourier Transform Infrarred (FTIR) mico-spectroscopy; the IR spectra are available from authors upon request.

3D X-ray micro-computed tomography scanning

X-ray microtomography images were acquired using a bench-top micro-CT built at the Physics Institute (IF), UNAM. A detailed description of the equipment is presented elsewhere [22]. The micro-CT system is based on an Oxford Instruments Apogee XTG5011 tungsten anode X-ray tube with a nominal focal spot size of 35 μm, coupled to a Rad-icon Shad-o-Box 2048 flat panel detector (Teledyne DALSA Inc.). The projection image data were collected at 50 kVp, 1 mA with an integration time of 500 ms per frame and 360 degree orbit in 1 degree steps. The images were corrected for flat-field non-uniformities, dead-pixels, and dark noise. The Feldkamp-Davis-Kress algorithm [23], a Hamming filter with 0.7 cut-off frequency and an in-house developed program written in MATLAB Release 2010b (The MathWorks, Inc.) were applied for tomographic reconstruction. Finally, the open source programs ImageJ [24] and OsiriX [25] were used for 3D image post-processing and displaying.

Photomicrographs and drawings

Regular and infrared-reflected photomicrographs were acquired using an apochromatic zoom micro-system combining regular and infrared-pass lens with LED and tungsten lamps and multiple image superimposition from >26 planes per image, as seen in [17]. Schematic drawings were hand traced by electronic pen using stereomicroscope, micrographs and CorelDraw X6 for graphic processing.

Anatomical Abbreviations

anm, antennomere; ant, antennae; cl, collum; co, coxa; cns, cones, ct, cuticle; cw, claw; ep, epiproct; gco, gonocoxae; gpd, gonopods; hc, head capsule; hyp, hypoproct; its, inner tissues; ico, intercoxal process; l, leg; lgs, longitudinal sulcus of the head capsule; mt, metatergite; mz, metazonite; p, paranota; pap, paraproct; par, preanal ring; pz, prozonite; s, trunk segment; se, seta; spr, spiniform accessory projection; spm, suture between the prozonite and metazonite; st, stipes; t, telopodite; To, Tömösváry organ; tt, apical lobes of telopodite; anatomical elements of the right and left sides are denoted as (r) and (l), respectively (Fig. 2, 3, 4, 5).

Terminology

The pattern of description and terminology follow [26–30]. Anatomical measurements are expressed in millimeters.

Nomenclatural Acts

The electronic edition of this article conforms to the requirements of the amended International Code of Zoological Nomenclature, and hence the new names contained herein are available under that Code from the electronic edition of this article. This published work and the nomenclatural acts it contains have been registered in ZooBank, the online registration system for the ICZN. The ZooBank LSIDs (Life Science Identifiers) can be resolved and the associated information viewed through any standard web browser by appending the LSID to the prefix "http://zoobank.org/". The LSID for this publication is: urn:lsid:zoobank.org: pub: 0096A7D5-0826-4BCE-907A-80476A24F77C. The electronic edition of this work was published in a journal with an ISSN, and has been archived and is available from the following digital repositories: PubMed Central, LOCKSS.

Results and Discussion

Systematic Paleontology

Class **Diplopoda** Blainville, in Gervais, 1844.

Subclass **Chilognata** Latreille, 1802/1803.

Infraclass **Helminthomorpha** Pocock, 1887.

Order **Polydesmida** Pocock, 1887.

Suborder **Leptodesmidea** Brölemann, 1916.

Family **Chelodesmidae** Cook, 1895.

Maatidesmus Riquelme et Hernández **gen. nov.**

ZooBank LSID: urn:lsid:zoobank.org:act:BB03262D-6BA7-48B4-8FA8 A06CFE7E0A01.

Etymology: Derived from the Maya word *maat-* (means "amber") and *-idesmus,* which is a common suffix in the Chelodesmidae.

Diagnosis: As for the only known species below.

Type species: *Maatidesmus paachtun* Riquelme et Hernández sp. nov.

Designated by monotypic species. Fig. 2–3, 5A. Movie S1.

ZooBank LSID: urn:lsid:zoobank.org:act:AFA5FAA8-12E3-4D0E-A09D-62078F640DF3.

Etymology: The specific epithet *paachtun* means *"stony-backed",* composed from the Maya elements*: paach-: "back"* plus *tun*: "stone", refers to conspicuous, lobulated dorsal sculpture in collum and metatergite in rings 2–5.

Holotype: LZ.MALM28, and only known specimen. An entire adult female, three-dimensionally preserved (Fig. 2–3.).

Horizon and locality: The amber-bearing beds at the Guadalupe Victoria site, Latitude 17° 07′ 58′N, Longitude 92° 48′ 19′ W (Fig. 1), near the town of Simojovel, State of Chiapas, México. These rocks belong to Mazantic shale and Balumtum sandstone strata dated as early-middle Miocene, ca. 23-15 Ma [11–15].

Diagnosis: Large-sized chelodesmid, adult female, with head+19 rings, 35.5 mm total length. Head wider than collum, vertex moderately granulated, with a deep vertigial sulcus extending from the top of antennal sockets; antenna clavate, long and robust, antennomere length relationships: (2, 6) > (3) > (4, 5) > (1, 7). Collum with a convex dorsum covered with margin lobations, metatergite in rings 2–5 heavily lobulated in three transverse rows arrangement; whereas metatergite in rings 6 and 7 with an asymmetric pattern of swellings rather than truly-lobed. Differs from extant representatives of the Chelodesmidae by its conspicuous, coarsely lobulated dorsal sculpture in collum and metatergite in rings 2–5. Paranota on all rings short, inflated, subrectangular,

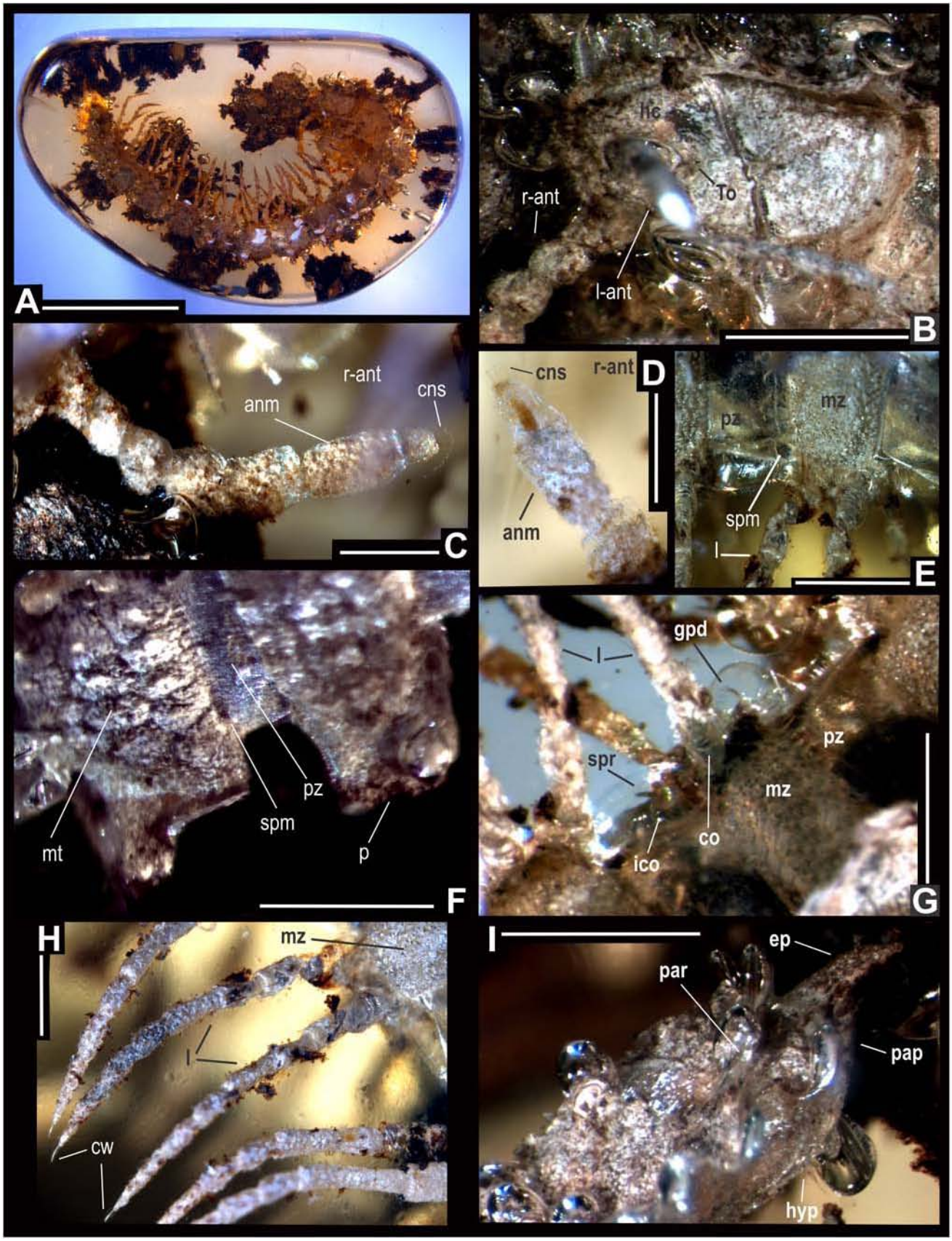
A
hc
r-ant
To
l-ant
B
r-ant
anm
cns
C
cns
r-ant
D
anm
pz
mz
spm
l
E
mt
pz
spm
p
F
gpd
l
pz
spr
mz
co
ico
G
H
mz
l
cw
I
ep
par
pap
hyp

Figure 4. *Anbarrhacus adamantis* nov. gen. and sp., holotype. (A): General view, scale bar 5 mm. (B): Head, collum and antenna, scale bar 1 mm (C): Right antenna, scale bar 0.5 mm. (D): Antennomeres 6–8 and cones in right antenna, scale bar…mm. (E): Lateral view of rings 4–5, scale bar 0.5 mm. (F): Dorsal view of paranota and metatergite in 6–7 rings, scale bar 1 mm. (G): Lateral view of gonopods in 7 ring, scale bar 0.5 mm. (H): Legs, scale bar 0.5 mm. (I): Telson, scale bar 1 mm. See anatomical abbreviations in the main text.
doi:10.1371/journal.pone.0105877.g004

dorsally roughened, tilted toward the body midline, with tick, minute, acute margins. In the longitudinal direction, dorsally, paranota+metatergite in rings 2–3, 17, 18 and 19 distinctly narrower than width of the rest of the rings. Epiproct wide, short, triangular, with caudal edged broadly blunt. Monotypic.

Description: – *General characteristics*: Fossil specimen LZ.MALM.28 represents an adult female with the entire trunk and head preserved (Fig. 2A–B). Distinguished by its conspicuous, coarse, lobulated dorsal sculpture in collum and metatergite in rings 2–5 (Fig. 2C, 3B–H, and 5A). Head wider than collum (Fig. 3G–I). Trunk composed of 19 segments with paranota and

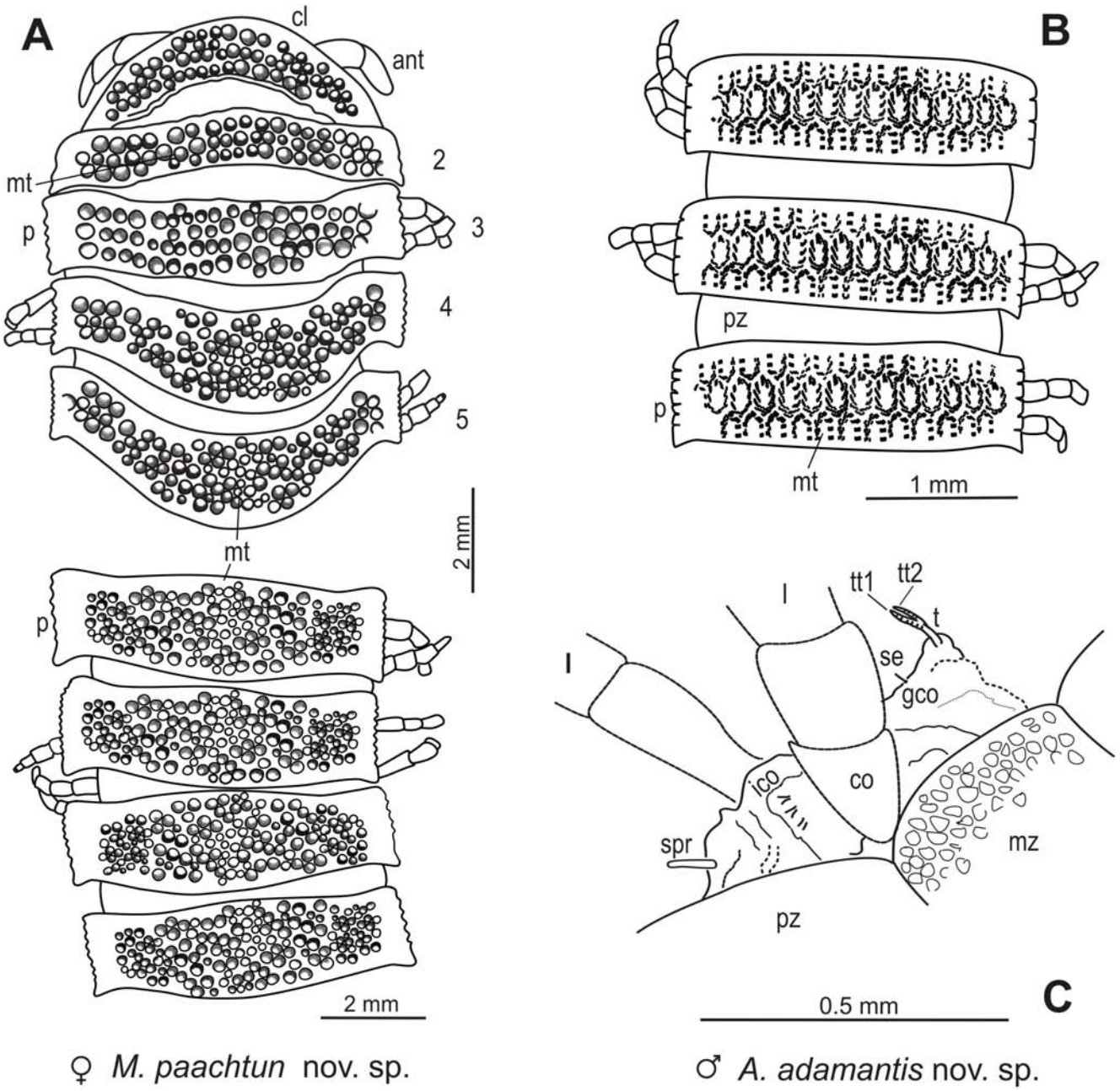

Figure 5. *Maatidesmus paachtun* nov. gen. and sp., schematic reconstruction, dorsal view. (A) collum, paranota and metatergite in rings 2–5 and mid-body rings. *Anbarrhacus adamantis* nov. gen. and sp., schematic reconstruction, dorsal view: (B) paranota and metatergite in rings 3–5. (C): inmature gonopods in ring 7. See anatomical abbreviations in the main text.
doi:10.1371/journal.pone.0105877.g005

telson, ca. 35.5 mm in length, 7.9 mm in maximum width, and W/L ratio of 22.2% (Fig. 3A–D). Rings 2–5 equal to collum in overall width, whereas posterior ring widths slightly increasing gradually to ring 17, thence gently narrowing over the last rings and telson (Fig. 3C–D, 3K, and 3J); Paranota inflated, subrectangular, dorsally roughened, tilted toward the body midline (Fig. 2B–C and 3A–G). Epiproct wide, short, triangular (Fig. 3C). Since amber is cloudy around female genitalia and this is a tiny structure, it cannot be clearly assessed.

Taphonomic features: a partial dorsal portion of rings 18–19 were accidentally scraped during amber polishing by collectors; accordingly, the preanal ring was scarcely altered in dorsal view, affecting the epyproct surface dorsally. The head is ventrally bent as seen in a defensive position. The body decay was dramatically interrupted by rapid polymerization of plant resin, which preserved intact soft tissues inside the fossil as shown in a cross section of inner body layers from the reconstructed X-ray tomography (Fig. 3G); although the cuticle is slightly recrystallized due to reacting with amber, it also preserves colored morphology. Copious embedded biodebris along and around the body, mostly insect parts from mosquitos and ants; there are also plant fragments and soil particles. The piece of amber is golden to orange yellow with translucent to cloudy glossiness, internally recrystallized with abundant transverse, small fractures (Fig. 2).

Coloration preserved in amber: Ground color in head and rings creamy white to nut-brown splatter (Fig. 2). All rings show slightly dissolved and recrystallized portions of cuticle as crystal-white patches, probably calcium carbonate salts. Head and antenna white. Collum whitish colored, most of the lobes nut-brown. Paranota generally from crystalline to creamy white, metaterga also nearly white with nut-brown lobes; upper part of prozona white and lower side creamy gray to nut-brown (Fig. 2C). Sterna pale to nut-brown. Legs white, ending in a nut-brown splashes (Fig. 2C).

Head: convex, slightly wider than collum, with a vertex moderately granulated, and deep vertigial sulcus extending from the top of antennal sockets; sockets slightly impressed ventrolaterally; frons elevated above level of clypeus and labrum. Cardo, stipes and gnathal lobe are prominent. Antenna clavate, long and robust, thicker than legs; antennomeres length relationships: (2, 6) > (3) > (4, 5) > (1, 7), apical cones are hardly distinguished (Fig. 3G–E, and 3I).

Collum: strongly convex anteriorly in dorsal view, with anterior margins broadly rounded, not hiding the head in lateral view; dorsal surface conspicuously lobed posteriorly, with posterior margins angled (Fig. 3D–F, and 3H).

Trunk: composed of 19 rings with paranota and telson (Fig. 3A–D). In the transverse direction, rings 2–5 equal to collum in overall width, consecutive ring widths increase gradually to ring 16, thence gently narrow over the last rings (17–19) and telson (Fig. 3C, 3D, 3K, and 3J); In the longitudinal direction, dorsal view, paranota+metatergite in rings 2 and 3 distinctly narrower than width of paranota+metatergite in consecutive rings, which gradually increase reaching a maximum width in mid-region and moderately decrease to ring 16, thence in rings 17–19 are as narrow as 2 and 3; between metazonite and prozonite waist striated; the prozonite surface almost smooth, metazonite surface finely granulated. Paranota on all rings short, inflated, subrectangular, dorsally roughened, tilted toward the body midline, with thick, minute, acute margins, and distinctly but irregularly toothed (Fig. 2C, 3B–C, 5A). The mid-dorsal surface of metatergite with at most three transversal rows of lobes in rings 2–5, whereas rings 6 and 7 with swellings randomly located (Fig. 2C, 5A); pleural tubercles conspicuous; sternites surface moderately setose; ozopores opening laterally as seen in rings 5, 7, 9–10, 12–13, and 15–16; there are not differences between segments with pores and without pores. Legs extended ventrally in all rings, long, slender, with elongated femora and tarsi, ending in a short claw. The podomere length relationships: femur > tarsus >prefemur > (postfemur, tibia) (Fig. 2C, 3B, and 3I).

Telson: Epyproct wide, short, triangular, with caudal edge broadly blunt, not extended beyond paraprocts due to taphonomic alteration; paraprocts semicircular, surface finely granular but the edges are smoother and scaly; hypoproct triangular but sharply truncate, posterior margin convex, apex acute, with setae on each side of the midline (Fig. 3C and 3J–K).

Remarks: – After the Paradoxosomatidae, the family Chelodesmidae is one of the most diverse polydesmidan group comprising 230 extant genera with nearly 450 species [31], whose distribution now extends to Africa, Middle America and South America [28]. At the present time, there are five living species of the Chelodesmidae recorded in Mexico assigned to the genera *Chondrodesmus, Rhaphandra* and *Eutyporhachis*, the latter is also present in the Chiapas Highlands [32–33]. *Maatidesmus paachtun* **gen. et sp. nov**. has in common several characters with the living representatives of the Chelodesmidae, including the shape of collum, paranota and telson, but differs by the conspicuous, coarsely lobulated dorsal sculpture in collum and metatergite in rings 2–5 (Fig. 2C, 3B–H, 5A). *M. paachtun* is the first fossil species of this family from the Neogene of Middle America. Other fossil chelodesmid form has been previously known from Dominican amber based on headless specimen [10].

Systematic Paleontology

Superfamily **Platyrhacoidea** Pocock 1895.

Family **Platyrhacidae** Pocock, 1895.

Anbarrhacus Riquelme et Hernández **gen. nov.**

ZooBank LSID: urn:lsid:zoobank.org:act:B1FD30A1-B55D-4205-8E99-C17F34386661.

Etymology: Derived from the Arabic voice *ánbar* (means "amber") and *–rhacus,* which is a common suffix in the Platyrhacidae.

Diagnosis: As for the only known species below.

Type species: *Anbarrhacus adamantis* Riquelme et Hernández **sp. nov**.

Designated by monotypic species. Fig. 4.

ZooBank LSID: urn:lsid:zoobank.org:act:DF667E57-51C8-4104-BC95-B2375DF3E5E4.

Etymology: The specific epithet *adamantis* is derived from *adamantus* (Latin): "diamond", refers to dorsal sculpture in collum and metatergite with a rhomboidal-pattern (Fig. 4 and 5B–C).

Holotype: IGM.4544, and only known specimen. Stadium 7 male, three-dimensionally preserved, almost complete; only left antenna is partially missing (Fig. 4).

Horizon and locality: Amber-bearing beds at the Guadalupe Victoria site, Latitude 17° 07′ 58′N, Longitude 92° 48′ 19′ W, near Simojovel de Allende, State of Chiapas, Mexico (Fig. 1). These rocks belong to Mazantic shale and Balumtum sandstone strata dated as early-middle Miocene [11–15].

Diagnosis: Small-sized Platyrhacidae, stadium 7 male **w**ith head+17 rings, 19.8 mm total length. Head moderately convex, rough, and setose, wider than collum. Antenna clavate, long, copiously covered with setae, antennomeres length relationships: 5>6> (2≈3≈4) > (1≈7), with four long, slender sensory cones. Distinguished by its granulated dorsal sculpture in paranota and metaterguite; paranota on all rings, wide, granulated, with thick, rounded margin, waist laterally striated; metatergite coarsely granulate, mid-dorsally ornamented in a rhomboidal-pattern, all

minute tubercles and setae multiple. Intercoxal process between legs in ring 7, irregular with distal, spiniform accessory projection. Gonopods immature, small, in situ on ring 7, gonocoxae bulbous, slightly crooked, with a long distal setae on medial surface; gonopodal telopodite shrunken, bipartite, apical lobes of the tibiotarsus laminate, striated and acute. Monotypic.

Description: – *General characteristics*. Fossil specimen IGM.4544 represents a stadium 7 male, which preserves the entire trunk and head with apical portion of left antenna missing (Fig. 4). Head convex, wider than collum (Fig. 4B). Trunk composed on 17 segments with paranota and telson, ca. 19.8 mm in length, 2.8 in maximum width, W/L ratio of 14.1%. Rings increasing gradually in width from collum to posterior 2/3 of the body and gently narrows over the last rings and telson; epiproct fairly long and spathulate (Fig. 4I). Paranota wide and granulate, metatergites ornamented in a rhomboidal-pattern (diamond-like) in mid-dorsal region (Fig. 4F). Legs long and slender, extended lateroventrally (Fig. 4H). Although relative immature, gonopods are exposed, small, in situ on trunk ring VII, gonocoxae bulbous, crooked, gonopodal telopodite shrunken, bipartite, apical lobes of the tibiotarsus minute, laminate, striated and acute (Fig. 4C and 5C).

Taphonomic features: left antenna partially broken, antennomeres 3–6 accidentally missing by polishing amber (Fig. 4B). Empty molds of bubbles are present all over the dorsal portion of the head and trunk; particularly, in the margins of paranota (Fig. 4A–B and 4I). It seems that these bubbles were produced as result of dissolved water vapor from soils during rapid amber hardening (polymerization). Decaying of carcass was drastically interrupted by resin polymerization; because of this the hard/soft tissues and true color morphology have been preserved (Fig. 4). Head and trunk slightly bent ventrolaterally; body randomly surrounded by blackish to brown soils and plant debris. The piece of amber is golden to citrine yellow with translucent glossiness, in a pebble-like shape and roughly polished (Fig. 4A).

Coloration preserved in amber: Most of the head and antenna from cream colored to nearly white, 6th antennomere of right antenna colorless, setiferous tubercles blackish-brown, clypeus darker, a conspicuous black patch above the Tömösváry organ, labrum pale yellowish (Fig. 4B–D). Collum gray to white, blackish in midline (Fig. 4B). Paranota generally cream colored with metaterga whitish gray; upper surface of prozona blackish gray and lower sides brownish. Sterna pale yellowish to brown and legs creamy white to pale yellowish (Fig. 4E–H).

Head: moderately convex, slightly wider than collum, densely covered with minute setae; surface in the vertex, frons and vertigial sulcus roughened; clypeus sparsely setose. Gnathochilarium with short median expansion, labral surface with several flat papillae, cardo, stipes, and gnathal lobe are appreciably well-defined. The Tömösváry organ is conspicuous below the antenna and between the incisura lateralis (Fig. 4B). Antenna clavate, long, copiously covered with setae, antennal length 2.5 mm. The antennomeres length relationships: $5>6>(2\approx3\approx4)>(1\approx7)$, with four long, slender sensory cones; 5^{th} and 6^{th} antennomeres with long sensitive setae near apex (Fig. 4B–D).

Collum: broadly rounded anteriorly, almost semicircular, laterally articulated with the rear of the head capsule, not hiding the head; dorsal surface granulated, with small rounded tubercles and setose, posterior margins irregular and rounded (Fig. 4B).

Trunk: Composed of 17 rings with paranota and telson (Fig. 4A). Trunk rings generally similar on structure, prozonite and metazonite separated by a well-defined striated waist (Fig. 4E–F). Metatergite mid-dorsally surface rough, granulated, with polygonal furrows in a rhomboid pattern, all setiferous tubercles multiple (Fig. 4F and 5B). Rings 16 and 17 with posterior margin of metatergite coarsely granulate. Pleural tubercles on all rings are conspicuous, variable in size. Prozonite surface polished, lightly smooth (4E–F). Paranota on all rings wide, arising low on body and slightly declined, with posterior margin rounded. Paranota dorsal surface roughened, in middle paranotal process with copious granules on anterior angle nearly rectangular; paranota lateral margins distinctly but irregularly toothed; anterior margin lightly convex, posterior lightly concave (Fig. 4F); paranota in rings 11 and 12 with posterior angle acute and not lateral marginal thickening. The posterior edge of the paranota and metatergite dorsally striated (Fig. 4F). Ozopore open dorsally in rings11 and 12, hard to distinguish in other rings. Sternites surface moderately setose, as wide as long. Spiracles small and pyriform as seen on ring 6. Legs extended lateroventrally on all rings, slender with elongated femora and tarsi, ending in a long claw; relative lengths of podomere are as a follows: femur >tarsus >prefemur > (postfemur, tibia) (Fig. 4H). Intercoxal process between legs in ring 7, irregular with distal, spiniform accessory projection (Fig. 4G).

Telson: Preanal ring with several large setae, epiproct spathulate in outline, fairly long, extending beyond the paraprocts, with caudal edged rounded-triangular and slightly acute; paraproct semicircular, each with setae; hypoproct sharply truncated (Fig. 4I).

Gonopods: relatively immature, small, in situ on ring 7; gonocoxae bulbous, slightly crooked, with a conspicuous setae on medial surface, posterior margin in plate greater almost the height of the sternites, gonopod telopodite thin, short, shrunken, bipartite, apical lobes of the tibiotarsus minute, laminate, striated and acute; gonopore inconspicuous due to body position (Fig. 4G and 5C).

Remarks: – *Anbarrhacus adamantis* **gen. et sp. nov**. is a stadium 7 male, consequently, the putative apomorphic characters from the male gonopods cannot be assessed unequivocally. The living species are typically diagnosed using male/female genitalia [26–27,30,34–35]. Other living species of the Platyrhacidae described upon female specimens have been considered species inquirenda [34]. At the present, there is no satisfactory treatment of platyrhacidan species that includes fossils in the available literature. Probabilities of finding adult male specimens with preserved, exposed genitalia in the fossil record are extremely low. In this context, *A. adamantis* shares somatic characters with several extant species of the family Platyrhacidae as seen in the genera *Nyssodesmus, Psammodesmus, Exallostethus, Platyrhacus and Hoffmanorhacus* [27,34–36]. Taxonomical affinities include the shape of collum, paranota, metatergites, epyproct, others, as described above. Thus, the specific relationships at the genus and species level of *A. adamantis* with living platyrhacidan millipedes are indicated by somatic characters; but distinguished from them by four long, slender sensory cones in antenna and the conspicuous, granulated dorsal sculpture in paranota and metaterguite. Also differs from them by the intercoxal process among legs in ring 7.

The extant representatives of Platyrhacidae comprise a greater diversity of about 37 genera and 180 species. Those are distributed in the Indo-Australian region from Myanmar to the Solomon Islands [37]; whereas the New World members of Platyrhacidae are found in the Neotropics from the southernmost Mexico to northern Brazil [30,33–36]. Here nine genera were proposed by Cook, 1895 [38], platyrhacids from South America have been reviewed by Chamberlin, 1941 [39] and platyrhacids from southern México, West Indies and Central America have been studied in significant works [34–36].

There are few living species of the Platyrhacidae recorded in México, i.e. *Exallostethus trinax* Hoffman, 1975 collected in the Chiapas Highlands [26]. Other species such as the first-described living forms of *Platyrhacus,* i.e. *P. bilineatus* and *P. mexicanus* Lucas, 1840 have been considered species inquirenda [34]. Thus, *A. adamantis* represents the first fossil species of the Platyrhacidae in the southernmost part of North America.

Conclusion

The 3D X-ray micro-CT scanning has revealed many of the diagnostic body parts of chelodesmid millipede embedded in cloudy, fractured amber with copious biodebris along and around the body. The micro-CT imaging also shows intact soft tissues inside the fossil chelodesmid, which is the first evidence of ancient soft tissue preservation in millipedes at any geological time. This demonstrates the potential of 3D X-ray microimaging using a lab-made technology. To our knowledge, such technique is first applied in the Chiapas amber arthropods.

On the other hand, several polydesmidan forms have been detected in the Chiapas amber samples belonging to private collections; they also contain many unidentified specimens (Riquelme, Hernandez-Patricio and Montejo-Cruz pers. obs.). Enthusiastic amber trading has produced a large gap in the fossil record of the Chiapas amber paleobiota, including Diplopoda. Accordingly, all fossil millipede species embedded in amber collected from Miocene strata in the Mountains of Chiapas are currently new to science. Both *M. paachtun* and *A. adamantis* share close affinities with their extant congeners and respective families. Millipedes show a primitive and very conservative morphology, younger fossil and living forms resemble those in the Late Paleozoic. In general terms, the fossil millipedes in the Chiapas amber are typically modern forms, but future findings and descriptions of new polydesmidan millipedes will probably show highly variable fossil forms at genus and species level only.

The Polydesmida fossil record is notoriously incomplete for global diversity analysis. However, the occurrence of *M. paachtun* and *A. adamantis,* which have been placed in extinct genera and restricted to Neogene of the Middle America amber, provides some additional insights into Polydesmida phylogeny and current Neotropical distribution from the southernmost North America to northern South America.

Supporting Information

Movie S1 *Maatidesmus paachtun* **gen. et sp. nov**. 3D X-ray micro-computed tomography.
(AVI)

Acknowledgments

F. Riquelme thanks the support of the PCB-UNAM-CONACYT-Doctoral program. We thank Biol. Francis Pimentel and Johanna Friessen from the MALM for access to the amber collection, Dr. Mario Ramos from the IGL-UNAM for help in the field, and Dr. Fernando Alvarez from the Sc. Faculty-UNAM for reviewing the manuscript. We also thank M.Sc. Jon D. Richey from the TX State University for help with the English edition, Biol. Susana Guzmán from the IB-UNAM for microphotography assistance and Enoch Ortiz from the IGL-UNAM for polishing the samples. We respectfully acknowledge the contributions of anonymous reviewers and editor whose refereeing and comments have improved the final published edition.

Author Contributions

Conceived and designed the experiments: FR. Performed the experiments: FR. Analyzed the data: FR MHP. Contributed reagents/materials/analysis tools: FR AMD MRV MMC JLRS JAO LZM. Contributed to the writing of the manuscript: FR. Designed the 3D X-ray micro-computed tomography imagining: AMD.

References

1. Hopkin SP, Read HJ (1992) The Biology of Millipedes. Oxford, UK: Oxford Univ Press. 233 p.
2. Sierwald P, Bond JE (2007) Current status of the myriapod class Diplopoda (Millipedes): taxonomic diversity and phylogeny. Annual Review of Entomology 52: 401–420.
3. Shear WA, Edgecombe GD (2010) The geological record and phylogeny of the Myriapoda. Arthropod Struct Dev 39: 174–190.
4. Wilson HM, Anderson LI (2004) Morphology and Taxonomy of Paleozoic millipedes (Diplopoda: Chilognatha: Archipolypoda) from Scotland. Journal of Paleontology 78 (1): 169–184.
5. Dzik J (1975) Spirobolid millipedes from the Late Cretaceous of the Gobi desert, Mongolia. Paleontologia Polonica 33: 17–24.
6. Müllerried FKG (1942) Fósiles raros de México I. El primer miriápodo fósil de México, encontrado en el estado de Puebla. Anales del Instituto de Biología 13: 711–717.
7. Wilson HM (2005) A new genus of Archipolypodan millipede from the Coseley Lagerstätte, Upper Carboniferous, UK. Palaeontology 48 (5): 1097–1100.
8. Keilbach R (1982) Bibliographie und Listeder Artentierischer Einschlüsse in fossilen Harzensowieihrer Aufbewahrungsorte. Deut Entomol Z, Neue Folge 29 (129–286): 301–491.
9. Spahr U (1992) Ergänzungen und Berichtigungen zu R. Keilbachs Bibliographie und liste der Bernsteinfossilien verschiedene Tiergruppen, ausgenommen Insecta und Araneae. Stuttg Beitr Naturk B 194: 1–77.
10. Santiago-Blay JA, Poinar GO (1992) Millipeds from Dominican amber, with the description of two new species (Diplopoda: Siphonophoridae) of Siphonophora. Ann Entomol Soc Am 85(4): 363–369.
11. Riquelme F, Alvarado-Ortega J, Ramos-Arias M, Hernández M, Le Dez I, et al. (2014) A fossil stemmiulid millipede (Diplopoda: Stemmiulida) from the Miocene amber of Simojovel, Chiapas, Mexico. Historical Biology 26 (4): 415–427.
12. Frost SH, Langenheim RL (1974) Cenozoic reef biofacies, tertiary larger Foraminifera and scleractinian corals from Chiapas, Mexico. De Kalb (IL): Northern Illinois University Press. 388 p.
13. Poinar GO (1992) Life in amber. Palo Alto (CA): Stanford University Press. 350 p.
14. Ferrusquía-Villafranca I (2006) The first Paleogene mammal record of Middle America: *Simojovelhyus pocitosense* (Helohyidae, Artiodactyla). Journal of Vertebrate Paleontology 26 (4): 989–1001.
15. Perrilliat MC, Vega FJ, Coutiño MA (2010) Miocene mollusks from the Simojovel area in Chiapas, southwestern Mexico. J South Am Earth Sci 30: 111–119.
16. Meneses-Rocha JJ (2001) Tectonic evolution of the Ixtapagraben, an example of a strike-slip basin in southeastern Mexico: implications for regional petroleum systems. In: Bartolini C, Buffler RT, Cantú-Chapa A, editors. The Western Gulf of Mexico Basin: tectonics, sedimentary basins, and petroleum systems. Vol. 75. Tulsa (OK): American Association of Petroleum Geologists Memoir, pp. 183–216.
17. Riquelme F, Northrup P, Ruvalcaba-Sil JL, Stojanoff V, Siddons DP, et al. (2014). Insights into molecular chemistry of Chiapas amber using infrared-light microscopy, PIXE/RBS, and sulfur K-edge XANES spectroscopy. Applied Physics A 116 (1): 97–109.
18. Graham A (1999) Studies in neotropicalpaleobotany. XIII. An Oligo-Miocene palynoflora from Simojovel (Chiapas, Mexico). America Journal of Botany 86 (1): 17–31.
19. Langenheim JH (1966) Botanical source of amber from Chiapas, Mexico. Ciencia 24: 201–211.
20. Langenheim JH (2003) Plant resins: chemistry, evolution, ecology and ethnobotany. Portland (OR): Timber Press, pp. 141–304.
21. Riquelme F, Ruvalcaba-Sil JL, Alvarado-Ortega J, Estrada-Ruiz E, Galicia-Chávez M, et al. (2014) Amber from México: Coahuilite, Simojovelite and Bacalite. MRS Proceedings 1618. doi:10.1557/opl.2014.466.
22. Martínez-Dávalos A (2010) An Overview of the Development and Evaluation of a Benchtop microCT Scanner. Proceedings of the XI Mexican Symposium on Medical Physics, AIP Conf Proc 1310: 7–11.
23. Feldkamp LA, Davis LC, Kress JW (1984) Practical Cone Beam Algorithm. JOSA A1: 612–619.
24. Rasband WS (2012) Image J, U. S. National Institutes of Health, Bethesda, Maryland: USA. Available: http://imagej.nih.gov/ij/ Accessed 2014 Aug 3.

25. Rosset A, Spadola L, Ratib O (2004) OsiriX: An Open-Source Software for Navigating in Multidimensional DICOM Images. J. Digit. Imaging 17 (3): 205–216.
26. Hoffman R (1975) A new genus and species of euryurid millipeds from Chiapas (Polydesmida: Platyrhacidae). Proceedings of the Biological Society of Washington 88 (20): 211–216.
27. Hoffman R (1975) Philippine Zoological Expedition, 1946–1947. Millipeds of the genus Polydesmorhachis Pocock (Polydesmida: Platyrhacidae). Fieldiana, Zoology 65 (6): 73–84.
28. Hoffman R (2001) A new, disjunct, diplopod genus from Espirito Santo, Brasil (Polydesmida: Chelodesmidae). Papéis Avulsos de Zoologia 49 (42): 557–562.
29. Mesibov R (2006) Dirt-encrusted and dragon millipedes (Diplopoda: Polydesmida: Paradoxosomatidae) from Queensland, Australia. Zootaxa 1354: 31–44.
30. Hoffman R, Martinez D, Florez E (2011) A new Colombian species in the millipede genus *Psammodesmus*, symbiotic host for bryophytes (Polydesmida: Platyrhacidae). Zootaxa 3015: 52–60.
31. Shear W (2011) Class Diplopoda de Blainville in Gervais, 1844. In: Zhang, Z.-Q. Animal biodiversity: An outline of higher-level classification and survey of taxonomic richness. Zootaxa 3148: 159–164.
32. Hoffman R (1999) Checklist of the millipedes of North and Middle America. Virginia Museum of Natural History Special Publication 8: 1–584.
33. Bueno-Villegas J, Sierwald P, Bond JE (2004) Diplopoda. In: Llorente BJ, Morrone JJ, Yáñez O, Vargas I, editors. Biodiversidad, Taxonomía y Biogeografía de Artrópodos de México: Hacia una síntesis de su conocimiento IV. México: UNAM, pp. 569–599.
34. Hoffman R (1953) A new Central American milliped of the genus Platyrhacus. Proceedings of the Entomological Society of Washington 55(5): 251–258.
35. Shelley RM, Martinez-Torres D (2013) The milliped family Platyrhacidae (Polydesmida: Leptodesmidea) in the West Indies: Proposal of Hoffmanorhacus n. gen.; description and illustrations of males of Proaspis aitia Loomis, 1941; redescription of Nannorrhacus luciae (Pocock, 1894); hypotheses on origins and affinities; and an updated New World familial distribution. Zootaxa 3626(4): 477–498.
36. Hoffman R (1960) A fourth contribution to the knowledge of neotropical platyrhacid millipeds (Diplopoda: Polydesmida). Proceedings of the United States National Museum 111(3424): 17–31.
37. Jeekel CAW (2007) An annotated bibliographical catalogue of the Indo-Australien Platyrhacidae (Diplopoda, Polydesmida). Myriapod Memoranda 10: 49–101.
38. Cook OF (1895) Introductory note on the families of Diplopoda. In Cook OF, Collins GN, editors. The Craspedosomatidae of North America. Ann New York Acad Sci vol 9, 1–9.
39. Chamberlin RV (1941) On a collection of millipedes and centipedes from northeastern Peru. Bulletin of the American Museum of Natural History 78(7): 473–535.

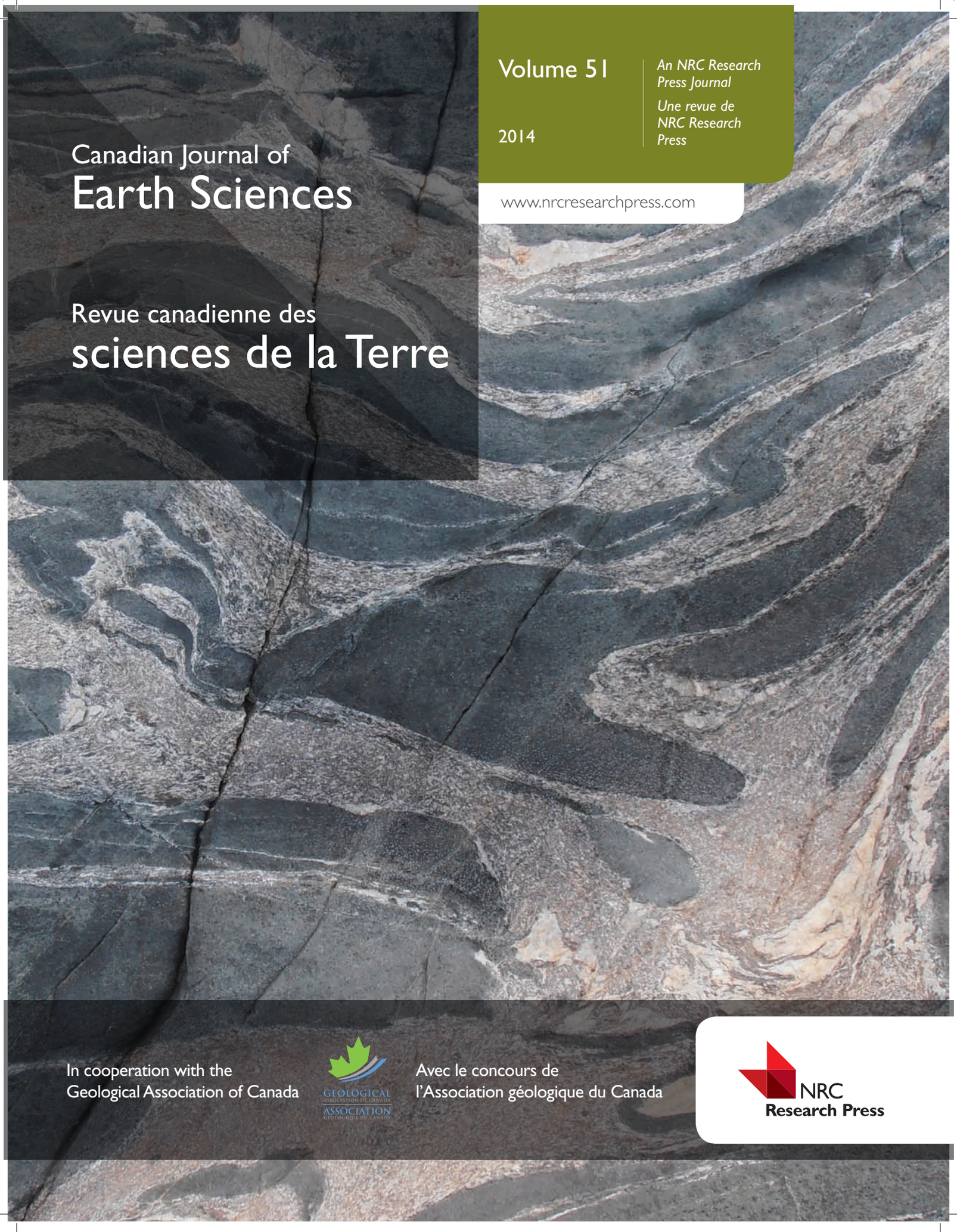

Canadian Journal of Earth Sciences

Revue canadienne des sciences de la Terre

Volume 51

2014

An NRC Research Press Journal

Une revue de NRC Research Press

www.nrcresearchpress.com

In cooperation with the Geological Association of Canada

Avec le concours de l'Association géologique du Canada

NRC Research Press

NRC Research Press

RAPID COMMUNICATION

A new chernetid pseudoscorpion from the Miocene Chiapas – Amber Lagerstätte, Mexico

Francisco Riquelme, Dulce F. Piedra-Jiménez, Víctor Córdova-Tabares, and Bibiano Luna-Castro

Abstract: ***Mayachernes maatiatus***, a new genus and species of pseudoscorpion of the family Chernetidae (Arachnida: Pseudoscorpionida), is described from the Miocene Chiapas – Amber Lagerstätte, south of Mexico. This new fossil species represents an adult male specimen with hard–soft tissues preserved in great detail. It differs from all other living chernetids by a combination of diagnostic characters. Anatomical data were collected using high-resolution microscopy with regular to infrared-reflected light. *Mayachernes maatiatus* is the first newly described fossil species of pseudoscorpion from the Chiapas amber. This taxon also adds to knowledge of the Chernetidae diversity in the southernmost part of North America at the Neogene.

Résumé : ***Mayachernes maatiatus***, un nouveau genre et espèce de pseudoscorpion de la famille Chernetidae (Arachnida: Pseudoscorpionida) est décrite provenant du Miocène Chiapas – Amber Lagerstätte, au sud du Mexique. Cette nouvelle espèce de fossil représente un spécimen adulte de sexe masculin avec des tissus durs et mous étonnamment préservée en détail. Ses caractères morphologiques le diffèrent de tous les autres chernétides vivants. Les données anatomiques ont été recueillies à l'aide d'un microscope utilisant les lumiere visible et passe-infrarouge lentilles. Cette découverte donne lieu à la première description, dans l'ambre du Chiapas, d'une espèce fossile de pseudoscorpion. Aussi ce taxon ajoute à la connaissance de la diversité de Chernetidae dans la partie la plus méridionale de l'Amérique du Nord au Néogène.

Introduction

Biology and life histories of pseudoscorpions (Arachnida: Pseudoscorpionida) have been widely investigated in several living species (Weygoldt 1969). Adaptive radiation of pseudoscorpions includes all subarctic environments. They occur in soil, litter, tree bark, grass, caves, fractured rocks, swamps muds, and seashore sands. Cladistics and molecular phylogeny have been examined elsewhere (Harvey 1992; Murienne et al. 2008). However, fossil preservation of pseudoscorpions is extremely rare. Fossil forms are poorly known except in amber. Their small, labile, chinitized cuticles are easily destroyed by deep burial and lithification. The oldest pseudoscorpion forms in the geological record date back to the Mid-Devonian argillaceous strata near Gilboa, New York, USA (Shear et al. 1989; Schawaller et al. 1991; Dunlop 1996). The only known Mesozoic occurrence of chernetid is a specimen embedded in amber from Cretaceous coal in Grassy Lake, Alberta, Canada (Schawaller 1991). In contrast, the majority of described fossil species are found in Cenozoic deposits from the Paleogene Baltic and Neogene Dominican Republic amber and younger copal sites from Madagascar and Colombia (i.e., Schawaller 1980; Judson 2003, 2010; Henderickx et al. 2012).

Little is known about fossil pseudoscorpions in the Chiapas amber, Mexico, which is botanically and geologically contemporary to the Dominican Republic amber (Langenheim 2003). A chernetid morphotype with uncertain taxonomic identity is the only fossil previously documented (Schawaller 1982). In the present work, the first fossil species of pseudoscorpion in the Chiapas amber is described and illustrated based on an adult male specimen. This fossil pseudoscorpion is diagnosed herein as *Mayachernes maatiatus* gen. et sp. nov. (family Chernetidae Menge, 1855). The fossil body is intact and shows true color morphology. Also cuticle and other tissues are gracefully preserved at detail. The morphology of *M. maatiatus* seems roughly similar to some living species of *Lustrochernes* clade. However, it separates from its extant congeners by a combination of diagnostic characters, such as the granulated sculpture and furrows on carapace, the trichobothria pattern on pedipalp, tarsus with basal tactile seta, tibia IV with two setae, and genitalia shape, among others.

According to Harvey (2013), the order Pseudoscorpionida globally comprises 26 extant families with 454 genera and 3533 species, whose record is constantly growing worldwide. Fossil pseudoscorpions have been placed in one family with 11 genera and 41 species (Harvey 2013). Diversity in Mexico is considerably high, currently represented by 18 extant families, with 64 genera and 167 species (nearly 4.7% of the global species richness) (Ceballos 2004; Córdova-Tabares and Villegas-Guzmán 2013; Villegas-Guzmán 2013; Francke 2014). As mentioned earlier in the text, there is one fossil pseudoscorpion known in Mexico (Schawaller 1982). The new species *M. maatiatus* placed into Chernetidae is restricted to Neogene amber of the Middle America, which includes Chiapas and the Antilles Islands amber (particularly the Dominican Republic).

Depositional environment and fossilization

Amber-embedded pseudoscorpion studied here comes from an amber site known as La Pimienta near Simojovel, Chiapas, which belongs to a Fossil Lagerstätte with early–middle Miocene age

Received 15 May 2014. Accepted 7 August 2014.

Paper handled by Associate Editor Jisuo Jin.

F. Riquelme. Posgrado en Ciencias Biológicas, Universidad Nacional Autónoma de México, Ciudad Universitaria, C.P. 04360, D.F., México.
D.F. Piedra-Jiménez. Laboratorio de Aracnología, Facultad de Ciencias, Universidad Nacional Autónoma de México, Ciudad Universitaria, Coyoacán, C.P. 04360, D.F., México.
V. Córdova-Tabares. Laboratorio de Acarología, Escuela Nacional de Ciencias Biológicas, Instituto Politécnico Nacional, Casco de Santo Tomás, C.P. 11340, D.F., México.
B. Luna-Castro. Museo del Ámbar de Chiapas, Diego de Mazariegos S/N, La Merced, C.P. 2924, San Cristóbal de las Casas, Chiapas, México.
Corresponding author: Francisco Riquelme (e-mail: riquelme.fc@gmail.com).

Fig. 1. Location of amber site: La Pimienta near Simojovel, Chiapas, south of Mexico.

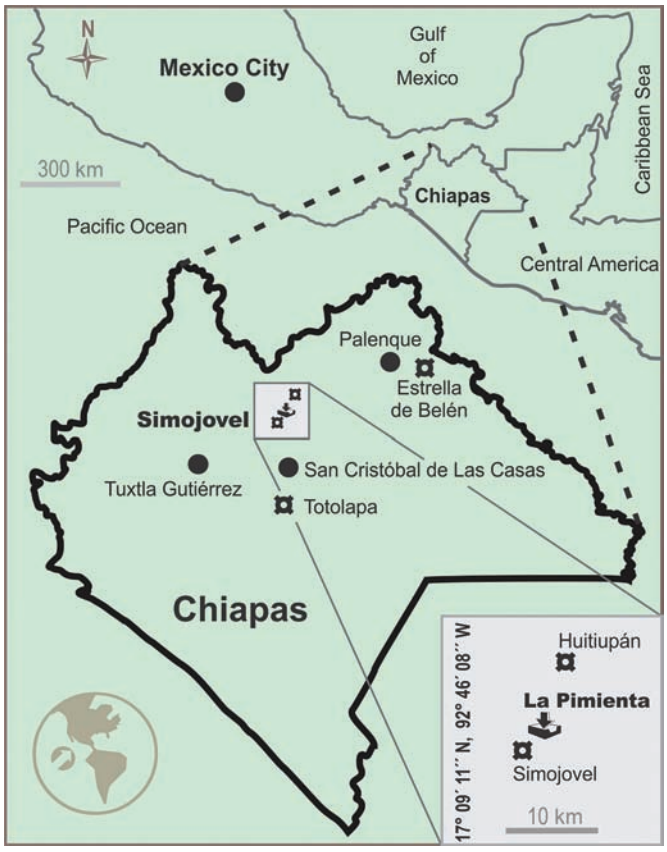

(Durán-Ruiz et al. 2013; Riquelme et al. 2014*a*, 2014*b*). Predominantly, fossil arthropods and plants are found almost intact in this conservation deposit, which extends over the Chiapas Highlands, south of Mexico (Fig. 1). Small-sized vertebrates are found less frequently. The outcrops containing amber are found near the towns of Simojovel, Huitiupán, Totolapa, Estrella de Belén, Paubuchil, Pueblo Nuevo Solistahuacán, Puente Nacional, El Bosque, Malpaso, Patelhó, and San Andrés Duraznal.

The associated strata of amber-bearing beds surrounding Simojovel have been commented and discussed in multiple contributions. Most authors agree that that the Chiapas amber is found in Mazantic shale and Balumtum sandstone strata dated as early to middle Miocene, ca 23–15 Ma. (Frost and Langenheim 1974; Poinar 1992; Perrilliat et al. 2010; Riquelme et al. 2014*a*). Another outcrop assigned to the La Quinta unit near Simojovel, dated as Late Oligocene has been mentioned as possibly containing amber (i.e., Poinar 1992). However, recent fieldwork in this area has failed to confirm the presence of this outcrop.

Taphonomy of arthropods, plants, and microorganisms in the Chiapas amber indicates an exceptional preservation of hard–soft tissues. Synchrotron-based physicochemical analysis suggests that organic decay was prevented because of rapid resin polymerization (Riquelme et al. 2014*b*). Palynoflora present on amber sediments indicate a mangrove-like environment (Graham 1999). Paleobotanical and chemical studies suggest a subtropical forest with Neotropical *Hymenaea* tree species recognized as the plant source of amber (Miranda 1963; Langenheim 1966, 2003; Poinar and Brown 2002; Calvillo-Canadell et al. 2009). The most recent revision of the organic mineral nomenclature and plant source of the Chiapas amber is given in Riquelme et al. (2014*c*).

Materials and methods

Fossil is embedded in a piece of golden yellow amber with translucent glossiness. This was collected from La Pimienta site, Municipality of Simojovel, Chiapas, south of Mexico (Fig. 1). The fossil specimen was scheduled as BL.MACH.2 and currently is housed at the Museo del Ámbar de Chiapas (MACH), located in San Cristóbal de Las Casas, Chiapas, Mexico. The amber collection BL.MACH is formally certified by the Instituto Nacional de Antropología e Historia (INAH), which protects the archeological and paleontological heritage in Mexico. The collection was curated by the present researchers (F. Riquelme, D.F. Piedra-Jimenez, and M. Montejo-Cruz sensu stricto). No specific permits were required for the specimen description and geology fieldwork.

Microimaging and measurements

Anatomical data were collected using high-resolution microscopy with regular to infrared-pass lens and light-emitting diode (LED) and tungsten lamps. The microimaging process includes multiple image superimposition of about >26 planes per image (Riquelme et al. 2014*a*, 2014*b*). Schematic drawings were hand traced by electronic pen using stereomicroscope, micrographs, and CorelDraw X6 for graphic processing (Riquelme et al. 2014*a*). Anatomical measurements were collected using the open-source program tpsDig V. 2.17 (Rohlf 2013). Measurements are given in millimetres, and dimension ratio is expressed as length/width (*L*/*W*).

Acronyms

INAH, Instituto Nacional de Antropología e Historia. MACH, Museo del Ámbar de Chiapas; BL.MACH, Bibiano Luna/Museo del Ámbar de Chiapas; UNAM, Universidad Nacional Autónoma de México.

Terminology

The pattern of description and terminology generally follow Muchmore (1990), Harvey (1992), Mahnert and Adis (2002), Judson (2007, 2010), and Gao and Zhang (2011).

Nomenclature

The nomenclatural acts as presented herein have been registered in ZooBank, the official website of the ICZN (International Commission on Zoological Nomenclature). The ZooBank LSID (Life Science Identifiers) for this publication is urn:lsid:zoobank.org:pub:D72CA395-188C-4DC7-B726-35277EB8B401.

Abbreviations

The following anatomical abbreviations are used in this study. On body: ab, abdomen; c, carapace; ch, chelicera; che, chela; cw, claw; cx, coxa; fe, femur; ff, fixed finger; gt, genitalia; l, leg; mf, movable finger; p, pedipalp; pa, patella; tf, transverse furrow; tr, trochanter. On chelicerae, the trichobothria pattern: exterior seta (*es*), basal seta (*b*), subbasal seta (*sb*), interior seta (*is*), laminal seta (*ls*), and galeal seta (*gs*) on the movable finger. On pedipalp, the trichobothria pattern: setae of movable finger: basal (*b*), subbasal (*sb*), subterminal (*st*), and terminal (*t*). Setae of fixed finger: exterior basal (*eb*), exterior subbasal (*esb*), exterior subterminal (*est*), exterior terminal (*et*), interior basal (*ib*), interior subbasal (*isb*), interior subterminal (*ist*), and interior terminal (*it*). Tactile seta (*TS*).

Results and discussion

Systematic paleontology

Class	Arachnida Cuvier, 1812
Order	Pseudoscorpionida De Geer, 1978
Superfamily	Cheliferoidea Risso, 1826
Family	Chernetidae Menge, 1855
Genus	***Mayachernes*** Riquelme, Piedra et Córdova gen. nov.

ZOOBANK LSID: urn:lsid:zoobank.org:act:D3054D71-8700-459E-8431-EE6729141279

Fig. 2. *Mayachernes maatiatus* gen. et sp. nov., holotype. (*a*) Laterodorsal view. (*b*) Lateroventral view. (*c*) Dorsal view. (*d*) General view. Scale bars 1 mm. Anatomical abbreviations, see main text.

ETYMOLOGY: Named after *Maya-* plus *-chernes* (common generic suffix in Chernetidae). The prefix *Maya-* is a patronymic for the Maya descendants who living in the Simojovel area, specifically the Tzotzil and Tzeltal, who have extracted amber from artisanal mines since pre-Columbian times.

DIAGNOSIS: As for the only known species in the following text.

TYPE SPECIES: ***Mayachernes maatiatus*** Riquelme, Piedra et Córdova sp. nov. Designated by monotypic species. Figures 2–4.

ZOOBANK LSID: urn:lsid:zoobank.org:act:44150A14-A02C-43BB-A67B-158805B4D6ED

ETYMOLOGY: The specific epithet *maatiatus* is derived from the ancient Maya voice *maat*, which means "amber".

HOLOTYPE: BL.MACH.2, the only specimen known, amber inclusion, an adult male three-dimensionally preserved. Figures 2, 3.

HORIZON AND LOCALITY: The amber-bearing beds in La Pimienta site, latitude 17°09′11″N, longitude 92°46′08″W; near the town of Simojovel de Allende, State of Chiapas, Mexico (Fig. 1). These rocks belong to the Mazantic shale and Balumtum sandstone strata dated as early–middle Miocene in age (Poinar 1992; Frost and Langenheim 1974; Perrilliat et al. 2010; Riquelme et al. 2014*a*).

DIAGNOSIS: Small-sized chernetid, adult male, 4.83 mm of total length, 2.40 mm without pedipalps, 2.20 mm without chelicera nor pedipalps. Carapace conspicuously sculptured with granules and two transverse furrows. Eyes or eyespots absent. Chelicerae about 1/3 as long as carapace, hand smooth, with four acuminate setae (*b*, *sb*, *ls*, *is*) and one in the movable finger (*gs*); movable finger moderately slender, with subapical lobe, at least two discernible teeth, apparently 20 plates in the serrula exterior, bearing five acuminate setae (*es* absent); galea with at least two rami; rallum with three blades. Pedipalp moderately stout, with dorsomedial protuberance in palpal patella; movable finger with 35 small, contiguous teeth and two accessory teeth; fixed finger with 16 accessory teeth; trichobothria *it* on fixed finger much closer to *et* than to *esb*, and farthest from the fingertip than the distance between *isb* and *ist*, *st* about midway between *t* and *sb*, *ist* closer to *isb* or *ib* than *it*, distance between *st* and *t* less than the distance of *t* from the fingertip, distance from *est* to *isb* more than five times as the distance between *esb* and *eb*. Tarsus IV with a basal tactile seta; tibia IV with two tactile setae; accessory tooth on claws absent. All tergites divided except XI. Genitalia placed anteriorly with respect to genital operculum, ejaculatory canal atrium with inverted triangle-shaped, dorsal apodeme elongate and darker.

DESCRIPTION: Holotype BL.MACH.2 represents an adult male with its entire body and true color morphology preserved almost intact. General characteristics are as follows: carapace subrectangular as typically diagnosed for Chernetidae, conspicuously granulated, slightly longer than wide, with two transverse furrows. Carapace and pedipalps moderately sclerotized; most setae acuminate. Eyes absent. Pedipalps moderately stout, pedipalp femur 2.42 times as long as broad, chelal hand with dorsal depression. Chelicera with five setae, chelicera movable finger moderately slender, with subapical lobe, at least two discernible teeth; rallum with three blades. All tergites divided except XI; genitalia well preserved, placed anteriorly with respect to genital operculum, ejaculatory canal atrium with inverted triangle-shaped. Legs long, with claw simple. *Mayachernes maatiatus* gen. et sp. nov. have close affinities with the living chernetids of the *Lustrochernes* clade (*sensu* Beier, 1932*a*), i.e., *Cordylochernes*, *Lamprochernes*, *Americhernes*, *Gomphochernes*, *Incachernes*, *Odontochernes*, *Mesochernes*. However, it differs predominantly but not exclusively from these related extant taxa by the following diagnostic characters: (*i*) different morphometric values as seen in living males; (*ii*) different carapace morphotype, heavily granulated with distinctly furrows on fossil specimen; (*iii*) tergite divisions, fossil only has tergite XI undivided; (*iv*) the trichobothria pattern on pedipalp fixed finger, particularly the *ist* closer to *isb* or *ib* than *it*, and *st* about midway between *t* and *sb* as seen in

Fig. 3. *Mayachernes maatiatus* gen. et sp. nov., holotype. (*a*) Laterodorsal view of carapace and chelicera; scale bar 0.5 mm. (*b*) Close view of chelicera; scale bar 100 μm. (*c*) Abdomen; scale bar 0.5 mm. (*d*) Genitalia in ventral view; scale bar 1 mm. (*e*) Pedipalp; scale bar 1 mm. (*f*) Right chela; scale bar 0.5 mm. (*g*) Left chela, scale bar 0.5 mm. (*h*) Legs in ventral view; scale bar 1 mm. (*i*) Legs in lateral view; scale bar 0.5 mm. (*j*) Close view of leg iv; scale bar 250 μm. Anatomical abbreviations, see main text.

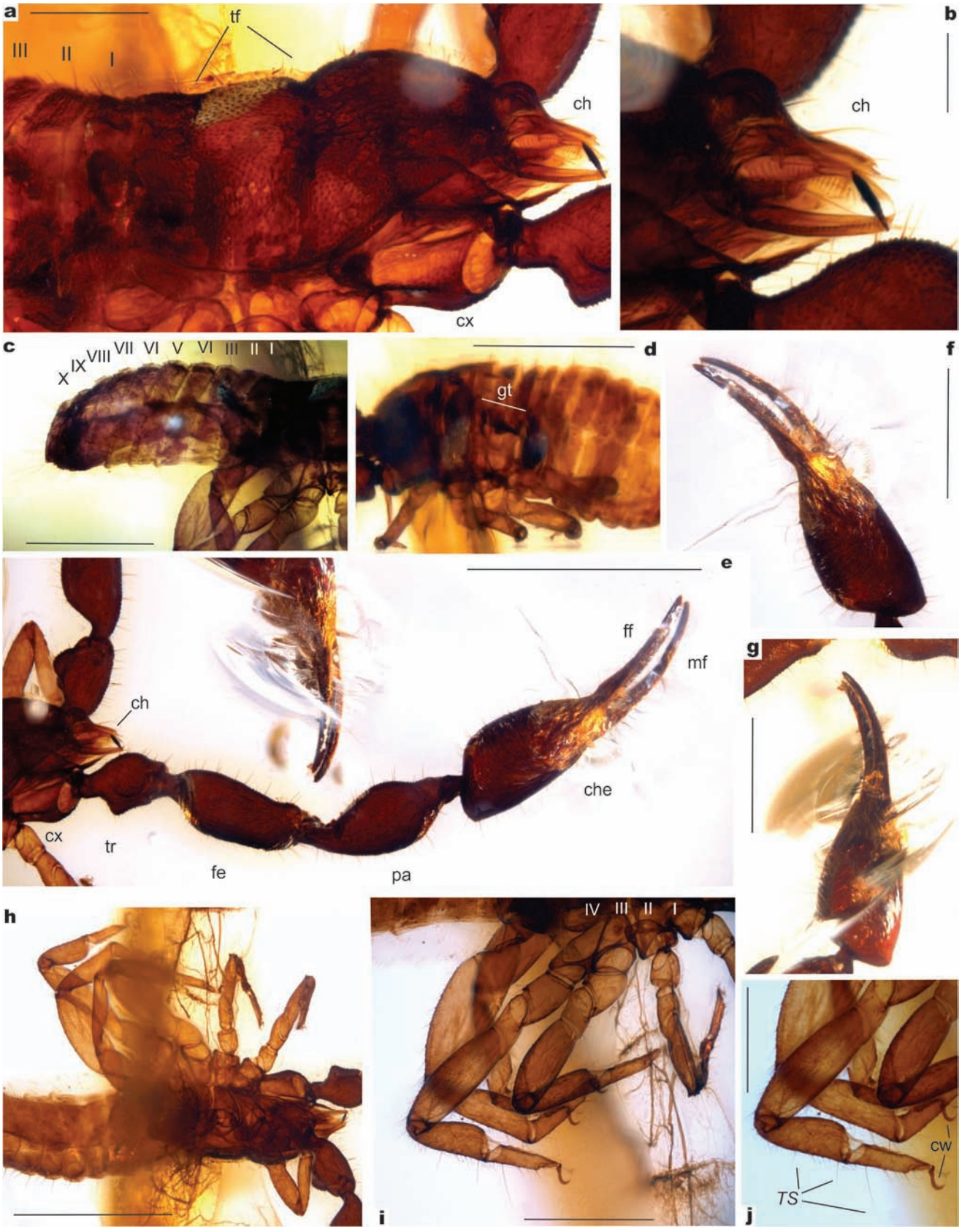

Fig. 4. *Mayachernes maatiatus* gen. et sp. nov., holotype, schematic representation. (*a*) Carapace, dorsal view. (*b*) Coxal area, ventral view. (*c*) Genitalia. (*d*) Chelicera, dorsal view. (*e*) Galea, dorsal view. (*f*) Rallum. (*g*) Right pedipalp. (*h*) The trichobothria pattern on chela, right pedipalp. (*i*) Leg I. (*j*) Leg IV. Scale bars 0.5 mm at (*a*–*b*) and (*h*–*j*); 0.2 mm at (*c*–*d*); 0.1 mm (*e*); 0.05 (*f*); and 1 mm (*g*).

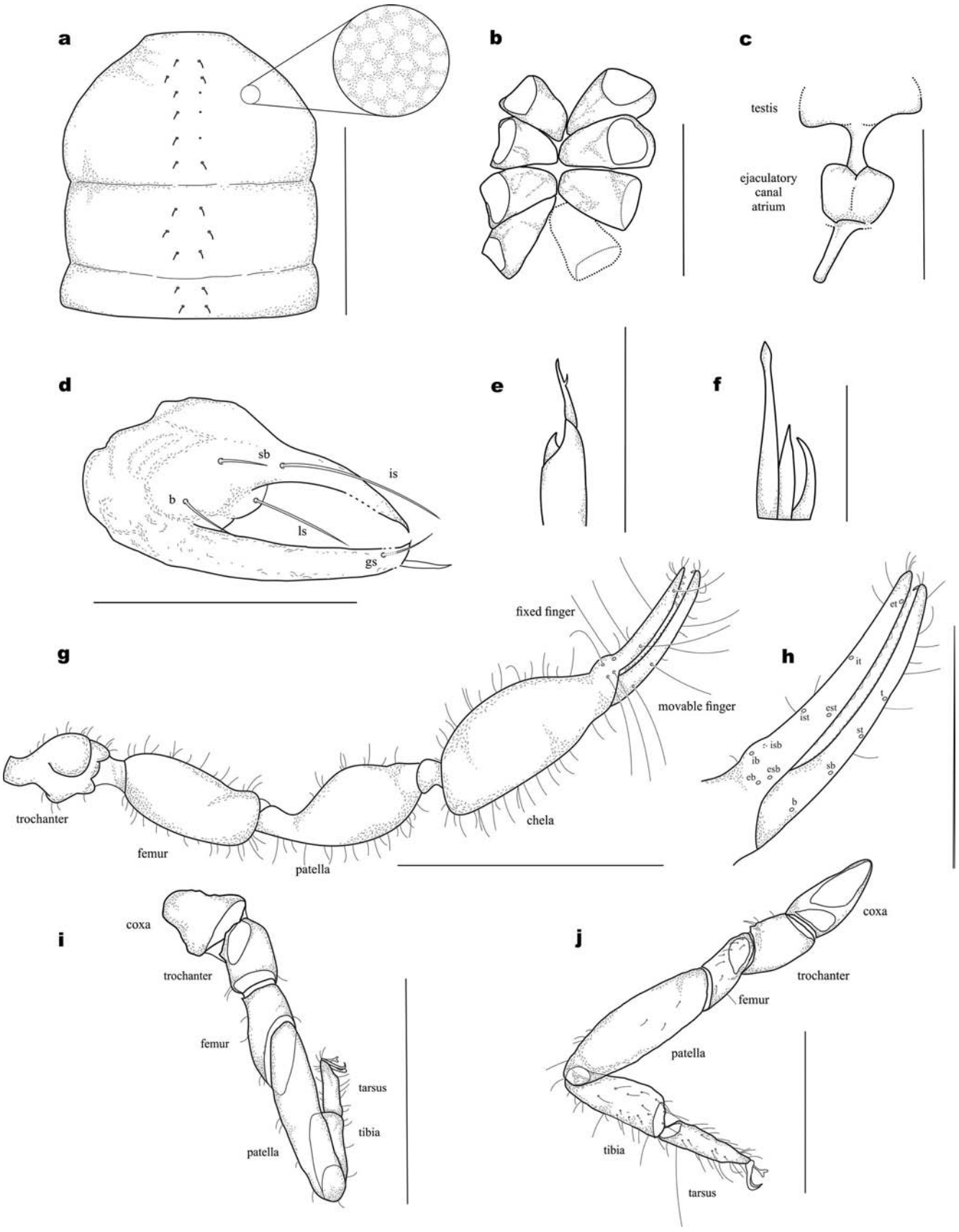

present fossil; (*v*) tarsus with tactile seta, tibia IV with two, on related living species significantly varies (Figs. 2, 3).

Taphomic features: Cuticle slightly mineralized owing to minerals (likely calcium carbonate salts) reacting with the organic acids in amber. This is clearly observed dorsally in the carapace. In contrast, abdomen seems labile, somewhat translucent, as consequence of internal tissue dehydration. There are diverse biodebris adjacent to body, mostly plant remains, such as dissolved leaf situated transversally (Figs. 2*a*, 2*b*). Particularly, there is an elongate blackish plant remain near the chelicera, slightly covering the apical portion of movable finger (Fig. 3*b*). Abundant dark soil, empty bubbles, and minerals particles are also present. The piece of amber is golden yellow with polished, translucent glossiness. A pattern of circular movements near the palps has been internally pressed into the amber at detail. This describes the dramatic movements by the palps during rapid amber hardening and the specimen's death (Figs. 2*a*, 2*b*). Accordingly, there are no fossilization artefacts with taxonomic interest.

Coloration preserved in amber: Carapace and palps reddish brown in ground color, legs and abdomen yellowish brown, somewhat translucent (Figs. 2, 3).

Carapace: Reddish brown, strong, subrectangular, slightly longer than wide (*L*/*W* ratio = 1.09) with two well-marked transverse furrows, the posterior one less deep and closer to the posterior carapace margin than to the anterior furrow (Figs. 2*c*, 3*a*, 4*a*); surface conspicuously sculptured with granules, conspicuously separated; eyes or eyespots absent; 19 observable setae; coxal area parallel-sided, pseudosternum absent, all coxae about the same size (Figs. 3*a*, 4*b*).

Abdomen: Yellowish brown; longer than wide (*L*/*W* ratio = 1.6); with tergites I–X divided, except XI; surface strongly striated; with nine setae on any tergal half, and 11 on any sternal half; tergite XI with long tactile setae; pleural membrane weakly rugose. Genitalia placed anteriorly with respect to genital operculum, testis partially visible, ejaculatory canal atrium with inverted triangle-shaped, dorsal apodeme elongate and darker, setae of genital operculum are not discernible or not preserved (Figs. 2*c*, 3*c*, 3*d*, 4*c*).

Chelicera: Reddish brown, about 1/3 as long as carapace, hand smooth with four acuminate setae (*b*, *sb*, *ls*, *is*) and one in the movable finger (*gs*); movable finger moderately slender, with subapical lobe, at least two discernible teeth (Fig. 4*d*); apparently 20 plates in the serrula exterior; galea with at least two rami (Figs. 3*a*, 3*b*, 4*e*); rallum composed of three blades (Fig. 4*f*).

Pedipalps: Reddish brown, moderately stout; surface of maxilla, trochanter, femur, and patella with granules; chela striate; trochanter with two round lateral humps; patella pedicel slender; chelal hand with dorsal depression (Figs. 3*e*–3*g*, 4*g*); movable finger with 35 small, contiguous teeth and two accessory teeth; fixed finger with 16 accessory teeth; fixed chelal finger with eight trichobothria and movable finger with four trichobothria in the next pattern: *it* on fixed finger much closer to *et* than to *esb*, and farthest from the fingertip than the distance between *isb* and *ist*, *st* about midway between *t* and *sb*, *ist* closer to *isb* or *ib* than *it*, distance between *st* and *t* less than the distance of *t* from the fingertip, distance from *est* to *isb* more than five times as the distance between *esb* and *eb* (Figs. 3*e*–3*g*, 4*g*, 4*h*). Venom tooth present in movable chelal finger (Figs. 3*e*–3*g*, 4*g*, 4*h*).

Legs: Yellowish brown; large, tarsus undivided; each leg with five segments beyond coxa; segment surface varying from almost smooth to weakly granular; legs III and IV with femora different in shape than I and II, with one prominent tactile seta at the base of tarsus (TS = 0.25) and tibia with two marginal tactile setae at middle and distal end; leg IV with oblique junction between femur and patella; claws simple, little longer than arolium (Figs. 3*h*–3*j*, 4*i*, 4*j*).

Dimensions, L/W *ratio*: Body total length 4.83, without pedipalps 2.40, without chelicera and pedipalps 2.20. Carapace: 0.78/0.71. Pedipalp: trochanter 0.37/0.27 (1.39); femur 0.63/0.26 (2.42); patella 0.63/0.29 (2.17); chela, with pedicel: 1.43/0.36 (3.97); chela, without pedicel: 1.33/0.36 (3.69); hand 0.73/0.36 (2.03); movable finger length 0.61 (0.46 times longer than length of hand without pedicel). Chelicera: 0.27/0.13 (2.08), movable finger length 0.19. Leg I: trochanter 0.12/0.1 (1.2), femur 0.22/0.11 (2), patella 0.4/0.09 (4.44); tibia 0.19/0.06 (3.17); tarsus 0.11/0.03 (3.67). Leg IV: trochanter 0.24/0.14 (1.71); femur 0.27/0.1 (2.6); patella 0.53/0.16 (3.31); tibia 0.34/0.12 (2.83); tarsus 0.27/0.07 (3.6).

REMARKS: *Mayachernes* gen. nov. is most closely related to the extant genera *Lustrochernes* (Beier, 1932*a*), *Lamprochernes* (Tömösváry, 1882), *Cordylochernes* (Beier, 1932*a*), *Americhernes* (Muchmore, 1976), *Gomphochernes* (Beier, 1932*a*), *Incachernes* (Beier, 1933), *Odontochernes* (Beier, 1932*a*), *Mesochernes* (Beier, 1932*a*), all putative members of the family Chernetidae. Taxonomic affinities include the presence of rallum with three setae and tarsus and tibia IV bearing tactile setae (except *Incachernes*), among others. However, *Mayachernes* consistently differs from its living congeners by the following considerations: *Mayachernes* differs from *Lustrochernes* by having a carapace with a granulated pattern instead of almost smooth. It also differs from *Lustrochernes* in the shape of palpal patella in male and the trichobothria pattern with *st* closer to *sb* than *t*, whereas *Mayachernes* has *st* about midway between *t* and *sb* (Beier 1932*b*).

In contrast, *Mayachernes* differs from *Lamprochernes* by having a palpal patella with conspicuous dorsomedial protuberance in male and two furrows in the carapace instead of a median furrow, a feature seen in *Lamprochernes*. Another difference is observed in tergites; *Mayachernes* has all tergites divided but XI. *Lamprochernes* has tergites I or II and XI undivided. *Mayachernes* also differs from *Lamprochernes* with trichobothria *ist* as close to *it* as to *isb* or *ib* or closer to *it* than to *isb* or *ib*, whereas *Mayachernes* has *ist* closer to *isb* or *ib* than *it* (Tömösváry 1882).

Mayachernes matches with *Cordylochernes* in the shape of the palpal patella in male but differs in dimension ratio (*L*/*W*) of tibia and tarsus on leg IV. *Mayachernes* has tibia and tarsus IV with a ratio of 2.83 and 3.6, respectively, rather than over five as described in *Cordylochernes*. It also differs in trichobothria *st* closer to *sb* than *t* as noted in *Cordylochernes* (Beier 1932*b*).

Additionally, *Mayachernes* distinguished from *Americhernes* by having trichobothria *ist* and *isb* closer than the distance between *it* and *ist*, instead of *it* closer to *ist* than the distance between *ist* and *isb* as seen in *Americhernes*. *Americhernes* also has carapace smooth, with single transverse furrow, and two eyespots. *Mayachernes* also differs from *Gomphochernes*, which has eyespots, carapace smooth, trichobothria *st* closer to *sb* than *t*, and claws with an accessory tooth, all absence in *Mayachernes* (Muchmore 1976; Beier 1932*b*).

Mayachernes may be separated from *Incachernes*, mainly because it has eyespots, distinct setae on tergites and carapace, palps dentate, trichobothria *it* farther from the fingertip than the distance between *isb* and *ist*, and *st* closer to *t* than *sb*, and lacks tactile setae on tibia IV. *Mayachernes* also differs from *Odontochernes* (with total length about 4 mm) by having different morphometric values. Besides, *Odontochernes* has claws with an accessory tooth. Lastly, *Mesochernes*, with distinct trichobothria *sb* much closer to *st* than *t* and slender legs (with tibia and tarsus five times longer than wide), also distinguished from *Mayachernes* (Beier 1932*b*, 1933).

Conclusion

The latest published review shows 23 extant genera with nearly 54 species of chernetids described in Mexico (Ceballos 2004; Villegas-Guzmán 2013). There are eight living species and one fossil form of chernetids currently documented in Chiapas, southern Mexico (Schawaller 1982; Córdova-Tabares and Villegas-Guzmán 2013). Biogeographically, Chiapas is located in a terrain between boundaries of North and Central America. The data as presented herein show that *Mayachernes maatiatus* gen. et sp. nov. is the first newly described fossil species of the family Chernetidae from the

Miocene Chiapas amber. Since the first attempt to document pseudoscorpions in the Chiapas amber *sensu* (Schawaller 1982), many fossils (including pseudoscorpions) have been missing on account of oligophrenic amber trading. This is influenced by civil and academic collectors who kept the fossils in their pockets. In this context, the occurrence of *M. maatiatus* falls into the large gap in the fossil record of Chiapas amber pseudoscorpions. According to data presented here, this fossil adds to knowledge of the Chernetidae biodiversity and extends the geochronologic range of pseudoscorpions to Neogene rocks in the southernmost part of North America.

Acknowledgements

F.R. was supported by the doctoral granting program CONACYT-PCB/UNAM. D.P.J. was financially supported by the scholarship UNAM-PAPIIT IN213612. Author contributions are as follows: specimen identification by F.R., D.P.J., and V.C.T.; description, measurements, microimaging, graphics, and critical insights by F.R. and D.P.J.; fossil acquisition by B.L.C.; paleontological fieldwork and writing by F.R. The authors declare no conflict of interest. We thank Adriana Kuhn for access to the MACH collection. We thank Dr. Mario Ramos (IGL–UNAM) for help in the field and Dr. Fernando Alvarez (Science Faculty, UNAM) for useful discussions and reviewing the manuscript. We also thank Jon D. Richey (Texas State University) for help with the English edition and Kilian Laclavetine (CNA–Sevilla) for French edition. Thanks go to Dr. Jose Luis Ruvalcaba (IF–UNAM) for supporting this research, Susana Guzmán (IB–UNAM) for microphotography assistance, and Maira Montejo (Science Faculty, UNAM) for help in the amber collection. We thank the anonymous reviewers and Associated Editor whose comments have improved the final published edition.

References

Beier, M. 1932*a*. Pseudoscorpionida II. Subord. C. Cheliferinea. Das Tierreich, **58**(i–xxi): 1–294.

Beier, M. 1932*b*. Zur Kenntnis der Lamprochernetidae (Pseudoscorpionidea). Zoologischer Anzeiger, **97**: 258–267.

Beier, M. 1933. Pseudoskorpione aus Mexiko. Zoologischer Anzeiger, **104**: 91–101.

Calvillo-Canadell, L., Cevallos-Ferriz, S., and Rico-Arce, L. 2009. Miocene *Hymenaea* flowers preserved in amber from Simojovel de Allende, Chiapas, Mexico. Review of Palaeobotany and Palynology, **160**(3–4): 126–134.

Ceballos, A. 2004. Pseudoscorpionida. *In* Biodiversidad, taxonomía y biogeografía de Artrópodos de México: hacia una síntesis de su conocimiento. *Edited by* Bousquets, J. et al. Facultad de Ciencias, UNAM-CONABIO, Mexico, **4**: 417–429.

Córdova-Tabares, V.M., and Villegas-Guzmán, G.A. 2013. Nuevos registros de Pseudoescorpiones (Arachnida: Pseudoscorpiones) en Chiapas, México. Acta Zoológica Mexicana, **29**(3): 596–613.

Dunlop, J.A. 1996. Arácnidos fósiles (con exclusión de arañas y escorpiones). *In* Volumen Monográphico: PaleoEntomologica. *Edited by* Melic, A. Boletin de la Sociedad Entomologica Aragonesa, **16**: 77–92.

Durán-Ruiz, C., Riquelme, F., Coutiño-José, M., Carbot-Chanona, G., Castaño-Meneses, G., and Ramos-Arias, M. 2013. Ants from the Miocene Totolapa amber (Chiapas, Mexico), with the first record of the genus *Forelius* (Hymenoptera, Formicidae). Canadian Journal of Earth Sciences, **50**: 495–502. doi:10.1139/cjes-2012-0166.

Francke, O.F. 2014. Biodiversity of Arthropoda (Chelicerata: Arachnida ex Acari) in Mexico. Revista Mexicana de Biodiversidad, **85**: 408–418.

Frost, S.H., and Langenheim, R.L. 1974. Cenozoic reef biofacies, tertiary larger Foraminifera and scleractinian corals from Chiapas, Mexico. Northern Illinois University Press, DeKalb. p. 388.

Gao, Z., and Zhang, F. 2011. A new genus and species of Chernetid pseudoscorpion (Pseudoscorpiones: Chernetidae) from Hainan Island, China. Entomological News, **122**: 432–440. doi:10.3157/021.122.0505.

Graham, A. 1999. Studies in neotropicalpaleobotany. XIII. An Oligo-Miocene palynoflora from Simojovel (Chiapas, Mexico). America Journal of Botany, **86**(1): 17–31.

Harvey, M.S. 1992. The phylogeny and classification of the Pseudoscorpionida (Chelicerata: Arachnida). Invertebrate Taxonomy, **6**: 1373–1435. doi:10.1071/IT9921373.

Harvey, M.S. 2013. Order Pseudoscorpiones. *In* Animal Biodiversity: An Outline of Higher-level Classification and Survey of Taxonomic Richness. *Edited by* Zhang, Z.Q. Addenda. Zootaxa, **3703**: 34–35.

Henderickx, H., Tafforeau, P., and Soriano, C. 2012. Phase-contrast synchrotron microtomography reveals the morphology of a partially visible new *Pseudogarypus* in Baltic amber (Pseudoscorpiones: Pseudogarypidae). Palaeontologia Electronica, **15**: 1–11.

Judson, M.L.I. 2003. Baltic amber pseudoscorpions (Arachnida, Chelonethi): a new species of *Neobisium* (Neobisiidae) and the status of *Obisium rathkii* Koch & Berendt. Geodiversitas, **25**: 445–450.

Judson, M.L.I. 2007. A new and endangered species of the pseudoscorpion genus Lagynochthonius from a cave in Vietnam, with notes on chelal morphology and the composition of the Tyrannochthoniini (Arachnida, Chelonethi, Chthoniidae). Zootaxa, **1627**: 53–68.

Judson, M.L.I. 2010. Redescription of *Chelifer eucarpus* DALMAN (Arachnida, Chelonethi, Withiidae) and first records of pseudoscorpions in copal from Madagascar and Colombia. Palaeodiversity, **3**: 33–42.

Langenheim, J.H. 1966. Botanical source of amber from Chiapas, Mexico. Ciencia, **24**: 201–211.

Langenheim, J.H. 2003. Plant resins: chemistry, evolution, ecology and ethnobotany. Timber Press, Portland. pp. 141–304.

Mahnert, V., and Adis, J. 2002. Pseudoscorpiones. *In* Amazonian Arachnida and Myriapoda. *Edited by* Adis, J. Pensoft Publishers, Sofia, Bulgaria. pp. 367–380.

Miranda, F. 1963. Two plants from the amber of Simojovel, Chiapas, Mexico, area. Journal of Paleontology, **37**: 611–614.

Muchmore, W.B. 1976. Pseudoscorpions from Florida and the Caribbean Area. 5. Americhernes, a new genus based upon Chelifer oblongus say (Chernetidae). The Florida Entomologist, **59**: 151–163.

Muchmore, W.B. 1990. Pseudoscorpionida. *In* Soil Biology Guide. *Edited by* Dindal. D.L. John Wiley and Sons, New York. pp. 503–527.

Murienne, J., Harvey, M.S., and Giribet, G. 2008. First molecular phylogeny of the major clades of Pseudoscorpiones (Arthropoda: Chelicerata). Molecular Phylogenetics and Evolution, **49**: 170–184 doi:10.1016/j.ympev.2008.06.002. PMID: 18603009.

Perrilliat, M.C., Vega, F.J., and Coutiño, M.A. 2010. Miocene mollusks from the Simojovel area in Chiapas, southwestern Mexico. Journal of South American Earth Sciences, **30**: 111–119. doi:10.1016/j.jsames.2010.04.005.

Poinar, G.O. 1992. Life in amber. Palo Alto (CA): Stanford University Press, pp. 29–46.

Poinar, G.O., and Brown, A.E. 2002. *Hymenaea mexicana* sp. nov. (Leguminosae: Caesalpiniodeae) from Mexican amber indicates Old World connections. Botanical Journal of the Linnean Society, **139**: 125–132.

Riquelme, F., Alvarado-Ortega, J., Ramos-Arias, M., Hernández, M., Le Dez, I., Lee-Whiting, T.A., and Ruvalcaba-Sil, J.L. 2014*a*. A fossil stemmiulid millipede (Diplopoda: Stemmiulida) from the Miocene amber of Simojovel, Chiapas, México. Historical Biology, **26**(4): 415–427. doi:10.1080/08912963.2013.778843.

Riquelme, F., Northrup, P., Ruvalcaba-Sil, J.L., Stojanoff, V., Siddons, D.P., and Alvarado-Ortega, J. 2014*b*. Insights into molecular chemistry of Chiapas amber using infrared-light microscopy, PIXE/RBS, and sulfur K-edge XANES spectroscopy. Applied Physics A., **116**(1): 97–109. doi:10.1007/s00339-013-8185-2.

Riquelme, F., Ruvalcaba-Sil, J.L., Alvarado-Ortega, J., Estrada-Ruiz, E., Galicia-Chávez, M., Porras-Múzquiz, H., et al. 2014*c*. Amber from México: Coahuilite, Simojovelite and Bacalite. MRS Proceedings. Vol. 1618. doi:10.1557/opl.2014.466.

Rohlf, F.J. 2013. The tpsDig program, ver. 2.17. The Stony Book University, NY, USA.

Schawaller, W. 1980. Erstnachweis tertiarer Pseudoskorpione (Chernetidae) in Dominikanischem Bernstein (Stuttgarter Bernsteinsammlung: Arachnida, Pseudoscorpionidea). Stuttgarter Beitrage zur Naturkunde (B), **57**: 1–20.

Schawaller, W. 1982. Der erste Pseudoskorpion (Chernetidae) aus Mexikanischem Bernstein. Stuttgarter Beiträge zur Naturkunde (B), **85**: 1–9.

Schawaller, W. 1991. The first Mesozoic pseudoscorpion from Cretaceous Canadian amber. Palaeontology, **34**: 971–976.

Schawaller, W., Shear, W.A., and Bonamo, P.M. 1991. The first Palaeozoic pseudoscorpions (Arachnida: Pseudoscorpionida). American Museum Novitates, **3009**: 1–17.

Shear, W., Schawaller, W., and Bonamo, P.M. 1989. Record of Palaeozoic Pseudoscorpions. Nature, **341**: 527–529. doi:10.1038/341527a0.

Tömösváry, Ö. 1882. Pseudoskorpiones Faunae Hungaricae. Mathematikai és Természettudományi Közlemények, **18**: 135–256.

Villegas-Guzmán. G.A. 2013. Pseudoescorpiones (Arachnida: Pseudoscorpiones) de la Laguna Colombia, Isla de Cozumel, Quintana Roo, México. *In* Entomología Mexicana. *Edited by* Equihua-Martinez, A., Estrada-Venegas, E. Sociedad Mexicana de Entomología, Mexico, **12**(1): 117–120.

Weygoldt, P. 1969. The Biology of Pseudoscorpions. Harvard University Press, Cambridge, Massachusetts, p. 156.

N. Jb. Geol. Paläont. Abh. 275/1 (2015), 93–106
Stuttgart, January 2015

Article

Fossil Jumping-bristletail from the Chiapas amber: *Neomachilellus (Praeneomachilellus) ezetaelenensis* sp. nov. (Microcoryphia: Meinertellidae)

Francisco Riquelme, Maira Montejo-Cruz, Bibiano Luna-Castro, and Luis Zuñiga-Mijangos

With 8 figures

Abstract: A new species of Jumping-bristletail, *Neomachilellus (Praeneomachilellus) ezetaelenensis* sp. nov. (Microcoryphia: Meinertellidae), is described from the Miocene amber collected in the Mountains of Chiapas, southwestern Mexico. This study is based on amber microcoryphian insects newly recovered from rocks near the towns of Simojovel, Totolapa and Estrella de Belén. These amber sites are part of a Conservation Lagerstätte with remarkable preserved paleobiota. On the basis on male and female specimens, *N. (Praeneomachilellus) ezetaelenensis* sp. nov., is illustrated and diagnosed herein by a combination of diagnostic characters. Morphological data were collected using high-resolution microscopy with regular to adapted infrared-pass lens. The subgenus *Praeneomachilellus* Sturm & Poinar, 1997 into the genus *Neomachilellus* Wygodzinsky, 1953 comprises one described fossil species from the Miocene Dominican Republic amber and one extant species from Puerto Rico. Thus, *N. (Praeneomachilellus) ezetaelenensis* is the first species of this group to be described in the Chiapas amber that adds insights into Microcoryphia biodiversity at the southernmost part of North America.

Key words: Miocene, Chiapas amber, Microcoryphia, Meinertellidae, *Neomachillelus*, Jumping-bristletail.

1. Introduction

Microcoryphians (= Archaeognatha) commonly called Jumping-bristletails are one of the earliest insect lineages. They are small, primitive, ectognathous wingless insects that currently live in temperate and tropical environments (Sturm & Machida 2001). Microcoryphians occur in soil, leaf litter, tree bark, fractured stones, nearby water-pounds, and rocky nearshores. Systematics of Microcoryphia Verhoeff, 1904 has been reviewed and discussed elsewhere (Sturm & Bach de Roca 1993; Mendes 2002). The order Microcoryphia comprises the families Meinertellidae, Machilidae, and some *incertae sedis* genera with extant and few fossil representatives distributed at both Hemispheres (Sturm & Machida 2001).

In spite of very poor fossil record of Microcoryphia, modern forms are found as fossils in amber at different deposits and geological ages. A few fossils have been recorded in amber from Lebanon, Myanmar, Spain, New Jersey, Baltic, Dominican Republic, Mexico (Chiapas), and Venezuela copal (Mendes & Wunderlich 2013; Getty et al. 2013).

Basal archaeognatha-like forms associated with Microcoryphia and its sister group Zygentoma (=Thysanura) are recorded as fragmentary fossils in Early to Middle Devonian strata from Quebec, Canada and New York, US, respectively (Shear et al. 1984; La-

www.schweizerbart.de
DOI: 10.1127/njgpa/2015/0453
0077-7749/2015/0453 $ 3.50

bandeira et al. 1988). The extinct Monura linage in a close position with Microcoryphia/Zygentoma insects shows a geochronologic range spanning from the Late Carboniferous to Middle Triassic (Bechly & Stockar 2011). Monura trace fossils are also found from the Late Carboniferous to Early Permian shales of North America (Getty et al. 2013). The oldest known fossil closely related to microcoryphian insects presumably is *Triassomachilis uralensis* Sharov, 1948 from the Early Triassic of Russia, but its taxonomical identity is still under debate (Sharov 1948, 1957; Sturm & Poinar 1998; Bechly & Stockar 2011; Mendes & Wunderlich 2013).

The unequivocal modern forms of microcoryphian insects comes from the Early Cretaceous amber, *Cretaceomachilis libanensis* Sturm & Poinar, 1998 (family Meinertellidae), from Lebanon, and *Macropsontus* sp., from Myanmar (Mendes & Wunderlich 2013). Other undescribed Microcoryphia or Zygentoma insects have been reported in the Early Cretaceous of Álava, Spain (Alonso et al. 2000) and the Late Cretaceous amber of New Jersey, US (Getty et al. 2013; Mendes & Wunderlich 2013). Several taxa from the Paleogene Baltic amber have been described and listed by Silvestri (1912). There is one species of the family Meinertellidae described in the Neogene Dominican Republic amber: *Neomachilellus (Praeneomachilellus) dominicanus* Sturm & Poinar, 1997. Another microcoryphian sub-fossil named as *Meinertellus* sp. was reported in Venezuela copal (Mendes 1997).

Lastly, there is one record in Chiapas amber previously published, which is based on a female specimen tentatively attributed to *Neomachilellus* (Wygodzinsky 1971). This fossil was collected near the town of Ixhuatán, as seen listed in the amber collection from the University of California with ≈1500 amber fossils (Wygodzinsky 1971). These were donated mostly by the Danish explorer and indigenist Franz Blom, who was active in Chiapas since the 1930s. Another male specimen from the American Museum of Natural History, NY, was also briefly mentioned by Sturm & Poinar (1997). Until now, the status of both specimens remains unclear. Recently, microcoryphian insects trapped in Chiapas amber are continuously collected in rocks near Simojovel, Totolapa, Huitiupán, Pueblo Nuevo Solistahuacán, San Andrés Duraznal and Estrella de Belén, in the Mountains of Chiapas.

The genus *Neomachilellus* (family Meinertellidae) comprises two subgenera: *N. (Neomachilellus*) with nearly 39 extant species and *N. (Praeneomachilellus)* with one fossil species and another extant (Sturm & Poinar 1997; Bach de Roca et al. 2009). Fossil species erected as *N. (Praeneomachilellus) dominicanus* Sturm & Poinar, 1997 was described in the Miocene Dominican amber; whereas the living species *N. (Praeneomachilellus) szeptyckii* is currently known from Puerto Rico (Bach de Roca et al. 2009).

In this context, the first species of microcoryphian insect in the Miocene Chiapas amber referred to here as *Neomachilellus (Praeneomachilellus) ezetaelenensis* sp. nov. is illustrated and described in the present paper. Diagnosis is based on fossil material newly recuperated from lignite/sandstones beds exposed surrounding Simojovel, Totolapa and Estrella de Belén, in the Mountains of Chiapas, Mexico. Fossil specimens have been delicately preserved showing anatomical characters (including true color) with taxonomical interest. Laboratory-adapted microscopy with regular to infrared-reflected lens has been used to collect all morphological data (Riquelme et al. 2014a).

Morphotype of the present fossil species corresponds largely with the extant representatives of the family Meinertellidae, which is the most derived clade of Microcoryphia (Sturm & Machida 2001). It exhibits small abdominal sterna, each of them with not more than one pair of eversible vesicles, pulvilli absent, and antennae lacking scales (Sturm & Bach de Roca 1992). Also matches with the genus *Neomachilellus* by having an adult body length ≥7 mm, body hypodermal pigmentation with reddish-brown to blackish in color, eyes large and rounded, paired ocelli wide, ♂ penis short and ♀ chaetotaxy on the ovipositor (Sturm & Poinar 1997). A full description and diagnosis is presented below, which is the aim of the present paper.

2. On the depositional environment

Geological setting of Chiapas amber has been reviewed in several paleontological and biostratigraphic studies. Most authors agree that amber-bearing beds are part of the Mazantic shale and Balumtum sandstone strata dated as early to middle Miocene, ca. 23-15 Ma (Frost & Langenheim 1974; Poinar 1992; Perrilliat et al. 2010; Riquelme et al. 2014a, among others). Preliminary paleontological prospections near Simojovel have also mentioned another amber outcrop within the La Quinta strata with late Oligocene in age (i.e. Frost & Langenheim 1974; Poinar 1992). However, recent geology fieldwork in such area cannot be confirmed this outcrop as yet. More supporting stratigraphic studies regarding the correlation between amber outcrops over the Mountains of Chiapas from Totolapa

Fig. 1. Location of amber sites in the Mountains of Chiapas, southwestern Mexico.

(southernmost site) to Estrella de Belén (northernmost site) are needed.

The available stratigraphic data and comments of amber outcrops near Simojovel and Totolapa is shown elsewhere (Frost & Langenheim 1974; Poinar 1992; Ferrusquía-Villafranca 2006, Perrilliat et al. 2010; Duran-Ruiz et al. 2013; Riquelme et al. 2014a, b, among others). Readers are urged to consult the sedimentary environment as presented in previous published studies. Palynology in amber sediments near Simojovel indicates a terrestrial-mangrove environment (Graham 1999). Estrella de Belén site near Palenque was discovered in 2010 by village farmers who give notice by the first time to an expedition represented by archeologist Martha Cuevas (INAH), and paleontologists Jesús Alvarado (IGL-UNAM) and Francisco Riquelme (PCB-UNAM) (Fig. 1). The amber-bearing beds in this site resemble those exposed near Simojovel and Totolapa. The amber section mainly consists of organic-rich lignite lenses derived from decomposition of plant residues and soils. There is non-fissile, coarse to fine grained sandstone variable in thickness associated with lignite. There are also ripple cross-lamination, interbedded friable shales, lenticular bedding of bentonite-like clay, brown to red iron oxides, abundant clay minerals and pyrite lumps. In fact, pyrite trapped in amber is frequently found in Estrella de Belén as unique characteristic no shared with other amber sites. Rocks are occasionally exposed angular or almost perpendicularly to the beading plane. This indicated a strong tectonic activity post-burial. According to above, lithology and sedimentary input is consistent with a terrestrial-fluvial environment close to the coast (Boggs 2009).

The amber sites in the Mountains of Chiapas are part of a Miocene Conservation Lagerstätte whose most conspicuous characteristic is that it shows an exceptionally preserved paleobiota (Riquelme et al. 2014a-c). The remarkably preservation of hard/soft tissues on plants, animals and microorganisms was caused by a rapid resin hardening, followed by a disruption of the organic decay (Riquelme et al. 2014c).

Plant source of Chiapas amber is attributed to an extinct legume tree species of the genus *Hymenaea* (*sensu* Langenheim 1966). Chiapas amber has chemical signatures in common with plant resin of living *H. courbaril* and *H. verrucosa*, which are now distributed in the tropics (Langenheim 2003; Riquelme et al. 2014d). Amber associated with *Hymenea* trees are also found in Dominican Republic, Cuba, Puerto Rico, Haiti and Jamaica (Poinar 1992; Iturralde-Vinent 2001; Langenheim 2003). It seems that *Hymenaea* amber forest were dispersal over near costal lands in the Neogene tropics of Middle America. There is also a tectonic and sedimentary evolution in common between Chiapas amber strata and those from the Caribbean, which extends from the Early Miocene to Pliocene (Iturralde-Vinent 2006). Therefore, paleobiota present in *Hymenaea* amber in the Miocene Middle America should be closely related at both taxonomical and paleobiogeographic level.

3. Materials and methods

Amber fossils studied here come from the following sites: La Pimienta site: Latitude 17°09'11" N, Longitude 92°46'08" W, Los Pocitos site: Latitude 17°08'32" N, Longitude 92°43'27" W, both are located near Simojovel. The Rio Salado site near Totolapa: Latitude 16°32'28" N, Longitude 92°41'5" W. Estrella de Belén site near Palenque: Latitude 17°29'2" N, Longitude 91°41'01" W. All amber sites are located in the State of Chiapas, southwestern Mexico (Fig. 1). Fossils are embedded in golden to orange yellow amber with translucent to cloudy glossiness. Fossils specimens are currently housed in the amber fossil collections of the Museo del Ámbar de Chiapas and Museo del Ámbar Lilia Mijangos that are located in San Cristóbal de Las Casas, Chiapas, Mexico. Both amber fossil collections are curated repositories formally certified by the Instituto Nacional de Antropología e Historia (INAH), which protect the archeological and paleontological heritage in Mexico. No specific permits were required for the specimen description and paleontology fieldwork.

Microimaging and measurements: Anatomical data were collected applying laboratory-based, high-resolution microscopy with regular to infrared-pass lens and LED/tungsten lamps. Multiple image superimposition with >23 planes per image were also applied for imaging processing and displaying (Riquelme et al. 2014a-c). Schematic drawings were hand traced by electronic pen using stereomicroscope, micrographs and CorelDraw X6 for graphic processing. Anatomical measurements are expressed in millimeters; these were collected using the open source program tpsDig V. 2.17 (Rohlf 2013).

Acronyms: INAH – Instituto Nacional de Antropología e Historia. MACH – Museo del Ámbar de Chiapas. MALM – Museo del Ámbar Lilia Mijangos. UNAM: Universidad Nacional Autónoma de Mexico.

Terminology: The pattern of description and terminology generally follows Wygodzinsky 1978, Sturm 1997, Sturm & Poinar 1997, and Bach de Roca et al. 2009, with the exception of the linguistic usage of roman numbers in terga, abdominal coxites and legs, in the following text the natural numbers are used as both ordinals and adjectives.

Abbreviations: The following anatomical abbreviations are used in the schematic representations: ast: abdominal sterna; ant: antennae; cx: coxa; cr: cerci; cn: conules; e: eye; fe: femur; fg: flagellum; lop: longitudinal process; h: hook-shaped projection; man: mandibles; mcf: median caudal filament; oce: ocellus; ovp: ovipositor; pd: pedicellus; Plp. Max: maxillary palp; Plp. Lab: labial palp; PP: legs; se: setae; scp: scapus; sp: spine; sty: stylet; ts: tarsus; tb: tibia; tp: triangular process; tr: trochanter.

Nomenclature: The nomenclatural acts as presented herein have been registered in ZooBank, the official website of the ICZN (International Commission on Zoological Nomenclature). The ZooBank LSID (Life Science Identifiers) for this publication is: urn:lsid:zoobank.org:pub:B7563ABF-E17C-4960-AA30-D8A32E342BFE.

4. Systematic paleontology

Order Microcoryphia Verhoeff, 1904 (=Archaeognatha Börner, 1904)
Family Meinertellidae Verhoeff, 1910
Genus *Neomachilellus* Wygodzinsky, 1953
Subgenus *Praeneomachilellus* Sturm & Poinar, 1997

Neomachillelus (Praeneomachilellus) ezetaelenensis
Riquelme & Montejo sp. nov.
(ZooBank LSID: urn:lsid:zoobank.org:act:E0C15BD0-9BE6-4276-9E19-518F2B001D65)
Figs. 2-8

Etymology: For the EZLN, acronym of the Ejército Zapatista de Liberación Nacional, which is an outcast, partisan indigenous group, who fight for their political and human rights in the Mountains of Chiapas, Mexico.

Type material: Holotype male BL.MACH.1, amber inclusion, entire specimen, collected in La Pimienta site and currently deposited at the Museo del Ámbar de Chiapas (Fig. 2A-B).

Allotype female BL.MACH.47, amber inclusion, entire specimen, collected in Los Pocitos site and currently deposited at the Museo del Ámbar de Chiapas, located in San Cristobal de las Casas, Chiapas, Mexico (Fig. 2C-D).

Referred material: Female BL.MACH.32, amber inclusion, entire specimen, collected in Guadalupe Victoria site (Fig. 3A). Female LZ.MALM.3, amber inclusion, entire

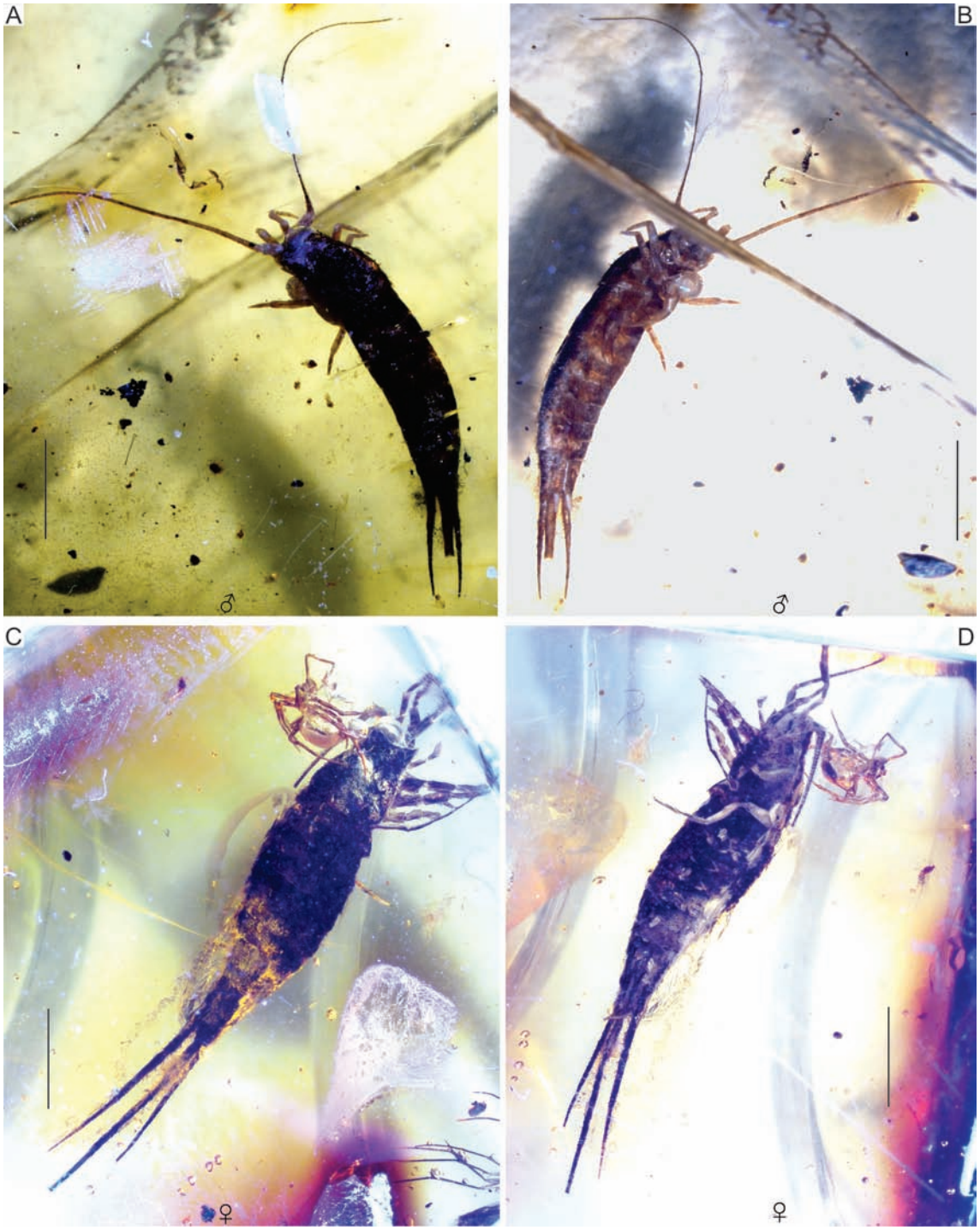

Fig. 2. *Neomachillelus (Praeneomachilellus) ezetaelenensis* sp. nov. **A-B** – Holotype male BL.MACH.1 in dorsal and ventral view. **C-D** – Allotype female BL.MACH.47 in dorsal and ventral view. Scale bars (mm): A-D= 2.

specimen, collected in La Pimienta site (Fig. 3B). Female LZ.MALM.33, amber inclusion, entire specimen, collected in the Río Salado site. Female LZ.MALM.34, amber inclusion, entire specimen, collected in the Estrella de Belén site.

Locality and horizon: La Pimienta, Los Pocitos and Guadalupe Victoria sites near the town of Simojovel; the Río Salado site near the town of Totolapa; and Estrella de Belén site near the town of Palenque. All sites are located in the

Fig. 3. *Neomachillelus (Praeneomachilellus) ezetaelenensis* sp. nov. **A** – Paratype female BL.MACH.32 in ventral view. **B** – Paratype female LZ.MALM.3 in ventral view. **C** – Closer ventral view of holotype male BL.MACH.1 and **D** allotype female BL.MACH.47, both specimens show maxillary palp, labial palp, coxosternites and legs. Scale bars (mm): A-B = 1; C-D = 2.

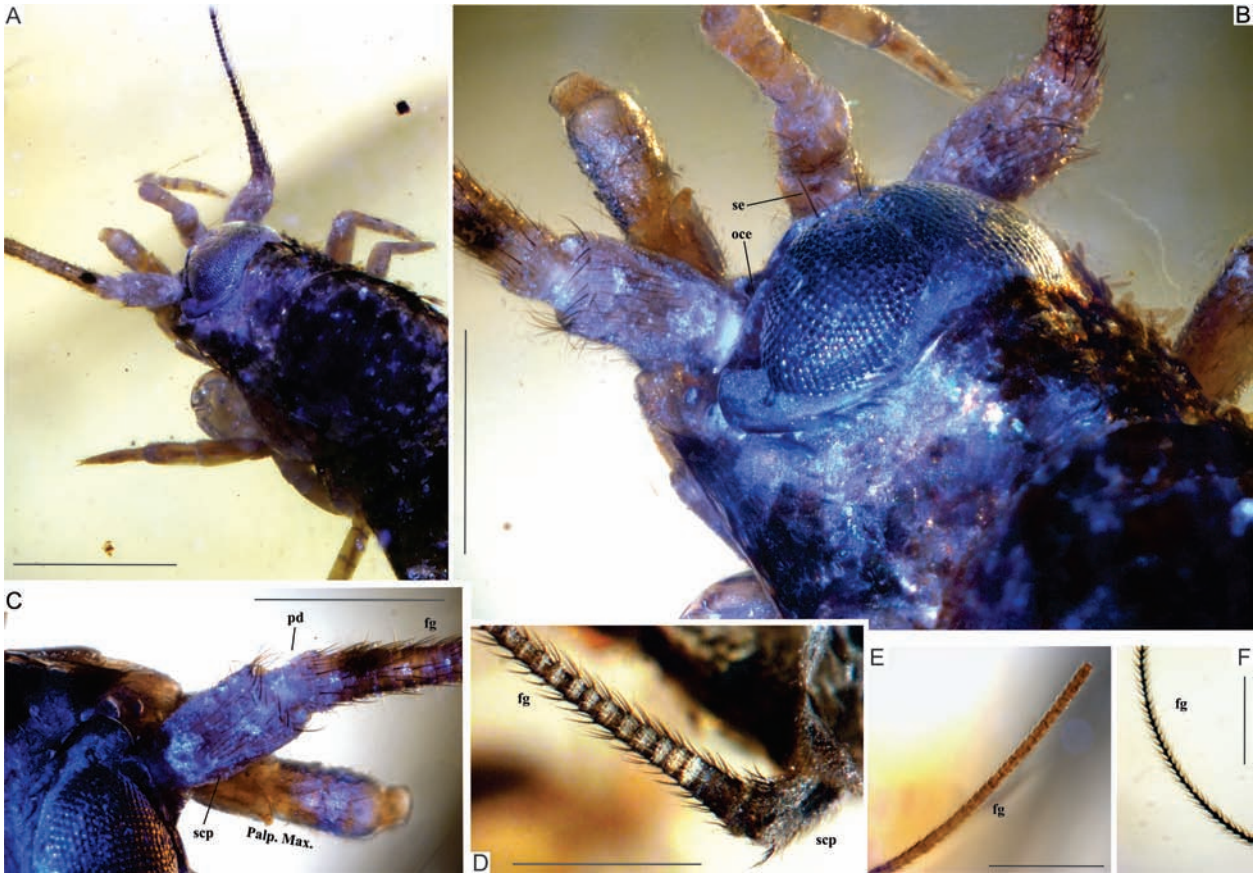

Fig. 4. *Neomachillelus (Praeneomachilellus) ezetaelenensis* sp. nov. **A** – Holotype male BL.MACH.1 in dorsolateral view showing head, eyes, ocellus, antennae, mouth-parts and terga. **B** – Closer view of head and eyes. **C** – Closer view of antennal segments: scapus, pedicellus and flagellum in holotype male BL.MACH.1 and **D-F** allotype female BL.MACH.47. Scale bars (mm): A = 1; B-F = 0.5. See abbreviations in the main text**.**

Mountains of Chiapas, southwestern Mexico (Fig. 1). Here the amber-bearing rocks belong to Mazantic shale and Balumtum sandstone strata dated as early-middle Miocene, ca. 23-15 Ma (Frost & Langenheim 1974; Poinar 1992; Perrilliat et al. 2010; Durán-Ruiz et al. 2013; Riquelme 2014a, b).

Diagnosis: Regular in size, average body length in adult male and female: ≈7 mm. Body with hypodermal pigment, reddish-brown to blackish in ground color. Bearing pigmented scales: in male dorsally reddish, with golden-yellow patches, ventrally lighter, somewhat yellowish; in female darker. Frons projecting an interocellar space below the eye midline with two conspicuous, long setae. Compound eyes contiguous, large, rounded, about as long as wide; brownish in ground color with golden reflection in male; lighter, barely pigmented, pale-yellow and silver reflection in female. Paired ocelli wide, sole-shaped, and extending medially in front of the eyes, dark-brown in color. Antennae elongated, lacking scales, with scapus about twice longer than wide, flagellum filiform, multi-annulled, each annulus with one row of setulae, 40-50 annuli by distal chain. Tergite margins with spiniform, lateral macrosetae. Legs reddish to yellowish, with restricted, darker, brownish patches; coxal stylets, scopulae absent on all legs; coxa 3 with tactile seta. ♂ Penis short. ♀ Ovipositor slender, setose, quaternary type; gonapophyses 8 and 9 with up 35 divisions, and 9 stylets bearing a spine.

Taphonomical features: Holotype male BL.MACH.1, trapped in amber, it preserves head, antennae, thorax, caudal appendages and true color morphology (Figs. 2A-B, 3C). Head and thorax complete, antenna slightly damage, the left maxillary palp broken, the apical portion of the median caudal filament is missing, lateral cerci broken. There are bubble molds near mouth-parts associated with gas emitted by the specimen. Fossilization of soft/hard tissues is extremely delicate, i.e. abundant tiny scales are spread everywhere. There are copious plant fragments, soil and insects remains surrounding body. There is also a conspicuous amber fracture near body in a ventral view. Amber piece is golden-yellow with translucent glossiness (Fig. 3C). There is a blue tone in eyes, antennal scapus, and head, with bluish to whitish patches, but only as a virtual image seeing

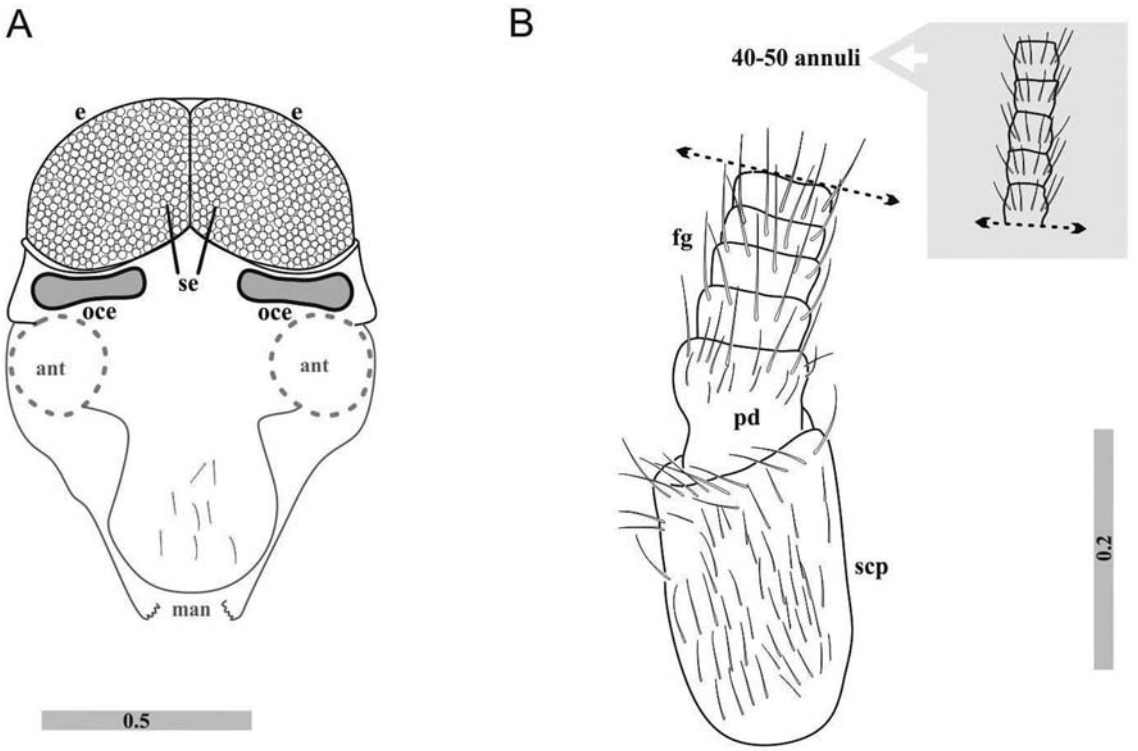

Fig. 5. *Neomachillelus (Praeneomachilellus) ezetaelenensis* sp. nov. **A** – Schematic reconstruction of head, eyes, ocellus and two conspicuous setae below the eye midline. **B** – Antennal segments: scapus, pedicellus, flagellum and annuli in distal portion. See abbreviations in the main text.

on the microscope (Fig. 4A-C). This is caused by refracted light shining on the mineral-rich ommatida, scales and cuticle; probably calcium phosphate.

Allotype female BL.MACH.47, trapped in amber, it preserves head, antennae, thorax, caudal appendages (lateral cerci apically broken), and also true color morphology (Figs. 2C-D, 3D). There is a spider near head, likely a male, a representative of the superfamily Araneoidea. There are also abundant bubble molds and cast, plant and soil fragments, disperse insect parts, mineral particles, and fractures. Amber piece is orange to golden-yellow with translucent glossiness (Fig. 2C-D).

Paratype females BL.MACH.32 and LZ.MALM.3 from Guadalupe Victoria and La Pimienta sites (Simojovel), respectively, as the allotype female in size and general morphology but less preserved, amber slightly varies in cloudiness and color (Fig. 3A-B). Paratype female LZ.MALM.33 from Totolapa as females from Simojovel but amber is typically orange-yellow with cloudy to translucent glossiness. Paratype female LZ.MALM.34 from Estrella de Belén as both Simojovel and Totolapa female specimens but amber is cloudier with more abundant plant remains, minerals and soil. According to above, there are no taphonomic artifacts caused by fossilization in any described specimen that affect size or morphotype.

Color in amber preservation: Male specimen reddish-brown to blackish in ground color, eyes brownish with golden reflection; female specimens as in male but darker, eyes lighter, pale-yellowish, with silver reflection (Figs. 2-4).

Description: Including statements about both male and female. Holotype BL.MACH.1, adult male, a regular-sized Meinertellidae, body length 7 mm. Allotype BL.MACH.47, adult female, body length: 7.2 mm. Body fusiform, subcylindrical, with hypodermal pigment, reddish-brown to blackish in ground color in male; whereas in female are darker. Bearing pigmented scales, in dorsal habitus reddish-brown to blackish, with golden-yellow patches, ventrally lighter, with reddish-brown somewhat yellowish (Figs. 2-3).

Head: Reddish-brown in male, blackish-brown in female; frons and clypeus slightly pigmented, brownish to yellowish in color, finely setose, somewhat protruding (Fig. 4A-B). Frons projecting an interocellar space below the eye midline with two conspicuous, long setae (Figs. 4B, 5A). Compound eyes contiguous, large, rounded, about as long as wide, the eye margins anteriorly blunt and triangular projected, posterolaterally convex and arch-shaped; eyes brownish in ground color with golden reflection in male; whereas lighter, pale-yellow, and silver reflection in female. Paired ocelli wide, sole-shaped, and extending medially in

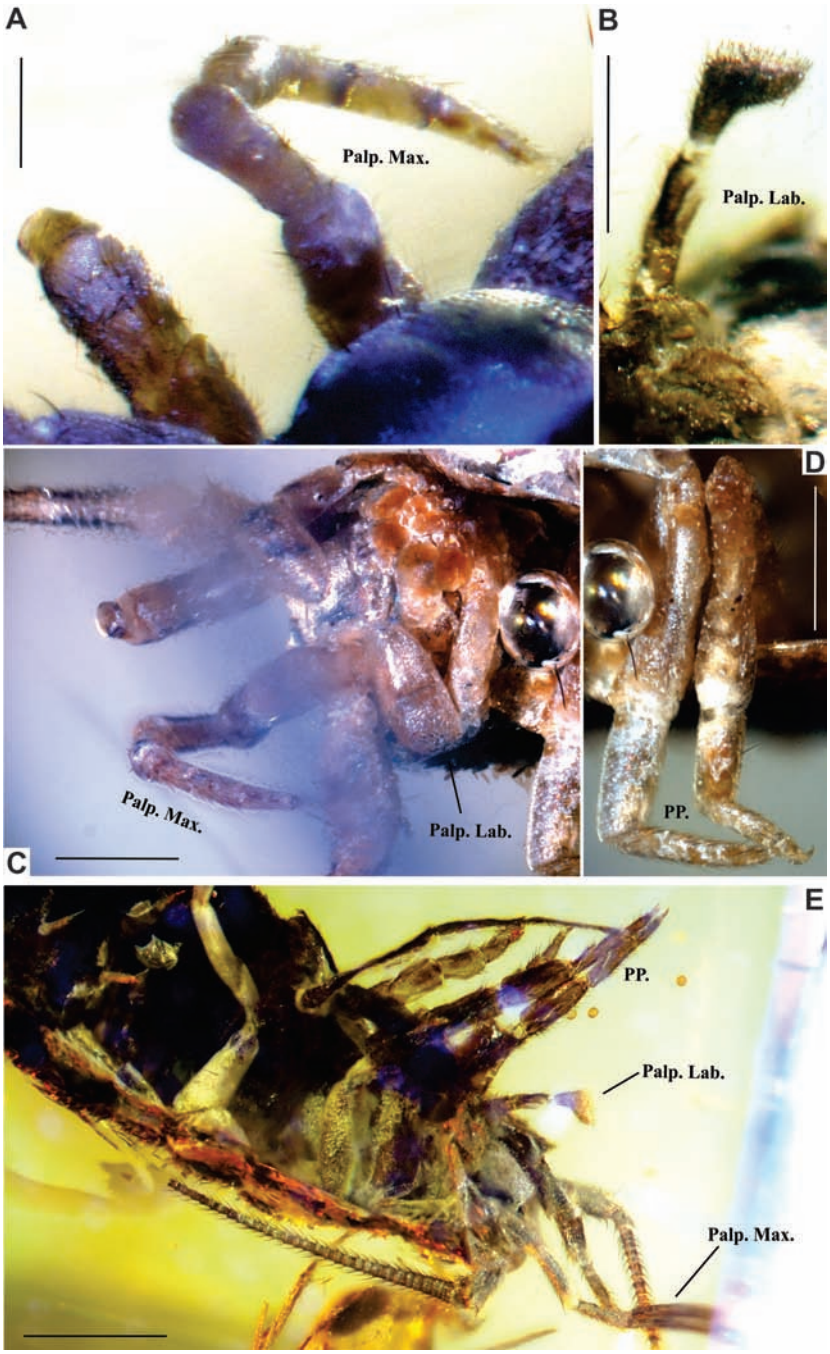

Fig. 6. *Neomachillelus (Praeneomachilellus) ezetaelenensis* sp. nov. **A** – Maxilliary palp on holotype male BL.MACH.1, dorsal view. **B** – Labial palp on allotype female BL.MACH.47, lateral view. **C** – Maxillary and labial palp on BL.MACH.1, ventral view. **D** – Legs on BL.MACH.1, ventral view. **E** – BL.MACH.47 in ventrolateral view showing maxillary palp, labial palp and legs. Scale bars (mm): A = 0.2; B-D = 0.5; E = 1. See abbreviations in the main text.

front of the eyes, dark brown in color, with lateral margins slightly pilose (Figs. 4B, 5A). Mandibles well toothed.

Antennae: Male antennal length: ≈7 mm; female antennal length: ≈5 mm. Antennae elongated, at least as long as the body, lacking scales; scapus about twice longer than wide, robust and setose; pedicellus short, almost as wider as scapus, with apically long setae, both scapus and pedicellus are brownish to somewhat yellowish in color (Fig. 4C-D).

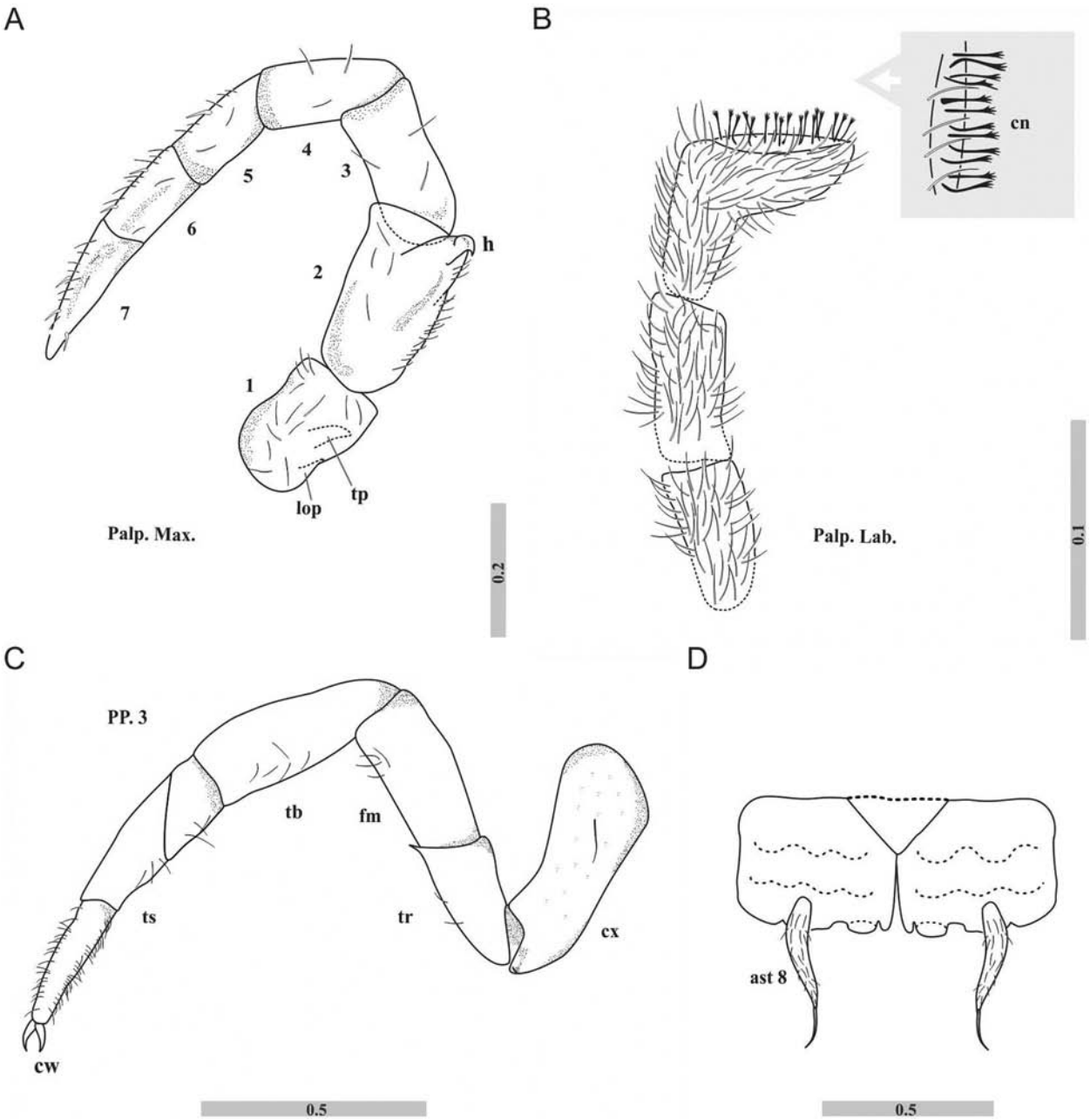

Fig. 7. *Neomachillelus (Praeneomachilellus) ezetaelenensis* sp. nov. **A** – Schematic reconstruction of maxillary palp on holotype male BL.MACH.1. **B** – Labial palp on allotype female BL.MACH.47 with details of the conules. **C** – Leg 3 and **D** coxosternite 8 on BL.MACH.1. See abbreviations in the main text.

Flagellum filiform, widened at the basal part, pigmented, dark-brown in color, distal part is becoming narrower, lighter, brownish; flagellum with multiple annuli, about 40-50 by distal chain, each annulus with one row of setulae (Figs. 4D-F, 5B).

Mouth-parts: ectognathous, reddish to yellowish-brown in ground color (Fig. 6). Maxillary palp obviously long, setose, 7-articulated, basal articles with dark pigmentation and distal articles becoming lighter (Fig. 6A). Article 1 with irregular reddish-brown patches, basally setae long, with chaetotaxy undetermined, dorsal longitudinal process barely longer than the triangular process; article 2 brownish pigmented, less setose than the previous one, with hook-shaped process present (with distal dorsal inner apophysis); article 3 and 4 yellowish-brown, as longer than 1 and 2, but article 3 bearing long setae, and article 4 with

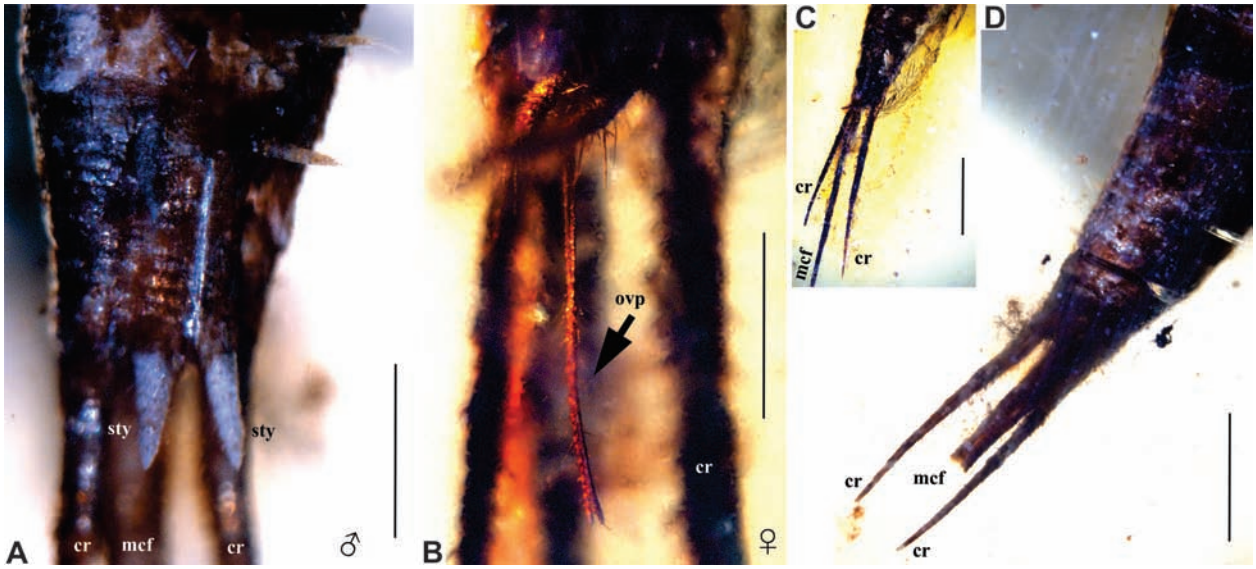

Fig. 8. *Neomachillelus (Praeneomachilellus) ezetaelenensis* sp. nov. **A** – Coxite 9 on holotype male BL.MACH.1. **B** – Close view (in focus) of the ovipositor on allotype female BL.MACH.47. **C** – Caudal appendages on BL.MACH.47 and **D** BL.MACH.1. Scale bars (mm): A-B = 0.5; C-D = 1. See abbreviations in the main text.

one hyaline spine; distal articles 5, 6 and 7 similar in size, less pigmented; article 5 and 6 lighter, with brown, annular patches, article 5 and 6 with one hyaline spine, and article 7 with five hyaline spines, two of them placed basally, other three apically. Distal article elongated, conical-shaped, with at least two, longitudinal brown patches; articles length relationships: (1: 2: 3: 4) > (5: 6: 7); the spine chaetotaxy in articles are described on male, whereas spines on female are hardly to distinguish due to body position. Labial palp yellowish-brown, basal article long, robust, finger-shaped (Fig. 6B). Article 2 shorter, article 3 widened, somewhat dark, all articles with setae long; labial palp on females with third article about twice wider than long, extensively darkened, apically enlarged and profusely covered with conules having distal expansions multiples. On the holotype male, article 3-labial palp distinctly stronger and apical conules shorter (Figs. 6A-C, 7A-B).

Thorax: Terga 2-3 arched, extending over pleura, dorsally bearing scales reddish-brown to blackish in color, ventrally becoming lighter; tergite margins with spiniform, lateral macrosetae (Figs. 2-3). Legs reddish to yellowish, with restricted, darker, brownish patches; coxal stylets and scopulae absent on all legs; legs 1 strong, broader than 2 and 3; coxa on leg 3 with tactile seta; tarsus on leg 1-3 setose, clearly pigmented, with erected setae; claws simple (Figs. 6D-E, 7C).

Abdomen: Abdominal sterna small, triangular-shaped, reddish-brown in color, somewhat yellowish, with golden patches (Fig. 3). Abdominal coxites lacking spines, stylets present on abdominal coxites 2-9, with long terminal spines, except in holotype male without terminal spine on stylets 9. Female specimens have regular terminal spines on stylets 9. Terminal spines generally longer than half of the stylets. One pair of eversible vesicles present on segments 1-7 (Figs. 7D, 8A).

Male genitalia: Penis not discernible, hidden by coxites 9, shorter than half length of coxites 9; parameres absent, coxites 9 enlarged, with stylets long, gross, lacking terminal spine (Fig. 8A).

Female genitalia: Ovipositor well-developed, slender, quaternary type (*sensu* Sturm & Bach de Roca 1993), average ovipositor length: ≈1.3 mm; gonapophyses 8 and 10 with up 35 divisions, stylets 9 bearing a spine. Distal divisions of gonapophyses with terminal spine as long as three most distal divisions; coxites 9 elongated, with stylet long, almost twice longer than stylet on coxites 1-8, and terminal spines long. Paratypes as female allotype are slightly variable in size and color of pigmented scales. Abdominal coxites, leg articles, and caudal appendages on several female are more setose than holotype male (Fig. 8B).

Caudal appendages: Dark, reddish to blackish-brown in color; median caudal filament length on holotype male (incomplete): ≈1.2 mm; copiously setose, lateral cerci length (incomplete): 2.5 mm; all three appendages with long, pointed setae, including spiniform setae; median caudal filament length on female allotype (apically broken): ≈5.3 mm, and lateral cerci length (broken): ≈4.8 mm (Fig. 8C-D).

Remarks: Penis in the holotype male is hidden by coxites 9 due to body position, but we can infer with confidence that penis should be shorter than half length of coxites 9. Also stylets 9 on holotype male lack the terminal spine (female specimens show a regular stylets 9 with terminal spine); stylets 9 are well-developed with lateral macrosetae as seen in adults. This non-regular feature in holotype male is not a fossilization artifact; neither a missing part caused by resin

hardening nor is related to organic decay (Fig. 8A). Although, this feature has not been formally described in other extant congeners, mature or immature specimens, however, it seems related to a temporal state of growth. Probably, such appendages were under regeneration because of accidental mislaying prior to being entombed in amber (M. Gaju-Ricart, pers. comm.). Fossils may show characters that have not been reported before in living specimens but microcoryphians from Miocene age are clearly modern forms. Typically, an intraspecific variability is observable. Since there is a gap of published studies about the Microcoryphia ontogeny, it would be premature establish such feature as a valid. Consequently, this non-regular feature is preliminary discarded in diagnosis of *N. (Praeneomachilellus) ezetaelenensis,* awaiting further references. Diagnosis is strongly supported by other critical, putative characters as presented above.

Contrasting with other described species of the subgenus, such as *N. (Praeneomachilellus) dominicanus* (fossil) and *N. (Praeneomachilellus) szeptyckii* (extant), the new fossil species *N. (Praeneomachilellus) ezetaelenensis* has in common the following diagnostic characters: average body length in adult male and female; body with hypodermal pigment; bearing pigmented scales, compound eyes contiguous, large and rounded; paired ocelli wide, sole-shaped, extending medially in front of the eyes; antennae elongated, lacking scales, with scapus about twice longer than wide, flagellum multi-annulled, each annulus with one whorl of setulae (this character only shared with extant species *N. (Praeneomachilellus) szeptyckii*, tergite margins with spiniform, lateral macrosetae; legs with restricted, darker, brownish patches, coxal stylet and scopulae absent; ♂ penis short, and ♀ ovipositor slender, setose, quaternary type, and reaching apex of stylets 9 with spines. By contrast, it is distinguish by having two conspicuous, long setae in the interocellar space, below the eye midline; also differs by having distinct pattern of pigmented scales, distinct eyes and ocelli color, different shape and chaetotaxy of labial palp, by having a tactile seta on coxa 3, and each antennal annulus with one row of setulae (the last character only differs from fossil species *N. (Praeneomachilellus) dominicanus*).

5. Conclusions

It was believed earlier that microcoryphians were rare in Chiapas amber probably due to ecological gap because their knowledge was limited to one specimen (Wygodzinsky 1971). However, currently microcoryphians are collected in all sites with different state of preservation. They are cosmopolitan insects in Chiapas amber. As presented here, the holotype male of *N. (Praeneomachilellus) ezetaelenensis* shows one of the most outstanding organic preservation as seen in fossil terrestrial arthropods. Previously, one species of Zygentoma, a sister taxon of Microcoryphia, have also been described in Chiapas amber by Mendes & Poinar (2013).

The latest review of the extant representatives of Microcoryphia in México shows 8 genera with 13 species. There are 4 genera with 6 species assigned to the family Machilidae and 4 genera with 7 species within the family Meinertellidae (Palacios-Vargas 2000; CONABIO checklist 2006). The Meinertellidae fauna in Mexico have a central-southern distribution. The New World extant representatives of the Machilidae are typically described in North America and the Meinertellidae occur generally in the Antilles, Central and South America. However, the family Meinertellidae is also recorded in the United States of America (Sturm 1997). For example, the present subgenus *N. (Praeneomachilellus),* to which is considered essentially Neotropical has also been mentioned in Georgia, USA (Sturm 1983, 1984). Accordingly, the occurrence of *N. (Praeneomachilellus) ezetaelenensis* also adds to knowledge of the New World Microcoryphia fauna, which is found since the Early Miocene (ca. 23 Ma) on the transitional physiographic region between North and Central America boundaries.

Acknowledgements

Author contributions are as follows: the specimen identification, description, microimaging, and graphics by FR and MMC; paleontological fieldwork and writing by FR; fossil acquisition by BLC and LZM. The authors declare no conflict of interest. We thank Adriana Kuhn from the MACH, for access to the amber collection. We also thank Francis Pimentel and Johanna Friessen, for access to the amber collection at the MALM. We thank Dr. Mario Ramos (IGL-UNAM), for help in the field, MSc Jon D. Richey (Texas State) for help with the English edition, and Biol. Susana Guzmán (IB-UNAM), for microphotography assistance. Thanks go to Dr. Jose Luis Ruvalcaba (IF-UNAM), for supporting this research, and Dra. Carmen Bach de Roca, for providing literature. We thank Drs. Miquel Gaju, Vladimir Kaplin, and Guenter Schweigert, whose comments, corrections and feedback have improved the final published edition. FR was financially supported by the PhD granting-program CONACYT-UNAM/PCB.

References

Alonso, J., Arillo, A., Barrón, E., Corral, J.C., Grimalt, J., López, J.F., López, R., Martínez-Delclòs, X., Ortuño, V., Peñalver, E. & Trincão, P.R. (2000): A new fossil resin with biological inclusions in Lower Cretaceous deposits from Álava (Northern Spain, Basque-Cantabrian Basin). – Journal of Paleontology, **74**: 158-178.

Bach De Roca, C., Mendes, L.F., Molero, R. & Gaju, M. (2009): A new *Neomachilellus* Wygodzinsky, 1953 (Mi-

crocoryphia: Meinertellidae) from Puerto Rico. – Acta Zoologica Cracoviensia, **52B** (1-2): 101-107.

Bechly, G. & Stockar, R. (2011): The first Mesozoic record of the extinct apterygote insect genus *Dasyleptus* (Insecta: Archaeognatha: Monura: Dasylepidae) from the Triassic of Monte San Giorgio (Switzerland). – Palaeodiversity, **4**: 23-37.

Boggs, S. (2009): Petrology of sedimentary rocks, 63-164; New York (Cambridge University Press).

CONABIO (2006): Catálogo de autoridades taxonómicas de los insectos sin alas (Apterygota: Insecta) de Mexico. Data Base SNIB-CONABIO (Comisión Nacional para el Conocimiento y Uso de la Biodiversidad), Mexico, p. 2.

Duran-Ruiz, C., Riquelme, F., Coutiño-José, M., Carbot-Chanona, G., Castaño-Meneses, G. & Ramos-Arias, M. (2013): Ants from the Miocene Totolapa amber (Chiapas, Mexico), with the first record of the genus *Forelius* (Hymenoptera, Formicidae). – Canadian Journal of Earth Sciences, **50**: 495-502.

Ferrusquía-Villafranca, I. (2006): The first Paleogene mammal record of Middle America: *Simojovelhyus pocitosense* (Helohyidae, Artiodactyla). – Journal of Vertebrate Paleontology, **26** (4): 989-1001.

Frost, S.H. & Langenheim, R.L. (1974): Cenozoic reef biofacies, Tertiary larger foraminifera and scleractinian corals from Chiapas, Mexico. – 388 pp.; De Kalb (Northern Illinois University Press).

Getty, P.R., Sproule, R., Wagner, D.L. & Bush, A.M. (2013): Variations in wingless insect trace fossils. Insights from neoichnology and the Pennsylvanian of Massachusetts. – Palaios, **28**: 243-258.

Graham, A. (1999): Studies in neotropicalpaleobotany. XIII. An Oligo-Miocene palynoflora from Simojovel (Chiapas, Mexico). – America Journal of Botany, **86** (1): 17-31.

Iturralde-Vinent, M.A. (2001): Geology of the amber-bearing deposits of the Greater Antilles. – Caribbean Journal of Science, **17** (3-4): 141-167.

Iturralde-Vinent, M.A. (2006): Meso-Cenozoic Caribbean paleogeography: Implications for the historical biogeography of the region. – International Geology Review, **48**: 791-827.

Labandeira, C.C., Beall, B.S. & Hueber, F.M. (1988): Early insect diversification: Evidence from a Lower Devonian bristletail from Quebec. – Science, **242**: 913-916.

Langenheim, J.H. (1966): Botanical source of amber from Chiapas, Mexico. – Ciencia, **24**: 201-211.

Langenheim, J.H. (2003): Plant resins: chemistry, evolution, ecology and ethnobotany, 141-304; Portland (Timber Press).

Mendes, L.F. (1997): On a new fossil Microcoryphia (Insecta: Apterygota) from South-American copal. – Boletim da Sociedade portuguesa de Entomologia, **6** (18) (168): 245-250.

Mendes, L.F. (2002): Taxonomy of Zygentoma and Microcoryphia: historical overview, present status and goals for the new millennium. – Pedobiologia, **46**: 225-233.

Mendes, L.F. & Poinar, G. Jr. (2013): Description of two new fossil Zygentoma from Mexico and the Dominican Republic. – Soil Organisms, **85** (1): 1-9.

Mendes, L.F. & Wunderlich, J. (2013): New data on thysanurans preserved in Burmese amber (Microcoryphia and Zygentoma Insecta). – Soil Organisms, **85** (1): 11-22.

Palacios-Vargas, J.G. (2000): Archaeognatha y Zygentoma. – In: Llorente Bousquets, J.E., González, S. & Papavero, N. (Eds.): Biodiversidad, taxonomía y biogeografía de artrópodos de Mexico Hacia una síntesis de su conocimiento, **2**: 285-291; México (Facultad de Ciencias, UNAM-CONABIO).

Perrilliat, M.C., Vega, F.J. & Coutiño, M.A. (2010): Miocene mollusks from the Simojovel area in Chiapas, southwestern Mexico. – Journal of South American Earth Science, **30**: 111-119.

Poinar, G.O. (1992): Life in amber, 29-46; Palo Alto (Stanford University Press).

Riquelme, F., Alvarado-Ortega, J., Ramos-Arias, M., Hernández, M., Le Dez, I., Lee-Whiting, T.A. & Ruvalcaba-Sil, J.L. (2014a): A fossil stemmiulid millipede (Diplopoda: Stemmiulida) from the Miocene amber of Simojovel, Chiapas, Mexico. – Historical Biology, **26** (4): 415-427.

Riquelme, F., Hernández-Patricio, M., Martínez-Dávalos, A., Rodríguez-Villafuerte, M., Montejo-Cruz, M., Alvarado-Ortega, J., Ruvalcaba-Sil, J.L. & Zúñiga-Mijangos, L. (2014b): Two flat-backed Polydesmidan millipedes from the Miocene Chiapas-Amber Lagerstätte, Mexico. – Plos One, **9** (8): e105877. doi: 10.1371/journal.pone.0105877

Riquelme, F., Northrup, P., Ruvalcaba-Sil, J.L., Stojanoff, V., Siddons, D.P. & Alvarado-Ortega, J. (2014c): Insights into molecular chemistry of Chiapas amber using infrared-light microscopy, PIXE/RBS, and sulfur K-edge XANES spectroscopy. – Applied Physics, (A), **116** (1): 97-109.

Riquelme, F., Ruvalcaba-Sil, J.L., Alvarado-Ortega, J., Estrada-Ruiz, E., Galicia-Chávez, M., Porras-Múzquiz, H., Stojanoff, V., Siddons, D.P. & Miller, L. (2014d): Amber from México: Coahuilite, Simojovelite and Bacalite. – MRS Proceedings, **1618**, doi:10.1557/opl.2014.466.

Rohlf, F.J. (2013): The tpsDig program, V. 2.17. New York (Stony Brook University).

Sharov, A.G. (1948): Triassic Thysanura from the Ural foreland. – Doklady Akademii Nauk SSSR, **61**: 517-519.

Sharov, A.G. (1957): Peculiar Paleozoic wingless insects belonging to a new order Monura (Insecta, Apterygota). – Doklady Akademii Nauk SSSR, **115**: 795-799.

Shear, W.A., Bonamo, P.M., Grierson, J.D., Rolfe, W.D.I., Smith, E.L. & Norton, R.A. (1984): Early land animals in North America: Evidence from Devonian age arthropods from Gilboa, New York. – Science, **224**: 492-494.

Silvestri, F. (1912): Die Thysanuren des baltischen Bernsteins. – Schriften der Physikalisch-Ökonomischen Gesellschaft zu Königsberg, **53**: 42-66.

Sturm, H. (1983): Contribución al conocimiento de los Machiloidea de Colombia (Archaeognatha: Insecta). – Caldasia, **13** (65): 787-816.

Sturm, H. (1984): Zur Systematik, Biogeographie und Evolution der südamerikanischen Meinertellidae (Machiloidea, Archaeognatha, Insecta). – Journal of Zoological Systematics and Evolutionary Research, **22**: 27-44.

Sturm, H. (1997): A new subgenus and two new species of the genus *Machilinus* (Meinertellidae, Archaeognatha=Microcoryphia, "Apterygota", Insecta) from Mexico. – Journal of the New York Entomological Society, **105** (1): 15-23.

Sturm, H. & Bach de Roca, C. (1993): On the systematics of the Archeognatha (Insecta). – Entomologia Generalis, **18**: 55-90.

Sturm, H. & Machida, R. (2001): Archaeognatha. – Handbuch der Zoologie, **37**: 213 pp.; Berlin (de Gruyter).

Sturm, H. & Poinar, G.O. Jr. (1997): A new *Neomachilellus* species from Miocene amber of the Dominican Republic and its phylogenetic relationships (Archaeognatha: Meinertellidae). – Entomologia Generalis, **22**:157-170

Sturm, H. & Poinar, G.O. Jr. (1998): *Cretaceomachilis libanensis*, the oldest known bristle-tail of the family Meinertellidae (Machiloidea, Archaeognatha, Insecta) from the Lebanese amber. – Deutsche Entomologische Zeitschrift, **45**: 43-48.

Wygodzinsky, P. (1953): Über einige Machiliden aus Indonesien. – Verhandlungen der naturforschenden Gesellschaft in Basel, **64** (29): 347-355.

Wygodzinsky, P. (1971): A note on a fossil machilid (Microcoryphia) from the amber of Chiapas, Mexico. – University of California Publications in Entomology, **63**: 101-102.

Wygodzinsky, P. (1978): Two new species of *Neomachilellus* Wygodzinsky (Meinertellidae, Microcoryphia) from the state of Amazonas, Brazil. – Acta Amazonica, **8**: 303-307.

Manuscript received: July 9th, 2014.
Revised version accepted by the Stuttgart editor: September 26th, 2014.

Addresses of the authors:

Francisco Riquelme, Posgrado en Ciencias Biológicas, Instituto de Física, Universidad Nacional Autónoma de México, Coyoacán, AP 20-364, D.F., México;
e-mail: riquelme.fc@gmail.com

Maira Montejo-Cruz, Facultad de Ciencias, Universidad Nacional Autónoma de México, Coyoacán, CP 04510, D.F., México;

Bibiano Luna-Castro, Museo del Ámbar de Chiapas, Diego de Mazariegos S/N, La Merced, CP 29249, San Cristóbal de las Casas, Chiapas, México;

Luis Zuñiga-Mijangos, Museo del Ámbar Lilia Mijangos, Diego de Mazariegos 23, CP 29218, San Cristóbal de Las Casas, Chiapas, México.

PLOS ONE

New fossil scorpion from the Chiapas Amber Lagerstätte

--Manuscript Draft--

Manuscript Number:	PONE-D-14-51462
Article Type:	Research Article
Full Title:	New fossil scorpion from the Chiapas Amber Lagerstätte
Short Title:	New fossil scorpion from the Chiapas Amber Lagerstätte
Corresponding Author:	Francisco Riquelme Universidad Nacional Autonoma de México Mexico City, MEXICO
Keywords:	Chiapas amber, Miocene, Scorpiones, Buthidae, Tityus.
Abstract:	A new species of scorpion is described based on entire adult male rarely preserved in a cloudy amber from Miocene rocks in the Chiapas Highlands, Mexico. The amber-bearing beds in Chiapas constitute a Conservation Lagerstätte with outstanding organic preservation inside plant resin. The new species is diagnosed by having putative characters that correspond largely with the genus Tityus Koch, 1836 (Scorpiones, Buthidae). Accordingly, it is now referred to as Tityus apozonalli sp. nov. Its phylogenetic position among fossil taxa of the family Buthidae from both Dominican and Mexican amber is testing herein. Close relationships with the extant Tityus-like clades that live now in the Neotropics are also discussed. This new taxon adds to knowledge of the New World scorpions rarely found in amber from the Neogene of Middle America.
Order of Authors:	Francisco Riquelme
	Gabriel Villegas-Guzmán
	Edmundo González-Santillán
	Víctor Córdova-Tabares
	Oscar F. Francke
	Dulce Piedra-Jiménez
	Emilio Estrada-Ruiz
	Bibiano Luna-Castro
Suggested Reviewers:	Jason Dunlop, Dr. Museum für Naturkunde. Leibniz Institute for Evolution and Biodiversity Science jason.dunlop@mfn-berlin.de He has qualified expertise and knowledge in systematic, phylogeny and paleontology of the Class Arachnida, including Scorpiones. He also has several published papers in amber fossils.
	Carlos Carlos Viquez Núñez, Dr. Curator, The Arachnids Collection. Biodiversity National Institute of Costa Rica cviquez@inbio.ac.cr He has qualified expertise and knowledge in systematic, phylogeny and anatomy of scorpions from the American Tropics such as the Family Buthidae.He also has several publications about the genus Tityus.
	W. David Sissom, Dr. West Texas A&M University dsissom@wtamu.edu He has qualified expertise and knowledge in systematic, biogeography, phylogeny and anatomy of scorpions.
Opposed Reviewers:	
Additional Information:	

New fossil scorpion from the Chiapas Amber Lagerstätte

Francisco Riquelme[1], Gabriel Villegas-Guzmán[2], Edmundo González-Santillán[3], Víctor Córdova-Tabares[2], Oscar F. Francke[4], Dulce Piedra-Jiménez[3], Emilio Estrada-Ruiz[5], Bibiano Luna-Castro[6]

[1]Posgrado en Ciencias Biológicas. Universidad Nacional Autónoma de México, Cuidad Universitaria, Coyoacán, D.F., México.

[2]Laboratorio de Acarología, Escuela Nacional de Ciencias Biológicas, Instituto Politécnico Nacional, D.F., México.

[3]Laboratorio de Aracnología, Facultad de Ciencias, Universidad Nacional Autónoma de México, Ciudad Universitaria, Coyoacán, D.F, México.

[4]Colección Nacional de Arácnidos, Instituto de Biología, Universidad Nacional Autónoma de México, Cuidad Universitaria, Coyoacán, D.F., México

[5]Laboratorio de Ecologia, Escuela Nacional de Ciencias Biológicas, Instituto Politécnico Nacional, D.F., México.

[6]Museo del Ámbar de Chiapas, La Merced, San Cristóbal de las Casas, Chiapas, México.

E-mail corresponding author: riquelme.fc@gmail.com

Running title: — New fossil scorpion from the Chiapas Amber Lagerstätte

Abstract

A new species of scorpion is described based on entire adult male rarely preserved in a cloudy amber from Miocene rocks in the Chiapas Highlands, Mexico. The amber-bearing beds in Chiapas constitute a Conservation Lagerstätte with outstanding organic preservation inside plant resin. The new species is diagnosed by having putative characters that correspond largely with the genus *Tityus* Koch, 1836 (Scorpiones, Buthidae). Accordingly, it is now referred to as *Tityus apozonalli* sp. nov. Its phylogenetic position among fossil taxa of the family Buthidae from both Dominican and Mexican amber is testing herein. Close relationships with the extant Tityus-like clades that live now in the Neotropics are also discussed. This new taxon adds to knowledge of the New World scorpions rarely found in amber from the Neogene of Middle America.

Keywords: Chiapas amber, Miocene, Scorpiones, Buthidae, *Tityus*.

Introduction

The fossil record of the order Scorpiones Koch, 1851 currently reaches 118 described species, for which there are 112 species from amber deposits worldwide [1][2][3]. A comprehensive list of fossil scorpions is recently given elsewhere [2]. Fossil amber scorpions are consistently found since the Early-Mid Cretaceous. The oldest amber scorpion is *Archaeobuthus estephani* Lourenço, 2001 (family Archaeobuthidae), from the Early Cretaceous amber of Lebanon [4]. Preliminary, *A. estephani* was considered as member of the superfamily Buthoidea Koch, 1837 [4]; as well as *Palaeoburmesebuthus grimaldii* Lourenço, 2002 (family Incertae sedis) from the Late Cretaceous amber of Myanmar [5]. However, a phylogenetic review of the order Scorpiones has placed *A. estephani* and *P. grimaldii* outside the Buthoidea [6]. A subsequent study based on a more complete second specimen of *Palaeoburmesebuthus* suggests that this does not match with Buthoidea and extant relatives [7]. Later, the holotype of *A. estephani* was newly reviewed and placed as extinct group outside the Buthoidea based on its orthobothriotaxic type F1 [8]. The later authors also presume that another primitive scorpion, *Protobuthus elegans* Lourenço and Gall, 2004 (family Protobuthidae), was initially misplaced [8]. *P. elegans* is a non-amber fossil found in sandstones from the Early Triassic Grès à Voltzia, France. This was tentatively considered as the earliest form associated with buthid scorpions [9]. However, Baptista and coworkers (2006) estimate that the type material of *P. elegans* is too fragmentary and lacks several diagnostic characters of buthid scorpions [8]. They conclude that *Protobuthus, Palaeoburmesebuthus* and *Archaeobuthus* are Mesozoic close relatives belonging to basal linages without extant descendants and suggest that the geological record of buthid scorpions is currently limited to the Cenozoic [8].

Fossils unequivocally belonging to the family Buthidae Koch, 1837 have been documented from the Paleogene Baltic amber [2][10][11]. These have been placed into several extinct taxa: *Paleolychas* Lourenço and Weitschat, 1996; *Paleoprotobuthus* Lourenço and Weitschat, 2000; *Paleoakentrobuthus* Lourenço and Weitschat, 2000; *Paleotityobuthus* Lourenço and Weitschat, 2000, *Paleoananteris* Lourenço and Weitschat, 2009 (also present in contemporary Rovno amber [11]); *Paleospinobuthus* Lourenço, Henderickx and Weitschat,

2005; *Paleoisometrus* Lourenço and Weitschat, 2005; and the presumably misplaced species *'Tityus' eogenus* Menge, 1869 [12].

In the Americas, the oldest known buthid form is a non-amber scorpion which dates back to the Paleogene; the extinct taxa *Uintascorpio halandrasorum* Perry, 1995 from the Eocene Green River Formation in western Rocky Mountains, USA [13][14]. In younger deposits of the Middle America amber at the Neogene, several buthid scorpions have been found predominantly in Mexico and the Dominican Republic [2][3][15]-[21]. A few species have been assigned to the genera *Centruroides* Marx, 1890, *Microtityus* Kjellesvig-Waering, 1966 and *Tityus* Koch, 1836; such as *Centruroides beynai* Schawaller, 1979 [15], seemingly a synonym of *Centruroides nitidus* Thorell, 1876 [2]*; Microtityus ambarensis* Schawaller, 1982[16][17]; *Tityus geratus* Santiago-Blay and Poinar, 1988 [18]; *Tityus (Brazilotityus) hartkorni* Lourenço, 2009 [19]; and *Tityus azari* Lourenço, 2013 [20], all from the Dominican Republic. Only one species, *Tityus knodeli* Lourenço, 2014, has been formally described from Chiapas, Mexico [3]. Accordingly, the genus *Tityus* is represented with complete certainty since the Neogene of Middle America.

The occurrence of fossil scorpions in Chiapas amber is very rare. There are only two fossils known in previously published studies [3][21]. One of them was tentatively placed within the genus *Centruroides* (status uncertain) [21], and *T. knodeli* as mentioned above [3]. Scorpions from the Chiapas amber are primarily modern forms that lived in an ancient mangrove-like environment at the Miocene. Thus, there are significant intraspecific variations that allow erecting new species closely related with those Neotropical living forms currently found in the Caribbean, Central and South America. In the present study, we illustrate and diagnose a new scorpion placed into the genus *Tityus*, family Buthidae, which is now referred to as *Tityus apozonalli* nov. sp. Description is based on a single, entire, adult male specimen preserved in colorful, recrystallized, cloudy amber. The morphology of *T. apozonalli* is fairly close to some living Tityus-like species from the '*Tityus clathratus*' clade, preliminary included within the '*Tityus (Archaeotityus)'* group (after Lourenço, 2006) because shows plesiomorphic characters among tityiod scorpions [22]. It also shares some ecological aspects with those groups as inhabitants of Neotropical forests. The phylogenetic position of *T. apozonalli* among fossil members of the family Buthidae from the Middle America amber is also examined herein. As well as brief revision of the family Buthidae according to fossil evidence.

On the fossil occurrence

Fossil studied here was collected in a hand-made pit at the Guadalupe Victoria site near Simojovel, Chiapas, south of Mexico (Fig. 1), which comprises two indian settlements: The Guadalupe Victoria I and II [23][24]. The crude amber piece was found by an indian local farmer who informed his discovery to the Museo del Ámbar in San Cristobal de Las Casas, Chiapas, to Director B. Luna in the strict sense. According to geographical references provided by the collector, a provenance analysis has been carried out in amber with infrared and X-ray spectroscopies. Provenance analysis has been complemented with field geology tracking the amber outcrop at the amber site commonly known as the Guadalupe Victoria site [23][24]. Accordingly, the present amber section consists of organic-rich lignite embedded in non-fissile, coarse to fine grained sandstone with variable thickness. A ripple cross-lamination, interbedded friable shales, stratified bentonite-like clay, copious brown to red iron oxides, pyrite and other secondary clay minerals are also observable. The organic-rich lignite is the result of plant decay and soil lithogenesis. The amber section overlies a transitional-marine sequence with abundant shells, corals, calcareous debris, bioclastic limestones and consolidated sandstones. The geological setting of the Simojovel area displays rhythmic sequences as a result of sea level fluctuations. This indicates land changes from transitional to terrestrial environments and associated climate fluctuations that span from the Oligocene-Miocene boundaries to mid-Pliocene [25]. Consequently, lithology and sedimentary record of amber section are consistent with a terrestrial-fluvial environment near a coastal plain [26]. Palynology in amber strata also suggests an ancient terrestrial-mangrove environment [27].

The available published paleontological and biostratigraphic data in the Simojovel area agrees that amber-bearing beds are part of the Mazantic shale and Balumtum sandstone strata with a relative age estimated in the Early to Middle Miocene, ca. 23-15 Ma. [23][24][28]-[30]. Another outcrop near Simojovel assigned to the La Quinta strata dated as late Oligocene has been mentioned as containing amber [28][29]. However, the location of that outcrop cannot be confirmed in current field studies. Other author also discusses the stratigraphic position of a section in the Los Pocitos site near Simojovel –this locality also contains amber lumps- by placing it in the Simojovel Formation, which informally correlates with the La Quinta Formation in the Late Oligocene [31]. However, this correlation is based on unpublished, unavailable

biostratigraphic report apparently using foraminifera as mentioned scarcely [31], which increased the confusion about the amber age. Geology of amber outcrops in the Mountains of Chiapas, from Totolapa to Estrella de Belén near Palenque, should be correlated by more supporting stratigraphic data in further published works.

The Guadalupe Victoria site near Simojovel along with other amber sites grouped in the Mountains of Chiapas constitute a Miocene Conservation Lagerstätte with paleobiota conspicuously preserved [23][24]. Those fossils show hard/soft tissues preservation in remarkable detail. The preservation potential has been influenced by a rapid resin hardening, followed by a restriction of chemical reactions and incomplete organic decay [32]. Since the initial work by Langenheim (1966), the plant source of Chiapas amber is assigned to an extinct legume tree species of the genus *Hymenaea,* because it shares chemical signatures with extant resins of the living tree species *H. courbaril* and *H. verrucosa* [33]-[35]. The recent biogeochemical features and organic mineral nomenclature of Chiapas amber has also been recently reviewed [36].

The Chiapas amber also shares botanical affinities with those fossil resins occurring in the Caribbean since the Miocene, such as amber from the Dominican Republic, Haiti, Puerto Rico, Cuba, and Jamaica [29][34][37]. These amber strata also have in common the regional tectonic setting (in the Caribbean Plate and the Central America formation) and a coeval sedimentary regimen with the Simojovel sites at the Miocene [38]. However, the age correlation of amber deposits exposed in Chiapas and the Caribbean group should be interpreted with caution, because there are significant differences in depositional ages (still unstudied) that should be considered at detail.

Material and Methods

The amber scorpion was collected in hand-made pit near the Guadalupe Victoria site, Latitude 17° 09′ 11′′ N, Longitude 92° 46′ 08′′ W, located near Simojovel, Chiapas, south of Mexico (Fig.1). Specimen is now housed at the Museo del Ámbar de Chiapas (MACH) located in San Cristóbal de Las Casas, Chiapas, Mexico. The amber collection of the MACH, including the fossil scorpion, is formally certified by the Instituto Nacional de Antropología e Historia (INAH), which protects the archeological and paleontological heritage in Mexico. No specific

permits were required for the specimen description and paleontological fieldwork, which complied with all relevant regulations.

Micrographs and measurements: Anatomical data were collected using a high-resolution microscopy with regular to adapted infrared-pass lens with LED/tungsten lamps as infrared source. A multiple image superimposition with >16 planes per image were applied for images processing and displaying [23][24][32]. Schematic drawings were hand traced by electronic pen using stereomicroscope, micrographs and CorelDraw X6 for graphic processing. Anatomical measurements (given in millimeters) were collected using the open source program tpsDig V. 2.17 [39]. Provenance analysis on amber was applied using infrared and X-ray spectroscopies [32][36], data are available upon request.

Phylogenetic analysis: The phylogenetic position of *Tityus apozonalli* sp. nov. among its fossils congeners from both Dominican and Mexican amber, Neogene, was analyzed using the TNT program [40]. Branch support values were calculated with the function tree bisection and reconnection (TBR) from existing trees, and character mapping and bootstrap values on a most parsimonious tree using a traditional heuristic search with 100,000 replicates. Table 1 shows the data matrix that includes the most informative morphological characters on the following fossil taxa: *Tityus hartkoni, T. azari, T. knodeli, and T. apozonalli*, *C. beynai* and *M. ambarensis*. *Palaeonanteris ukrainensi*s from Rovno amber, Paleogene [11], was used as outgroup by its relatively basal condition and comparable plesiomorphic characters. Distribution of qualitative and quantitative characters among taxa has been listed in Appendix 1.

Acronyms: BLMACH: Bibiano Luna/ Museo del Ámbar de Chiapas. INAH: Instituto Nacional de Antropología e Historia. MACH: Museo del Ámbar de Chiapas. UNAM: Universidad Nacional Autónoma de Mexico.

Terminology: The pattern of description and terminology generally follow Stahnke, 1970 [41]. The trichobothria pattern follows Vachon, 1974 [42][43]. Metasomal carinae follows Soleglad and Sissom, 2001 [44]. Pedipalp chela carinae follows Prendini, 2000 [45], modified by Acosta et al., 2008 [46]. Sternum follows Soleglad and Fet, 2003 [47]. The linguistic usage of roman numbers on tergites and metasoma segments was modified; in the following text the natural numbers were used as both ordinals and adjectives.

Nomenclature: The electronic edition of this article conforms to the requirements of the amended International Code of Zoological Nomenclature, and hence the new names contained herein are available under that Code from the electronic edition of this article. This published work and the nomenclatural acts it contains have been registered in ZooBank, the online registration system for the ICZN. The ZooBank LSIDs (Life Science Identifiers) can be resolved and the associated information viewed through any standard web browser by appending the LSID to the prefix "http://zoobank.org/". The LSID for this publication is: (will be adding after revision). The electronic edition of this work was published in a journal with an ISSN, and has been archived and is available from the following digital repositories: PubMed Central, LOCKSS

Results and Discussion

Systematic Paleontology

Order: Scorpiones Koch, 1851
Superfamily: Buthoidea Koch, 1837
Family: Buthidae Koch, 1837
Genus: Tityus Koch, 1836

Tityus apozonalli Riquelme sp. nov. ZooBank LSID: (will be adding after revision). Figs. 2-8

Diagnosis: small-sized tityoid form, 17.8 mm of total length, reddish-brown in ground color, sparsely infuscated, pedipalp fingers + manus and legs pale yellowish. Carapace poorly emarginated anteriorly and carinae macrosculpture inconspicuous. Median eyes large. Sternum subtriangular type 1-like. Chelicerae fixed finger distinctly infuscated, with short dentition, and median denticle moderately large. Pedipalp fixed finger dentition: PD= 9 and RD= 10, MD= 9 rows of denticles; PD and RD slightly imbricated, dislocated from median rows. Movable finger PD= 11, RD= 12, MD= 10 rows of medial denticles. Trichobothrial pattern Type A, probably orthobothriotaxic, partially visible. Pectinal tooth count 29; teeth subequal in size, relative large, fulcra present. Leg tibial spur absent, prolateral pedal spur reduced, retrolateral pedal spur

moderate. Ungues short and strongly curved. Metasomal consecutive length increases progressively from segment **1** to **5**, hardly varies in width. Vesicle elongated, globose, oval-shaped, slightly granulose, with long macrosetae. Aculeus moderately large, arcuate, pale yellowish, bearing two laterodorsal macrosetae. Subaculear tubercle strong, conspicuously spiniform, lanceolate**,** pale yellowish, as long as one quarter of aculeus, with at least two ventrobasal granules and two visible lateral macrosetae.

Derivation of name: from the Náhuatl voice "*apozonalli",* this term was given to amber in the pre-Columbian times by the Aztecs. Literally means "sea bubble" or "sea foam".

Type material: BLMACH.18, amber inclusion, three-dimensionally preserved, entire adult male and only specimen known (Fig. 2-3). Currently is housed at the Museo del Ámbar de Chiapas (MACH), located in San Cristóbal de Las Casas, Chiapas, Mexico.

Locality and Horizon: The Guadalupe Victoria site, latitude 17° 07′ 58′′N, longitude 92° 48′ 19′′ W, located in the Municipality of the Simojovel de Allende, Chiapas, Mexico (Fig. 1). The amber-bearing beds are part of the Mazantic shale and Balumtum sandstone strata in the Early-Middle Miocene (≈23-15 Ma).

Taphonomic features: The specimen is embedded in golden yellow amber, tinged with orange, showing cloudy to weakly translucent glossiness, with abundant microfractures obliquely placed (Fig. 2). There is a recrystallization pattern (wave-shaped) close to the body, which is a consequence of different crystallization stages during resin hardening (Fig. 2) Both fractures and recrystallization have darkened some minute anatomical elements, i.e. trichobothria, carinae and macrosculpture, which are hard to distinguish (Fig.3). Typically, there is soil, plant remains, insect parts, bubble molds and undetermined minerals embedded together with the scorpion (Fig. 2). Most portions of carapace and tergites are compressed, almost obliterated, and somewhat translucent, as a consequence of the organic decay (Fig. 2). This suggests that organic acids in amber have dissolved the cuticle. Amber is still chemically reactive in the depositional environment; this affects the organic preservation at different levels [32]. However, pedipalps, chelicerae, caudal segments and telson are less dissolved, staying tightly sclerotized (Figs. 3,5,

and 7). Undetermined salts are spread under sternites. These are secondary reactive products from the resin hardening. Pectines and adjacent sternites are slightly bleached (Fig. 5). Legs are also translucent, flattened, with inner soft-tissues heavily degraded (Fig. 7A). Telson is basally broken close to anus. The true color morphology pattern is well-preserved in general (Figs. 7B-C).

Color in amber preservation*:* reddish-brown in ground color, somewhat translucent (Figs. 2B-C). Carapace, chelicerae, pedipalp femur + patella reddish-brown, sparsely infuscated (Fig. 3). Pedipalp fingers + manus pale yellowish. Median ocular tubercle black (Fig. 3). Mesosoma segments: tergites reddish-brown, heavily infuscated (Fig. 2C); sternites **3-4** whitish, others reddish-brown; pectines also whitish (Fig. 5). Legs pale yellowish, with moderate brownish markings (Fig. 7A). Metasomal segments and telson reddish-brown, infuscated (Figs. 7B-C).

Description: Holotype BLMACH.18, amber inclusion, adult male, small-sized tityoid, 17.8 mm of total length (Fig.2).

Prosoma: Carapace size 2.9 length and 3.3 width, reddish-brown, mildly infuscated, poorly emarginated anteriorly, sublinear; carinae macrosculpture inconspicuous, most sulci and setation hardly distinguishable, anterior median notch absent. Posteromedial sulcus broad and deep. Median ocular tubercle with few minute, dusky granulates; median eyes large (≈0.23). Two lateral ocelli, one third the size of median eyes. Sternum type 1-like, almost obliterated and flattened, but profile clearly subtriangular with median depression and paired lobes slightly visible (Figs. 2B-C)

Chelicerae: size 1.1 length and 0.7 width, reddish-brown, almost smooth. Movable finger with internal and external distal denticles opposable, in line, about the same size. Ventral margin with a row of four smaller denticles. Dorsal margin with a moderate median denticle. Subdistal third with a row of marginal macrosetae. Serrula undiscernible. Fixed finger distinctly infuscated, with short dentition, median denticle moderately large, with a few, short, thin macrosetae ventrolaterally (Fig. 3A).

Pedipalps: size 8.9 in total length; pedipalp segments size (length / width) and (ratio): femur= (2.16/ 0.88), (r=2.45); patella= (2.42/ 1.04), (r=2.32); chela= (3.65 / 0.91), (r= 4.01);

movable finger length= (2.55); fixed finger length== (2.60). Femur + patella reddish-brown and sparsely infuscated. Fingers + manus pale yellowish, manus tinged with brownish striations, finger somewhat translucent. Carinae in Femur: dorsal prolateral, dorsal retrolateral, , ventral prolateral and prolateral submedian with scattered irregular subserrate granules; other carinae undiscernible. On Patella: dorsal prolateral, dorsal retrolateral, ventral retrolateral, and ventral prolateral carinae finely crenulated; dorsal median costated to finely crenulated; prolateral median and prolateral ventrosubmedian finely crenulated; other carinae undiscernible. On Chela: Dorsal median carina costate; other carinae undiscernible. Pedipalp chela moderate. Fingers lacking scalloping, oblique. Pedipalp fixed finger dentition: PD= 9 and RD= 10, MD= 9 rows of denticles; PD and RD slightly imbricated, dislocated from median rows. Movable finger PD= 11, RD= 12, MD= 10 rows of medial denticles, distal row of one to three denticles missing. Trichobothrial pattern Type A, probably orthobothriotaxic, several trichobothria hardly distinguishable due to resin fossilization (Figs. 3B-C and 4).

Mesosoma: size 4.3 in total length; tergites reddish-brown, heavily infuscated, with minute wrinkles. Macrosculpture carinae in tergites **1-6** hardly distinguishable. Carinae on tergite **7**: dorsal lateral and lateral supramedian strongly protruding and finely granular. Sternites **3-4** whitish; whereas sternites **5-7** typically reddish-brown. Sternites **3–7** ventral submedian crenulated, with coarse-to-fine granules; ventral lateral margins with carinae moderately strong, granular (Figs. 2A-B). On sternite **7**: posterolateral carinae coarsely granular; other carinae undiscernible. Genital operculum subtriangular, longitudinally divided, male genital papillae weakly visible. Pectinal tooth count 29 (left side partially covered by leg patella **3**), average pectines: 2.61; teeth relative large, subequal in size, average tooth length: 0.40, fulcra present (Figs. 5 and 6).

Legs: All segments pale yellowish, some portions hyaline and flattened, moderately setose. Dorsally granulated but basitarsi and telotarsi almost smooth. Patella strong, carinae prolateral dorsal, retrolateral dorsal and retrolateral median with moderate, subserrated granules. Setation on tarsi: retrolateral ventral with row of minor macrosetae. Tibial spur absent, prolateral pedal spur reduced, retrolateral pedal spur moderate. Ungues short and strongly curved (Fig. 7A).

Metasoma: segments moderately strong, reddish-brown and infuscated, all bearing macrosetae. Consecutive length increases progressively from segment **1** to **5**, hardly varies in

width, measurements are as follows (length /width) and (ratio): Segment **1**= (1.26/1.23) (r= 1.02); **2**= (1.61/1.02) (r= 1.57); **3**= (1.64/1.15) (r=1.42). **4**= (2.33/1.12) (r=2.08); **5**= (2.49/1.22) (r=2.04). Carinae on segment **1**-**5**: dorsal lateral median finely serrated, with distal spiniform projection. On segment **1**: lateral inframedian moderate, on segments **2**-**5**: strong, all serrated. On segments **1**-**5**: ventral submedian costate and strong. On segments **1**-**2**: ventral lateral moderate, on segments **3**-**5**: strong, all serrated. On segment **5**: ventral median moderate and finely serrated. From segment **1** to **5** carinal setation: ventral lateral counts 2:2:2:2:3, others undiscernible and/or not preserved (Figs. 7B-C and 8).

Telson: size 2.82 length and 0.96 width, reddish-brown, sparsely infuscated. Vesicle size 1.3 length and 0.9 width, elongated, globose, oval-shaped, slightly granulose, with long macrosetae. Aculeus moderately large, arcuate, pale yellowish, with laterobasally microserration and laterodorsally bearing two visible macrosetae. Subaculear tubercle well-developed, strong, lanceolate, conspicously spiniform, sharp, pale yellowish, about 1/4 as long as aculeus, with at least two minute granules situated ventrobasally and two lateral macrosetae (Figs. 7B-C and 8).

Remarks: *Tityus apozonalli* sp. nov. morphologically resembles those small-sized living forms belonging to the *'Tityus (Archaeotityus)'* clade *sensu* Lourenço, 2006 that includes '*Tityus clathratus*' and '*Tityus columbianus'* morphotypes currently distributed in the Caribbean Islands, Central America and northern South America [22]. It shares markedly the presence of fulcra and strong, spiniform subaculear tubercle [22][48]. However, it considerably differs by the following diagnostic characters: (i) the morphometric values; (ii) the variation on the color and infuscation pattern; (iii) the pedipalp finger dentition that count on fixed finger PD= 9 and RD= 10, MD= 9 rows, on movable finger PD= 11, RD= 12, MD= 10 rows; (iv) the pectinal dentition that count 29; (v) the variation in the subaculear tubercle size and bearing setae. *T. apozonalli* also shares the presence of fulcra with others amber scorpions assigned to *Tityus* from the Dominican Republic [18]-[20], whereas fulcra are vestigial in *T. knodeli* from Chiapas. However, *T. apozonalli* may be primarily separated by its previously described amber fossil congeners, such as *T. geratus*, *T. (Brazilotityus) hartkorni*, *T. azari*, *M. ambarensis*, and *T. knodeli,* according to the significant variation present on the color/infuscation pattern, as well as the pedipalp fingers and pectinal dentition.

Regarding the phylogenetic status of *T. apozonalli* among its fossil buthid congeners from both Dominican and Mexican amber, the results of the phylogenetic analysis show a single most parsimonious tree with length= 23, consistency index (CI) = 82 and retention index (RI) = 77 (Fig. 9). The resulting cladogram indicates a closer position of *T. apozonalli* with *T. azari* and *T. (Brazilotityus) hartkorni* from Dominican amber and clearly separates for its sister groups of *Centruroides* and *Microtityus* (Fig. 9). Accordingly, *T. apozonalli* shows a plesiomorphic condition instead of *T. knodeli* (previously described in Chiapas amber) that seems more derived. This is consistent with a plesiomorphic condition that is shared by the '*Tityus clathratus*' morphotypes, preliminary classified into '*Tityus (Archaeotityus)'* group [22]. Today there are many extant forms of '*Tityus clathratus*' clade that currently lives in the Neotropics of Central and northern South America [48]. The distribution of the new species, *T. apozonalli,* is limited to the Chiapas amber in the southernmost part of North America at the Miocene.

The current distribution of the living buthid scorpions is worldwide except Antarctica [6]. As shown by the fossil record, the family Buthidae is represented by modern forms that occur since the Paleogene of Europe with several genera found in Baltic amber, as well a single genus *Uintascorpio* found in the Paleogene of North America [13][14] (Fig.10). Several published contributions suggest that extant buthid scorpions from Asia, Africa and South America have a Gondwanaland relationship [6]. Although there is a notable gap in the Mesozoic fossil record (Fig.10), it has been preliminary considered that the buthid scorpions emerged in Gondwana (nearly the Permian-Triassic boundaries) as predicted by the current worldwide distribution [6]. The superfamily Buthoidea with two families: Buthidae and Microcharmidae, is considered monophyletic, neither Achaeobuthidae nor *Palaeoburmesebuthus* (family Incertae sedis) are included in the Buthoidea [6]. The assignment of the Triassic family Protobuthidae into Buthoidea is still inconclusive (Fig.10). Also, the placement of the family Microcharmidae Lourenço, 1996 as separated from the Buthidae is still under debate [6][49]. Based on mesosomal anatomy other authors propose a synonymy of Microcharmidae = Buthidae [51].

On the other hand, the genus *Tityus* is typically a New World group. The fossil specimen '*Tityus' eogenus* from the Baltic amber in Central Europe was initially misplaced [12]. Currently the type material of '*Tityus' eogenus* is missing; the revision is not possible [12]. There are also two buthid species found in the recent Madagascar copal (less than 250 years old) that were assigned to the genera *Microcharmus* (family Microcharmidae) and *Palaegrosphus* [49][50].

However, these may be considered as extant species, not belonging to the fossil record or even subfossil due to the recent depositional age of copal (Fig.10).

Conclusion

Tityus apozonalli sp. nov. brings the number of known scorpions in Chiapas amber to three. However, the fossil record also includes at present other four unidentified specimens -likely tityoid morphotypes- now kept in some private collections and several missing specimens as result of amber fossil trading. Historically, invaluable Chiapas amber fossils have been accumulated in anachronistic and pretentious collections that illegally extract fossils outside Mexico. Unfortunately, the type material of *T. knodeli* and *Centruroides*-like specimen that were mentioned earlier falls into this ambiguous context [3][21]. Thus, the specimens revision for comparison is basically prohibited and information unverifiable. Also the provenance of amber pieces is questionable because Mexican amber is roughly equal to Dominican, i.e. on color, glossiness, general composition, associated plant source, similar paleobiota and geological age [33]-[36]. Amber scorpions are merrily wanted because of their rarity. Fossil collectors that not guarantee the provenance and repository typically pay good money for them, but their egocentric opportunism are shitting on the methodology basically. Accordingly, *T. apozonalli* is the first fossil scorpion in the Chiapas amber with unquestionable repository and provenance, which is not trivial.

Endemism and species richness of scorpion fauna in Mexico is conspicuously high for worldwide criteria, with today nearly 258 species assigned to 26 genera and 7 families, including Buthidae, Chactidae, Diplocentridae, Euscorpiidae, Iuridae, Superstitioniidae and Vaejovidae, which are distributed in both Nearctic and Neotropical environments [52][53]. The average number of known species from Mexico currently is nearly *13.5%* of the worldwide diversity [53]. But the number is growing regularly as new species are described and taxonomic categories re-evaluated. The family Buthidae in Mexico comprises several extant species of the genus *Centruroides,* which is widely distributed in the territory [53][54], another extant species of *Tityopsis* Armas, 1974 that was found in Oaxaca near Chiapas [55], and two fossil species of *Tityus* from the Chiapas amber that now includes *T. apozonalli* [3]. The fossil Centruroides-like morphotype earlier reported needs revision [21].

Notably, there are no living species of the genus *Tityus* previously described in Mexico. *Tityus* essentially shows a Neotropical distribution from northern South America to Central America and the Caribbean Islands [22]. Fossil tityiods from Chiapas amber now extend the geographical range of *Tityus* to the southernmost part of North America. According to Lourenço (2014), the primitive tityiods were likely replaced by opportunistic *Centruroides* that now are prevalent in southern Mexico [3]. However, the sedimentary and tectonic evolution in southern Mexico must play an important role in the extinction and dispersal of the Chiapas amber paleobiota, which includes the scorpion fauna, since the beginning of the Miocene to mid-Pliocene, ca. 23-5 Ma [56]. Accordingly, the extinction and consequent dispersion to new endemic areas was probably induced by land changes [56]. The current distribution of tityiod scorpions supports this hypothesis.

The biogeographic relationships between multiple species of *Tityus* distributed in the northern South America and the Caribbean Islands are pointed out in several contributions [22][57][58]. As noted, the presence of discernible fulcra in *T. apozonalli* from Chiapas as shown in other small-sized fossil tityoids from the Middle America amber seems to be a relict that shares with the present-day morphotypes of the '*Tityus (Archaeotityus)'* group now living extensively from the northern South America to the Caribbean islands. This also suggests an intense radiation at least since the Neogene in the Neotropics of Southernmost North America.

Acknowledgements

We thank Adriana Kuhn for access to the MACH collection and Susana Guzmán (IB-UNAM) for microphotography assistance. Thanks go to Dr. José Luis Ruvalcaba (IF-UNAM) for supporting this research.

References

[1] Dunlop JA, Penney D, Tetlie OE, Anderson LI (2008) How many species of fossil arachnids are there. The Journal of Arachnology 36:267–272.

[2] Dunlop JA, Penney D, Jekel D (2014) A summary list of fossil spiders and their relatives. In Platnick, N.I. (ed.) The world spider catalog, version 15.0. American Museum of

Natural History, online at http://research.amnh.org/entomology/spiders/catalog/index.html. Accessed 2014 Aug.

[3] Lourenço WR (2014) A new species of scorpion from Chiapas amber, Mexico (Scorpiones: Buthidae). Revista Ibérica de Aracnología 24: 59–63.

[4] Lourenço WR (2001) A remarkable scorpion fossil from the amber of Lebanon. Implications for the phylogeny of Buthoidea. Comptes Rendus de l'Académie des Sciences Paris, Sciences de la Terre et des Planètes 332: 641-646.

[5] Lourenço WR (2002) The first scorpion fossil from the Cretaceous amber of Myanmar (Burma). New implications for the phylogeny of Buthoidea. Comptes Rendus Palevol 1: 97-101.

[6] Soleglad ME, Fet V (2003) High-level systematics and phylogeny of the extant scorpions (Scorpiones: Orthosterni). Euscorpius, 11: 1175.

[7] Santiago-Blay, J.A., Fet, V., Soleglad, M.E., P. R. Craig (2004b). The second Cretaceous scorpion from Burmese amber (Arachnida: Scorpiones). Journal of Systematic Palaeontology, 2, pp 147-152.

[8] Baptista C, Santiago-Blay JA, Soleglad ME, Fet V (2006) The Cretaceous scorpion genus, Archaeobuthus, revisited (Scorpiones: Archaeobuthidae). Euscorpius, 35: 1-40.

[9] Lourenço WR, Gall JC (2004) Fossil scorpions from the Buntsandstein (Early Triassic) of France. Comptes Rendus Palevol, 3: 369–378.

[10] Lourenço WR (2009) A synopsis of the amber scorpions, with special reference to the Baltic fauna. In: Zugleich Kataloge der oberösterreichischen Landermuseen. Denisia, 26 (86): 131-136.

[11] Lourenço WR, Weitschat W (2009) A new species of *Palaeonanteris* Lourenço & Weitschat, 2001, fossil scorpion from Ukrainian amber (Scorpiones, Buthidae). Boletín Sociedad Entomológica Aragonesa, 45: 231-235.

[12] Lourenço WR, Weitschat W (2009) More than 120 years after its description, the enigmatic status of the genus of the Baltic amber scorpion ”Tityus eogenus” MENGE, 1869 can finally be clarified. Mitteilungen aus dem Geologisch-Paläontologischen Institut der Universität Hamburg 79: 183-193.

[13] Perry ML (1995) Preliminary description of a new fossil scorpion from the middle Eocene Green River Formation, Rio Blanco County, Colorado. In Averett, W.R. (ed.). The

Green River Formation in Piceance Creek and Eastern Uinta Basins. Grand Junction, Colorado: Grand Junction Geological Society, p. 131–133.

[14] Santiago-Blay JA, Soleglad ME, Fet V (2013) A redescription and family placement of *Uintascorpio* Perry, 1995 from the Parachute Creek Member of the Green River Formation (Middle Eocene) of Colorado, USA (Scorpiones: Buthidae). Revista Ibérica de Aracnología 10: 7−16.

[15] Schawaller W (1979) Ersnachweis eines Skorpions in Dominikanischem Bernstein (Stuttgarter Bernsteinsammlung: Arachnida; Scorpionida) . Stuttgarter Beiträge zur Naturkunde Ser. B (Geologie und Paläontologie) 45: 15.

[16] Schawaller, W. (1982) Zwei weitere Skorpione in Dominikanischem Bernstein (Stuttgarter Bernsteinsammlung: Arachnida; Scorpionida). Stuttgarter Beiträge zur Naturkunde Ser. B (Geologie und Paläontologie) 82: 14.

[17] Santiago-Blay JA, Schawaller W, Poinar Jr GO (1990) A new specimen of *Microtityus ambarensis* (Schawaller 1982) (Scorpiones: Buthidae), fossil scorpion from Hispaniola: evidence of the taxonomic status and possible biogeographic implications. Journal of Arachnology 18:115-117.

[18] Santiago-Blay JA, Poinar, Jr. G.O. (1988) A fossil scorpion, *Tityus geratus* new species (Scorpiones: Buthidae) from Dominican amber. Historical Biology 1: 345-354.

[19] Lourenço WR (2013) A new species of Tityus C. L. Koch, 1836 (Scorpiones: Buthidae) from Dominican Amber. Euscorpius 156: 1-5.

[20] Lourenço WR (2009) A new species of Tityus C. L. Koch, 1836 (subgenus Brazilotityus Lourenço, 2006) from the Dominican Amber (Scorpiones: Buthidae). Euscorpius 83: 1-5.

[21] Santiago-Blay, J.A. Poinar, Jr. G.O. (1993) First scorpion (Buthidae: Centruroides) from Mexican amber (lower Miocene to upper Oligocene). The Journal of Arachnology 21:147-151.

[22] Lourenço WR (2006) Nouvelle proposition de decoupage sous-générique du genre Tutyus C.L. Koch, 1836 (Scorpions, Buthidae). Boletín Sociedad Entomológica Aragonesa 39: 55-67.

[23] Riquelme F, Alvarado-Ortega J, Ramos-Arias M, Hernández M, et al. (2014) A fossil stemmiulid millipede (Diplopoda: Stemmiulida) from the Miocene amber of Simojovel, Chiapas, Mexico. Historical Biology 26 (4): 415-427.

[24] Riquelme, F., Hernández-Patricio, M., Martínez-Dávalos,A., Rodríguez-Villafuerte, M., Montejo-Cruz,M., Alvarado-Ortega, J., Ruvalcaba- Sil, J.L., and Zúñiga-Mijangos, L. (2014): Two flat-backed Polydesmidan millipedes from the Miocene Chiapas-Amber Lagerstätte, Mexico. Plos One 9(8): e105877. doi: 10.1371/journal.pone.0105877

[25] Meneses-Rocha JJ (2001) Tectonic evolution of the Ixtapagraben, an example of a strike-slip basin in southeastern Mexico: implications for regional petroleum systems. In: Bartolini C, Buffler RT, Cantú-Chapa A, editors. The Western Gulf of Mexico Basin: tectonics, sedimentary basins, and petroleum systems. Vol. 75. Tulsa (OK): American Association of Petroleum Geologists Memoir, pp. 183–216.

[26] Boggs S (2009) Petrology of sedimentary rocks: New York, Cambridge University Press, p. 63-164.

[27] Graham A (1999) Studies in neotropicalpaleobotany. XIII. An Oligo-Miocene palynoflora from Simojovel (Chiapas, Mexico). America Journal of Botany 86 (1): 17-31.

[28] Frost, S.H., and Langenheim R.L. 1974. Cenozoic reef biofacies, tertiary larger Foraminifera and scleractinian corals from Chiapas, Mexico. De Kalb (IL): Northern Illinois University Press, p. 388.

[29] Poinar GO (1992) Life in amber. Palo Alto (CA): Stanford University Press. 350p.

[30] Perrilliat MC, Vega FJ, Coutiño MA (2010) Miocene mollusks from the Simojovel area in Chiapas, southwestern Mexico. Journal of SouthAmerican Earth Science 30: 111-119.

[31] Ferrusquía-Villafranca I (2006) The first Paleogene mammal record of Middle America: *Simojovelhyus pocitosense* (Helohyidae, Artiodactyla). Journal of Vertebrate Paleontology 26 (4): 989–1001.

[32] Riquelme F, Northrup P, Ruvalcaba-Sil JL, Stojanoff V, Siddons DP, et al. (2014). Insights into molecular chemistry of Chiapas amber using infrared-light microscopy, PIXE/RBS, and sulfur K-edge XANES spectroscopy. Applied Physics A 116 (1): 97-109.

[33] Langenheim JH (1966) Botanical source of amber from Chiapas, Mexico. Ciencia 24:201–211.

[34] Langenheim JH (2003) Plant resins: chemistry, evolution, ecology and ethnobotany. Portland (OR): Timber Press, pp. 141–304.

[35] Cunningham A, Gay ID, Oehlsclager AC, Lanhenheim J (1983) 13CNMR and IR analyses of structure, aging and botanical origin of Dominican and Mexican ambers. Phytochemestry 22 (4):965-968.

[36] Riquelme F, Ruvalcaba-Sil JL, Alvarado-Ortega J, Estrada-Ruiz E, et al. (2014) Amber from México: Coahuilite, Simojovelite and Bacalite. MRS Proceedings 1618, doi:10.1557/opl.2014.466.

[37] Iturralde-Vinent MA (2001) Geology of the amber-bearing deposits of the Greater Antilles. Caribbean Journal of Science 17 (3/4): 141-167.

[38] Iturralde-Vinent MA (2006) Meso-Cenozoic Caribbean Paleogeography: Implications for the Historical Biogeography of the Region. International Geology Review 48: 791-827.

[39] Rohlf FJ (2013) tpsDig, ver 2.17. New York, Department of Ecology and Evolution, State University of New York at Stony Brook.

[40] Goloboff PA, Farris JS, Nixon KC (2008) TNT, a free program for phylogenetic analysis. Cladistics, 24:1-13.

[41] Stahnke HL (1970) Scorpion nomenclature and mensuration. Entomological News 81:297-316.

[42] Vachon M (1974) Étude de caractéres utilisés pour classer les familles et les genres de scorpions (Arachnides). Bulletin du Muséum National d´Historie Naturelle, sér. 3 104:857958.

[43] Vachon M (1975) Sur l'utilisation de la trichobothriotaxie dubras des pédipalpes des Scorpions (Arachnides) dans le classement des genres de la famillа des Buthidae Simon. Comptes Rendus Academie de Sciences (D) 281:15.

[44] Soleglad ME, Sissom WD (2001) Phylogeny of the family Euscorpiidae: a major revision. In V. Fet, P.A.Selden (editors), Scorpions 2001. In memoriam Gary A. Polis: 25111. British Arachnological Society, UK.

[45] Prendini L (2000) Phylogeny and classification of the superfamily Scorpionoidea Latreille 1802 (Chelicerata: Scorpiones): An exemplar approach.Cladistics, 16: 1–78.

[46] Acosta LE, Candido DM, Buckup RH, Brescovit AD (2008) Description of Zabiusgah (Scorpiones,Buthidae), a new species from southern Brazil, with an update about the generic diagnosis. Journal of Arachnology 36: 491-501.

[47] Soleglad ME, Fet V (2003) The scorpion sternum: Structure and phylogeny (Scorpiones: Orthosterni). Euscorpius 5: 1–34.

[48] Lourenço WR (1984) Analyse taxonomique des scorpions du groupe *Tityus clathratus* Koch, 1845 (Scorpiones, Buthidae). Bulletin du Muséum national d'Histoire naturelle, Paris, 4e sér., 6 (A2): 349-360.

[49] Lourenço WR (2009) A new sub-fossil scorpion of the genus *Microcharmus* Lourenço from Malagasy copal (Scorpiones, Microcharmidae). Boletín Sociedad Entomólogica Aragonesa 44: 135–137.

[50] Lourenço WR, Henderickx H (2012) Another new sub-fossil species of scorpion of the genus *Palaeogrosphus* Lourenço, 2000 from Malagasy copal (Scorpiones: Buthidae). Euscorpius 137: 1−4.

[51] Volschenk ES, Mattoni CI, Prendini L (2008) Comparative anatomy of the mesosomal organs of scorpions (Chelicerata, Scorpiones), with implications for the phylogeny of the order. Zoological Journal of the Linnean Society, 154: 651-675.

[52] Sissom WD, Hendrixson BE (2005) Scorpion diversity and patterns of endemism in northern Mexico. InJ Cartron, E.C.Ceballos, and R.S.Felger (eds.), Biodiversity, ecosystems, and conservation in northern Mexico 122–137. Oxford University Press, NewYork.

[53] Francke OF (2014) Biodiversity of Arthropoda (Chelicerata: Arachnida ex Acari) in Mexico. Revista Mexicana de Biodiversidad 85: 408-418.

[54] de Armas LF, Martín-Frías E, Estévez-Ramírez J (2003) Lista anotada de las especies mexicanas del género *Centruroides* Marx, 1890 (Scorpiones: Buthidae). Revista Ibérica de Aracnología 8: 93-98.

[55] de Armas LF, Martín-Frías E (1998) Presencia del género *Tityopsis* en México y descripción de una especie nueva (Scorpiones: Buthidae). Anales de la Escuela Nacional de Ciencias Biológicas 43:45-49.

[56] Riquelme F, Hill DE (2013) Insights into amber salticids from the Neogene of Middle America, with the first report of Marpissinae (Araneae: Salticidae) from the Chiapas amber. Peckhamia 106.2: 1-5.

[57] Armas LF, de Abud-Antun AJ (2004) Adiciones al género *Tityus* C. L. Koch, 1836 en República Dominicana, con la descripción de dos especies nuevas (Scorpiones: Buthidae). Revista Ibérica de Aracnología 10: 53−64

[58] Lourenço WR (1999) Origines et affinités des scorpions des Grandes Antilles: Le cas particulier des éléments de la famille des Buthidae. Biogeographica, 75(3): 131-144.

Figure captions

Figure 1

Location of the Guadalupe Victoria site near Simojovel, Chiapas, Mexico.

Figure 2

Tityus apozonalli sp. nov. [A]: Amber piece, arrow indicates the position of fossil inclusion, scale bar 10 mm. [B]: General view of fossil scorpion, scale bar 5 mm. [C]: Close view of the holotype male BLMACH.18, scale bar 2 mm.

Figure 3

Tityus apozonalli sp. nov. A: Dorsal view of chelicera and partial carapace with median eyes, scale bar 1 mm. B: Left pedipalp, scale bar 2 mm. C: Right pedipalp, scale bar 2 mm.

Figure 4

Tityus apozonalli sp. nov. Schematic reconstruction of left pedipalp in dorsal view, which shows discernible carinae and the pedipalp movable finger dentition.

Figure 5

Tityus apozonalli sp. nov. A: general view of sternites and pectines, note the whitish color on pectines and adjacent sternites, scale bar 2 mm. B: Closer view of pectines, scale bar 1 mm.

Figure 6

Tityus apozonalli sp. nov. Schematic reconstruction of sternum and pectines showing fulcra and the number of pectinal teeth, punted arrow indicate the partially visible portion as covered by leg.

Figure 7

Tityus apozonalli sp. nov. A: Legs, scale bar 2 mm. B: Metasoma segments and telson, scale bar 2mm. C: Closer view of telson, scale bar 1 mm.

Figure 8

Tityus apozonalli sp. nov. Schematic reconstruction of the metasoma segments and telson showing aculeus and subaculear tubercle.

Figure 9

The phylogenetic status of *Tityus apozonalli* sp. nov. among fossil buthids from the Middle America amber, Neogene, inferred from data matrix in Table 1. Characters are described in Appendix 1. Strict consensus tree based on quantitative and qualitative characters: Length= 23, CI= 82, and RI= 77. Black circles represent synapomorphies and white circle homoplasies. Numbers above circles indicate characters and numbers below branches indicate bootstrap values.

Figure 10

Time-scale tree that shows the family Buthidae diversity since the Paleogene (Cenozoic) and extinct close relatives in the Mesozoic, according to the current fossil record. The family Protobuthidae is here considered as a basal linage outside the superfamily Buthoidea after Batista et al. (2003) [8] and *Microcharmus* [49] is considered into Buthidae (= Microcharmidae) after Volschenk et al. (2008) [52]. Note that both copal taxa *Palaeogrosphus* and *Microcharmus* are not part of the geological record.

Supplementary Table 1
Data Matrix

Taxa	1	2	3	4	5	6	7	8	9	10	11	12	13
Palaeonanteris ukrainensis	2	0	1	0	0	?	0	1	1	1	0	1	1
Tityus knodeli	0	0	1	1	0	0	0	0	0	0	1	0	1
Tityus azari	1	1	1	1	1	1	1	1	1	2	1	0	0
Tityus(Brazilotityus) hartkoni	2	1	1	1	1	1	1	1	1	1	1	0	0
Tityus apozonalli	1	2	1	2	2	2	?	?	1	1	0	1	2
Centruroides beynai	0	0	1	2	?	0	0	0	?	0	1	0	2
Microtytyus ambarensis	0	?	1	0	?	0	0	0	0	0	0	0	2

Supplementary Apendix 1

List of characters scored for phylogenetic analysis according to Stahnke, 1970 [41] except for the trichobothria pattern *sensu* Vachon, 1974 [42][43], pedipalp chela carinae *sensu* Prendini, 2000 [45], modified by Acosta *et al.*, 2008 [46]. Length values are expressed in millimeters.

1. Body size: (0) 12-13, (1) 17-17.8, (2) 18-32.
2. Finger fixed teeth: (0) 5-12, (1) 14-15, (2)18-32.
3. Trichobothria Type A: (0) absent, (1) present.
4. Pectinal teeth: (0) 10-12, (1) 19-20, (2) 29-30.
5. Movable finger teeth: (0) 5-12, (1) 14-15, (2) 30-33.
6. Carapace length: (0) 5-12, (1) 14-15, (2) 30-33.
7. Femur length pedipalp: (0) 1.0-1.8, (1) 2.0-2.5, (2) 2.6-3.4.
8. Patella length pedipalp: (0) 1.3-1.8, (1) 2.5-2.6, (2) 3.1-4.5.
9. Chela length: (0) 2.0-2.3, (1) 3.6-3.9, (2) 4.0-5.2.
10. Movable finger length: (0) 0.8-1.5, (1) 2.5-2.7, (2) 3.0-4.9.
11. P/R pedal spurs: (0) absent, (1) present.
12. Tibial spur: (0) absent, (1) present
13. Fulcra: (0) absent, (1) vestigial, (2) present.

PECKHAMIA 106.2, 29 August 2013, 1—5 ISSN 2161—8526 (print)
urn:lsid:zoobank.org:pub:3D989741-FCA4-4FDC-A5C5-88C67741BC33 (registered 27 AUG 2013) ISSN 1944—8120 (online)

Insights into amber salticids from the Neogene of Middle America, with the first report of Marpissinae (Araneae: Salticidae) from the Chiapas amber

Francisco Riquelme [1] and David E. Hill [2]

[1] Instituto de Fisica, Universidad Nacional Autónoma de México, AP 20-364, D.F., México, *email corresponding author:* riquelme.fc@gmail.com
[2] 213 Wild Horse Creek Drive, Simpsonville, South Carolina 29680-6513, USA.

Abstract. The genera and species of fossil salticids from the European Baltic amber (Paleogene) are more diverse than salticids from the geologically younger Neogene deposits of Dominican and Chiapas amber. However, the latter are more diverse than Baltic amber at the subfamily level and also include close relatives of modern species. This diversity may reflect the presence of ancestor taxa for extant North American groups. The relatively modern forms of the Neogene suggest a broader divergence since the Miocene within the tropics. Here we add the discovery of a fossil salticid that appears to be a marpissine (cf. *Maevia* C. L. Koch, 1846) from the Miocene Chiapas amber (southern México). The tectonic and sedimentary evolution of South México, Central America and the Antilles from the Paleogene to Neogene that caused short-term cyclical changes in climate may have also driven the early dispersal and introduction of marpissines from Middle America into southern North America.

Key words: Chiapas amber, Miocene, Middle America, Salticidae, Marpissinae

Resumen. Los géneros y las especies de saltícidos fósiles del ámbar Báltico en Europa (Paleógeno) son más diversos que los saltícidos de los más recientes depósitos de ámbar del Neógeno de República Dominicana y Chiapas. Sin embargo, estos últimos son más diversos que los del ámbar del Báltico a nivel de subfamilias y también muestran parentescos cercanos con especies modernas. Las formas relativamente modernas del Neógeno sugieren una más amplia divergencia desde el Mioceno en los trópicos. Se incluye aquí el descubrimiento de un saltícido fósil, según parece marpissino (cf. *Maevia* C. L. Koch, 1846), en el ámbar de Chiapas (Mioceno) al sur de México. La evolución tectónica y sedimentaria del Sur de México, Central América y las Antillas durante el Paleógeno al Neógeno que causó cambios cíclicos de periodos cortos en el clima también puede haber conducido a una temprana dispersión e introducción de marpissinos desde la América Media hacia el sur de Norte América.

Palabras clave: Ámbar de Chiapas, Mioceno, América Media, Salticidae, Marpissinae

Introduction

Fossil spiders, including amber salticids, have been fully cataloged based on criteria used for living spiders (Dunlop, Penney and Jekel, 2013). Several monographs of amber and copal spiders from the Cretaceous to Tertiary of Europe, Africa, Asia and America have also been published separately by Wunderlich (2004a, 2008, 2011, and 2012), reflecting his use of different criteria. Fossil representatives of the Salticidae occur in the amber deposits of the Paleogene and Neogene of Europe and the Americas (Wunderlich, 2004a; Penney and Selden, 2011; Dunlop, Penney and Jekel, 2013). This includes the Paleogene amber deposits from Bitterfeld, Baltic, Rovno and younger (Neogene) strata from the Dominican Republic. These recent reviews do not include the salticid records from the Neogene Chiapas amber (Southern México) that were previously published by Petrunkevitch (1971) and García-Villafuerte and Penney (2003). Both reports of Chiapas salticids were associated with the Simojovel quarries that belong to the Lower Miocene Balumtum and Mazantic Shale strata. Petrunkevitch (1971) described a representative of Salticidae *incertae sedis* since this specimen was too poorly preserved to identify further, while García-Villafuerte and Penney (2003) described a representative of the genus *Lyssomanes*. Additionally, a putative new member of the subfamily Marpissinae (Araneae: Salticidae) from the Chiapas amber is reported here for the first time. Although limited, this fossil record increases our knowledge of

the amber salticids from the Neogene of Middle America, complementing previously published fossil records from Dominican amber.

Material and Methods

The piece of amber containing the salticid shown here was collected in the Rio Salado locality near the town of Totolapa, 66 km south of Simojovel, State of Chiapas, southern México. A first stratigraphy report of the Totolapa amber outcrops can be found in Duran-Ruiz *et al.* (2013: Fig. 1-2). Totolapa amber is currently thought to be Lower Miocene in age. The single specimen BL-MACH48 is currently housed at the Museo del Ámbar de Chiapas, San Cristobal de Las Casas, Chiapas, México.

Results and Discussion

This putative member of the subfamily Marpissinae (Araneae: Salticidae) is tentatively placed in the genus *Maevia* C. L. Koch, 1846 (Figure 1).

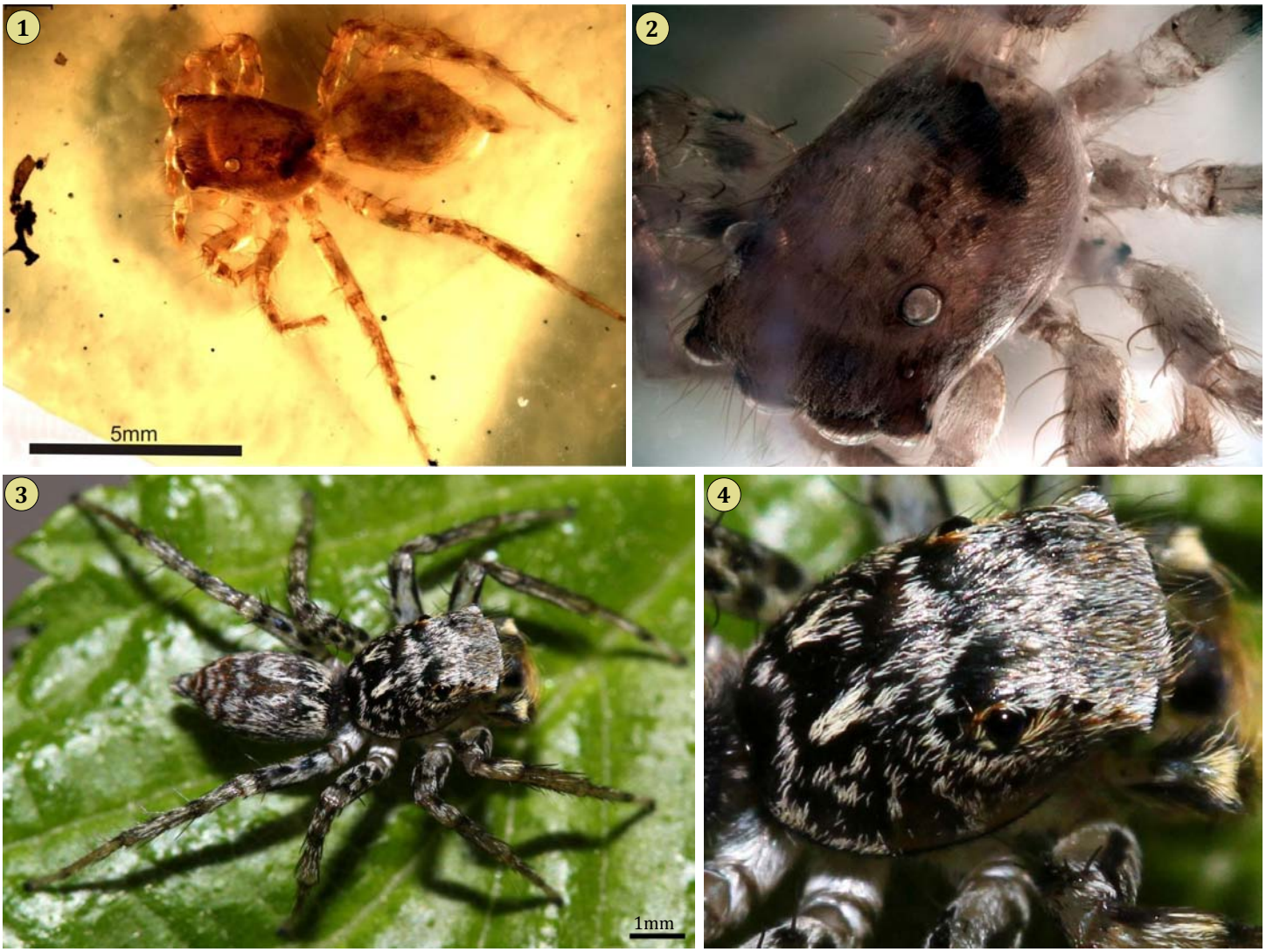

Figure 1. **1,** A single specimen preliminarily identified as new member of the Marpissinae from the Miocene Totolapa amber, Chiapas, México. **2,** Closer view of the of prosoma from (1). **3,** ♂ *Maevia inclemens* (Walckenaer 1837), 'light form' from the forest understory of southern Greenville County, South Carolina, USA (12 MAY 2012). **4,** Detail of prosoma from (3). In many details including size, carapace shape, placement of eyes, relative leg lengths, and setation, the amber specimen resembles this living *Maevia*.

This specimen is presently being studied and a formal description at the species level will be published when this has been completed. The fossil record of salticids from North America is unknown to date, so the discovery of this fossil marpissine in the Miocene Chiapas amber at the physiographic boundaries between southern North America and Central America can have a major impact on our hypotheses regarding the minimum age of the origin and divergence of related taxa.

The Chiapas amber is associated with a resin-producing tree of the genus *Hymenaea* that formed a dominant plant cover in temperate, subtropical and tropical areas from the Miocene until recently (Langenheim, 2003). The paleobiological affinities of the Neotropical Chiapas amber that are shared with Dominican amber, including the *Hymenaea* forest, mangrove-like environments, and their coeval faunas, are suggested elsewhere (Poinar, 1992; Langenheim, 2003; Solórzano-Kraemer, 2010; Penney, 2008; others). In this context, according to Wunderlich (2004b) the fossil record of salticids in Dominican amber is most abundant at the subfamily level reflecting a higher diversity than the Baltic amber. Penney (2008) reported that the family Salticidae has the second most abundant fossil spider record in Dominican amber, after Theridiidae. The amber salticids of Chiapas mentioned above expand the known subfamily diversity of Neotropical America during the Tertiary. Accordingly, the diversity of these Miocene salticids may reflect the presence of ancestor taxa for the recent North American groups.

The hypothesis of salticid origin during the Upper Cretaceous on the basis of the molecular phylogenetics and available biogeography literature has been reviewed elsewhere (Hill and Richman, 2009). Penney (2010) saw a need to integrate the fossil record into this kind of analysis. In this sense, the huge gap in the Mesozoic fossil record of salticids including the Cretaceous fossiliferous amber and the absence of relative modern forms in the Eocene Baltic amber (Wunderlich, 2004b) have suggested that the divergence of salticid groups occurred during the Cenozoic instead of the Mesozoic (Wunderlich, 2004b; Penney, 2010; Penney and Selden, 2011). Some of the most 'primitive' or basal salticids representing few subfamilies are known from the Eocene Baltic amber, suggesting a poor diversification of modern groups during the lower part of the Cenozoic (Wunderlich, 2004b). According to Wunderlich, a significant divergence may have started after the Eocene Baltic amber extinction during the Oligocene (when we have a fossil record gap), persisting into the Miocene. Hill and Richman (2009) also suggested that the divergence and rapid speciation of the salticids probably took off in the Paleocene-Miocene. The subfamily diversity and the presence of relatively modern forms of salticids from the Middle American amber indicate a broader divergence of salticids since the Miocene within the tropics.

Geological notes on the Miocene Chiapas amber with implications for salticid dispersal

Central America lies at the western end of the Caribbean plate (James, 2007; Bundschuh and Alvarado, 2007). Its geological history is clearly important to biodispersal between North and South America. Central America is part of a complex of fragmented continental, oceanic and volcanic arc crust between the larger continental masses of North and South America. This includes pre-Mesozoic blocks, Mesozoic and Cenozoic units (James, 2007; Bundschuh and Alvarado, 2007). The Caribbean plate is thought to have a Pacific origin, moving from north to south (Bundschuh and Alvarado, 2007; others). Readers are urged to consult the abundant available literature for a more detailed discussion, which is only briefly mentioned here. The tectonic and sedimentary evolution of so-called Middle America includes southern México, Central America and the Antilles (James, 2007; Bundschuh and Alvarado, 2007). This evolution drastically modified paleobasins in this area and also affected climate change in a manner that is consistent with the early introduction of marpissines from Neogene ancestors in Middle America to southern North America.

It is important to note that the Neogene Dominican and Chiapas amber strata, as part of the geological history of the Middle America, shared the same time scale and orogeny at convergent boundaries during

the geological evolution of southern México and Central America (James, 2007). This and their similar nearshore depositional regimes spanning the Lower to Middle Miocene eventually favored similar patterns of biodispersal in the two areas.

Wunderlich (2004a), Penney (2008), and Penney and Selden (2011) suggested that nearly all families and genera of fossil spiders from Dominican amber are still extant in the same geographical area. The accuracy of this statement can be a subject of debate, but this diversity may also reflect a center of origin for several groups. Poinar (1992) and Nudds and Selden (2008) compared the Dominican fossil assemblages with the similar, living tropical biota. They suggested that paleobiota trapped in Dominican amber was forced to disperse and became extinct due to climatic fluctuations during the ice ages (Neogene to Pleistocene), which altered the poles and also affected the tropics. According to this hypothesis, plant and animal groups could retreat back to Central and South America, and elsewhere to Australasia. Because this approach is based on a general climate inference (glaciation cycles), it remains to be demonstrated in accordance with the geological history of the Dominican Republic region as part of the Central America orogenies.

On the other hand, the Chiapas amber deposits of southern México are part of the Mazantic Shale and Balumtum Sandstone strata ranging from Lower to Middle Miocene (ca. 23-13 Ma). These are associated with nearshore and lowland continental settings (Perrilliat *et al.*, 2010). The geological evolution of Chiapas from the Oligocene to Pliocene is also linked to the formation of Central America (Meneses-Rocha, 2001; Bundschuh and Alvarado, 2007; Mandujano-Velázquez and Keppie, 2009; others). The tectonic phenomena and sedimentary input that formed the Mountains of Chiapas (where the Chiapas amber is now collected) during the Oligocene-Miocene altered the distribution of basins and generated and modified barriers to dispersal (Meneses-Rocha, 2001). This caused changes in local ecosystems and represents a potential driver of diversification, forcing the dispersal of Chiapas amber paleobiota.

Accordingly, the intense tectonic activity by a general uplift that thrust and folded the basal rocky units during the Oligocene-Miocene of Chiapas (ca. 28-13 Ma) and a subsidence post-orogenic phase ending at the Lower Pliocene (ca. 5 Ma) significantly altered the paleogeography of the region (Riquelme *et al.*, 2013: Fig. 2). The rising blocks triggered by tectonics produced mountain ranges, marine sea level fluctuations, and also affected climatic processes progressively. Thus, the shoreline was forced to recede toward the north and cyclic alternation of depositional environments occurred, alternating from lacustrine to alluvial and stream-flood systems that reflect episodic, severe climate changes (Meneses-Rocha, 2001). This is consistent with the Oligocene to Miocene depositional record in the Chiapas amber area. The rocks exposed here show alternate, compositional changes in carbonate, siliciclastic and organic-rich carbonaceous beds that suggest a system eventually controlled by short-term cyclical changes in climate (Riquelme *et al.*, 2013). It seems that the dispersal and extinction of Chiapas amber paleobiota took place in allopatry by land changes. This was followed by a forced dispersion to new areas over long periods of time spanning the Miocene to Pliocene.

Acknowledgments

We thank the PhD-granting program in Biological Sciences at the UNAM, financially supported by CONACYT. We also thank Thomas A. Lee-Withing (RIP) at the UNICACH, M. Ramos-Arias, J. Alvarado-Ortega (IGL-UNAM) and J. L. Ruvalcaba-Sil (IF-UNAM) for field support, Susana Guzmán (IREKANI-IB-UNAM) for photomicrography assistance, and Ma. C. Perrilliat for access to the CNP-IGL-UNAM.

Corrigendum to Peckhamia 106.1

When this article was first published (Riquelme & Hill 2013, Peckhamia 106.1) the catalogue number was listed in error as IGM6264. This has now been corrected to BL-MACH48. The authors apologise for this error.

References

Bundschuh, J., and G. E. Alvarado (eds.). 2007. *Central America: Geology, Resources, and Hazards.* Taylor and Francis, London. Vol. 1- 2.

Dunlop, J. A., D. Penney and D. Jekel. 2013. A summary list of fossil spiders and their relatives. In Platnick, N. I. (ed.) The world spider catalog, version 13.5 American Museum of Natural History, *Online at:* http://research.amnh.org/iz/spiders/catalog/Fossils13.5.pdf

Durán-Ruiz, C., F. Riquelme, M. Coutiño-José, G. Carbot-Chanona, G. Castaño-Meneses, and M. Ramos-Arias. 2013. Ants from the Miocene Totolapa amber (Chiapas, México), with the first record of the genus *Forelius* (Hymenoptera, Formicidae). Canadian Journal of Earth Sciences, in press.

García-Villafuerte, M. A. and D. Penney. 2003. *Lyssomanes* (Araneae, Salticidae) in Oligocene-Miocene Chiapas amber. The Journal of Arachnology 31: 400-404.

J**ames, K. H. 2007.** Structural geology: From local elements to regional synthesis. In: *Central America: Geology, Resources, and Hazards* (J. Bundschuh and G. Alvarado, eds.). Taylor and Francis, London. Vol. 1: 1-45.

Hill, D. E. and D. B. Richman. 2009. The evolution of jumping spiders (Araneae: Salticidae): a review. Peckhamia 75.1: 1-17.

Langenheim, J.H. 2003. *Plant Resins: Chemistry, Evolution, Ecology and Ethnobotany*. Timber Press. 586 p.

Mandujano-Velázquez, J. J. and J. D. Keppie. 2009. Middle Miocene Chiapas fold and thrust belt of Mexico: a result of collision of the Tehuantepec Transform/Ridge with the Middle America Trench. Special Publications of the Geological society, London 327: 55-69.

Meneses-Rocha, J. J. 2001. Tectonic evolution of the Ixtapa graben, an example of a strike-slip basin in southeastern Mexico: implications for regional petroleum systems. In: *The Western Gulf of Mexico Basin: Tectonics, Sedimentary Basins, and Petroleum Systems* (C. Bartolini, C. Buffler and A. Cantú-Chapa, eds.). Memoirs of the American Association of Petroleum Geologists 75: 183-216.

Nudds, J. R. and P. Selden. 2008. Dominican amber. In: *Fossil Ecosystems of North America: A Guide to the Sites and their Extraordinary Biotas* (J. R. Nudds and P. Selden, eds.). Manson Publishing, 233-258.

Penney, D. 2008. *Dominican Amber Spiders: A Comparative Palaentological-neontological Approach to Identification, Faunistics, Ecology and Biogeography*. Siri Scientific press, Manchester. 178 p.

Penney, D. 2010. The evolution of jumping spiders (Araneae: Salticidae): the palaeontological evidence. Peckhamia 81.1: 1-3.

Penney, D. and P. A. Selden. 2011. *Fossil Spiders: The Evolutionary History of a Mega-diverse Order*. Siri Scientific press, Manchester. 128 p.

Perrilliat M. C., F. J. Vega and M. A. Coutiño. 2010. Miocene mollusks from the Simojovel area in Chiapas, southwestern Mexico. Journal of South American Earth Science 30: 111-119.

Petrunkevitch, A. I. 1971. Chiapas amber spiders II. University of California Publications in Entomology 63: 1–44.

Poinar Jr., G. O. 1992. *Life in Amber.* Stanford University Press. 350 p.

Riquelme, F., J. Alvarado-Ortega, M. Ramos-Arias, M. Hernández, I. Le Dez, T. A. Lee-Whiting and J. L. Ruvalcaba-Sil. 2013. A fossil stemmiulid millipede (Diplopoda: Stemmiulida) from the Miocene Amber of Simojovel, Chiapas, México. Historical Biology, in press.

Riquelme, F. and D. E. Hill. 2013. Insights into amber salticids from the Neogene of Middle America, with the first report of Marpissinae (Araneae: Salticidae) from the Chiapas. Peckhamia 106.1: 1-5.

Solórzano-Kraemer, M. M. 2010. Mexican Amber. In: *Biodiversity of Fossils in Amber from the Major World Deposits* (D. Penney, ed.). Siri Scientific Press, Manchester. 42-56.

Wunderlich, J. 2004a. *Fossil Spiders in Amber and Copal*. Beiträge zur Araneologie, Verlag J. Wunderlich 3a-3b: 1908 p.

Wunderlich, J. 2004b. Fossil jumping spiders (Araneae: Salticidae) in Baltic and Dominican amber, with remarks on Salticidae subfamilies. Beiträge zur Araneologie, Verlag J. Wunderlich 3: 1761–1819.

Wunderlich, J. 2008. *Fossil and Extant Spiders (Araneae) - Fossile und Heutige Spinnen*. Beiträge zur Araneologie, Verlag J. Wunderlich 5: 1-870.

Wunderlich, J. 2011. *Extant and Fossil Spiders (Araneae) - Heutige und Fossile Spinnen*. Beiträge zur Araneologie, Verlag J. Wunderlich 6: 1-640.

Wunderlich, J. 2012. New fossil spiders (Araneae) of eight families in Eocene Baltic amber, and revisions of selected taxa. Beiträge zur Araneologie, Verlag J. Wunderlich 7: 94–149.

CAPÍTULO 3 CONCLUSIONES Y PESPECTIVAS

Respuestas a interpretaciones previas

Los estudios mineralógicos actuales en resinas fósiles están basados en técnicas analíticas de la geoquímica orgánica. A partir de los cuales se han establecido un amplio número de variedades minerales válidas (Vavra, 1993). El arsenal de técnicas incluye desde la combinación de cromatografía acoplada a espectrometría de masas, termólisis, resonancia magnética nuclear de Carbono 13, hasta la espectroscopia de infrarrojo (IR) (Anderson, 1992; Beck *et al*., 1964; Langenheim y Beck, 1968; Lambert, 1989; Derrick *et al*., 1999; Bray y Anderson, 2009; Tappert *et al*., 2011). Esta última, la espectroscopia IR, es considerada como el método más empleado en la caracterización de las afinidades botánicas o quimiotaxonomia, tanto de resinas fósiles como recientes (Vandenabeele *et al*., 2003; Trevisani *et al*., 2005). La espectroscopia IR también ha aventajado significativamente en su capacidad instrumental como en la acumulación de datos espectrales para estudios comparativos (Wolfe *et al*., 2009). Para nuestro conocimiento, el presente trabajo muestra el primer análisis de espectroscopia IR en resinas fósiles usando una fuente de luz Sincrotrón. Este método muestra una ventaja significativa en la quimiotaxonomia de resinas fósiles, puesto que colecta espectros IR con mayor rapidez y mejor definición en muestras sin preparar. Además se obtienen mapeos de distribución química asociada a la estructura del material. Lo cual representa una ventaja en la diagnosis de caracteres químicos de cada variedad o especie de resina.

El presente estudio puede representar un estado-del-arte del análisis de espectroscopia IR en las variedades de ámbar de México, dado que muestra los espectros IR característicos para cada una de las variedades actualmente conocidas (Riquelme *et al*, 2014b). Sin embargo, en futuros trabajos se requiere una ampliación significativa del muestreo para cada localidad y tipo de ámbar. Lo cual ampliará la librería de espectros para estudios comparativos y permitirá identificar variaciones de acuerdo a la alteración diagenética o marcadores específicos entre diferentes afloramientos asociados a la paleogeografía.

Por otra parte, en la mineralogía moderna existe poco consenso sobre la distinción entre especies y variedades de minerales orgánicos. El ámbar es formalmente reconocido como una especie de mineral orgánico en las clasificaciones más aceptadas de Dana y Nickel-Strunz, entre otras (Dana, 2014; Strunz, 2014). Sin embargo, los criterios para caracterizar variedades y/o especies de resinas fósiles, son todavía ambiguos. Diferentes criterios son aplicados indistintamente. Por su naturaleza de polímero semicristalino, el ámbar no puede ser caracterizado por técnicas estructurales tradicionales de difracción de rayos-X. Dado que es una resina fósil de ocurrencia natural, la cristalización es parcial y no definida, a diferencia de los minerales inorgánicos donde la estructura cristalina da lugar a un patrón de difracción claramente definido. En el ámbar, la cristalización ocurre a nivel de moléculas en vez de átomos o iones (Callister, 2000). En análisis preliminares en el laboratorio, los patrones de difracción estándar de la Coahulita, Simojovelita y Bacalita, muestran una fase amorfa fuertemente traslapada (obs. pers.). Esto sugiere que la muestra no es cristalina. Sin embargo, esto ocurre probablemente porque el tamaño y orientación de los cristales en la resina fósil está por debajo de los límites de detección.

La limitante técnica y metodológica para obtener patrones de difracción en resinas fósiles de manera rutinaria, ha sido la mayor causa de inconsistencias en su caracterización mineral. Se ha considerado como especie tipo de ámbar, la descrita inicialmente como Succinita. Esta resina proviene de los depósitos del Mar del Báltico, en Europa, con una edad de depósito estimada en el Eoceno Temprano (Vavra, 1993; Langenheim, 2003). Pero el resto de los ámbares descritos posteriormente como variedades, no comparten ni la misma morfología ni la composición química. Tampoco comparten características estratigráficas, edad geológica o la fuente paleobotánica. Nuevas variedades de resinitas fósiles y ámbares en diferentes depósitos del mundo son descritas continuamente con características específicas, tanto estructurales como composicionales. Es momento de una nueva revisión de la nomenclatura de resinas fósiles y los criterios diagnósticos que definen especies y/o variedades.

En este contexto, la clasificación adoptada en este trabajo está basada en criterios morfológicos, composicionales y de afinidad botánica (Riquelme *et al*, 2014b). Lo cual representa una metodología que desestima la ambigüedad de criterios producida por la caracterización mineral tradicional. La cual adopta de manera poco eficiente criterios fisicoquímicos aplicables solo a minerales inorgánicos característicos. Pero que en minerales

orgánicos no son determinados por las mismas técnicas analíticas o son irrelevantes. En este trabajo, además de la estructura y composición del ámbar, es considerada también su naturaleza fósil. Por lo tanto, su biología, representada por su afinidad botánica, la cual es considerada como un carácter diagnóstico válido para establecer variedades y/o especies. Posiblemente, uno de los rasgos más significativos.

Consecuentemente, se presentan aquí, por primera vez, los ámbares de México incluidos en la nomenclatura de minerales orgánicos, en comparación con las resinas y resinitas fósiles de otros depósitos en el mundo (Riquelme *et al*, 2014b). Los resultados de la microespectroscopía IR soportan la descripción de la Coahuilita como una nueva variedad de ámbar en México. También proporcionan los primeros datos diagnósticos que definen la afinidad botánica de la Bacalita. Actualmente, ambos son el registro más antiguo de ámbar en México, con una edad estimada en el Cretácico Tardío. Estos ámbares están asociados con el paleoambiente y las afinidades botánicas de otras resinas fósiles de América del Norte, depositadas en edades geológicas semejantes (Riquelme *et al*, 2014b). Trabajos futuros de caracterización de los ámbares de México, incluyendo metodologías complementarias a la espectroscopia de IR, como la cromatografía acoplada a espectrometría de masas y difracción de rayos-X de bajo ángulo, contribuirán a una más precisa definición de las propiedades fisicoquímicas y la fuente paleobotánica de estas resinas fósiles.

Durante las décadas pasadas, el ámbar del Mioceno de Chiapas fue el único ámbar conocido con certeza en México. Esta variedad de ámbar, descrita aquí como Simojovelita, forma parte del llamado ámbar del Neógeno de la América Media, que incluye el ámbar de Republica Dominicana y las Antillas (Riquelme y Hill, 2013). Estos ámbares comparten una fuente botánica similar, asociada con la planta leguminosa del género *Hymenaea.* Así como una edad geológica contemporánea y un ambiente de depósito semejante entre sí. Lo cual es consistente con la evolución tectónica y sedimentaria del sur de México, Centroamérica y las Antillas, insertadas en la Placa del Caribe y la formación de Centroamérica, la cual se extiende desde inicios del Mioceno al Plioceno (Iturralde-Vinent, 2001).

Nueva plataforma experimental = nuevos datos

La paleobiología usa los métodos y principios de la biogeoquímica para obtener datos y evidencias a nivel molecular del material fósil con implicaciones directas en su biología, ecología, tafonomía, biogeografía y procesos evolutivos. En este contexto, se han obtenido aquí los primeros datos sobre la preservación de la materia orgánica embebida en el ámbar de Chiapas. De acuerdo a los resultados presentados en este trabajo, la concentración de azufre orgánico es un elemento importante en la composición del ámbar, que tiende a aumentar de acuerdo con los procesos biogeoquímicos que transforma la resina en ámbar a través del tiempo geológico. Interacciones químicas complejas se producen entre la resina durante su deposición y enterramiento. Además, el cambio químico que ocurre durante la maduración geológica en ámbar (*ambarización*) ha sido considerado como un proceso básicamente oxidativo (Langenheim, 2013). Sin embargo, los datos obtenidos por XANES muestran que la mayor parte de las especies de azufre están entre un rango de baja oxidación y reducción, lo que sugiere que la maduración de la resina o ambarización se produce bajo reacciones con escasez de oxigeno o son favorecidas en un ambiente pobre en oxígeno (Riquelme *et al.*, 2014a). Lo cual difiere de la opinión general sobre la ambarización=oxidación de las resinas. Esto lleva a revisar los procesos de transformación en otro tipo de ámbares.

Aunque esta investigación tiene implicaciones importantes para el ámbar Chiapas, se requiere de más análisis y discusión para evaluar si las especies de azufre pueden funcionar como biomarcadores altamente informativos para otros ámbares fosilíferos distribuidos en todo el mundo y a edades geológicas diferentes.

Por otra parte, el azufre orgánico detectado en el ámbar de Chiapas es un marcador indicativo de la solidificación acelerada de la resina. Este azufre puede tener la función de aditivo en la estructura de polímero de la resina, promoviendo un rápido endurecimiento (Callister, 2000; Riquelme *et al.*, 2014a). Por lo tanto, prácticamente sella la materia orgánica atrapada en su interior y restringe significativamente la degradación orgánica, limitando el intercambio gaseoso y el ataque bacteriano. La encapsulación de la materia orgánica también proporciona una mayor estabilidad contra cambios químicos durante los procesos diagenéticos del enterramiento y litificación de los sedimentos portadores del ámbar.

Resultados como los mostrados aquí, basados en los de métodos y técnicas de espectroscopias de infrarrojo y rayos-X usando una fuente de luz Sincrotrón, son pioneros en el estudio del material fósil. Así pues, sus perspectivas y aplicaciones son múltiples en trabajos futuros.

Nuevas técnicas en microimagen

Los análisis de imagen microscópica en inclusiones orgánicas atrapadas en ámbar, es un importante tópico con interés taxonómico y tafonómico, que hasta ahora resulta muy problemático de resolver, debido principalmente a la opacidad característica de las resinas fósiles. Microtomografía de rayos-X usando una fuente de luz Sincrotrón se ha aplicado exitosamente en muestras de ámbar del Báltico. Pero es una técnica costosa y su acceso es limitado. La microscopía con filtros infrarrojos y planos apocromáticos, así como la microtomografía computarizada de rayos-X en 3D diseñada en el laboratorio por Martínez-Martínez-Dávalos (2012), tal como se han empleado en el presente trabajo, demuestran que son técnicas adecuadas para medir, documentar y analizar inclusiones orgánicas con interés taxonómico y tafonómico (Riquelme *et al.*, 2011; 2013; 2014c). Algunas de ellas, como alternativas a técnicas de microimagen más costosas y todavía inaccesibles.

La nueva práctica de fotomicrografía usando filtros infrarrojos en muestras de ámbar y resinas subfósiles, tiene la ventaja de que proporciona información rápida y detallada sobre las inclusiones orgánicas y la estructura de la resina. En este trabajo, se emplea por primera vez esta técnica. Encontrar nuevas herramientas y materiales para mejorarla, será esencial para utilizarla de manera rutinaria (Riquelme *et al*., 2011, 2014a).

Por otra parte, las imágenes 3D obtenidas mediante microtomografía computarizada de rayos-X (Martínez-Dávalos, 2012) ha revelado muchas de las partes diagnosticas de un ejemplar de milpiés preservado en una muestra de ámbar nublado, con abundante suelo, restos de plantas, y microfracturas, los cuales dificultaban su descripción. La imagen 3D reveló igualmente tejidos blandos intactos en el interior del ejemplar, lo cual representa la primera evidencia de la conservación de tejidos blandos en un fósil de milpiés de cualquier depósito o tiempo geológico. Previamente, se ha utilizado exitosamente la microtomografía de rayos-X con una fuente de luz Sincrotrón para analizar fósiles en ámbar (Tafforeau *et al*., 2006; Lak *et al.*, 2008; Perreau y

Tafforeau, 2011). Pero las imágenes que se han obtenido en el presente trabajo, son las primeras de este tipo para un fósil, de cualquier sedimento o edad geológica, obtenida bajo esta técnica en México. Esto demuestra el potencial de la microtomografía de rayos-X, como una tecnología hecha en el laboratorio, para obtener imágenes microscópicas del material fósil (Martínez-Dávalos, 2012; Riquelme *et al.*, 2014c)

Inclusiones orgánicas

Las nuevas especies de artrópodos terrestres en el ámbar de Chiapas aquí descritas, se suman a la biodiversidad de sus respectivos órdenes y amplían su rango geocronológico a los estratos del Mioceno en la parte más meridional de América del Norte.

Los fósiles proporcionan evidencias para comprender ciertas tendencias evolutivas y permiten comprobar hipótesis filogenéticas (Shcherbakov *et al*., 2011). En este contexto, la sistemática paleontológica de inclusiones orgánicas en ámbar enfrenta varios retos, metodológica y conceptualmente: (1) La colecta de ejemplares con una certeza mínima de su horizonte geológico. (2) La identificación de nuevos morfotipos mediante la obtención de nuevas técnicas microscópicas que permitan visualizar los rasgos diagnósticos. (3) El uso de los principios y prácticas de la sistemática de especies actuales que soporten nuevas hipótesis filogenéticas y biogeográficas. (4) El uso de los métodos y conocimientos de las ciencias de la tierra que generan correlaciones sobre la dispersión y extinción de los taxa.

En los trabajos publicados producto de esta investigación se abordaron estos tópicos centrales en la diagnosis y descripción de nuevas especies (e.g. Riquelme *et al*, 2014, 2014c). En su medida, se buscó también presentar correlaciones con las especies actuales e inferencias sobre su dispersión actual. Sin embargo, quedan por discutir y presentar relaciones filogenéticas más extensas para diferentes taxa, los cuales estarían orientados a reconstruir sus historias evolutivas y patrones biogeográficos comparando las diversidad y distribución geográfica actual de los respectivos grupos. Pero como esto requiere del uso de nuevas herramientas y teorías de la sistemática moderna, las cuales quedan fuera de los objetivos de este proyecto, se proponen como una línea a investigar y desarrollar en trabajos futuros.

Históricamente, fósiles invaluables en el ámbar de Chiapas han sido acumulados en colecciones anacrónicas y pretenciosas que extraen fósiles ilegalmente fuera de México.

Desafortunadamente, el material tipo de los dos escorpiones, por ejemplo, que fueron reportados previamente para el ámbar de Chiapas, cae bajo este contexto ambiguo (Santiago-Blay y Poinar, 1993; Lourenço, 2014). En general, este fenómeno se aplica para muchos otros ejemplares en el ámbar de Chiapas. Por lo cual, la revisión de los ejemplares está básicamente restringida y la información no es verificable. Igualmente, la procedencia de los ámbares es cuestionable, ya que el ámbar Mexicano es muy parecido, física y químicamente, al ámbar Dominicano. Es decir, comparten similitudes en color, brillo, consistencia, composición química general, fuente vegetal y biología de las inclusiones orgánicas (Cunningham *et al*., 1983; Langenheim de 2003, Riquelme *et al*, 2014b). La información proporcionada por los intermediarios que ofrecen los fósiles puede ser típicamente malinterpretada o insidiosa. De manera complementaria a las referencias geográficas proporcionadas por los colectores, se requieren también análisis químicos y microscópicos para distinguir claramente la naturaleza del ámbar. De acuerdo a lo anterior, la procedencia de los fósiles descritos en ese trabajo fue examinada a detalle y forman parte de colecciones públicas registradas ante el Instituto Nacional de Antropología e Historia (INAH). Un registro público que fue promovido por el presente autor y que fue compartido por los coleccionistas, quienes mostraron un interés genuino por preservar este patrimonio paleontológico. De esta manera, quedó asegurado su resguardo y protección, lo que garantiza que la información generada por este material fósil es verificable y de acceso abierto a la academia y público en general.

El fenómeno de colecta y venta de ámbar con inclusiones orgánicas en Chiapas es muy complejo. Inicia en su forma actual, desde la primera mitad del siglo XX. Sin embargo, trabajos futuros de campo en el área deben también involucrar la parte sociocultural y enfocarse en la formación de colecciones públicas integradas a los museos locales. Con esto se garantiza el repositorio y estudio formal del material fósil, lo cual no es trivial.

3.1 MATERIAL COMPLEMENTARIO

S1. Video (.avi)

Microtomografía computarizada de rayos-X

Espécimen: Milípedo, polidésmido, inclusión en ámbar de Chiapas

Referenciado en Riquelme *et al*., 2014. Plos One

3.2 OTRAS CONTRIBUCIONES

Publicaciones de divulgación: Artículo y Libro.

1. Riquelme, F. 2012. Ámbar, la vida inmóvil. **Arqueología Mexicana** 115: 82-87.

2. Ámbar y Copal de México. 2014. Editado por **Riquelme** F., Ruvalcaba Sil J.L., Bucio L. **Instituto de Física, UNAM,** p. 100. †En prensa (Fig. 29).

Congresos internacionales

1. The Geological Society of America, Cordilleran Section - 108th Annual Meeting. Querétaro, México, marzo de 2012. Cartel. https://gsa.confex.com/gsa/2012CD/finalprogram/

2. Second Mexican Synchrotron Radiation Users' Meeting (MESYRUM). Science and Engineering Division of the University of Guanajuato, León, México, junio de 2012. Ponencia, http://www.fisica.ugto.mx/~mesyrum/.

3. Synchrotron Radiation in Art and Archaeology. The Metropolitan Museum of Art (MMA). New York, NY, E.E.U.U., junio de 2012. Ponencia. . http://www.bnl.gov/sr2a/

4. IX Congreso Internacional de Ingeniería, Universidad Autónoma de Querétaro. Querétaro, México, mayo de 2013. Ponencia.

5. VII Congreso Latinoamericano de Paleontología/XIII Congreso Mexicano de Paleontología. Guanajuato, México, septiembre de 2013. 5 ponencias.

6. XXII International Material Research Conference (IMRC). Cancún, México, noviembre de 2013, Cartel. http://www.mrs-mexico.org.mx/imrc2013/

7. IV Congreso Latinoamericano de Aracnología. Michoacán, México, julio de 2014. 2 ponencias. http://congresoaracnologiamexico.org/index.html

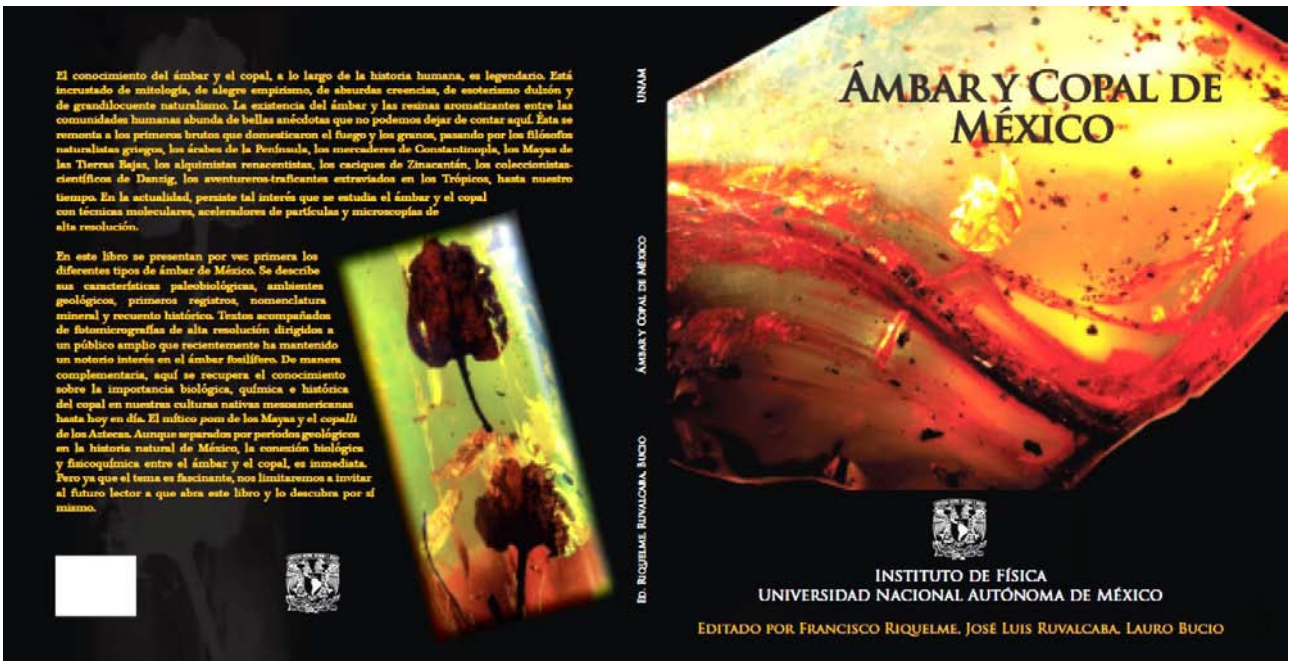

29. Libro Ámbar y Copal de México, portada y contraportada tentativo.

REFERENCIAS

Agricola, G. 1546. **De Natura Fossilium** (Textbook of Mineralogy). Traducción Bandy, M.C y Bandy, J. A. (2004), Courier Dover Publications, p. 240.

Anderson, K.B., Winans, R.E., Botto, R.E. 1992. The nature and fate of natural resins in the geosphere-II. Identification, classification and nomenclature of resinites. **Organic Geochemistry** 18: 829-841.

Anderson, K. B., Crelling, J. C.1995. Introduction (Amber, Resinite, and Fossil Resins), **American Chemical Society Symposium Series** 617, xi–xvii.

Anderson, K. B. 1996. New Evidence Concerning the Structure, Composition, and Maturation of Class I (Polylabdanoid) Resinites. Amber, Resinite, and Fossil Resins. **American Chemical Society Symposium Series** 617: 105-129.

Anderson, K.B. 1997. The nature and fate of natural resins in the geosphere- VII. A radiocarbon (14C) age scale for description of inmature natural resins. an invitation to scientific debate. **Organic Geochemistry** 25: 251-253.

Azar, D., Engel, M., Jarzembowski, E., Krogmann, L., A. Nel, A., Santiago-Blay, J. 2013. **Insect Evolution in an Amberiferous and Stone Alphabet**. Proceedings of the 6th International Congress on Fossil Insects, Arthropods and Amber. Brill Academic Pub. p. 210.

Beck, C., Wilbur, E., Meret, S. 1964. Infrared spectra and the origin of amber. **Nature** 201: 256-257.

Behrensmeyer, A. K., Kidwell, S, Gastaldo R.A. 2000. Taphonomy and paleobiology. **Paleobiology** 26 (4): 103-147.

Blom, F. 1959. Historical notes relating to the pre-Columbian amber trade from Chiapas. **Mitteilungen aus dem Museum für Volkerkunde in Hamburg** 25: 24-27.

Boggs, S. 2009. **Petrology of Sedimentary Rocks**. Cambridge Unicersity Press, 311-555.

Bray, P.S., Anderson, K.B. 2009. Identification of Carboniferous (320 million years old) class Ic amber. **Science** 326 (5949): 132-134.

Briggs, D.E.G. 2003. Exceptionally Preserved Fossils. En: **Palaeobiology II**. Editado por Briggs, D.E.G., Cowther, P.R., Blackwell Publishing, Malden, E.E.U.U., p. 328-332.

Buddhue, J.D. 1935. Mexican Amber. **Rocks and Minerals** 10: 170-171.

Callister, W.D. 2000. Polymer structures. En: **Material Science and Engineering.** John Wiley and Sons, MA. E.E.U.U., p. 446-514.

Carr, G.L., Williams, G.P.1997. Infrared microspectroscopy with synchrotron radiation. En: Accelerator-Based Infrared Sources and Applications, **SPIE Conference Proceedings** 3153: 51-59.

Cunningham, A., Gay, I.D., Oehlsclager, A.C., Lanhenheim, J. 1983. 13CNMR and IR analyses of structure, aging and botanical origin of Dominican and Mexican ambers. **Phytochemestry** 22 (4):965-968.

Dana Classification, 8th edition: Organic Compounds**.** www.mindat.org, último acceso 8.21.2014.

Derrick, M.R, Stulik, D., Landry, J.M. 1999. **Infrared Spectroscopy in Conservation Science**. The Getty Conservation Institute, p. 235.

Dumas, P., Miller, L. 2003. The use of synchrotron infrared microspectroscopy in biological and biomedical investigations. **Vibrational Spectroscopy** 32: 3-21.

Dunlop, J. A. 1996. Arácnidos fósiles (con exclusión de arañas y escorpiones). En: **Volumen Monográphico: PaleoEntomologica**. Editado por Melic, A. Boletin de la Sociedad Entomologica Aragonesa **16**: 77-92.

Dunlop, J.A., Penney, D., Tetlie, O.E. and Anderson, L.I. 2008. How many species of fossil arachnids are there? **The Journal of Arachnology** 36:267-272.

Dunlop, J.A., Penney, D. and Jekel, D. 2014. A summary list of fossil spiders and their relatives. En: **The world spider catalog, version 15.0**, American Museum of Natural History. Editado por Platnick, N.I., http://research.amnh.org/entomology/spiders/catalog/index.html, ultimo acceso 8.21.2014.

Durán Ruiz, C.A. 2012. **Estudio de himenópteros incluidos en el ámbar de Totolapa, Chiapas.** Tesis de Licenciatura. Universidad de Ciencias y Artes de Chiapas. Tuxtla Gutiérrez, Chiapas, p.72.

Durán-Ruiz, C., Riquelme, F., Coutiño-José, M., Carbot-Chanona, G., Castaño-Meneses, G., Ramos-Arias, M. 2013. Ants from the Miocene Totolapa amber (Chiapas, México), with the first record of the genus *Forelius* (Hymenoptera, Formicidae). **Canadian Journal of Earth Sciences** 50 (5): 495-502.

Durham, J. W. 1957. Amber through the ages. **Pacific Discovery** 10 (2), 3-5.

Eguiluz de Antuñano, S. 2001, Geologic evolution and gas resources of the Sabinas Basin in northeastern Mexico. En C. Bartolini, R. T. Buffler, and A. Cantú-Chapa (eds), The western Gulf of Mexico Basin: Tectonics, sedimentary basins, and petroleum systems. **AAPG Memoir** 75: 241-270.

Estrada-Ruiz, E., Upchurch, G.R., and Cevallos-Ferriz, S.R.S. 2008. Flora and climate of the Olmos Formation (Upper Campanian-Lower Maastrichtian), Coahuila, Mexico: a preliminary report. **Gulf Coast Association of Geological Societies Transactions** 58: 273-283.

Feldkamp, L.A., Davis, L.C., Kress, J.W. 1984. **Practical Cone Beam Algorithm**. JOSA A1: 612-619.

Flank, A.M., Cauchon, G., Lagarde, P., Bac, S., Janousch, M., Wetter, R., Dubuisson J.M. , Langlois, F., Idir, M., Moreno, T., Vantelon, D. 2006. LUCIA, A Microfocus soft XAS beamline. **Nuclear Instruments and Methods in Physics Research** (B) 246: 269-274.

Frost, S.H., Langenheim, R.L. 1974. **Cenozoic reef biofacies, tertiary larger Foraminifera and scleractinian corals from Chiapas, Mexico**. De Kalb (IL), Northern Illinois University Press, p. 388.

Graham, A. 1999. Studies in neotropicalpaleobotany. XIII. An Oligo-Miocene palynoflora from Simojovel (Chiapas, Mexico): **American Journal of Botany** 86 (1):17-31.

Grimaldi, D.A. 2000. **Studies on Fossils in Amber, with Particular Reference to the Cretaceous of New Jersey**. Editado por D. Grimaldi. Leiden, Netherlands: Backhuys, p. 504.

Grimaldi, D.A. 1996. Amber**: Window to the Past.** Abrams, New York, p. 216.

Goodwin, M.B., Grant, P.G., Bench, G., Holroyd, P.A. 2007. Elemental composition and diagenetic alteration of dinosaur bone: Distinguishing micron-scale spatial and compositional heterogeneity using PIXE. **Palaeogeography, Palaeoclimatology, Palaeoecology** 253: 458-476.

Harvey, M. S. 1992. The phylogeny and classification of the Pseudoscorpionida (Chelicerata: Arachnida). **Invertebrate Taxonomy** 6: 1373-1435.

Harmanand, P., Mitton, S. 2002. **Cambridge Scientific Minds**. Cambridge University Press, UK, p. 352.

Henderickx, H., Tafforeau, P., and Soriano, C. 2012. Phase-contrast synchrotron microtomography reveals the morphology of a partially visible new *Pseudogarypus* in Baltic amber (Pseudoscorpiones: Pseudogarypidae). **Palaeontologia Electronica** 15: 1-11

Hopkin S.P., Read H.J. 1992. **The Biology of Millipedes**. Oxford, UK: Oxford Univ Press, p. 233.

Hurd, P.D., Smith, R.F., Durham, J.W. 1962. **Fossiliferous amber of Chiapas, México**. Ciencia 2: 107-118.

Iturralde-Vinent, M.A. 2001. Geology of the amber-bearing deposits of the Greater Antilles**. Caribbean Journal of Science** 17 (3/4): 141-167.

Iturralde-Vinent, M.A. 2006. Meso-Cenozoic Caribbean Paleogeography: Implications for the Historical Biogeography of the Region. **International Geology Review** 48: 791-827.

Johansson, S.A.E., Campbell, J.L., Malmqvist, K.G. 1995. **Particle-Induced X-ray Emission Spectrometry (PIXE)**. En: Widefrodner, J.D. (Ed.), Chemical Analysis: Series of monograph on analytical chemistry and its applications, John Wiley & Sons, New York, 133.

Johnson, M.E., Ledesma-Vazquez, J., Clark, H.C., Zwiwbel, J.A. 1996. Coastal evolution of Late Cretaceous and Pleistocene rocky shores: Pacific rim of northern Baja California, Mexico. **Geological Society of America Bulletin** 108: 708-721.

Johnson, M.E., Ledesma-Vazquez, J., Baarli, B. G. 2006. Vertebrate Remains on Ancient Rocky Shores: A Review with Report on Hadrosaur Bones from the Upper Cretaceous of Baja California (México). **Journal of Coastal Research** 223:574-580.

Judson, M.L.I. 2010. Redescription of *Chelifer eucarpus* DALMAN (Arachnida, Chelonethi, Withiidae) and first records of pseudoscorpions in copal from Madagascar and Colombia. **Palaeodiversity** 3: 33-42.

Keilbach, R. 1982. Bibliographie und Listeder Artentierischer Einschlüsse in fossilen Harzensowieihrer Aufbewahrungsorte. **Deut Entomol Z, Neue Folge** 29 (129–286): 301-491.

Lambert, J.B., Frye, J.S., Lee, T.A., Welch, C.J., Poinar Jr., G. 1989. Analysis of Mexican amber by carbon-13 NMR spectroscopy. **Archaeological Chemistry** 4: 381-388.

Langenheim, J. H., Beck, C.W. 1965. Infrared spectra as a means of determining botanical sources of amber. **Science** 149: 52-54.

Langenheim, J.H. 1966. Botanical Source of Amber from Chiapas, Mexico (Fuente botánica del ámbar de Chiapas, México). **Ciencia** 24 (5-6): 201-210.

Langenheim, J.H., Beck, C.W. 1968. **Catalogue of infrared spectra of fossil resins (ambers) I. North and South America**. Botanical Museum Leaflets-Harvard University, vol. 22 (3): 65-120.

Langenheim, J.H. 1969. Amber: a botanical inquiry. **Science** 163: 1157-1169.

Langenheim, I.H. 1995. Biology of amber-producing trees: focus on case studies of *Hymenaea* and *Agathis*. **American Chemical Society Symposium Series** 617: 1-31.

Langenheim, J. H. 2003. **Plant resins: chemistry, evolution, ecology and ethnobotany**. Timber Press, p.586.

Langenheim, R.L., Budduhe, J.D., Jelinek, G. 1965. Age and occurrence of the fossil resins bacalite, kansasite and jelinite. **Journal of Paleontology** 39: 283-287.

Lak, M., Néraudeau, N., Nel, A., Cloetens, P., Perrichot, V., Tafforeau, P. 2008. Phase Contrast X-Ray Synchrotron Imaging: Opening Access to Fossil Inclusions in Opaque Amber. **Microscopy and Microanalysis** 14: 251-259.

Lee-Whiting, T. A. 2004. **Ámbar de Chiapas: historia, ciencia y estética**. Gobierno del Estado de Chiapas, México, p. 276.

Lourenço, W.R. 2014. A new species of scorpion from Chiapas amber, Mexico (Scorpiones: Buthidae**)**. **Revista Ibérica de Aracnología** 24: 59-63.

Lourenço, W.R. and Weitschat, W. 2005. A new genus and species of fossil scorpion from a different kind of Baltic amber (Scorpiones, Buthidae). **Mitteilungen aus dem Geologisch-Paläontologischen Institut der Universität Hamburg** 89: 183-188.

Lowe, L., Ruvalcaba, J.L. 2000. Provenance studies of amber by PIXE. **UNAM-IIA-Arqueometría** 6: 41-48.

Lowe, L. 2004. **El ámbar en Chiapas y su distribución en Mesoamérica**. UNAM-IIF-Centro de Estudios Mayas, México, p. 171.

Maldague, X.P. 2001. T**heory and practice of infrared technology for nondestructive testing**. Wiley, E.E.U.U., p. 684.

Martínez-Dávalos, A. 2010. An Overview of the Development and Evaluation of a Benchtop microCT Scanner. Proceedings of the XI Mexican Symposium on Medical Physics, **AIP Conference Proceedings** 1310: 7-11

Martínez-Hernández, E., Almeida-Leñero, L., Reyes-Salas, M. and Betancourt-Aguilar, Y. 1980. Estudio palinógico para la determinación de ambientes en la cuenca Fuentes-Río Escondido (Cretácico Superior), región de Piedras Negras, Coahuila. UNAM, **Instituto de Geología Revista** 4: 167-185.

Mendes, L. F. 1997. On a new fossil Microcoryphia (Insecta: Apterygota) from South-American copal. **Boletim da Sociedade portuguesa de Entomologia** 6 (18) (168): 245–250.

Mendes, L.F. 2002. Taxonomy of Zygentoma and Microcoryphia: historical overview, present status and goals for the new millennium. **Pedobiologia** 46: 225–233.

Meneses-Rocha, J.J. 2001.Tectonic evolution of the Ixtapa graben, an example of a strike-slip basin in southeastern Mexico: implications for regional petroleum systems. En: **The Western Gulf of Mexico Basin: tectonics, sedimentary basins, and petroleum systems**, vol. 75. Editado por Bartolini, C., Buffler, R.T., Cantú-Chapa, A., Tulsa, Oklahoma. American Association of Petroleum Geologists Memoir, p. 183–216.

Miller, J.L. 1994. **Principles of infrared technology: a practical guide to the state of the art.** The University of Michigan, E.E.U.U., p. 578.

Morra, M.J., Fendorf, S.E., Brown, P.D. 1997. Speciation of sulfur in humic and fulvic acids using X-ray absorption near-edge spectroscopy (XANES). **Geochimica et Cosmochimica Acta** 61: 683-688.

Morris, W.J. 1981. A new species of Hadrosaurian dinosaur from the Upper cretaceous of Baja California-? *Lambeosaurus laticaudus*. **Journal of Paleontology** 55 (2): 453-462.

Müllerried, F.K.G. 1942. Fósiles raros de México I. El primer miriápodo fósil de México, encontrado en el estado de Puebla. **Anales del Instituto de Biología** 13: 711-717.

Murienne, J., Harvey, M. S., and Giribet, G. 2008. First molecular phylogeny of the major clades of Pseudoscorpiones (Arthropoda: Chelicerata). **Molecular Phylogenetics and Evolution** 49: 170-184.

Penney, D. 2010. **Biodiversity of Fossils in Amber from the Major World Deposits**. Siri Scientific Press, p.304.

Perreau, M. and Tafforeau, P. 2011. Virtual dissection using phase-contrast X-ray synchrotron microtomography: reducing the gap between fossils and extant species. **Systematic Entomology** 36: 573-580.

Perrilliat, M., Vega, F., Coutiño, M. 2010. Miocene mollusks from the Simojovel area in Chiapas, southwestern Mexico. **Journal of South American Earth Sciences**, 30: 111-119.

Poinar, G. 0. 1992. **Life in amber**. Palo Alto: Stanford University Press, E.E.U.U., p. 29-46.

Poinar G.O, and Brown A.E. 2002. *Hymenaea mexicana* sp. nov. (Leguminosae: Caesalpiniodeae) from Mexican amber indicates Old World connections. **Botanical Journal of the Linnean Society** 139: 125–132.

Potts, P.J., Bowles J.F.W., Reed S. J. 6 Cave, M. R. 1995. **Microprobe Techniques in the Earth Sciences**. Chapman and Hall, London, p. 432.

Prieto-Márquez, A., Chiappe, L.M., Joshi, S.H. 2012. The Lambeosaurine Dinosaur *Magnapaulia laticaudus* from the Late Cretaceous of Baja California, Northwestern Mexico. **Plos One** 7(6): 1-32.

Rasband, W.S. 2012. **Image J**, U. S. National Institutes of Health, Bethesda, Maryland, E.E.U.U., http://imagej.nih.gov/ij/: ultimo acceso 8.21.2014.

Ravel, B., M. Newville. 2005. ATHENA, ARTEMIS, HEPHAESTUS: data analysis for X-ray absorption spectroscopy using IFEFFIT**. Journal of Synchrotron Radiation** 12, 537-541.

Riquelme, F., J. L. Ruvalcaba-Sil & J.Alvarado-Ortega. 2009, Palaeometry: Non-destructive analysis of fossil materials. **Boletín de la Sociedad Geológica Mexicana** 61 (2): 177-183.

Riquelme, F., Ruvalcaba-Sil, J. L., Alvarado-Ortega, J., Espinosa- Matías, S.; Martínez, M. C. Rodriguez, I., Perrilliat, M. C.; Ortiz, E.; Guzman, S.; Durán, C. A., Coutiño, M. A.; G. Carbot, G. 2011. Procesing and displaying 3D images of fossil insect and plants preserved in amber based on Apochromatic-zoom microscopy and Infrared microimaging. Proceedings of the XI InterAmerican Congress of Microscopy, **Acta Microscopica** 20, Supp. B, p. 3.

Riquelme, F. 2012. Ámbar, la vida inmóvil. **Arqueología Mexicana** 115: 82-87.

Riquelme, F., Alvarado-Ortega, J., Ruvalcaba-Sil, J. L., Aguilar-Franco, M., Porras-Múzquiz, H. 2013. Chemical fingerprints and microbial biomineralization of fish muscle tissues from the Late Cretaceous Múzquiz Lagerstätte, Mexico. **Revista Mexicana de Ciencias Geológicas** 2: 417-435.

Riquelme, F., Hill, D. E. 2013. Insights into amber salticids from the Neogene of Middle America, with the first report of Marpissinae (Araneae: Salticidae) from the Chiapas amber. **Peckhamia** 106.2: 1-5.

Riquelme, F., Alvarado-Ortega, J., Ramos-Arias, M., Hernández, M., Le Dez, I., Lee-Whiting, T. A., and Ruvalcaba-Sil J.L. 2014. A fossil stemmiulid millipede (Diplopoda: Stemmiulida) from the Miocene amber of Simojovel, Chiapas, Mexico. **Historical Biology** 26 (4): 415-427.

Riquelme, F., Northrup, P., Ruvalcaba-Sil, J.L., Stojanoff, V., Siddons, D.P., and Alvarado-Ortega, J. 2014a. Insights into molecular chemistry of Chiapas amber using infrared-light microscopy, PIXE/RBS, and sulfur K-edge XANES spectroscopy. **Applied Physics A** 116 (1): 97-109.

Riquelme, F., Ruvalcaba-Sil, J.L., Alvarado-Ortega, J., Estrada-Ruiz, E., Galicia-Chávez, M., Porras-Múzquiz, H., Stojanoff, V., Siddons, D.P., Miller, L. 2014b. Amber from México: Coahuilite, Simojovelite and Bacalite. **MRS Proceedings** 1618: doi:10.1557/opl.2014.466.

Riquelme, F., Hernández-Patricio, M., Martínez-Dávalos,A., Rodríguez-Villafuerte, M., Montejo-Cruz,M., Alvarado-Ortega, J., Ruvalcaba- Sil, J.L., and Zúñiga-Mijangos, L. 2014c. Two flat-backed Polydesmidan millipedes from the Miocene Chiapas-Amber Lagerstätte, Mexico**. Plos One**. En prensa.

Rosset, A., Spadola, L., Ratib, O. 2004. OsiriX: An Open-Source Software for Navigating in Multidimensional DICOM Images. **Jounal of Digital Imaging** 17 (3): 205-216.

Ruvalcaba-Sil, J.L. 2008. Las técnicas de origen nuclear: PIXE y RBS. En: **La Ciencia y el Arte.** Editado por Del Egido, M.A., Calderón, T., Instituto del Patrimonio Histórico Español: IPHE-CSIC, Madrid, p. 151-172.

Ruvalcaba Sil, J.L, Manzanilla, L., Melgar, E., Lozano Santa Cruz, R. 2008. PIXE and Ionoluminiscence for mesoamerican jadeite characterization. **X-ray Spectrometry** 37: 96-99.

Santiago-Blay, J.A., Poinar, G.O. 1992. Millipeds from Dominican amber, with the description of two new species (Diplopoda: Siphonophoridae) of Siphonophora. **Annals of the Entomological Society of America** 85(4): 363–369.

Santiago-Blay, J.A. and Poinar, G.O. 1993. First scorpion (Buthidae: Centruroides) from Mexican amber (lower Miocene to upper Oligocene). **The Journal of Arachnology** 21:147-151.

Schawaller, W. 1980. Erstnachweis tertiarer Pseudoskorpione (Chernetidae) in Dominikanischem Bernstein (Stuttgarter Bernsteinsammlung: Arachnida, Pseudoscorpionidea). Stuttgarter **Beitrage zur Naturkunde** (B) **57**: 1-20.

Schawaller, W. 1982. Der erste Pseudoskorpion (Chernetidae) aus Mexikanischem Bernstein. Stuttgarter **Beiträge zur Naturkunde** (B) **85**: 1-9.

Schawaller, W. 1991. The first Mesozoic pseudoscorpion from Cretaceous Canadian amber**. Palaeontology** 34: 971-976.

Schweitzer, M. H., R. Avci , T. Collier , M. B. Goodwind. 2008. Microscopic, chemical and molecular methods for examining fossil preservation. **Comptes Rendus Palevol** 7: 159-184.

Sham, T.K. 2002. **Chemical Applications of Synchrotron Radiation. Part II: X-ray applications**. World Scientific, Singapore, p. 1227.

Shcherbakov, D., Engel, M., Sharkey, M. 2011. **Advances in the Systematics of Fossil and Modern Insects.** Honouring Alexandr Rasnitsyn. PenSoft Publishers LTD, p.542.

Shear, W., Schawaller, W., and Bonamo, P. M. 1989. Record of Palaeozoic Pseudoscorpions. **Nature** 341: 527-529.

Shear, W. 2011. Class Diplopoda de Blainville in Gervais, 1844. In: Zhang, Z.-Q. Animal biodiversity: An outline of higher-level classification and survey of taxonomic richness. **Zootaxa** 3148: 159-164.

Sierwald P., Bond, J.E. 2007. Current status of the myriapod class Diplopoda (Millipedes): taxonomic diversity and phylogeny. **Annual Review of Entomology** 52: 401-420.

Solórzano-Kraemer, M.M. 2010. Mexican Amber. En: **Biodiversity of fossils in amber from the major world deposits**. Editado por Penney, D., Manchester, Siri Scientific Press, 42-56.

Stankiewicz, A., Poinar, H.N., Briggs, D.E.G., Evershed, R.P., George O. Poinar, G.O. 1998. Chemical Preservation of Plants and Insects in Natural Resins. **Proceeding of the Royal Society of London (B)** 265: 641-647.

Strunz Classification: Organic Compounds. www.mindat.org, último acceso 8.21.2014.

Sturm, H., Bach de Roca, C. 1993. On the systematics of the Archeognatha (Insecta). **Entomologia Generalis** 18:55-90.

Sturm, H., Poinar, G. O. Jr. 1997. A new Neomachilellus species from Miocene amber of the Dominican Republic and its phylogenetic relationships (Archaeognatha: Meinertellidae). **Entomologia Generalis** 22:157-170.

Sturm, H., Machida, R. 2001. **Archaeognatha**. Walter de Gruyter, Berlin, Series Handbuch der Zoologie 37, p. 213.

Tafforeau, P., Boistel, R., Boller, E., Bravin, A., Brunet, M., Chaimanee, Y., Cloetens, P., Feist, M., Hoszowska, J., Jaeger, J.-J., Kay, R.F., Lazzari, V., Marivaux, L., Nel, A., Nemoz, C., Thibault, X., Vignaud, P., Zabler, S. 2006. Applications of X-ray synchrotron microtomography for non-destructive 3D studies of paleontological specimens. **Applied Physics A** 83:195-202.

Tappert R., Wolfe, A. P., McKellar, R. C., Tappert, M. C., Muehlenbachs, K. 2011. Characterizing modern and fossil gymnosperm exudates using micro-Fourier Transform Infrared spectroscopy. **International Journal of Plant Science** 172(1): 120-138.

Trevisani, E., Papazzoni, C.A., Ragazzi, E., Roghi. G. 2005. Early Eocene amber from the ‘‘Pesciara di Bolca’’ (Lessini Mountains, Northern Italy). **Palaeogeography, Palaeoclimatology, Palaeoecology** 223:260-274.

Vandenabeele, P., Grimaldi, D.M., Edwards H**,** Moens, L. 2003. Raman spectroscopy of different types of Mexican copal resins. **Spectrochimica Acta Part A**: Molecular and Biomolecular Spectroscopy 59 (10): 2221-2229.

Vavra N. 1993. Chemical Characterization of Fossil Resins ("Amber"). A Critical Review of Methods, Problems and Possibilities: Determination of Mineral Species, Botanical Sources and Geographical Attribution. **Proceedings of a Symposium held in Neukirchen am Großvenediger 1990 Abh.Geol**. (B-A): 147-157.

Weistschat, W., Wichard, W. 2002. **Atlas of Plants and animals in Baltic Amber**. Editorial Dr. Friedrich Pfeil, Munich, p.256.

Weygoldt, P. 1969. **The Biology of Pseudoscorpions**. Harvard University Press, Cambridge, Massachusetts, p. 156.

Wilson, H.M., Anderson, L.I. 2004. Morphology and Taxonomy of Paleozoic millipedes (Diplopoda: Chilognatha: Archipolypoda) from Scotland. **Journal of Paleontology** 78 (1): 169-184.

Wolfe, A. P., Tappert, R., Muehlenbachs, K., Boudreau, M., McKellar, R. C., Basinger, J. F., Garrett, A. 2009. A new proposal concerning the botanical origin of Baltic amber. **Proceedings of Royal Society (B)** 276: 3403-341.

Xia, K., Weesner, F., W. F. Bleam, W. F., Bloom, P.R., Skyllberg, U. L., Helmke, P.A. 1998. XANES studies of oxidation states of S in humic substances from different environmental settings. **Soil Science Society of America Journal** 62, 1240-1246.

Yefremov, I. 1940. Taphonomy: new branch of paleontology. **Pan-American Geologist** 74: 81-93.

Zittel, Karl Alfred von. 1901. **History of geology and palæontology to the end of the nineteenth century**. W. Scott., Londres, U.K., p. 15-16.